
Coral-based Reconstructions of Southern Caribbean Climate during the Mid- to Late Holocene

Dissertation

for the doctoral degree in natural sciences
(Dr. rer. nat.)

at the
Faculty of Geosciences of Bremen University

submitted by
Cyril Giry

Tag des öffentlichen Kolloquiums

28.06.2011

MARUM Building 1, Raum 2070, 16.15.

Gutachter der Dissertation

Prof. Dr. Gerold Wefer

Prof. Dr. Gerrit Lohmann

Weitere Mitglieder des Prüfungsausschusses

Prof. Dr. Dierk Hebbeln

Prof. Dr. Gerhard Bohrmann

Dr. Thomas Felis

Anne Seidenglanz

Declaration

Name: Cyril Giry

Date: 21 April 2011

Address: Kleine Annenstrasse, 17a
28199, Bremen

Herewith I declare that

- I. this document and the accompanying data has been composed by myself, and describes my own work
- II. Material from the published or unpublished work of others, which is referred to in the dissertation, is credited to the author in the text.
- III. This work has not been submitted for any other degree.

Bremen, 21 April 2011

.....
(Signature)

Table of contents

| | |
|---|-------------|
| <i>Table of contents</i> | <i>I</i> |
| <i>Table of Figures</i> | <i>V</i> |
| <i>Table of tables</i> | <i>IX</i> |
| <i>ABSTRACT</i> | <i>XI</i> |
| <i>ZUSAMMENFASSUNG</i> | <i>XIII</i> |
| <i>ACKNOWLEDGMENTS</i> | <i>XV</i> |
| <i>Abbreviations</i> | <i>XVII</i> |
| | |
| 1. Introduction | 1 |
| 1.1 The potential of the Caribbean for Holocene climate reconstructions | 1 |
| 1.2 State-of-the-art, coral-based paleoclimatology | 3 |
| 1.3 Coral Sr/Ca, a temperature proxy | 5 |
| 1.4 Coral $\delta^{18}\text{O}$, a combined temperature and salinity proxy | 8 |
| 1.5 Coastal deposits on Bonaire, the “Great climate archive” | 11 |
| 1.5.1 <i>Diploria strigosa</i> (Dana, 1846) | 12 |
| 1.5.2 Collection of coral cores and microsampling | 14 |
| 1.6 Bonaire, regional setting | 14 |
| 1.6.1 Geography and Geology | 14 |
| 1.6.2 Oceanographic setting | 15 |
| 1.6.3 Climatic setting | 17 |
| 1.7 Motivations and Objectives | 21 |
| 1.7.1 Motivations | 21 |
| 1.7.2 Objectives | 22 |
| 1.8 Thesis outline | 23 |
| | |
| 2. Manuscripts | 25 |
| 2.1 Geochemistry and skeletal structure of <i>Diploria strigosa</i>, implications for coral-based climate reconstruction | 27 |
| 2.1.1 Introduction | 28 |
| 2.1.2 Material and Methods | 29 |
| 2.1.2.1 Regional and climatic settings | 29 |
| 2.1.2.2 Coral core collection and preparation | 30 |
| 2.1.2.3 Microsampling of coral skeleton | 31 |
| 2.1.2.4 Sr/Ca and stable isotope analyses | 33 |
| 2.1.3 Results | 33 |
| 2.1.3.1 Mean geochemical composition of skeletal elements | 33 |
| 2.1.3.2 Subseasonally-resolved Sr/Ca, $\delta^{18}\text{O}$ and $\delta^{13}\text{C}$ records | 35 |
| 2.1.3.3 Geochemical variability within the theca | 36 |
| 2.1.4 Discussion | 37 |
| 2.1.4.1 Kinetic fractionation within a corallite | 37 |

| | |
|--|-----------|
| 2.1.4.2 Temperature dependence of climate proxies in <i>Diploria strigosa</i> | 40 |
| 2.1.4.3 Implications for coral-based climate reconstruction | 41 |
| 2.1.5 Conclusion | 43 |
| 2.2 Assessing the potential of Southern Caribbean corals for reconstructions of Holocene temperature variability | 45 |
| 2.2.1 Introduction | 46 |
| 2.2.2 Material and Methods | 47 |
| 2.2.2.1 Regional setting | 47 |
| 2.2.2.2 Coral sampling and ^{230}Th /U-dating | 48 |
| 2.2.2.3 Diagenetic investigations | 48 |
| 2.2.2.4 Microsampling | 48 |
| 2.2.2.5 Sr/Ca analyses | 49 |
| 2.2.2.6 Coral chronology | 49 |
| 2.2.3 Results and discussion | 50 |
| 2.2.3.1 Preservation of coral skeleton | 50 |
| 2.2.3.2 Coral Sr/Ca record | 50 |
| 2.2.3.3 Southern Caribbean interannual SST variability at 2.35 ka BP | 52 |
| 2.2.4 Conclusions | 52 |
| 2.3 Mid- to late Holocene changes in tropical Atlantic temperature seasonality and interannual to multidecadal variability documented in southern Caribbean coral records | 55 |
| 2.3.1 Introduction | 56 |
| 2.3.2 Material and Methods | 58 |
| 2.3.2.1 Climatic setting of the study area | 58 |
| 2.3.2.2 Coral collection and diagenetic investigations | 59 |
| 2.3.2.3 ^{230}Th /U-dating of corals | 61 |
| 2.3.2.4 Microsampling, Sr/Ca analyses, chronology construction, time series analyses | 61 |
| 2.3.2.5 Model description and experimental setup | 62 |
| 2.3.3 Results | 62 |
| 2.3.3.1 Preservation of coral skeletons | 62 |
| 2.3.3.2 Modern coral Sr/Ca-SST relationships | 64 |
| 2.3.3.3 Coral Sr/Ca-based SST variations throughout the mid- to late Holocene | 66 |
| 2.3.3.3.1 Coral Sr/Ca-based variations in mean SST | 66 |
| 2.3.3.3.2 Coral Sr/Ca-based SST seasonality | 67 |
| 2.3.3.3.3 Coral Sr/Ca-based interannual SST variability | 67 |
| 2.3.3.3.4 Coral Sr/Ca-based inter- to multidecadal SST variability | 68 |
| 2.3.4 Discussion | 69 |
| 2.3.4.1 Warming of the western tropical Atlantic over the last 6.2 ka | 69 |
| 2.3.4.2 Forcing of SST seasonality in the western tropical Atlantic over the last 6.2 ka | 69 |
| 2.3.4.3 Source of prominent quasi-biennial SST variability over the last 6.2 ka | 71 |
| 2.3.4.4 Sources of interannual SST variability over the last 6.2 ka | 71 |

| | |
|---|------------|
| 2.3.4.5 Change in the seasonal pattern of interannual SST variability at 2.35 ka | 72 |
| 2.3.4.6 Enhanced inter- to multidecadal SST variability in the mid-Holocene | 74 |
| 2.3.5 Conclusion | 74 |
| 2.4 Seasonal to multidecadal variability of sea surface hydrology in the southern Caribbean during the mid- to late Holocene | 83 |
| 2.4.1 Introduction | 84 |
| 2.4.2 Regional setting of the study area | 85 |
| 2.4.3 Material and Methods | 87 |
| 2.4.4 Results | 88 |
| 2.4.4.1 Modern coral $\delta^{18}\text{O}$ -SST relationship | 88 |
| 2.4.4.2 Mid- to late Holocene changes in southern Caribbean Sea surface hydrology | 89 |
| 2.4.4.2.1 Variation in mean $\delta^{18}\text{O}_{\text{sw}}$ | 90 |
| 2.4.4.2.2 Seasonal changes of sea surface hydrology | 90 |
| 2.4.4.2.3 Interannual to multidecadal $\delta^{18}\text{O}_{\text{sw}}$ variability | 93 |
| 2.4.4.3 Relationship between $\delta^{18}\text{O}_{\text{sw}}$ and SST | 96 |
| 2.4.5 Discussion | 96 |
| 2.4.5.1 $\delta^{18}\text{O}_{\text{sw}}$ changes of the western tropical Atlantic over the last 6.2 ka | 96 |
| 2.4.5.2 Annual $\delta^{18}\text{O}_{\text{sw}}$ cycles over the last 6.2 ka: local precipitations Vs. oceanic advection | 97 |
| 2.4.5.2.1 Reduced local precipitations at present | 97 |
| 2.4.5.2.2 Pronounced local precipitations in the mid-Holocene | 99 |
| 2.4.5.2.3 Mid- to late Holocene transition | 100 |
| 2.4.5.3 Control of surface winds on SST and sea surface hydrology | 101 |
| 2.4.5.4 Enhanced multidecadal variability at 6.2 ka | 104 |
| 2.4.6. Conclusion | 106 |
| 3. Summary and conclusions | 109 |
| 4. Outlook - Future research directions | 113 |
| 4.1 <i>Biological effects on geochemical proxies in corals</i> | 113 |
| 4.2 <i>Climate reconstructions from Pleistocene corals</i> | 113 |
| 4.3 <i>The importance of monthly resolved tropical Atlantic coral records</i> | 114 |
| 4.4 <i>Extended coral-based reconstructions of mid-Holocene climate</i> | 114 |
| References | 116 |

Table of Figures

| | |
|---|----|
| Figure 1.1: Concept of the INTERDYNAMIC Project CaribClim | 2 |
| Figure 1.2: Map of published subannual coral-derived climate records | 5 |
| Figure 1.3: Oxygen isotopic composition and coral growth | 9 |
| Figure 1.4: Oxygen isotopic composition of global sea surface waters ($\delta^{18}\text{O}_{\text{sw}}$) | 10 |
| Figure 1.5: Coastal deposits on Bonaire, the “Great climate archive” | 11 |
| Figure 1.6: Fossil <i>Diploria strigosa</i> (Dana, 1846) on Bonaire | 12 |
| Figure 1.7: Living <i>Diploria strigosa</i> brain coral on Bonaire | 13 |
| Figure 1.8: Mesoskeletal architecture of <i>D. strigosa</i> | 13 |
| Figure 1.9: Growth pattern of <i>D. strigosa</i> corallite | 15 |
| Figure 1.10: Map of the Caribbean Sea depicting Bonaire | 15 |
| Figure 1.11: Temperature/salinity diagram for the water column of the Caribbean | 16 |
| Figure 1.12: Sea surface salinity map and oceanographic setting of the western tropical Atlantic and the Caribbean | 17 |
| Figure 1.13: Monthly mean climatology of environmental parameters at Bonaire | 18 |
| Figure 1.14: Correlation map between Niño3.4 (DJF) index and global SST (MAM) | 19 |
| Figure 1.15: Correlation map between NAO (DJF) index and global SST (MAM) | 20 |
| Figure 1.16: Correlation map between AMO index and global SST | 21 |

Manuscript I

| | |
|--|----|
| Figure 2.1: Monthly sea surface temperature climatology for Bonaire | 30 |
| Figure 2.2: Presentation of mesoskeletal architecture of <i>Diploria strigosa</i> skeleton | 31 |
| Figure 2.3: Scheme of the microsampling experiments performed | 32 |
| Figure 2.4: Sr/Ca, $\delta^{18}\text{O}$ and $\delta^{13}\text{C}$ annual cycles from four sampling paths | 34 |
| Figure 2.5: Geochemical signature of four different microsampling profiles | 35 |
| Figure 2.6: Geochemical variability within a thecal wall of <i>D. strigosa</i> | 36 |
| Figure 2.7: Mean geochemical composition across thecal wall of three <i>D. strigosa</i> | 39 |

Manuscript II

| | |
|---|----|
| Figure 2.8: Location of Bonaire and coastal deposits | 47 |
| Figure 2.9: Diagenetic screening of the 2.35 ka fossil coral skeleton | 49 |
| Figure 2.10: 40-year long monthly resolved Sr/Ca record from 2.35 ka coral | 51 |

Manuscript III

| | |
|---|----|
| Figure 2.11: SST maps around Bonaire for March and October | 57 |
| Figure 2.12: Monthly Bonaire SST and Niño3.4 DJF index | 58 |
| Figure 2.13: X-radiograph positive prints of Bonaire <i>Diploria strigosa</i> coral slabs | 60 |
| Figure 2.14: Diagenetic screening of Bonaire <i>Diploria strigosa</i> corals | 63 |
| Figure 2.15: Spectral analyses of monthly coral Sr/Ca records and Bonaire SST data | 65 |
| Figure 2.16: SST changes throughout the mid- to late Holocene, comparison between Bonaire coral Sr/Ca-SST and western tropical Atlantic temperature reconstructions | 66 |
| Figure 2.17: Comparison between seasonal insolation changes at the latitude of Bonaire and coral Sr/Ca-derived SST seasonality | 68 |
| Figure 2.18: SST seasonality anomaly at 6 ka inferred from coral Sr/Ca-SST records and COSMOS-aso numerical simulations | 70 |
| Figure 2.19: Monthly and seasonal time series for Bonaire SST data, 2.35 ka and 6.22 ka coral Sr/Ca records and corresponding spectral analyses | 73 |
| Suppl. Figure 1: Map of Bonaire showing locations of coral samples | 77 |
| Suppl. Figure 2: Year-to-year variability of SST seasonality inferred from Bonaire coral Sr/Ca records and instrumental SST data and corresponding spectral analyses | 78 |
| Suppl. Figure 3: Interdecadal bandpass filtered Sr/Ca-SST time series of coral Sr/Ca records with length > 20 years and their standard deviation | 79 |
| Suppl. Figure 4: Cross-spectral analysis between monthly time series of Bonaire SST and Niño3.4 Index | 80 |
| Suppl. Figure 5: Cross-spectral analysis between monthly time series of Bonaire SST and NAO Index | 85 |

Manuscript IV

| | |
|--|----|
| Figure 2.20: Modern oceanographic setting of the Caribbean and western North Atlantic | 86 |
| Figure 2.21: ENSO control on Bonaire SST and rainfall variability | 87 |
| Figure 2.22: Monthly resolved coral Sr/Ca, $\delta^{18}\text{O}$ and $\Delta\delta^{18}\text{O}$ records from <i>Diploria strigosa</i> corals from Bonaire | 89 |
| Figure 2.23: Change in southern Caribbean hydrology throughout the mid- to late Holocene, comparison between mean coral $\Delta\delta^{18}\text{O}$ and Cariaco Basin Ti record | 90 |
| Figure 2.24: Coral $\delta^{18}\text{O}$ seasonality inferred from Bonaire coral records | 91 |
| Figure 2.25: Composite annual Sr/Ca-SST and $\delta^{18}\text{O}$ -SST cycles from Bonaire coral records and corresponding phase angles between two time series | 91 |
| Figure 2.26: Response of reconstructed coral $\Delta\delta^{18}\text{O}$ annual cycle to different proxy-SST regression slopes. | 92 |

| | |
|---|-----|
| Figure 2.27: Composite annual coral $\Delta\delta^{18}\text{O}$ cycles for individual Bonaire coral records | 93 |
| Figure 2.28: Spectral analyses of monthly coral $\Delta\delta^{18}\text{O}$ records and Bonaire rainfall data | 94 |
| Figure 2.29: Quasi-biennial, interannual, near-decadal and multidecadal Gaussian bandpass filtered coral $\Delta\delta^{18}\text{O}$ time series from individual records with length > 20 years and corresponding standard deviation | 95 |
| Figure 2.30: Linear regressions between Gaussian bandpass filtered coral $\Delta\delta^{18}\text{O}$ and Sr/Ca-SST time series with length > 20 years | 96 |
| Figure 2.31: Modelled and observed annual cycle of water transport by the Florida Current in comparison with monthly mean climatology of modern coral geochemical data and environmental parameters | 98 |
| Figure 2.32: Control of surface wind strength on both SST and SSS at Bonaire | 103 |
| Figure 2.33: enhanced multidecadal climate variability in the mid-Holocene as documented in monthly coral Sr/Ca and $\Delta\delta^{18}\text{O}$ records of the 6.2 ka coral. | 105 |

Table of tables

| | |
|--|----|
| Table 1.1: Published Sr/Ca-SST relationships for <i>Porites</i> sp. corals | 6 |
| Table 1.2: Published Sr/Ca-SST relationships for corals other than <i>Porites</i> sp. | 7 |
| Table 1.3: Details of the coral Sr/Ca records from Bonaire | 64 |
| Supp. Table 1: Details of the U-Th ages for Bonaire corals | 77 |

ABSTRACT

Knowledge about climate variability is essentially based on observational climate data that are often too short to fully understand the underlying mechanisms with sufficient accuracy. Instrumental records of climate are sparse and become spatiotemporally incomplete before the middle of the 20th century thus, limiting our understanding of the Earth's climate system prior to the instrumental data period. Recent changes in climate are often attributed to anthropogenic global warming. However, to validate such an assumption, patterns of climate variability must be firmly established for periods of reduced anthropogenic forcing. The reconstruction of key climate parameters, such as sea surface temperature (SST) and salinity (SSS), in records extending beyond the relatively short instrumental period are a prerequisite. Additionally, since the reconstructions from climate archives usually focused on the long-term changes (i.e., centennial to millennial scales), there is a clear need to better understand the patterns of short-term (i.e., seasonal to multidecadal scales) climate variability, which are often overlooked in paleoclimatology but relevant for the predictability of hazardous climate phenomena. The aim of the present study is to document the natural range of short-term climate variability in the tropical Atlantic during periods of reduced human activity. Analyses were conducted on several annually-banded *Diploria strigosa* (Dana, 1846) fossil coral colonies of Holocene age found in the coastal deposits on Bonaire (southern Caribbean Sea).

Accurate climate reconstructions from fossil *Diploria strigosa* corals require a good understanding of the geochemical climate proxies incorporated in their skeleton. Potential complications of coral-based derived climate reconstruction associated with sampling of their skeleton were investigated. It was found that accurate microsampling along the centre of the thecal wall of *D. strigosa* is a prerequisite for generating robust climate reconstructions. Based on this conclusion, the first monthly-resolved coral Sr/Ca-based sea surface temperature record from a well-dated fossil *D. strigosa* coral was generated in a second study. The potential of the fossil coral records for reconstruction of southern Caribbean Sea temperature variability was assessed by investigating secondary modifiers of coral Sr/Ca temperature proxy, such as growth rate and diagenesis. As no diagenetic alterations and no correlation between the coral Sr/Ca and growth rate were found, it was concluded that the fossil corals from Bonaire are exceptional high-resolution climate archives.

Since the aforementioned studies indicate the great potential of fossil *D. strigosa* corals for past climate reconstructions, advantages were taken from three modern and three fossil corals colonies found on Bonaire to investigate the pattern of SST variability recorded in approximately 295 years of monthly-resolved decades-long coral Sr/Ca records. The three modern coral records revealed discrepancies in the mean Sr/Ca value and the amplitude of reconstructed annual cycle that were considered for accurate reconstruction of past SST variability inferred from the six fossil coral records. Fossil coral records indicate orbital-control on low-latitude Atlantic SST seasonality that was further supported by model simulation. The coral records indicate that Bonaire SST during the mid- to late Holocene was characterised by persistent quasi-biennial and prominent interannual to multidecadal scale variability. However, the magnitude of SST variations has varied over the last 6.2 ka and the reasons for these changes were attributed to air-sea interactions emanating from both the Atlantic and Pacific Oceans. Moreover, a coral record at 2.35 ka BP indicated more pronounced interannual variability that was consistent with a strengthening of El Niño/Southern Oscillation at that time.

The last study investigated seasonal to multidecadal variability of the sea surface hydrology recorded in the coral $\Delta\delta^{18}\text{O}$ (a proxy of oxygen isotopic composition of sea water, $\delta^{18}\text{O}_{\text{sw}}$) from the nine corals. This was achieved by applying paired coral Sr/Ca and $\delta^{18}\text{O}$ measurements on individual coral samples. While wetter conditions were found in the mid-Holocene, the short-term changes of Caribbean Sea surface hydrology were attributed to both the evaporation/precipitation (E/P) ratio and the advection of fresh water by wind-driven surface currents. Modern corals $\Delta\delta^{18}\text{O}$ seasonal cycles revealed that oceanic advection of freshwater dominates at Bonaire today, whereas enhanced summer precipitation governed the annual hydrological signal in the mid-Holocene. Moreover, the persistent positive relationship between reconstructed SST and SSS was found for time scales ranging from seasonal to multidecadal suggesting some unique processes controlled the short-term variability of these two oceanographic parameters. Since the E/P ratio can not explain such a systematic relationship, we assumed that the amount of precipitation over northern South America and the oceanic advection of tropical water by surface wind-driven

currents are critical factors responsible for changes in southern Caribbean sea surface hydrology on seasonal to multidecadal time scales.

Finally, while the short instrumental data might already contain anthropogenic imprints, the total number of 295-years of the coral Sr/Ca and $\delta^{18}\text{O}_{\text{sw}}$ records used in this study provided relevant insight into the natural short-term variability of the tropical Atlantic climate. It was found that such short-term variability over the last 6.2 ka have arisen mainly from the dynamics internal to the climate system itself and the magnitude of such changes has exceeded corresponding variability known from the short instrumental data period. Consequently, this study strongly supports that a better understanding of changes in the magnitude of modes of climate variability and their interactions is critical for the successful predictions of tropical Atlantic climate in a changing climate.

ZUSAMMENFASSUNG

Das Wissen über Klimaschwankungen beruht im Wesentlichen auf instrumentellen Klimadaten, diese Zeitreihen sind aber häufig zu kurz, um die treibenden Mechanismen genau verstehen zu können. Noch vor Mitte des 20. Jahrhunderts waren instrumentelle Klimaaufzeichnungen rar, daher war vor dieser Zeit sowohl die zeitliche als auch die räumliche Datenabdeckung lückenhaft. Unser Verständnis vom Klimasystem der Erde ist so weitestgehend auf den Zeitraum der instrumentellen Datenaufzeichnung beschränkt.

Als Ursache der jüngsten Klimaschwankungen wird oft anthropogener Einfluss diskutiert. Um diese Annahme zu validieren, müssen jedoch Muster in der Klimavariabilität in der präindustriellen Zeit untersucht werden. Grundvoraussetzung dafür ist die Rekonstruktion von klimatischen Schlüsselparametern, wie der Meeresoberflächentemperatur (SST) und –salinität (SSS) über den relativ kurzen instrumentellen Zeitraum hinaus. Die auf Klimaarchive gestützte Rekonstruktion von Schlüsselparametern konzentriert sich oft auf Langzeitveränderungen (z.B. Zeiträume von Jahrhunderten bis Jahrtausenden). Für die Vorhersagbarkeit von Klimarisiken ist aber gerade das Verständnis von Mustern der kurzfristigen Klimaveränderung (z.B. von saisonalen Zeiträume bis zu mehreren Jahrzehnten) wichtig, diese werden allerdings oft von der Paleoklimatologie übersehen. Das Ziel der vorliegenden Arbeit ist es, die natürliche Spanne kurzfristiger Klimavariabilität im tropischen Atlantik für die Zeit vor der Industrialisierung zu dokumentieren. Hierzu wurden Analysen an mehreren jährlich gebänderten holozänen Korallen (*Diploria strigosa*, Dana, 1846) durchgeführt, die aus Küstenablagerungen von Bonaire (südliche Karibik) stammen.

Für genaue Klimarekonstruktionen mit Hilfe fossiler Korallen bedarf es eines guten Verständnis der im Skelett eingeschlossenen geochemischen Proxies. Potenzielle Probleme von korallenbasierten Klimarekonstruktionen, die bei der Beprobung der Skelette auftreten könnten, wurden untersucht. Es stellte sich heraus, dass eine exakte Mikrobeprobung entlang des Zentrums der Thekenwand von *D. strigosa* für eine zuverlässige Klimarekonstruktion unabdingbar ist. Unter Berücksichtigung dieser Schlussfolgerung wurde in einer zweiten Studie die erste monatlich aufgelöste Meeresoberflächentemperaturrekonstruktion erstellt, die auf Sr/Ca einer exakt datierten fossilen *D. strigosa* basiert. Durch Untersuchungen sekundärer Steuerungsfaktoren des Sr/Ca Temperaturproxies, nämlich der Wachstumsrate und der Diagenese, wurde das Potential fossiler Korallen für die Rekonstruktionen von Temperaturschwankungen des südlichen karibischen Meeres bemessen. Da weder diagenetische Veränderungen noch eine Korrelation von Sr/Ca mit Wachstumsraten gefunden wurden, konnte die Schlussfolgerung gezogen werden, dass die fossilen Korallen Bonaires als außergewöhnlich hoch-aufgelöste Klimaarchive betrachtet werden können. Die zuvor erwähnten Arbeiten weisen auf den großen Nutzen von fossilen *D. strigosa* Korallen für die Klimarekonstruktionen hin. Dieses Potenzial wurde an drei rezenten und sechs fossilen Korallenkolonien von Bonaire genutzt, um Muster der SST über zusammengerechnet 295 Jahre in monatlich aufgelösten, jahrzehntelangen Korallen-Sr/Ca-Aufzeichnungen zu untersuchen. Die drei rezenten Zeitreihen offenbarten Diskrepanzen im durchschnittlichen Sr/Ca Wert und der Amplitude der rekonstruierten Jahreszyklen. Dies wurde für die genaue Rekonstruktion der vergangenen SST-Schwankungen, die von den sechs fossilen Korallenaufzeichnungen hergeleitet wurde, berücksichtigt. Die fossilen Korallenaufzeichnungen sprechen für eine orbital kontrollierte atlantische SST Saisonalität für Standorte in niedrigen Breiten, die später durch Modellsimulationen bekräftigt wurde. Die Korallen-Aufzeichnungen zeigen, dass die SST Bonaires während des mittleren bis späten Holozäns durch quasi-zweijährliche und zwischenjährliche bis multi-dekadische Schwankungen charakterisiert war. Jedoch variierte die Magnitude der Schwankungen während der letzten 6.2 ka. Die Gründe für diese Veränderungen werden mit Atmosphäre-Ozean-Interaktionen in Verbindung gebracht, die sowohl vom Atlantischen als auch vom Pazifischen Ozean stammen. Darüber hinaus deutet eine Korallen-Zeitreihe für 2.35 ka BP eine stärker betonte zwischenjährliche Variabilität an, die mit einer Intensivierung der El Niño/Südliche Oszillation für diese Zeit übereinstimmt.

Die letzte Arbeit untersucht saisonale bis multi-dekadische Schwankungen der Meeresoberflächenhydrologie in $\Delta\delta^{18}\text{O}$ - Aufzeichnungen (ein Proxy für die Sauerstoff-Isotopie des Meerwassers, $\delta^{18}\text{O}_{\text{sw}}$) von neun Korallen. Diese Schwankungen wurden durch die parallele Anwendung von Sr/Ca und $\delta^{18}\text{O}$ bestimmt. Für das mittlere Holozän konnten feuchte Bedingungen nachgewiesen werden. Kurzfristige Veränderungen in der Meeresoberflächenhydrologie in der Karibik werden sowohl vom Verhältnis von Evaporation und Niederschlag (E/P) als auch der Advektion von Süßwasser durch windgetriebene Oberflächenströmungen gesteuert. In modernen

Korallen zeigt $\Delta\delta^{18}\text{O}$ saisonale Schwankungen, die deutlich machen, dass die ozeanische Advektion von Süßwasser heute in Bonaire der dominierende Faktor ist, wohingegen ein erhöhter Niederschlag in den Sommermonaten das Jahressignal im mittleren Holozän prägt. Außerdem wurde für saisonale bis multi-dekadische Zeitspannen eine durchgehend positive Korrelation zwischen der rekonstruierten SST und SSS nachgewiesen. Daraus lässt sich die Schlussfolgerung ziehen, dass einige individuelle Prozesse die Kurzzeitschwankungen dieser beiden ozeanographischen Parameter kontrollieren. Da das E/P-Verhältnis diesen systematischen Zusammenhang für die saisonale bis multi-dekadische Veränderungen der Oberflächenhydrologie des südlichen Karibischen Meeres nicht erklären kann, nehmen wir an, dass die entscheidenden Faktoren der Niederschlag über dem nördlichen Südamerika und die ozeanische Advektion (durch Wind induzierte Oberflächenströmung) des tropischen Wassers sind.

Da davon ausgegangen werden kann, dass instrumentelle Daten zur Klimavariabilität einem anthropogenen Einfluss unterliegen, bietet die in dieser Studie durchgeführte Untersuchung von Sr/Ca und $\delta^{18}\text{O}_{\text{sw}}$ von insgesamt 295 jährlichen Dichtebändern in Korallen einen wichtigen Einblick in die natürliche, kurzfristige Klimavariabilität des tropischen Atlantiks. Es wurde herausgefunden, dass solche kurzfristigen Klimaveränderungen über die letzten 6,2 ka im Atlantik hauptsächlich auf der Eigendynamik des Klimasystems beruhen. Das Ausmaß ihrer Variabilität überschreitet die momentane Veränderung des Klimas, die auf die Aufzeichnungen der letzten Jahre gestützt ist, deutlich. Daher führt diese Studie zu einem besseren Verständnis über das Ausmaß und den Modus von Klimaschwankungen. Dieses Zusammenspiel ist für die Vorhersage des Klimas im tropischen Atlantik in einer sich verändernden Welt wichtig.

ACKNOWLEDGMENTS

The three years of this PhD position were funded by the Deutsche Forschungsgemeinschaft (DFG) through the Special Priority Programme INTERDYNAMIC, Project CaribClim.

First of all, I would like to thank my supervisor Prof. Dr. Gerold Wefer for providing me with an excellent scientific environment at MARUM during this project, and for advising me with accurate suggestions throughout. I'm extremely grateful to Dr. Thomas Felis who thought for this unique interdisciplinary PhD project. Thomas, thank you for providing me through day to day interaction with your expertise on coral paleoclimatology, for your patience, for encouraging me every time was necessary, for your help, for introducing me to so many people, and for your showing me how science actually works – all of these have largely contributed to the completion of this Thesis. I am also very grateful to my advising committee Prof. Dr. G. Lohmann, Dr. J. Pätzold and Dr. H. Kuhnert for their advices, supports, comments and individual expertises that greatly contributed to the completion of this Thesis. I owe many thanks to Prof. Dr. G. Lohmann for his support with climate simulations.

Fieldwork for this study was made possible by the Government of the Island Territory of Bonaire with strong support from Elsmarie Beukenboom (STINAPA Bonaire National Parks Foundation). Thanks to Dr. S.R. Scheffers for his great support over the last three years and to Prof. Dr. A. Scheffers (Southern Cross University, Australia) for initiating this collaboration. I'm very grateful for the excellent lab assistances provided by Dr. M. Kölling and Dr. M. Segl and their respective team. Many thanks to Dr. J. Pätzold for support with coral drilling and discussion, to M. Vermeij for help with temperature data, to Dr. M. Zuther for X-ray diffraction analyses and to Dr. K. Baumann for Scanning Electron Microscopy imaging. I owe special thanks to Nadja for her excellent work with the micro-balance.

I very much enjoyed the chance of being part of the DFG SPP Integrated Analysis of Interglacial Climate Dynamics (INTERDYNAMIK) for thoughtful insight into proxy-model intercomparison. Consequently, I owe many thanks to Prof. Dr. M. Schulz and Dr. A. Paul for coordinating this research program, to Dr. D. Scholz and Prof. Dr. A. Mangini and his technicians for support with U-series datings, and finally to Claudia and Wei for the great collaboration over the last three years.

A great thank you goes to Adelheid, Nicolas, Isabelle, Jolanthe, Birgit and Carmen for their help within the administration's world. The past and present staff members of GLOMAR (Bremen International Graduate School for Marine Sciences) are acknowledged for their educational and financial supports.

I'm also grateful to Prof. Dr. G. Haug and Gaudenz Deplazes for the introduction to the laminated sediment world of Cariaco Basin during my stay at ETH Zurich, to Prof. Dr. E. Bard, Dr. F. Rostek, Dr. L. Vidal and Dr. K. Tashikawa, for sharing their expertise and comments on this project during my stay at CEREGE.

I'm very grateful to Sebastian and Hiske for their help with all kind of German-related issues, to Mark for support with English and to James for support with English and intensive discussions. Thanks to my past and present office-mates, especially Enqing, for respecting my working style. I am also very grateful to many scientists from the University of Bremen for the great time spent in Bremen. The list of names is long, too long for being included in the acknowledgement section because I'm so grateful to all of them that it would need one additional chapter to acknowledge all very nice and friendly people met in Bremen over the last three years. I owe many thanks to the non-scientists left in my native country, my family and all my friends, who encouraged me though the distance.

Last, but not least, I would like to thank Sonja for her immeasurable understanding, her patience and love.

Abbreviations

| | |
|-----------------------------------|--|
| AD | Anno Domini |
| AMO | Atlantic Multidecadal Oscillation |
| AMOC | Atlantic meridional overturning circulation |
| AO | Arctic Oscillation |
| AWP | Atlantic Warm Pool |
| BP | Before Present, refers to years before 1950 AD |
| CC | Caribbean Current |
| CLLJ | Caribbean Low-Level Jet |
| $\delta^{13}\text{C}$ | Stable carbon isotopic composition in per mil (‰) relative to Vienna-Pee Dee Belemnite (VPDB) |
| $\delta^{18}\text{O}$ | Stable oxygen isotopic composition in per mil (‰) relative to Vienna-Pee Dee Belemnite (VPDB) |
| $\delta^{18}\text{O}_{\text{sw}}$ | Stable oxygen isotopic composition of seawater |
| $\Delta\delta^{18}\text{O}$ | Residual Stable oxygen isotopic composition, also referred to as $\delta^{18}\text{O}_{\text{sw}}$ |
| ENSO | El Niño/Southern Oscillation |
| GC | Guyana Current |
| ITCZ | Intertropical Convergence Zone |
| ka | Thousand years before present |
| NAO | North Atlantic Oscillation |
| NBC | North Brazilian Current |
| NTA | North Tropical Atlantic |
| QBO | Quasi-Biennial Oscillation |
| SEM | Scanning Electron Microscopy |
| Sr/Ca | Strontium (Sr) to Calcium (Ca) ratio of caragonitic coral skeleton |
| SSS | Sea Surface Salinity |
| SST | Sea Surface Temperature |
| TAV | Tropical Atlantic Variability |
| VPDB | Vienna-Pee Dee Belemnite |
| VSMOW | Vienna Standard Ocean Mean Water |
| XRD | X-Ray Diffraction |
| yr | Year(s) |

1. Introduction

Severe changes in climate have been observed in recent decades, including extreme droughts; heat waves; extreme winters; heavy precipitations; and the increasing intensity of devastating tropical cyclones. Such extreme climate conditions have had a large impact on societies and economies, which emphasise the importance of the climate sciences for better understanding the underlying mechanisms and predicting such extreme events. Recent discussions attributed current climate change to the influence of human activities on climate, mainly through increasing greenhouse gas concentrations in the atmosphere due to the burning of fossil fuels. Such an influence from humans on climate is also referred to as anthropogenic forcing. In a recent report, the Working Group I of the Intergovernmental Panel on Climate Change (IPCC) assessed the physical aspects of the climate system and climate change that is of relevance for policymakers (Solomon et al., 2007). It was found that, although climate system is characterised by its own natural variability, recent warming of global surface temperature is indeed induced by anthropogenic forcing. For the prediction of future climate, the IPCC uses a compilation of climate models to simulate the effects of anthropogenic emission of carbon dioxide CO₂ into the atmosphere. Climate models used for such predictions are essentially based on and validated by observational data available for the past few decades. However, these records are too short to fully investigate low-frequency climate variability and to understand the forcing mechanisms involved with sufficient accuracy. For example, instrumental records of environmental parameters are sparse and become spatio-temporally incomplete before 1950 thus, limiting our understanding of Earth's climate system prior to the instrumental data period. For this purpose, paleoclimatology provides records of past climate conditions in order to expand our understanding of the climate variability in time and space beyond this short and sparse instrumental data period.

Paleoclimatology uses a variety of climate archives to reconstruct past climate change. For example, terrestrial archives such as tree rings, ice cores and stalagmites provide reconstructions of past precipitation and air temperature, while marine archives such as sediments cores and corals provide records of past sea surface temperature (SST) and hydrology. Warm water corals offer a unique opportunity to investigate past changes of both SST and hydrology recorded in their annually-banded skeleton. Therefore, the present study takes advantage of warm water corals to study naturally occurring climate variability during period of reduced anthropogenic forcing with highly-resolved temporal resolution (i.e., subseasonal resolution).

1.1 The potential of the Caribbean for Holocene climate reconstructions

The Holocene is a geological period which began approximately 12,000 years ago and continues to the present. The Holocene and especially the mid- to late Holocene or the last 6,000 years are of particular interest for paleoclimatology and the understanding of rapid climate changes because the abundant and well-detailed proxy reconstructions from diverse range of locations have provided relevant insights into the past climate variability on millennial time scales, as well as

shorter time scales such as centennial and decadal (cf reviews by Mayewski et al., 2004; Wanner et al., 2008). Although external forcing (i.e., orbital forcing) did not drastically change with respect to glacial/interglacial cycles, the Earth's climate system over the last 6,000 years has experienced significant short-term changes in climate (Hodell et al., 1991; deMenocal et al., 2000b; Haug et al., 2001; Hodell et al., 2001). These changes in climate imply that forcing of external (i.e., solar variability) or internal (i.e., change of the thermohaline circulation and reorganisation of atmospheric circulation, among others) nature are potential mechanisms responsible for rapid changes of climate observed in the high and low latitudes over the last 6,000 years.

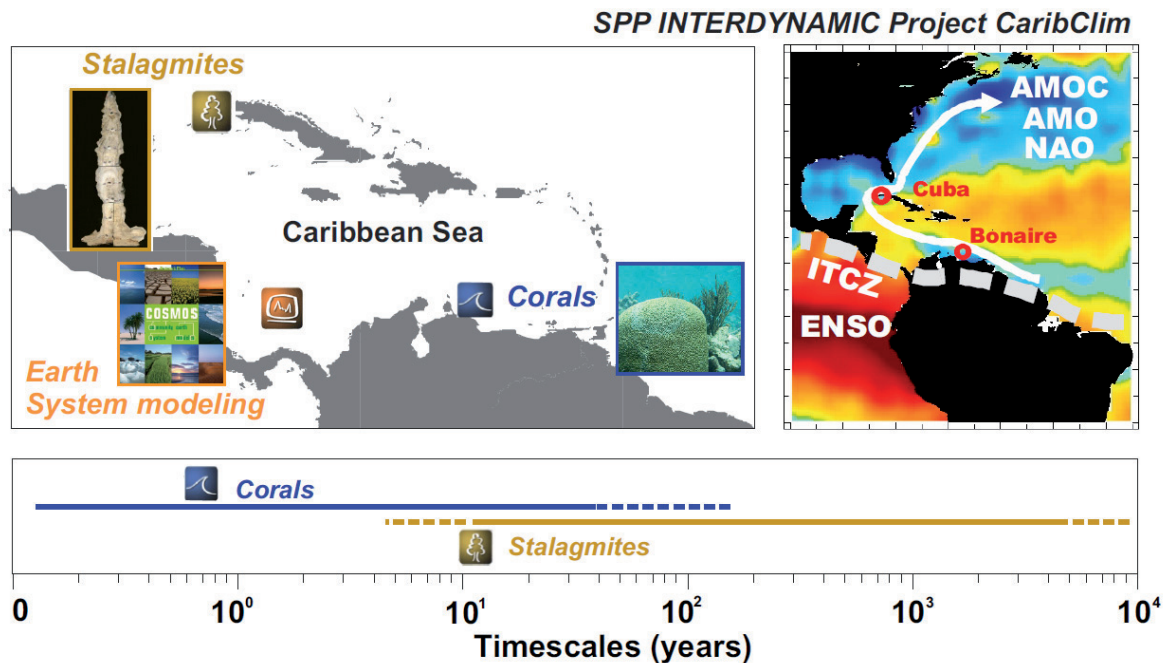


Figure 1.1: INTERDYNAMIC Project CaribClim identifies climate variability in the Caribbean region on a wide range of time scales during the Holocene by using stalagmite records from Cuba and coral records from Bonaire. While Bonaire coral records allow for assessing subseasonal to interdecadal scales variability of the Southern Caribbean Sea surface, stalagmite records allow for investigating interdecadal to millennial scale variability in the Northern Caribbean precipitations. On this broad range of time scales, Caribbean climate is linked to the mean latitudinal position of the Intertropical Convergence Zone (ITCZ); the Pacific El Niño/Southern Oscillation (ENSO); the North Atlantic Oscillation (NAO); the Atlantic Multidecadal Oscillation (AMO); and the Atlantic Meridional Overturning Circulation (AMOC).

In the tropics, the Caribbean Sea is located between the Atlantic and Pacific Oceans and offers a very promising study site for investigating the role of both oceanic and atmospheric circulation in modulating regional climate. Paleoclimate reconstructions of the tropical Atlantic inferred from sediment cores and speleothems have provided evidence for variable hydrological conditions over the last few millennia (e.g., Curtis et al., 1996; deMenocal et al., 2000a; Haug et al., 2003; Lachniet et al., 2004; Cruz et al., 2009). On orbital time scales, southern Caribbean rainfall changes are linked to the mean position of the Intertropical Convergence Zone (ITCZ) (Haug et al., 2001), which is controlled by a meridional SST gradient in the equatorial sector. Moreover, ocean circulation in the Caribbean is linked to heat transport from low- to high-latitude through the western boundary current, namely the Gulf Stream (Lund et al., 2006), which further controls the position and strength of the zonal band of maximum rainfall (Zhang and Delworth, 2005). On shorter time

scales, such as interannual to multidecadal, the dynamic of the ITCZ is influenced by natural modes of ocean/atmosphere variability of specific periodicity, such as the El Niño/Southern Oscillation (ENSO); the North Atlantic Oscillation (NAO); and the Atlantic Multidecadal Oscillation (AMO), emanating from tropical and subtropical oceans (see in depth review by Marshall et al., 2001a; Hurrell et al., 2006). The competing influence of these modes of climate variability on the tropical Atlantic climate is called the Tropical Atlantic Variability (TAV) (Hurrell et al., 2006). Moreover, the Caribbean offers exceptional high-resolution marine and terrestrial climate archives such as corals and stalagmites, which provide the unique opportunity to investigate pattern of Caribbean climate variability during the Holocene on a broad range of time scales ranging from seasonal to millennial.

For this purpose, the present study was conducted within the DFG Priority Programme 1266 INTERDYNAMIC (Integrated Analysis of Interglacial Climate Dynamics) project CaribClim which aims at identifying forcing mechanisms of seasonality and interannual to centennial climate variability in the Caribbean region during the Holocene. CaribClim combines fossil coral records from Bonaire (MARUM, University of Bremen); stalagmites from Cuba (Heidelberger Akademie der Wissenschaften, University of Heidelberg); and climate model simulations (Alfred Wegener Institute for Polar and Marine Research, Bremerhaven) to gather insights about the natural range of climate variability on these time scales. Ultimately, this combination of stalagmite and coral records with numerical simulations will unravel the role of the ENSO, AMO, NAO, solar activity, and Atlantic thermohaline circulation (THC) in the reconstructed climate changes (Figure 1.1). The scientific questions addressed in this project are:

- **What is the natural range of seasonality and interannual to centennial Caribbean climate variability during the Holocene?**
- **Did the amplitudes and periodicities of interannual to centennial Caribbean climate variability change during the Holocene?**
- **Did the strength of the seasonal cycle of hydrologic balance (and temperature) change during the Holocene in the Caribbean?**
- **Which forcing mechanisms control the reconstructed climate variations (ENSO, AMO, TAV, NAO, solar, THC)?**

Since this well-designed interdisciplinary project involves different institutions working on three different state-of-the-art climate sciences, the present PhD work uses corals from the southern Caribbean Sea as high-resolution marine archives, and addresses the scientific questions displayed above with special focus on time scales ranging from seasonal to multidecadal.

1.2 State-of-the-art, coral-based paleoclimatology

Tropical coral reefs are complex ecosystems that have existed in tropical and subtropical Oceans for millions of years to form prominent geological structures. Their distribution is restricted to well-defined shallow warm water regions. During their growth, massive corals incorporate a large array of geochemical elements into their aragonitic skeleton and form bands of varying density that

have been proven to follow the annual cycles of key environmental parameters (Knutson et al., 1972). When 5-10 mm slices are cut along the vertical growth axis, these annual density band couplets are apparent on X-radiographs, which make these massive coral skeletons significant archives of past tropical climates and environments. In comparison with other climate archives (i.e., tree rings, ice cores, speleothems, varved sediment) massive tropical corals have several characteristics that make them unique marine archives (e.g., Felis and Pätzold, 2003; Lough, 2010):

- Annual density bands enable absolute chronological control
- Rapid and continuous linear growth (~1cm/yr) allow for annual and subseasonal sampling resolution
- Growth of several meter high colonies provide coral records of several decades up to centuries
- The large range of geochemical tracers incorporated into the calcium carbonate skeleton reflects environmental conditions of the ambient seawater in which the coral grew
- Key oceanographic parameters such as sea surface temperature (SST) and salinity (SSS) can be quantitatively assessed from the coral skeleton
- Calcium carbonate from the coral skeleton is datable with either radiocarbon ^{14}C or U-series methods
- Good preservation of the coral skeleton after death allows for high-resolution paleoclimate reconstruction of well-dated subseasonally resolved time-windows of the distant past

The state-of-the art coral-based paleoclimatology benefits of the above criteria in order to reconstruct critical oceanographic parameters such as SST and SSS at high temporal resolution. The generation of long subannually resolved climate reconstruction has significantly improved our understanding of the variability of the tropical and subtropical climate system (e.g., Cole et al., 1993; Gagan et al., 1998; Felis et al., 2000; Tudhope et al., 2001; Cobb et al., 2003; Felis et al., 2004; Linsley et al., 2006; Abram et al., 2008; Hetzinger et al., 2008; Kilbourne et al., 2008; Abram et al., 2009). Extensive coral-based paleoclimatology studies have been carried on long-lived massive corals from the Pacific and Indian Oceans because of the importance of the ENSO systems and Indian Ocean Dipole and the abundance of the genus *Porites* sp.. However, the generation of coral-based climate records from the tropical Atlantic have been hindered by questioning the validity of geochemical proxies measured in the tropical Atlantic corals due to their more complex skeletal architecture (Veron, 2000). So far, decade-long and continuous subseasonally resolved coral records in the Caribbean and western Atlantic are underrepresented, especially coral records covering periods aged of 2,000 years or more (Figure 1.2). Exceptions include the work by Winter et al., (2003) (data not published) which showed orbital-control on the Caribbean seasonality recorded in a unique 4-year long coral record from the northern Caribbean, which grew during the Eemian (~126,000 years ago).

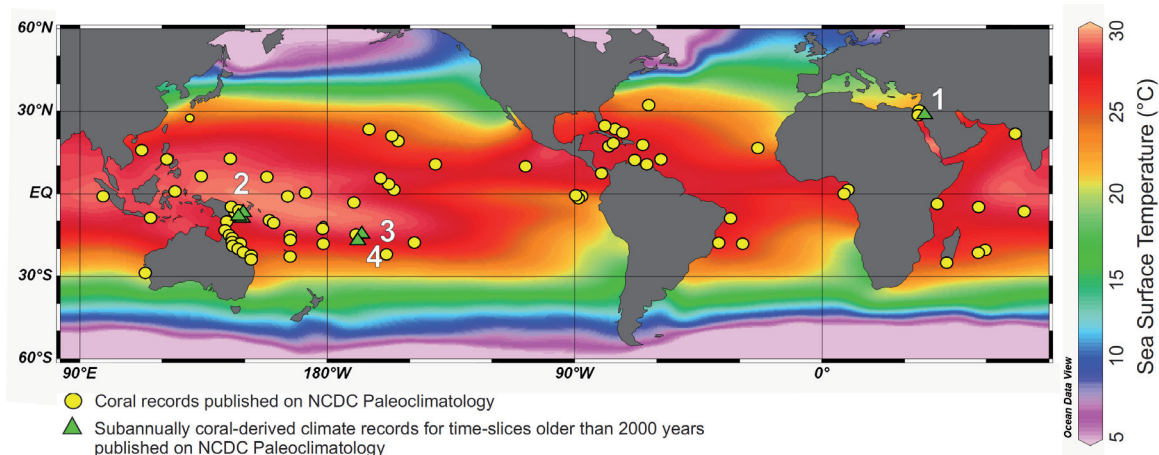


Figure 1.2: Global annual-mean sea surface temperature (SST) from World Ocean Atlas 05 (Locarnini et al., 2006). Yellow circles represent locations of published coral-derived climate records from NCDC Paleoclimatology website (in November 2010) and green triangles indicate locations of published subannual coral-derived climate records on NCDC Paleoclimatology website that extend beyond 2000 years BP: 1) Felis et al., (2004); 2) Tudhope et al., (2001); 3) Corrège et al., (2004); 4) Kilbourne et al., (2004).

Given that subseasonally coral-derived climate records have primarily focused on using the genus *Porites* sp. from the Indo-Pacific region, similar coral-based climate reconstruction from the western Atlantic are, however, underrepresented. Therefore, it is of crucial importance to find suitable corals from the Caribbean and western Atlantic in order to assess natural range of seasonal to interdecadal climate variability in this sector. Recent studies on *Diploria strigosa* brain coral from the Caribbean have demonstrated the potential of this Atlantic coral for capturing the seasonal and interannual climate variability in its skeleton (Hetzinger et al., 2006; Hetzinger et al., 2010). Geochemical climate proxies have been successfully calibrated against SST (Hetzinger et al., 2006) and have proven capable of recording the multidecadal variability of the tropical Atlantic climate and hurricane activity (Hetzinger et al., 2008; Hetzinger et al., 2010). Consequently, *D. strigosa* from the Caribbean is a potential recorder of past temperature and hydrology variability that can expand our understanding of the natural range of western tropical Atlantic climate variability.

1.3 Coral Sr/Ca, a temperature proxy

Sea surface temperature (SST) is one of the most critical environmental parameters influencing regional and global climate variability, and therefore it is one of the most critical oceanographic parameters for predicting future climate scenarios through numerical simulations. Trace elements (i.e., Sr, Mg, and U) incorporated in coral skeletons are widely used as robust paleothermometers. The ratios of strontium/calcium (Sr/Ca), magnesium/calcium (Mg/Ca), and uranium/calcium (U/Ca) are largely determined by the temperature-dependent distribution coefficient of Sr/Ca, Mg/Ca, and U/Ca between aragonite and sea water. As ambient temperature increases, the Sr/Ca and U/Ca ratios of the coral skeleton decrease while its Mg/Ca ratio increases.

Since the pioneering work by Smith et al., (1979) and Beck et al., (1992), the Sr/Ca ratio of coral skeleton is the most extensively used proxy for reconstructing past SSTs. A large number of successful climate reconstructions using coral Sr/Ca further emphasise that this trace elemental ratio is an excellent temperature proxy (e.g., Beck et al., 1992; McCulloch et al., 1994; Alibert and McCulloch, 1997; Gagan et al., 1998; Hughen et al., 1999; Swart et al., 2002; Winter et al., 2003; Cohen and Hart, 2004; Corrège et al., 2004; Felis et al., 2004; Pfeiffer et al., 2006; Goodkin et al., 2008b; Abram et al., 2009; Asami et al., 2009; Felis et al., 2009; Felis et al., 2010; Hetzinger et al., 2010).

Table 1.1: Table of published Sr/Ca-SST relationships for near-monthly sampling resolution. $Sr/Ca = m \cdot SST + b$, where m is the slope and b the intercept.

| Author | Year | Slope (mmol/mol. $^{\circ}C^{-1}$) | Intercept (mmol/mol) | Specie | Source of SST | Location |
|------------------------------------|------|--|-------------------------|-----------------------------|------------------|---|
| Gagan | 1998 | -0.066 | 10.78 | <i>Porites lutea</i> | Local SST | Pacific, Australia |
| | | -0.064 | 10.73 | <i>Porites lutea</i> | Local SST | Pacific, Australia |
| | | -0.0616 | 10.68 | <i>Porites lutea</i> | Local SST | Pacific, Australia |
| Smith Marshall and McCulloch | 1979 | -0.071 | 10.94 | <i>Multiple Porites sp.</i> | | Pacific, Atlantic |
| | 2002 | -0.0575 | 10.4 | <i>Porites lutea</i> | Local SST | Pacific, Australia |
| Alibert and McCulloch | 1997 | -0.0579 | 10.38 | <i>Multiple Porites sp.</i> | Local SST | Pacific, Australia |
| Linsley | 2004 | -0.053 | 10.65 | <i>Porites lutea</i> | IGOSS | Pacific, Fiji |
| Felis | 2009 | -0.051 | 10.333 | <i>Porites sp.</i> | Local SST | Pacific NW, Ogasawara |
| Felis | 2004 | -0.0597 | 10.781 | <i>Porites sp.</i> | Local SST | Red Sea, Aqaba Indian Ocean, Madagascar |
| Zinke | 2004 | -0.05 | 10.323 | <i>Porites lobata</i> | GISST | |
| Quinn and Sampson | 2002 | -0.052 | 10.073 | <i>Porites lutea</i> | Local SST | Pacific, N. Caledonia |
| | | -0.061 | 10.383 | <i>Porites lutea</i> | GISST | Pacific, N. Caledonia |
| Corrège | 2000 | -0.0657 | 10.73 | <i>Porites sp.</i> | ERSST | Pacific, N. Caledonia |
| Corrège | 2006 | -0.0576 | 10.407 | <i>Porites sp.</i> | Local SST | Pacific, N. Caledonia |
| Shen | 1996 | -0.0514 | 10.286 | <i>Porites sp.</i> | Local SST | Pacific, Taiwan |
| Mean for all corals | | -0.059 | 10.525 | | | |

As ambient temperature increases, corals incorporate less Sr into their calcium carbonate and thus, record the temperature of the ambient sea water as they grow (Smith et al., 1979; Beck et al., 1992). Recent analytical improvements in the application of Sr/Ca paleothermometry came with the development of a new high-precision method of Sr/Ca determination, via Inductively Coupled Plasma Atomic Emission Spectrophotometer that compares very regularly coral samples values to a reference solution (Schrag, 1999).

During the formation of the aragonitic coral skeleton, both Sr and Ca are incorporated into the skeletal structures. Sr^{2+} mainly substitutes to Ca^{2+} in crystal lattice (Kinsman and Holland, 1969). Since the chemistry of Sr^{2+} is very similar to that of Ca^{2+} , their behaviour is similar. The Sr/Ca ratio in coral skeleton is believed to be predominantly controlled by two factors, the Sr/Ca activity ratio of seawater and the Sr/Ca distribution coefficient (DSr) between aragonite and sea water (Smith et al., 1979). Therefore, when Sr is taken from a well defined solution, the coral Sr/Ca concentration can be predicted by its distribution coefficient:

$$DSr = (Sr/Ca)_{coral} / (Sr/Ca)_{seawater}$$

While Sr and Ca are very conservative elements in seawater (5.1×10^6 yr for Sr and 1.1×10^6 yr for Ca) (Broecker and Peng, 1982), the Sr/Ca ratio of seawater is influenced by weathering of exposed aragonite on the continental shelves during low-sea level stand (Stoll and Schrag, 1998). Moreover, small changes in coral skeleton Sr/Ca concentration have been observed due to coral symbionts, biological activity, as well as other local effects (de Villiers et al., 1994; de Villiers et al., 1995; Shen et al., 1996; de Villiers, 1999; Cohen et al., 2002).

Table 1.2: Table of published Sr/Ca-SST relationships for corals other than *Porites* sp.. $\text{Sr/Ca} = m \cdot \text{SST} + b$, where m is the slope and b the intercept.

| Author | Year | Slope (mmol/mol. $^{\circ}\text{C}^{-1}$) | Intercept (mmol/mol) | Specie | Source of SST | Location |
|-------------------------------------|------|---|-------------------------|----------------------------------|------------------|----------------------|
| Indo-Pacific corals | | | | | | |
| Smith | 1979 | -0.071 | 11.01 | <i>Pocillopora damicornis</i> | Local SST | Pacific, Hawaii |
| | | -0.089 | 11.64 | <i>Montipora verrucosa</i> | Local SST | Pacific, Hawaii |
| De Villiers | 1994 | -0.0763 | 11.004 | <i>Pocillopora eydouxi</i> | Local SST | Pacific, Hawaii |
| | | -0.0675 | 10.646 | <i>Pavona clavus</i> | Local SST | Pacific, Galapagos |
| Corrège | 2004 | -0.06 | 10.57 | <i>Diploria heliopora</i> | Local SST | Pacific, Indonesia |
| Yu | 2004 | -0.0305 | 9.6 | <i>Goniopora</i> sp. | ? | South China Sea |
| Atlantic corals | | | | | | |
| Cardinal | 2001 | -0.045 | 10.03 | <i>Diploria labyrinthiformis</i> | COADS | Atlantic, Bermuda |
| Hetzinger | 2006 | -0.041 | 9.986 | <i>Diploria strigosa</i> | SODA SST | Atlantic, Guadeloupe |
| Smith | 2006 | -0.0324 | 10.054 | <i>Montastraea faveolata</i> | Local SST | Atlantic, Florida |
| | | -0.0321 | 10.083 | <i>Montastraea faveolata</i> | Local SST | Atlantic, Florida |
| Swart | 2002 | -0.0377 | 9.994 | <i>Montastraea annularis</i> | Local SST | Atlantic, Florida |
| Goodkin | 2005 | -0.0358 | 10.1 | <i>Diploria labyrinthiformis</i> | Local SST | Atlantic, Bermuda |
| Goodkin | 2007 | -0.0376 | 10.1 | <i>Diploria labyrinthiformis</i> | Local SST | Atlantic, Bermuda |
| | | -0.0436 | 10.3 | <i>Diploria labyrinthiformis</i> | Local SST | Atlantic, Bermuda |
| | | -0.0429 | 10.3 | <i>Diploria labyrinthiformis</i> | Local SST | Atlantic, Bermuda |
| Maupin | 2008 | -0.039 | 10.008 | <i>Siderastrea siderea</i> | Local SST | Atlantic, Florida |
| Mean for Indo-Pacific corals | | -0.066 | 10.745 | | | |
| Mean for Atlantic corals | | -0.039 | 10.096 | | | |

Despite the promise of coral Sr/Ca paleothermometry, there are several outstanding concerns that have hindered the acceptance and validity of coral Sr/Ca as a robust paleothermometer: 1) each modern coral calibrated to instrumental SST shows a different coral Sr/Ca-SST relationship in both slope and intercept (e.g., Table 1.1 and 1.2); and 2) coral-based SST reconstructions in the tropical ocean for the Last Glacial Maximum (LGM) have shown SST conditions 2 to 4 times cooler than given by other marine paleoproxies (Beck et al., 1992; Guilderson et al., 1994), both implying that the Sr/Ca ratio in coral skeleton is not a simple a thermodynamic relationship (Marshall and McCulloch, 2002; Lough, 2004)

These all demonstrate that the coral Sr/Ca ratio is critical in its application as an absolute proxy of the past SST and therefore, judicious strategies should be used to extract robust estimations of the coral Sr/Ca-derived SST variability. One of the major aspects of this study is to better understand the incorporation of Sr into the coral skeleton of *Diploria strigosa* brain coral from

Bonaire in order to robustly assess past changes of SST recorded in skeletal Sr/Ca ratio of fossil corals.

1.4 Coral $\delta^{18}\text{O}$, a combined temperature and salinity proxy

The $\delta^{18}\text{O}$ of coral skeleton is influenced by both temperature and oxygen isotopic composition of ambient seawater ($\delta^{18}\text{O}_{\text{sw}}$). To first approximate the $\delta^{18}\text{O}_{\text{sw}}$ is linearly related to the sea surface salinity (SSS) (Urey, 1947). $\delta^{18}\text{O}_{\text{sw}}$ is relevant to paleoclimatology because it is closely related to the balance between precipitation and evaporation, and therefore its reconstruction could yield important information about past changes in hydrological cycle. However, because the $\delta^{18}\text{O}$ composition of coral skeletons is a function of both SST and $\delta^{18}\text{O}_{\text{sw}}$ (Weber and Woodhead, 1972), it is generally difficult to separate the effects of SST and $\delta^{18}\text{O}_{\text{sw}}$ by using coral $\delta^{18}\text{O}$ only. Therefore, in conjunction with the coral Sr/Ca-based SST reconstruction, coral $\delta^{18}\text{O}$ can be used to reconstruct $\delta^{18}\text{O}_{\text{sw}}$, a critical oceanographic parameter. Several studies have used paired coral Sr/Ca and $\delta^{18}\text{O}$ in order to assess past changes in the hydrological cycle recorded in the coral skeletons (McCulloch et al., 1994; Gagan et al., 1998; Ren et al., 2003; Zinke et al., 2004; Sun et al., 2005; Linsley et al., 2006; Pfeiffer et al., 2006; Cahyarini et al., 2008; Deng et al., 2009; Felis et al., 2009; Hetzinger et al., 2010).

Basically, $\delta^{18}\text{O}$ is a measure of the ratio between heavy and light oxygen isotopes ^{18}O and ^{16}O , respectively, in reference to a standard. This oxygen isotope ratio is reported in part per thousand or "per mil" (‰) and is calculated as follows:

$$\delta^{18}\text{O} = (((^{18}\text{O}/^{16}\text{O})_{\text{sample}} / (^{18}\text{O}/^{16}\text{O})_{\text{standard}}) - 1) * 1000$$

where the standard has a known isotopic composition such as Vienna Standard Mean Ocean Water (VSMOW). Reviews of this relationship can be found in Swart (1983), Swart et al., (1996a), and Leder et al., (1996).

Pioneer studies by McCulloch et al., (1994) and Gagan et al., (1998; 2000) attempted to quantitatively separate the effects of SST from those of $\delta^{18}\text{O}_{\text{sw}}$ on skeletal $\delta^{18}\text{O}$, by using paired coral $\delta^{18}\text{O}$ and Sr/Ca analysis on the same coral samples. The authors estimated the relationship of coral $\delta^{18}\text{O}$ and SST, as well as Sr/Ca and SST, using univariate linear regression equations. These equations are then used to convert both proxies to temperature units, in order to subtract the temperature component from coral $\delta^{18}\text{O}$ as described below:

$$\delta^{18}\text{O}_{\text{coral}} = \delta^{18}\text{O}_{\text{SST}} + \delta^{18}\text{O}_{\text{sw}}$$

where

$$\delta^{18}\text{O}_{\text{SST}} = \gamma_1 / \beta_1 (\text{Sr/Ca}_{\text{coral}})$$

therefore,

$$\delta^{18}\text{O}_{\text{sw}} = \delta^{18}\text{O}_{\text{coral}} - \gamma_1 / \beta_1 (\text{Sr/Ca}_{\text{coral}})$$

where $\delta^{18}\text{O}_{\text{SST}}$ and $\delta^{18}\text{O}_{\text{sw}}$ are the temperature and seawater oxygen isotopic component of the measured $\delta^{18}\text{O}_{\text{coral}}$, respectively. Here, γ_1 and β_1 are the $\delta^{18}\text{O}$ -SST and Sr/Ca-SST regression slopes, respectively.

As the absolute values of coral $\delta^{18}\text{O}$ and Sr/Ca are often delicate to interpret (Linsley et al., 1999; Felis et al., 2003; Suzuki et al., 2005), Ren et al., (2003) proposed to omit the intercept values of coral $\delta^{18}\text{O}$ -SST and Sr/Ca-SST regressions by calculating the first derivatives of the two proxies. Later on, Cahyarini et al., (2008) proposed to remove the mean value from its variable in order to focus on the first order variability as described below:

$$\delta^{18}\text{O}_{\text{sw norm}} = (\delta^{18}\text{O}_{\text{coral}} - \delta^{18}\text{O}_{\text{coral mean}}) - \gamma_1/\beta_1 (\text{Sr/Ca}_{\text{coral}} - \text{Sr/Ca}_{\text{coral mean}})$$

It is well known that carbonate organisms do not precipitate their calcium carbonate in isotopic equilibrium with ambient seawater (Weber and Woodhead, 1970; Swart, 1983; McConnaughey, 1989; Swart et al., 1996a). However, the degree of this disequilibrium is constant within a coral colony (McConnaughey, 1989). These geochemical disequilibria or the so-called "vital effects" are not necessarily constant within a coral genus (Weber and Woodhead, 1970; Erez, 1978; Felis et al., 2003; Suzuki et al., 2005), within an individual polyp (Land et al., 1975; Pätzold, 1992), nor within the same skeletal element (Allison and Finch, 2004; Juillet-Leclerc et al., 2009). There are indications that these disequilibria are influenced by numerous biological mechanisms during calcification of the coral skeleton (Weber and Woodhead, 1970; Erez, 1978; Juillet-Leclerc and Reynaud, 2010). Felis et al., (2003) showed that mean coral $\delta^{18}\text{O}_{\text{sw}}$ is strongly dependent on the mean annual extension rates mainly due to the extension-rate related kinetic isotope disequilibrium effects (McConnaughey, 1989). However, it has been suggested that this disequilibrium is reduced in coral skeleton growing at a rate greater than 0.6 cm/year (Felis et al., 2003) (Figure 1.3). All of these emphasise, once again, that judicious strategies should be considered to robustly assess past variations of SSS derived from paired coral $\delta^{18}\text{O}$ and Sr/Ca measurements.

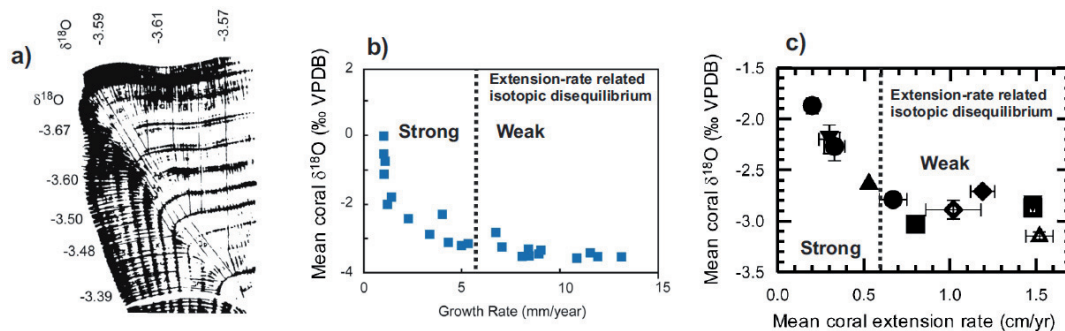


Figure 1.3: Oxygen isotopic composition and coral growth. a) X-radiography positive print and oxygen isotopic composition at the surface of *Pavana clavus* coral head from Punta Pitt, San Cristobal Island (Galápagos). b) Relationship between skeletal $\delta^{18}\text{O}$ and skeletal extension (growth) rate for this coral colony. a) and b) were redrawn and slightly modified from McConnaughey (1989) after Hetzinger (2007) c) Mean extension rate versus mean coral $\delta^{18}\text{O}$ of porites coral colonies from the Gulf of Aqaba, Red Sea (modified from Felis et al., (2003)). Dashed lines indicate minimum growth rate value (0.6cm/year) where extension-rate related kinetic isotopic disequilibria have reduced effect on mean coral $\delta^{18}\text{O}$ (Felis et al., 2003).

The oxygen isotopic composition of sea water ($\delta^{18}\text{O}_{\text{sw}}$) and SSS co-vary in the surface ocean waters on a global scale (Schmidt et al., 1999 "Global Seawater Oxygen-18 Database - v1.20" <http://data.giss.nasa.gov/o18/data/>). The positive relationship between the $\delta^{18}\text{O}_{\text{sw}}$ and SSS is a critical relationship in paleoclimatology, because in combination with thermodynamic properties of the ambient sea water it provides the chance to estimate the density of sea water, an important oceanographic parameters involved in the meridional overturning circulation in the North Atlantic. Both parameters are largely related to the hydrological cycle, with higher SSS and $\delta^{18}\text{O}_{\text{sw}}$ values observed in regions where evaporation exceeds precipitation, whereas lower values are characteristic of regions dominated by precipitation and river runoff (Figure 1.4). Furthermore, both parameters of the surface waters are influenced by oceanic advection and diffusion processes. Since the relationship between SSS and $\delta^{18}\text{O}_{\text{sw}}$ has been extensively studied in past few decades (Craig and Gordon, 1965; Schmidt, 1999; Delaygue et al., 2000), a unique study performed on Caribbean seawater (Watanabe et al., 2001) yielded to the conclusion that seasonal variation of $\delta^{18}\text{O}_{\text{sw}}$ is mostly governed by SSS changes. The $\delta^{18}\text{O}_{\text{sw}}$ -SSS relationship from these data is:

$$\delta^{18}\text{O}_{\text{sw}} = 0.204 (\pm 0.03) \times \text{SSS} - 6.54 (\pm 0.68) \quad (r = 0.93, N = 20)$$

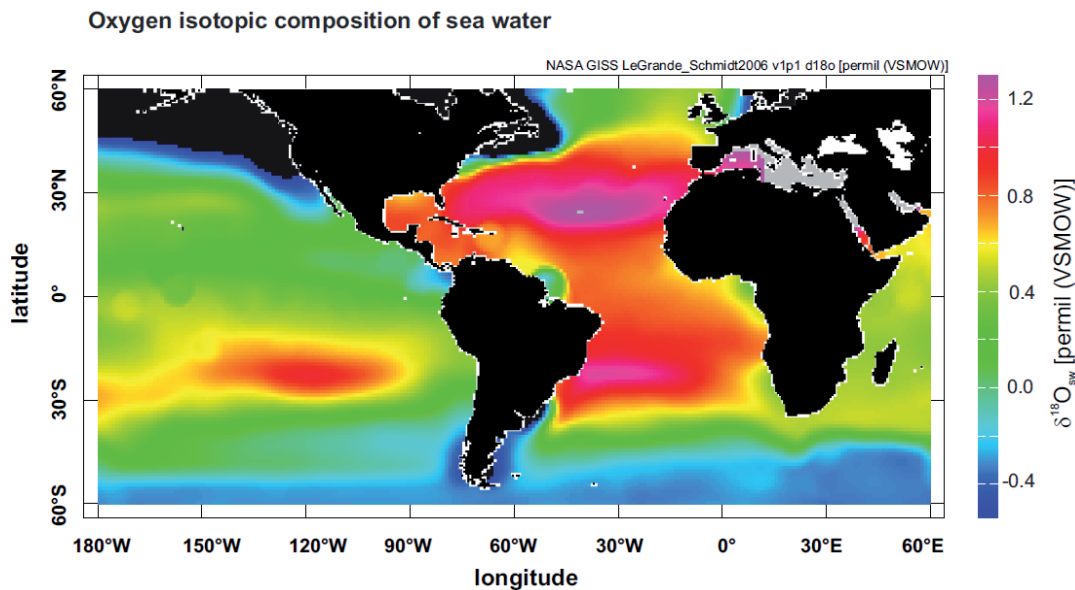


Figure 1.4: Oxygen isotopic composition of sea surface waters ($\delta^{18}\text{O}_{\text{sw}}$) from NASA GISS LeGrande_Schmidt2006 v1p1 d18o (LeGrande and Schmidt, 2006). All surface delta values are reported with respect to V-SMOW. Note that the Amazon River discharge is a prominent source of more negative $\delta^{18}\text{O}_{\text{sw}}$ in the western tropical Atlantic, whereas the subtropical gyre shows more positive $\delta^{18}\text{O}_{\text{sw}}$ values due to excessive evaporation.

Consequently, reconstruction of past changes in Caribbean SSS on time scales ranging from seasonal to multidecadal can be achieved from the reconstructed $\delta^{18}\text{O}_{\text{sw}}$ inferred from the paired coral Sr/Ca and $\delta^{18}\text{O}$ measurements. Such an approach performed on tropical Atlantic corals will provide unique insights on the variations of hydrological cycle in the southern Caribbean Sea on these time scales.

1.5 Coastal deposits on Bonaire, the “Great climate archive”



Figure 1.5: Coastal deposits on Bonaire (southern Caribbean Sea) can reach up to 10 meters above sea level and consist of coral debris with size ranging from a decimetre to a meter (Photo: Jurgen Pätzold).

Bonaire is arguably the most pristine coral reef environment in the Caribbean (Source: NOAA-National Oceanic Atmospheric Administration). The living coral reefs of Bonaire were extensively studied in the 1970's (Bak, 1975; Bak, 1977; Focke, 1978) and mapped at a scale of 1:4000 in an Atlas by Van Duyl (1985). The percentage of coral cover is relatively high compared to other Caribbean islands. Therefore, Bonaire reef environment represents one of the healthiest reef ecosystem in the Caribbean region, which attracts many SCUBA divers from around the world for adventures in this so-called "Diver's Paradise". The reef fringes along the west and south coast of Bonaire with only very few interruptions, forming a terrace of between 20 to greater than 50m wide to a drop off at about 8-15m depth.

The coral debris and boulders found on coastal deposits on Bonaire (Figure 1.5) indicate phases of flourishing reef growth in the past thousands years. Dating of these corals debris indicates that Bonaire coral reef growth occurred during the Holocene up until present (Scheffers 2004). The size of corals debris, the distance from the shoreline as well as the elevation above sea-level where these megaclasts are found (Figure 1.5), indicate that Bonaire have been struck by extreme wave-events during the Holocene. However, no consensus exists on the nature of the transport of these megaclasts (i.e., of hurricane and/or tsunami origin) (Scheffers, 2004; Morton et al., 2008; Scheffers et al., 2009; Engel et al., 2010). Although the origin of such impressive coastal deposits is still not clear, the megaclasts on Bonaire (Figure 1.5) provide numerous fossil corals that should be used to assess climate variability of the southern Caribbean Sea, which is documented in their coral skeleton (Figure 1.6).



Figure 1.6: Fossil (dead) *Diploria strigosa* (Dana, 1846) on Bonaire. The surface of a fossil coral shows meandroid growth form with a single skeletal wall (meandering white edge) separating two adjacent corallites. These features are characteristic of *D. strigosa* brain corals (Photo: Thomas Felis).

1.5.1 *Diploria strigosa* (Dana, 1846)

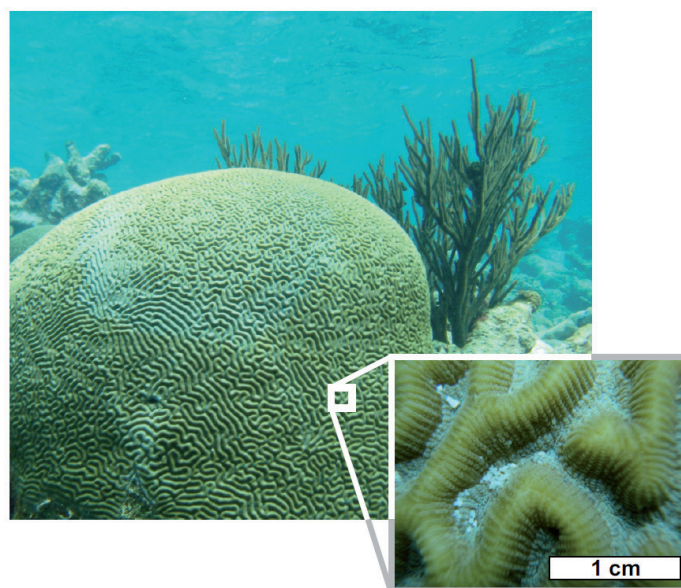


Figure 1.7: Living *Diploria strigosa* brain coral on Bonaire.

Diploria strigosa (Dana, 1846), commonly known as “symmetrical brain coral”, forms smoothed hemispherical dome colonies with a typical smooth and regular colony surface. *D. strigosa* has a meandroid (brain coral) growth form that is characterised by sinuous arrangement of interconnected polyps (Figure 1.7). *D. strigosa* is commonly present in most Caribbean reefs in water depth between 0 and 15 m (Van Duyl, 1985; Human and Deloach, 2008).

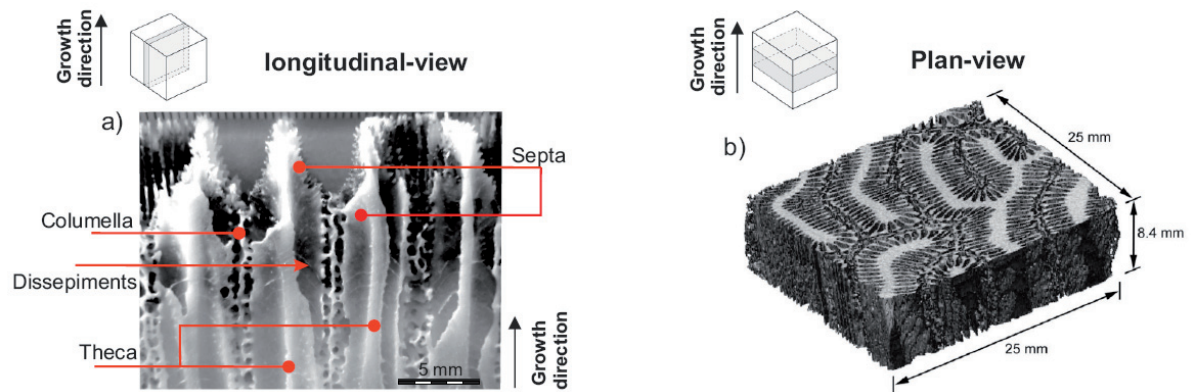


Figure 1.8: Mesoskeletal architecture of *Diploria strigosa* observed on a) a longitudinal view image of a coral slab cut along major growth axis and b) plan-view X-ray computed tomography images of a 25×25×25 mm coral sample (modified from Helmle et al., (2000)). Name of various mesoskeletal elements are given.

Diploria sp. is characterised by three main brain coral specimens, *Diploria strigosa*; *Diploria labyrinthiformis* (Linnaeus, 1758) commonly referred as “grooved” brain coral; and *Diploria clivosa* (Ellis and Solander, 1786) referred as “knobby” brain coral. The architectural organisation of the corallite allows for distinction between species. For instance, *D. labyrinthiformis* has a very distinct ambulacral groove formed by costae of adjacent corallites (e.g., Cohen et al., 2004). The ambulacrum clearly distinguishes *D. labyrinthiformis* from *D. strigosa* and *D. clivosa* which have a relatively similar skeletal architecture. However, *D. clivosa* has a rough irregular colony surface with slightly smaller and irregular valleys (4-8 mm wide) and more septae (Veron, 2000) than *D. strigosa*.

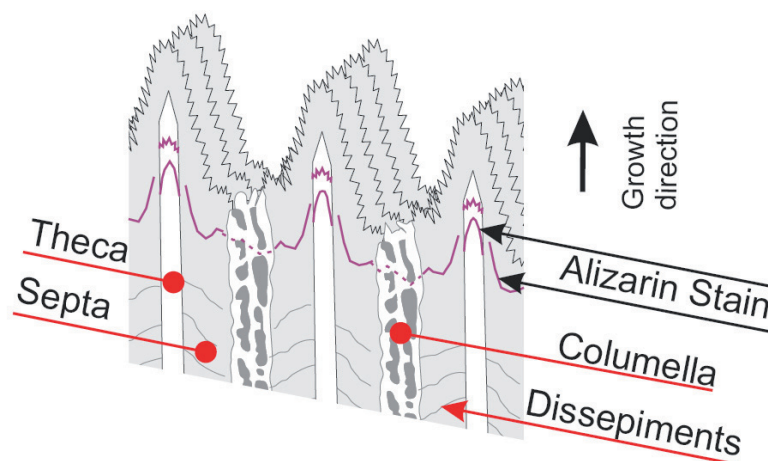


Figure 1.9: Cross-section sketch of *Diploria strigosa* corallite giving names of various skeletal structures. The alizarin stain lines (pink lines) depict the pattern of coral growth and calcification of coral skeleton at the time of staining experiment (modified from Dodge et al., (1984)).

Polyps are often connected and usually convoluted (Figure 1.7), except near the colonies' edge. These meandering continuous corallite valleys are usually 5 to 9 mm wide; regular in appearance; and comprise a continuous spongy structure in the middle called columella. The columella is surrounded by thinner vertical walls called septae that extend towards the corallite wall to form septotheca or theca (Figure 1.8). Adjacent corallites share a common thecal wall and no

exothecal structures are present. As the colony grows, coral tissue is lifted by the polyps which secrete new floors called dissepiments. Rare alizarin experiment on *Diploria strigosa* skeleton revealed that the theca wall has a convoluted growth form (Dodge et al., 1984) and that septal materials precipitated at the same time are calcified on the outer edge of the colony surface (Figure 1.9).

1.5.2 Collection of coral cores and microsampling

Hurricane and/or tsunami deposits found on the coast of Bonaire (Figure 1.5) provide numerous fossil corals of Holocene age that can be used to reconstruct past climate variability. Since fossil coral colonies were transported by wave-energy, the surface of the colony has been eroded, and therefore the shape of the colony was not a criterion for selection in the field. Six fossil *Diploria strigosa* coral colonies found on Bonaire coastal deposits were drilled along the main growth axis, and two additional colonies were drilled from dead *D. strigosa* colonies found in a storm deposit formed by hurricane Ivan in 2004 (Scheffers and Scheffers, 2006). These six fossil and two sub fossil *D. strigosa* colonies were identified in the field with respect to the following criteria:

- Meandering growth form
- Interconnected corallites
- Corallites width comprises between 6 to 9 mm
- Adjacent corallites separated by one exothecal wall

Inland coral-coring was performed using electric-powered core-barrel. The later was flushed with water from the inside in order to flush out the cut debris that would hinder/block the drilling process at the cutting edge. For calibration purposes, a short core was recovered from a living *D. strigosa* coral by Dr. S.R. Scheffers and B. Sommer.

Microsampling of the coral skeleton was performed using a milling machine (Proxxon FF 400) equipped with a micrometer-control table (Proxxon KT 400) which allows 3-dimensional sampling with an accuracy of 50 µm. The micrometer-control table was equipped with a PVC structure designed at MARUM in order to facilitate stabilisation of the corals slabs prerequisite for accurate microsampling of the dense and sinuous skeletal walls of *D. strigosa*.

1.6 Bonaire, regional setting

1.6.1 Geography and Geology

The Caribbean Sea is bounded to the south by South America, to the west by Central America, to the north by Greater Antilles and to the east by Lesser Antilles. In the southern Caribbean Sea, Bonaire (12°10'N, 68°15'W) is located approximately 100 km north of the coast of Venezuela (Figure 1.10). Bonaire island is one of the five islands that form the Netherlands Antilles (Leeward Islands: Bonaire, Curacao; Windward Islands: St Marteen, Saba and St Eustatius).

Bonaire is a crescent-shaped island, orientated NW-SE approximately, 40 km long, by 11 km at its widest point with a surface area of 288 km². Bonaire lies on a conservative plate boundary, where the South America and Caribbean tectonic plates meet and slide one to another. Along with the other ABC Islands (Aruba-Bonaire-Curacao) off Venezuela's north coast, Bonaire has been moving eastward at a slow but steady rate. The ABC Islands are located on the Southern rim of Caribbean plate and are separated by 2000m deep water. Together these form a discontinuous ridge of tertiary submarine volcanoes, uplifted and covered by Plio-Pleistocene reef limestones.

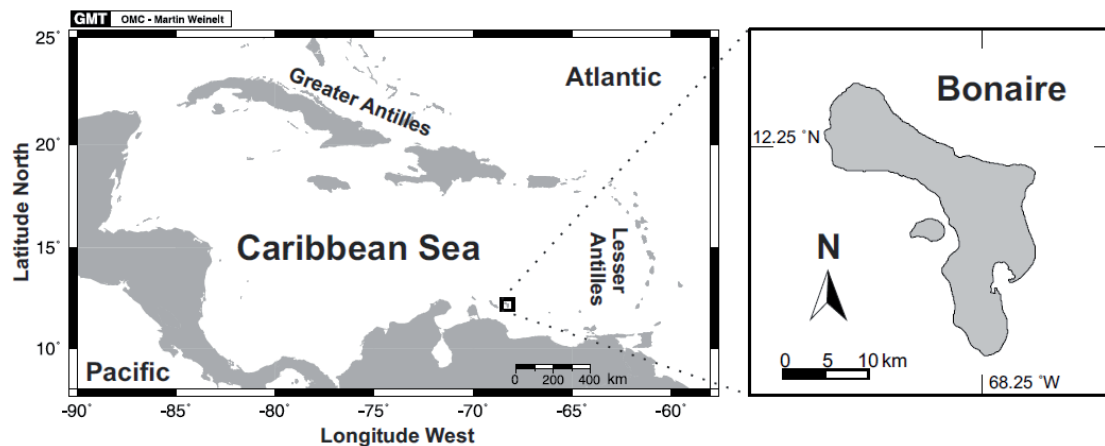


Figure 1.10: Map of the Caribbean Sea showing the location of Bonaire .

The geology of Bonaire is complex with the core of the island consisting of folded and faulted rocks of volcanic origins and silica-rich sediment formed during the Cretaceous (~120 Myr BP). Overlying this are fossil reefs terraces that developed during high sea-level stand during interglacial periods (de Buisonjé, 1974). Due to the slow uplift motion, these Pleistocene reef terraces are now exposed a few meters above sea-level. De Buisonjé (1974) distinguished four uplifted reef-terraces that should correspond according to Kim et al., (1999) to the last interglacial periods characterised by a high sea-level stand.

1.6.2 Oceanographic setting

The Caribbean Sea is a suboceanic basin of the western Atlantic spanning latitudes 9°N-22°N and longitudes 89°W-60°W. Water masses present in this semi-enclosed basin have complex physical characteristics that are linked to the climate conditions in the tropics and subtropics. The early study by Wüst (1964) described the hydrography of the Caribbean Sea and found that the surface water masses have different physical properties (i.e., salinity and temperature) than that of the underlying water masses. The upper water (0-200m depth) in the Caribbean is composed of two water masses (Figure 1.11). The high salinity Subtropical Under Water (SUW) (Wüst, 1964; Gordon, 1967), formed in the subtropical gyre where evaporation exceeds precipitation, sinks at a depth of approximately 100m, below the fresher surface water referred to as Caribbean Surface Water (CSW) (Wüst, 1964).

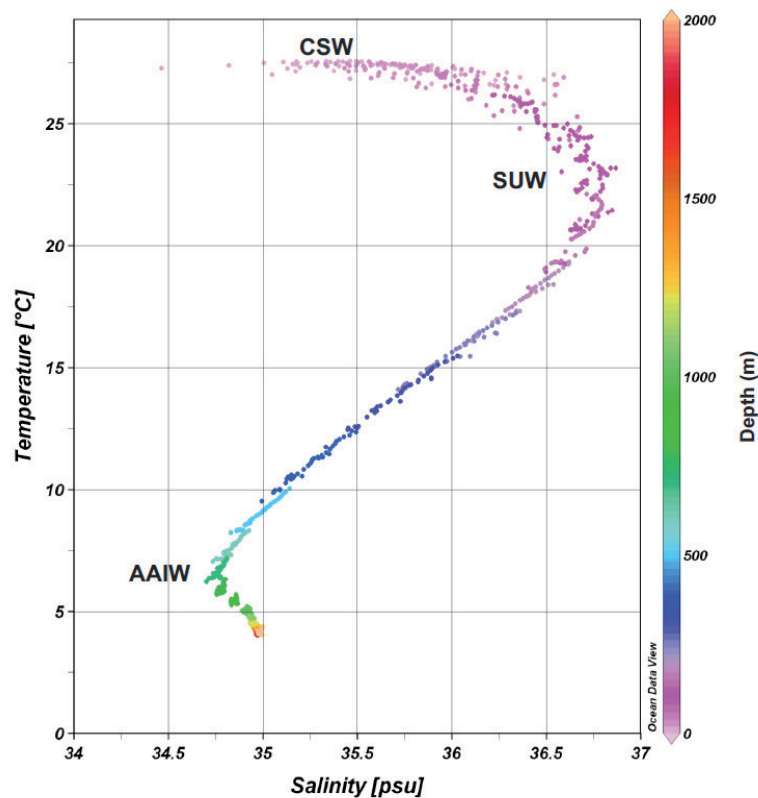


Figure 1.11: Temperature/salinity diagram for the water column (<2000m) of the Caribbean. Water masses constituting the Caribbean water are indicated: Caribbean Surface Water (CSW) (Wüst, 1964), Subtropical Under Water (SUW) (Wüst, 1964), and Antarctic Intermediate Water (AAIW) (Wüst, 1964; Morrison and Nowlin, 1982). Data are from World Ocean Atlas 05 (Antonov et al., 2006).

The CSW is a mixture of fresh water from the Amazon and Orinoco river discharges and the equatorial Atlantic surface water, which enter the Caribbean via the Guyana Current (GC) (Figure 1.12), whereas the SUW enters the Caribbean mainly via the North Equatorial Current (NEC). Merged together, these two water masses are transported by the Caribbean Current (CC), which is the dominant surface flow in the Caribbean bringing warm water northwestward into the Gulf of Mexico via the Loop Current (LC), and the Florida Strait via the Florida Current (FC) to ultimately contributing to the northward flowing western boundary current (Figure 1.12).

The inflow of the Atlantic water masses into the Caribbean is controlled by the strength of the North Atlantic thermohaline circulation and trade winds ultimately linked to the Intertropical Convergence Zone (ITCZ) (Johns et al., 2002). The total flow through the Caribbean ($\sim 28 \text{ Sv}$, $1 \text{ Sv} = 1 \text{ Sverdrup} = 10^6 \text{ m}^3 \text{ s}^{-1}$) displays a seasonal cycle that is stronger in the far southern Caribbean (Johns et al., 2002). A meridional hydrographic section at 66°W revealed that the highest velocities of the Caribbean Sea are found near the southern boundary along the coast of Venezuela and Netherland Antilles (Hernández et al., 2000; Fratantoni, 2001) suggesting that the southern Caribbean Sea is highly sensitive to seasonal changes of Atlantic inflow to the Caribbean. Outflow from the Caribbean shows maximum values in spring and summer, and minimum values in autumn (Schott et al., 1988; Molinari et al., 1990; Larsen, 1992; Johns et al., 2002). From spring to summer, the maximum inflow to the Southern Caribbean Sea appears to result from a

strengthened North Brazilian Current (NBC) and Guyana Current which enters the Caribbean through the southernmost Lesser Antilles Passages (Müller-Karger et al., 1989; Chérubin and Richardson, 2007). The reduction of Atlantic inflow to the Caribbean during the second half of the year is caused by the development of cyclonic circulation that deflects fresher Atlantic water eastward and reduces the strength of the GC (Müller-Karger et al., 1989; Johns et al., 2002).

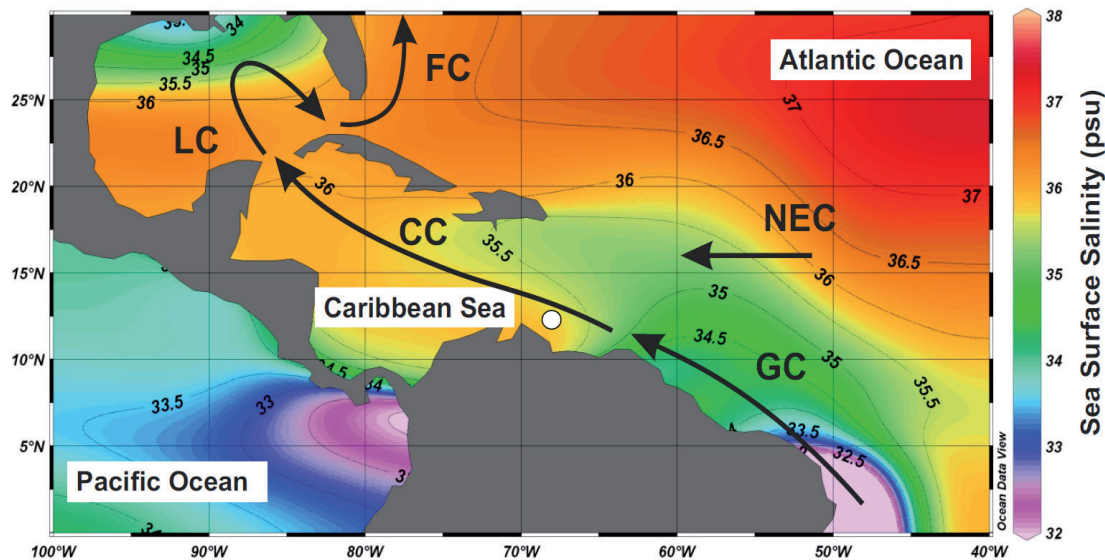


Figure 1.12: Sea surface salinity (SSS) map and modern oceanographic setting of the Caribbean and western Atlantic showing schematically majors surface current systems. White circle indicates the study site (Bonaire). Major surface currents are indicated: Guyana Current (GC), Caribbean Current (CC), Loop Current (LC), Florida Current (FC), North Equatorial Current (NEC). Salinity data are from World Ocean Atlas 05 (Antonov et al., 2006) averaged over one annual cycle.

Consequently, seasonal changes of the Atlantic inflow into the Caribbean and its advection of the fresher tropical water mixed with Amazon and Orinoco river discharges contribute to the seasonality of SSS in the Caribbean. In addition to the freshwater supply from the tropical rivers, the Caribbean SSS is further controlled by seasonal changes in the evaporation/precipitation ratio (Etter et al., 1987).

1.6.3 Climatic setting

Annual cycle:

The tropical Atlantic and the Caribbean Sea are primarily forced by the co-varying pattern of SST and trade winds associated with the seasonal migration of the ITCZ (Hastenrath, 1984). However, during the northernmost extent of the Atlantic ITCZ, its zonal band of maximum rainfalls does not reach Bonaire today. Therefore, the climate of Bonaire is tropical arid, characterised by low annual rainfall (~500 mm/yr), high air temperature (~27°C), and high evaporation rate due to the year-long easterly trade winds.

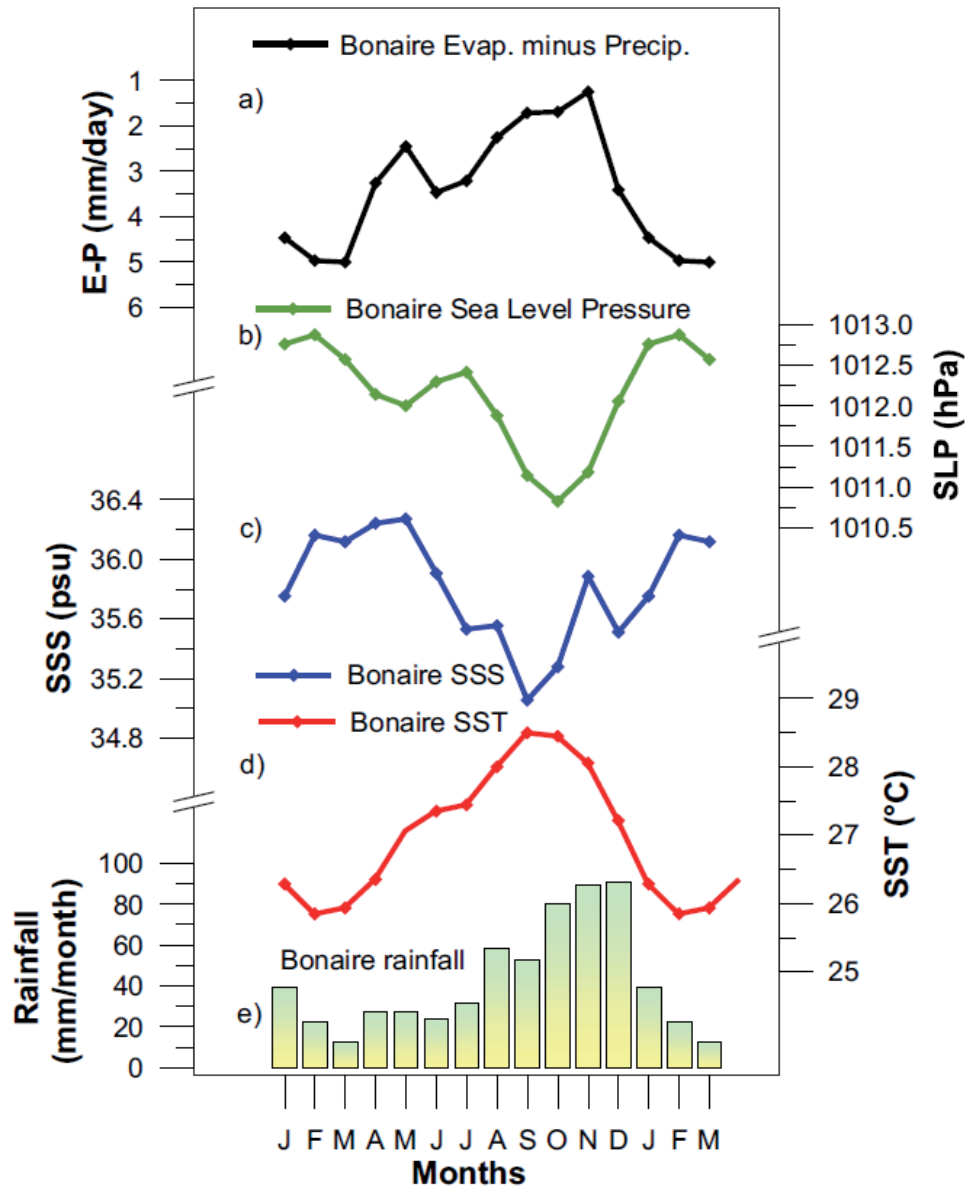


Figure 1.13: Monthly mean climatology of environmental parameters at the study site, Bonaire: a) Evaporation minus Precipitation (E-P) from NCAR CGD CAS tn430 era15 in a grid box centred at 67.5°W and 12.55°N (available at <http://iridl.ldeo.columbia.edu/SOURCES/.NCAR/.CGD/.CAS/.tn430/.era15/.t42f/.CLIMATOLOGY/.c7993/.EP/>); b) Sea Level Pressure from KAPLAN COADS_SLPclim slp in a 4° x 4° gridbox (Kaplan et al., 2000); c) Sea Surface Salinity (SSS) climatology from World Ocean Atlas 09 (Antonov et al., 2010) in a 1° x 1° grid box; climatology; d) Sea Surface Temperature (SST) climatology for 1970-2000 from ERSSTv3b (Smith et al., 2008) in a 2° x 2° gridbox; e) Climatology of monthly mean precipitation for 1970-2000 from UEA CRU Hulme Global prcp in a grid box centred at 67.5°W and 12.5°N (Hulme et al., 1998). Note that positive annual mean E-P values indicate that net evaporation.

Sea surface temperature (SST) displays a well-marked seasonal cycle of about ~2.9 °C in amplitude, ranging from 25.7 °C in February/March to 28.6 °C in September/October with annual mean of 27 °C (Smith et al., 2008). The rainy season starts in October and ends around the beginning of January. A secondary rainy season occurs in July-August and only very limited rainfalls events are recorded during dry months (Martis et al., 2002) (Figure 1.13). The sea surface salinity (SSS) data from World Ocean Atlas 2009 (Antonov et al., 2010) indicate an annual cycle of about 1 psu in amplitude, with more saline conditions in May and less saline conditions in

September. An annual cycle of sea level pressure (SLP) shows lower values in autumn and higher values in winter, which indicates the weakening and strengthening of the trade winds, respectively, during these times. According to these seasonal changes in the mean state of the atmosphere, the evaporation/precipitation ratio also shows a rapid shift between November and January towards more evaporation. This suggests that the hydrological balance of the southern Caribbean Sea is drastically changed due to the enhancement of the trade winds associated with the southward displacement of the ITCZ at this time.

Interannual to multidecadal variability: Unlike the tropical Pacific, where a single mode of climate variability (i.e., El Niño/Southern Oscillation, ENSO) dominates at interannual time scales, the climate of the tropical Atlantic and Caribbean is subject to multiple competing influences of the remote and local forcing that are tied to the dynamics of the ocean/atmosphere interaction of both the Pacific and Atlantic Oceans. Several mechanisms have been proposed to explain the origin of the variability observed in the tropical north Atlantic climate (e.g., Marshall et al., 2001a; Xie and Carton, 2004; Kushnir et al., 2006). On interannual time scales, these mechanisms include coupled ocean/atmosphere interaction from the tropical Pacific ENSO (Curtis and Hastenrath, 1995; Enfield and Mayer, 1997; Giannini et al., 2000; Saravanan and Chang, 2000) and the extratropical north Atlantic, namely the North Atlantic Oscillation (NAO) (Nobre and Srukla, 1996; Sutton et al., 2000; Giannini et al., 2001a; Czaja et al., 2002).

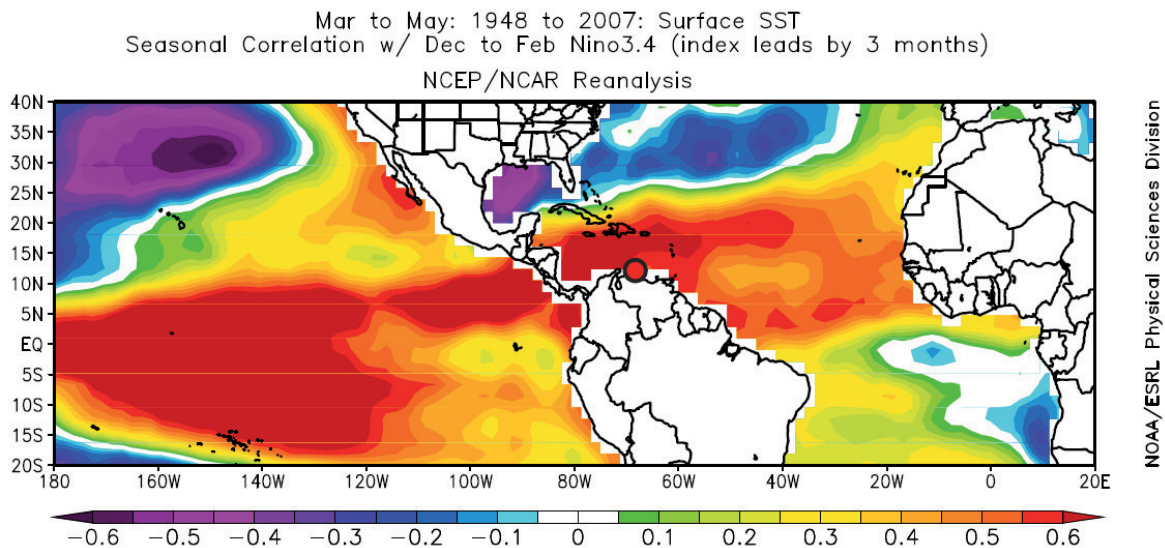


Figure 1.14: Correlation map between December-January-February El Niño3.4 index and March-April-May global sea surface temperature (SST) for the period 1948-2007 (Smith et al., 2008). Location of Bonaire is indicated (red dot).

ENSO appears to be the dominant mode of climate variability controlling north tropical Atlantic SST variability on interannual time scales, where about 50-80% of anomalous SST variability is associated with Atlantic warming occurring 4-5 months after the mature phase of Pacific warm events (Enfield and Mayer, 1997; Sutton et al., 2000) (Figure 1.14). Consequently, the Atlantic warming occurs as a result of the weakening of Northeast trade winds, which in turn

reduces the latent and sensible heat loss over the region (Enfield and Mayer, 1997; Giannini et al., 2001b; Alexander and Scott, 2002; Chiang et al., 2002). In addition, ENSO conditions are known for modulating Atlantic hurricane activity (Smith et al., 2010). The frequency and intensity of hurricanes are reduced in El Niño years, whereas they are enhanced in La Niña years (Gray, 1984; Saunders et al., 2000). However, hurricanes are complex phenomena and ENSO is just one factor among others influencing its activity in the tropical Atlantic. For example, SST in the Atlantic (Landsea, 1999; Goldenberg et al., 2001), the Quasi-biennial Oscillation (Gray, 1984), and the North Atlantic Oscillation (Elsner et al., 2000; Molinari and Mestas-Nuñez, 2003) are all critical environmental factors influencing Atlantic hurricane activity.

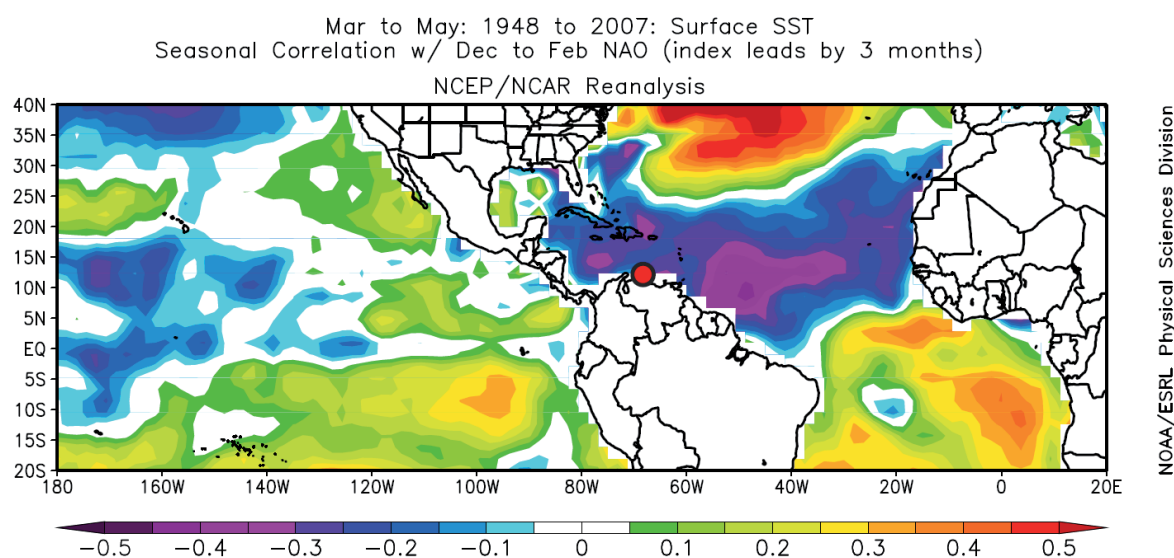


Figure 1.15: Correlation map between December-January-February North Atlantic Oscillation (NAO) index (Hurrell, 1995) and March-April-May global sea surface temperature (SST) for the period 1948-2007 (Smith et al., 2008). Location of Bonaire is indicated (red dot).

An important mode of climate variability affecting the Caribbean climate on an interannual time scale has an extratropical origin, the North Atlantic Oscillation (Hurrell, 1995). The NAO is defined as the difference in sea-level pressure over Iceland and Azores in winter. In low-latitudes, this SLP gradient influences the strength of trade winds and therefore the sensible and latent heat flux that in turn influences the north tropical Atlantic SST (George and Saunders, 2001; Giannini et al., 2001a) and the position of the ITCZ (Xie and Carton, 2004) (Figure 1.15). A positive NAO phase, implies a stronger than normal SLP in the north Atlantic subtropical high, which suppresses Caribbean rainfall indirectly via the anomalously cold SST associated with anomalies in the surface wind speed at these tropical latitudes. During the negative phase of the NAO, the trade winds diminish due to the weaker meridional SLP gradient, thus enabling SST to increase and precipitation to occur in the Caribbean.

It has been reported that the pattern of teleconnection from these modes of interannual climate variability to the tropical Atlantic have strong seasonality (Sutton and Hodson, 2005). Moreover, correlation in the recurrence of a positive phase of the NAO during the winters, coinciding with the warm ENSO conditions can produce statistically significant anomalies in the

seasonal and interannual Caribbean climate. Giannini et al., (2001a) found that interdecadal changes in ENSO teleconnection to the Caribbean region and the resulting interactions between ENSO and NAO has increased in the last 20 years in comparison with decades before this period. Observational and model-based studies have identified a significant decadal to interdecadal scale variability (period of 8-20 year) in SST, precipitation and hurricane activity of the tropical Atlantic. However, no consensus exists on the origin of the climate variability on these time scales (e.g., Carton et al., 1996; Chang et al., 1997; Marshall et al., 2001a). On multidecadal time scales, the Atlantic Multidecadal Oscillation (AMO) (Kerr, 2000) plays a critical role in controlling both SST and rainfall in the Caribbean (Enfield et al., 2001; Sutton and Hodson, 2005) (Figure 1.16). Forcing mechanisms responsible for the leading large-scale pattern of the AMO remain controversial primarily because of the limited instrumental record (Latif et al., 2006). Nevertheless, recent observational and model-based studies mentioned that changes in the strength of the oceanic thermohaline circulation could drive the associated multidecadal climate variability (Delworth and Mann, 2000; Knight et al., 2005). Additional evidence arose from a recent study which identified low-frequency variability of the NBC transport as an indicator of multidecadal variability of the surface return flow of the AMOC (Zhang et al., 2011).

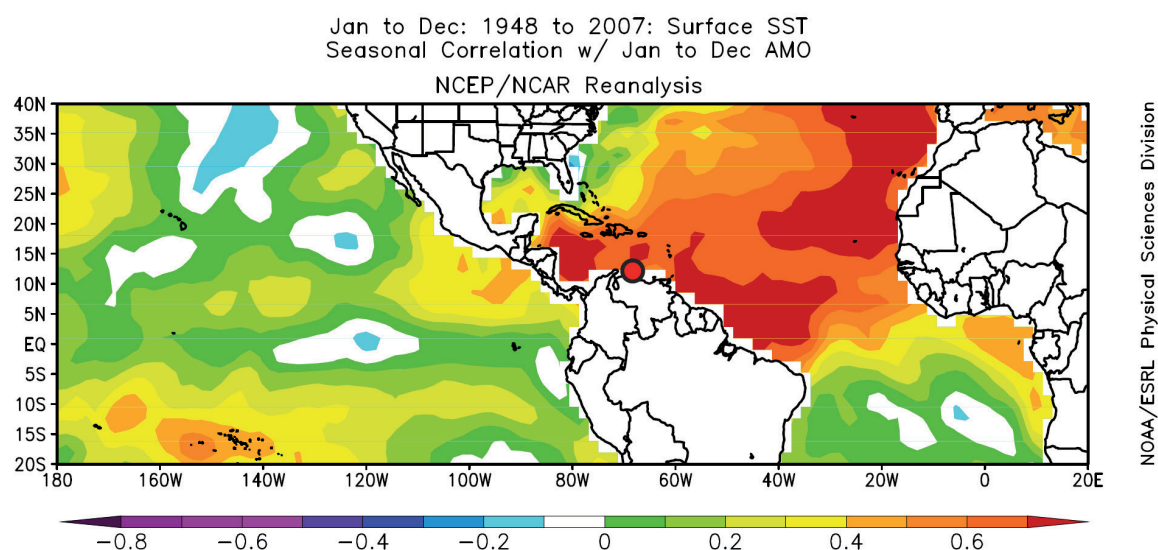


Figure 1.16: Correlation map between Atlantic Multidecadal Oscillation (AMO) index (Enfield et al., 2001) and global sea surface temperature (SST) for the period 1948-2007 (Smith et al., 2008). Location of Bonaire is indicated (red dot).

1.7 Motivations and Objectives

1.7.1 Motivations

The tropical Atlantic climate is characterised by a large seasonal cycle and clear interannual to multidecadal variability that are often linked to hazardous climate phenomena in this region (Gray, 1984; Wang et al., 2008a). However, knowledge of climate variability on these time scales is limited by short and sparse instrumental data in this region where reliable observations

extend back to 1950 AD. Proxy reconstructions in this sector that extend beyond this relatively short instrumental period have primarily focused on low-frequency (i.e., multidecadal to millennial time scales) rather than focusing on higher-frequency (i.e., seasonal to multidecadal timescales) climate variability (e.g., Hodell et al., 1991; Rühlemann et al., 1999; Haug et al., 2001; Lea et al., 2003; Tedesco and Thunell, 2003; Richey et al., 2007). Consequently, subseasonally resolved reconstructions of tropical Atlantic climate that extend beyond this instrumental data period are needed in order to assess its natural short-term variability. Such proxy reconstructions of the Caribbean climate can be achieved by using fossil corals found on the coastal deposits of Bonaire.

Since the Pleistocene, *Diploria strigosa* is a common reef-building coral from the western Atlantic and Caribbean reefs (Bak, 1975; Budd and Johnson, 1999) that produces annual density bands (Helmle et al., 2000), resists the power of storm-generated wave that are frequent in the Caribbean sector (Scheffers and Scheffers, 2006), and can grow up for several decades up to centuries. Corals of this species have dense and solid skeletal walls that are less affected by diagenesis compared to thinner and porous coral skeleton. Kuhnert et al., (2005) showed for the first time the potential of paired coral Sr/Ca and $\delta^{18}\text{O}$ measurements for reconstructing climate variability recorded in the coral skeleton of *D. strigosa*. Later on Hetzinger et al., (2006) showed that this brain coral is an excellent high-resolution archive of tropical Atlantic climate variability. So far, *D. strigosa*, has not been used to reconstruct the tropical Atlantic climate that extends beyond pre-industrial times. Consequently, using fossil *D. strigosa* corals from Bonaire which grew during this period of reduced human influence on climate will shed more light on the natural range tropical Atlantic climate variability. Ultimately, this study questions the stability of the well-defined features of tropical Atlantic climate known from instrumental data (i.e., seasonality and interannual to multidecadal climate variability) and aims at identifying forcing mechanisms responsible for its natural variability. The accurate reconstruction of past tropical Atlantic climate variability under well-known background climate states (i.e., period of higher summer insolation during the mid-Holocene, and periods of reduced/enhanced ENSO activity) will enable the robust assessment of the sensitivity of tropical Atlantic climate to various forcing mechanisms.

1.7.2 Objectives

The main objective of this dissertation is to robustly evaluate the natural range of seasonality and interannual to multidecadal climate variability in the southern Caribbean Sea over the last 6,000 years by using massive *Diploria strigosa* brain corals. For this purpose, monthly resolved well-dated records from fossil corals, which grew during key periods of the Holocene, are accurately generated. As the skeletal structure of tropical Atlantic corals is often more complex than that of *Porites* sp., the coral genus commonly used for paleoclimate reconstructions, an accurate strategy is designed for the generation of long and robust climate records from the skeleton of fossil *D. strigosa* corals from Bonaire.

In a first step, the geochemical composition of the coral skeleton of *Diploria strigosa* is investigated. Here the potential complications of derived coral-based climate reconstruction associated with sampling its complex skeletal architecture is discussed and an accurate

microsampling technique is defined. The second step aims at evaluating the potential of fossil *D. strigosa* from Bonaire for paleothermometry of the southern Caribbean Sea recorded in the Sr/Ca ratio of coral skeleton. For this task, a well-dated fossil coral is screened for diagenesis and the trace elemental Sr/Ca composition is examined at near-monthly resolution. In order to assess the robustness of the first order variability of the Sr/Ca time series, the effect of coral growth rate on the SST-proxy is investigated. Since both the first and second steps help to identify the most judicious strategy for the robust reconstruction of past climate variability using brain corals from Bonaire, a unique microsampling technique is applied to several pristine fossil coral colonies in order to accurately investigate at near-monthly resolution (~12 samples/year) the natural range of SST seasonality and interannual to multidecadal variability of the Southern Caribbean Sea recorded in coral Sr/Ca. Finally in the next step, paired coral Sr/Ca and $\delta^{18}\text{O}$ measurements are applied on individual coral samples in order to investigate the natural variability of the southern Caribbean hydrological cycle on these time scales.

1.8 Thesis outline

This PhD dissertation is composed of four chapters, with **Chapter 1** giving background relevant to the motivations and objectives of this thesis in order to place the present study in the relevant scientific context. Achieved steps are then outlined. All references are provided in a single reference list at the end of this thesis. A short summary of the different chapters is given below.

The results presented in **Chapter 2** consist of a series of papers and manuscripts that have been published or are ready for submission to international peer-reviewed scientific journals. Description of the materials and methods used for the individual subsections are presented in each study. Finally, a brief overview of the content of each manuscript is given in the following four paragraphs:

Chapter 2.1 investigates the skeletal structure and geochemical composition of *Diploria strigosa*. It is well known that the geochemical composition is not necessarily constant within a coral genus, neither within an individual polyp nor within the same skeletal element. All these geochemical heterogeneities can have a critical effect on the reconstructed climate records retrieved from specific coral skeletons. In this chapter, the mesoscale geochemical heterogeneity of the climate proxies is investigated for a *D. strigosa* coral colony and the most robust microsampling strategy is defined for the generation of accurate climate reconstruction from its skeleton.

In **Chapter 2.2**, the first monthly-resolved coral Sr/Ca record from a fossil *Diploria strigosa* coral from Bonaire using the microsampling strategy defined in Chapter 2.1 is described. The potential of the fossil corals from Bonaire for reconstruction of the southern Caribbean Sea temperature variability is assessed by investigating secondary modifiers of the coral Sr/Ca temperature proxy, such as growth rate and diagenesis.

In **Chapter 2.3**, based on the findings of the previous chapters (i.e., chapter 2.1 and 2.2), monthly-resolved Sr/Ca records are generated from multiple fossil and modern *Diploria strigosa* corals from Bonaire. Three modern corals allow for evaluating the uncertainty associated with using

multiple coral *D. strigosa* colonies from Bonaire for paleothermometry. Whereas, monthly resolved coral Sr/Ca records from six fossil corals allow for quantifying the natural range of SST variability in this region. About 295 years of coral Sr/Ca records provide a unique insight into seasonality and interannual to multidecadal variability of southern Caribbean Sea SST during well-distributed Holocene time slices. Finally this study identifies periods of pronounced SST variability that are unprecedented in the short instrumental data period.

In **Chapter 2.4**, variability of sea surface hydrology on seasonal to multidecadal time scales is investigated for Holocene time slices. The mean position of the ITCZ fluctuates on glacial/interglacial cycles according to the strength of the Atlantic meridional overturning circulation (AMOC) which further modulate Caribbean surface hydrology. However, due to a lack of suitable high-resolution marine archives little is known on short-term variability (i.e., seasonal to multidecadal) of low latitude hydrological cycle which could contribute to rapid changes in the strength of the AMOC. Here we reconstruct seasonality and interannual to multidecadal variability of sea surface hydrology of the southern Caribbean Sea by applying paired coral Sr/Ca and $\delta^{18}\text{O}$ measurements on pristine and well-dated annually-banded corals from Bonaire. Finally, comparison of reconstructed oxygen isotopic composition of sea water ($\delta^{18}\text{O}_{\text{sw}}$ that is related to salinity) with reconstructed SST inferred from coral Sr/Ca allows for identifying potential forcing mechanisms responsible for short-term variability of the southern Caribbean sea surface hydrology.

Chapter 3 summarises the major findings and implications of the four manuscripts. Finally, future research directions are proposed in **Chapter 4**.

2. Manuscripts

2.1 Manuscript I

Giry, C., T. Felis, M. Kölling, S. Scheffers (2010): *Geochemistry and skeletal structure of *Diploria strigosa*, implications for coral-based climate reconstruction*, ***Palaeogeography, Palaeoclimatology, Palaeoecology***, 298, 378-387.

2.2 Manuscript II

Giry, C., T. Felis, S. Scheffers, C. Fensterer (2010): *Assessing the potential of Southern Caribbean corals for reconstructions of Holocene temperature variability*. **IOP Conference Series: Earth and Environmental Science**, 9, 012021, doi:10.1088/1755-1315/9/1/012021.

2.3 Manuscript III

Giry, C., T. Felis, M. Kölling, D. Scholz, W. Wei and S. Scheffers: *Mid- to late Holocene changes in tropical Atlantic temperature seasonality and interannual to multidecadal variability documented in southern Caribbean coral records*. Submitted to ***Earth and Planetary Science Letters***

2.4 Manuscript IV

Giry, C., T. Felis, M. Kölling and S. Scheffers: *Seasonal to multidecadal variability of sea surface hydrology in the southern Caribbean during the mid- to late Holocene*. In preparation for ***Paleoceanography***

2.1 Geochemistry and skeletal structure of *Diploria strigosa*, implications for coral-based climate reconstruction

Cyril Giry¹, Thomas Felis¹, Martin Kölling¹ and Sander Scheffers²

¹ MARUM - Center for Marine Environmental Sciences, University of Bremen, 28359 Bremen, Germany

² Marine Ecology Research Centre, Southern Cross University, Lismore, NSW 2480, Australia

Published in *Palaeogeography, Palaeoclimatology, Palaeoecology*

Abstract: Geochemical tracers incorporated into the skeleton of reef-building corals are ideal proxies for reconstructing environmental parameters of ambient seawater such as temperature and salinity at subseasonal resolution. However, validation concerns of these environmental proxies due to the complex skeleton of some tropical Atlantic corals have hindered such coral-based environmental reconstructions in this region compared to the tropical Pacific. In order to identify complications associated with the complex skeletal architecture of the massive brain coral *Diploria strigosa*, we performed microsampling experiments along and across individual skeletal elements. We demonstrate that the mesoscale heterogeneity of Sr/Ca, $\delta^{18}\text{O}$ and $\delta^{13}\text{C}$ is a systematic feature of *D. strigosa* and is linked to different vital effects between skeletal elements. The thecal wall is significantly depleted in Sr, ^{18}O and ^{13}C compared to the adjacent septa and columella and differences between apparent temperature signatures of several degrees are greater for Sr/Ca suggesting that this temperature proxy is more sensitive to skeletal mixing than $\delta^{18}\text{O}$. Parallel subseasonal microsampling experiments performed along individual skeletal elements of a single corallite of a *D. strigosa* coral which grew at a rate of 0.65 cm/year allow for investigating potential biases associated with its complex skeletal mesoarchitecture. Highest correlation between Sr/Ca and $\delta^{18}\text{O}$ from skeletal material retrieved from the centre of the thecal wall suggests that microdrilling the theca provides the best environmental signal compared to adjacent microsampling profiles. Moreover, based on monthly-mean climatology, the temperature dependence of Sr/Ca for this profile is comparable to previous calibrations published from faster growing *D. strigosa*. Based on these results, we conclude that accurate microsampling along the centre of the thecal wall of *D. strigosa* is a prerequisite for generating robust climate reconstructions from its skeleton.

Citation: Giry, C., T. Felis, M. Kölling, S. Scheffers, Geochemistry and skeletal structure of *Diploria strigosa*, implications for coral-based climate reconstruction, *Palaeogeography, Palaeoclimatology, Palaeoecology*, 298, 378-387, 2010.

2.1.1 Introduction

Massive scleractinian corals are unique high-resolution marine archives that have improved the knowledge of the tropical and subtropical climate system. Key oceanographic parameters such as sea surface temperature (SST) and sea surface salinity (SSS) inferred from long-lived annually-banded coral colonies make this marine archive ideal for long subseasonal reconstructions of past climate variability. The inverse relationship between SST and the strontium (Sr) to calcium (Ca) ratio in coral skeleton (Smith et al., 1979; Beck et al., 1992) provides salinity independent records of local SSTs. The $\delta^{18}\text{O}$ of coral skeleton varies in response to changes in both temperature and seawater $\delta^{18}\text{O}$ which is linearly related to SSS (Carriquiry et al., 1994; Wellington et al., 1996). Therefore, combining $\delta^{18}\text{O}$ and Sr/Ca provide a unique opportunity to estimate subseasonal temperature and salinity changes back through time (Gagan et al., 1998).

The state-of-the-art, coral-based climate reconstruction has primarily focused on using the genus *Porites* from the Indo-Pacific. Generation of long subannually resolved climate reconstructions from this genus that extend beyond the sparse and short instrumental data period have significantly expanded our understanding of the variability of tropical and subtropical climate systems (Cole et al., 1993; Gagan et al., 1998; Felis et al., 2000; Felis et al., 2004; Linsley et al., 2006; Hetzinger et al., 2008). To date, such reconstructions in the tropical western Atlantic and the Caribbean are spatially and temporally underrepresented. Exceptions are limited to

the studies by Winter et al., (1991), Swart et al., (1996a), Winter et al., (2000), Watanabe et al., (2001), Kuhnert et al., (2002), Winter et al., (2003), Kuhnert et al., (2005), Goodkin et al., (2005), Greer and Swart (2006), Goodkin et al., (2008a; 2008b), Kilbourne et al., (2008), Maupin et al., (2008) and Saenger et al., (2008; 2009). Attempts using tropical Atlantic corals to generate long subseasonally resolved climate reconstructions have been delayed by questioning the validity of geochemical proxies measured in their skeleton as a tracer of environmental conditions (Cohen et al., 2001; Cohen et al., 2002; Swart et al., 2002) and by physical problems associated with sampling the skeleton of large-polyped corals (Leder et al., 1996; Swart et al., 2002; Cohen and Thorrold, 2007).

The skeletal mesoarchitecture of many Atlantic corals is relatively more complex than that of *Porites* sp. (Veron, 2000). Early studies have shown that the complex skeletal architecture of large-polyped corals is generally associated with variable isotopic fractionations within a single corallite (Land et al., 1975; Pätzold, 1992). Pätzold (1992) sought for understanding of the geochemical variability within coral species which is a prerequisite prior to generating accurate time series of environmental reconstructions. Recent studies on Atlantic corals such as *Montastraea* sp., *Siderastrea* sp. and *Diploria* sp. have demonstrated that successful climate records can be generated by following a single skeletal element, usually the solid thecal wall (Leder et al., 1996; Swart et al., 1996b; Swart et al., 2002; Kuhnert et al., 2005; Hetzinger et al., 2006; Moses et al., 2006; Smith et al., 2006; Goodkin et al., 2008b; Maupin et al., 2008;

Saenger et al., 2008). However, the intracorallite variability of climate proxies and its implication for paleoclimate reconstruction remains still unknown for most of these corals.

In this study, we focus on the brain coral *Diploria strigosa* (Dana, 1846), an important reef building, shallow water coral of the Caribbean region (Bak, 1977). *D. strigosa* has been in high abundance since the early Pliocene (Budd and Johnson, 1999), and forms massive and large colonies which generally resist the power of storm-generated waves frequent in the Caribbean and suffer less damage overall than branching corals (Woodley et al., 1981; Scheffers and Scheffers, 2006). The species produces distinct annual density bands (Helmle et al., 2000), and has recently provided relevant information on climate variability of the tropical and subtropical Atlantic Ocean recorded in Sr/Ca and $\delta^{18}\text{O}$ ratios (Kuhnert et al., 2005; Hetzinger et al., 2006; Hetzinger et al., 2008; Hetzinger et al., 2010). Early use of *Diploria labyrinthiformis* from Bermuda has presented some difficulties to extract the full range of seasonality from its slow-growing (3–4 mm/year) skeleton (Cohen and Hart, 2004; Goodkin et al., 2005). The complex growth pattern of *D. labyrinthiformis* appears to exacerbate some problems seen in coral-based climate reconstructions. Due to variable subannual skeletal extension rate as well as seasonal changes of the convoluted shape of the skeletal walls, microsampling along the dense thecal wall produces an artificial environmental signal that is dampened toward seasons when the skeleton is thickened (Cohen and Hart, 2004; Goodkin et al., 2005). Cohen et al., (2007) have proposed that fine scale microsampling along the centres of the convoluted septa walls by laser ablation can

resolve the full annual cycle of Sr/Ca-based SST. For long coral-based climate reconstructions, however, the laser ablation technique is less convenient compared to the commonly used millimetre-scale sampling methods also referred to as conventional microsampling (Asami et al., 2009; Felis et al., 2009). Recent studies on fast-growing *D. strigosa* coral colonies (~1cm/year) from the Caribbean have demonstrated the potential of conventional microsampling techniques for capturing the seasonal and interannual SST variability in the thecal walls of *D. strigosa*. Coral Sr/Ca and $\delta^{18}\text{O}$ have been successfully calibrated against SST (Hetzinger et al., 2006) and have proven capabilities to record the multidecadal variability of tropical Atlantic climate and hurricane activity (Hetzinger et al., 2008). Therefore, *D. strigosa* from the Southern Caribbean is a potential recorder of past temperature and hydrology variability of the western tropical Atlantic (Giry et al., 2010a). However, the influence of the complex growth processes of this brain coral on the incorporation of geochemical proxies remains unknown for this coral species. Therefore, this study contributes to a better understanding of the geochemistry of the complex skeletal architecture of this massive brain coral in order to assess the fidelity and circumvent potential sources of uncertainties of proxy-based climate reconstructions.

2.1.2 Material and Methods

2.1.2.1 Regional and climatic settings

Bonaire (Netherlands Antilles) is a small island in the Southern Caribbean Sea situated ~100 km north of the Venezuelan coastline (~12°10'N, 68°18'W). This open-ocean island belongs to the Leeward Antilles

and lies at the southern edge of the hurricane belt (Meyer et al., 2003; Bries et al., 2004). Frequent tropical storms and hurricanes passing north of Bonaire create high seas and intense wave actions that can cause considerable damage to the reefs (Meyer et al., 2003; Bries et al., 2004; Scheffers and Scheffers, 2006) and significant shoreline modifications (Scheffers et al., 2009). Coastal deposits commonly found on Bonaire such as polymodal clasts ranging in size from sand to coarse boulders suggest that the coastline of Bonaire is still highly sensitive to extreme wave events (Scheffers, 2004; Scheffers and Scheffers, 2006). Bonaire megaclasts derived from adjacent coral reefs and subadjacent reef terraces highlight the strength of extreme wave events of either hurricane or tsunami origins that took place during the Holocene (Scheffers, 2004; Morton et al., 2008; Scheffers et al., 2009).

The modern climate of Bonaire is tropical arid characterized by low annual rainfall (~ 500 mm/year), high evaporation rate peaking in summer and high annual mean SST (~27.4°C) ranging from 26.0°C (February) to 28.7°C (September) (Smith et al., 2008). Monthly instrumental SST based on ERSST.v3b (Smith et al., 2008) was extracted for the Bonaire gridbox centred at 12°N; 68°W. The monthly mean climatology was calculated for a 30-year period of interest (1900-1929) and compared to present-day conditions (1980-2009) (Figure 2.1).

2.1.2.2 Coral core collection and preparation

On the east coast of Bonaire (12°4.910'N; 68°13.913'W), a 33-cm-long core was drilled from a dead *Diploria strigosa* colony

(BON-9-A) found in a storm deposit formed by hurricane Ivan in 2004 (Scheffers and Scheffers, 2006). This coral was dated with U-series at 1912 ± 8 AD at the Forschungsstelle Radiometrie, Heidelberger Akademie der Wissenschaften, Germany. The coral core was sectioned into 6-7 mm thick slabs parallel to the major growth axis. Slabs were cleaned for 10 min in an ultrasonic bath, and then placed in a drying oven at 50°C overnight and X-rayed for 7 min at 45 kV. X-radiographs of the slabs provide a picture of density variations within the coral slab. Observed density variations within the slabs reflect two features; the clear annual density-banding pattern associated with seasonal changes in thickness of skeletal elements (Helmle et al., 2000) and the skeletal bulk-density variations associated with the position and orientation of different skeletal elements relative to the X-ray beam (Le Tissier et al., 1994) generally oriented parallel to the growth direction.

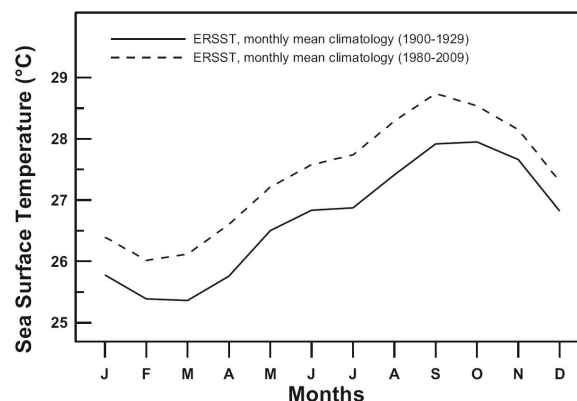


Figure 2.1: Monthly sea surface temperature (SST) climatology for Bonaire based on ERSST.v3b (Smith et al., 2008) (2°× 2° gridbox, centred at 12°N; 68°W) was calculated for the periods 1900-1929 (solid line) and 1980-2009 (dashed line). The amplitude of the annual SST cycle has not significantly changed during the last century ranging from 2.7 °C to 2.6 °C for the periods 1900-1929 and 1980-2009, respectively.

2.1.2.3 Microsampling of coral skeleton

Diploria strigosa commonly known as “symmetrical brain coral” has a smooth regular colony surface and a meandroid (brain coral) growth form with sinuous arrangement of interconnected corallites (Dana, 1846; Veron, 2000). Meandering continuous corallite valleys are usually 6 to 9 mm wide, regular in appearance and comprise a continuous spongy structure in the middle called columella. The columella is surrounded by thinner vertical walls called septae that extend toward the corallite wall to form septotheca or theca (Figure 2.2). Adjacent corallites share a common thecal wall and no exothecal structures are present. As the colony grows, coral tissue is lifted by the polyps which secrete a new floor called dissepiment. A rare alizarin staining experiment performed on *D. strigosa* skeleton (Dodge et al., 1984) reveals

that the thecal wall has a convoluted growth form and that septa walls are formed on the outer edge of the colony surface above the theca precipitated at the same time.

The position and orientation of individual skeletal elements within the coral slab are identified by combining both naked-eye observations of the slab-surface and density variability inferred by X-radiographs (Figure 2.2). A corallite valley orientated perpendicular to the surface of the slab has been selected for the following experiments (Figure 2.3). In order to investigate the geochemical variability across and along the corallite, two microsampling experiments with a constant sampling depth of 1.5-2 mm were performed using a milling machine Proxxon FF 400 equipped with a micrometer-control table Proxxon KT 400 which allows 3-dimensional

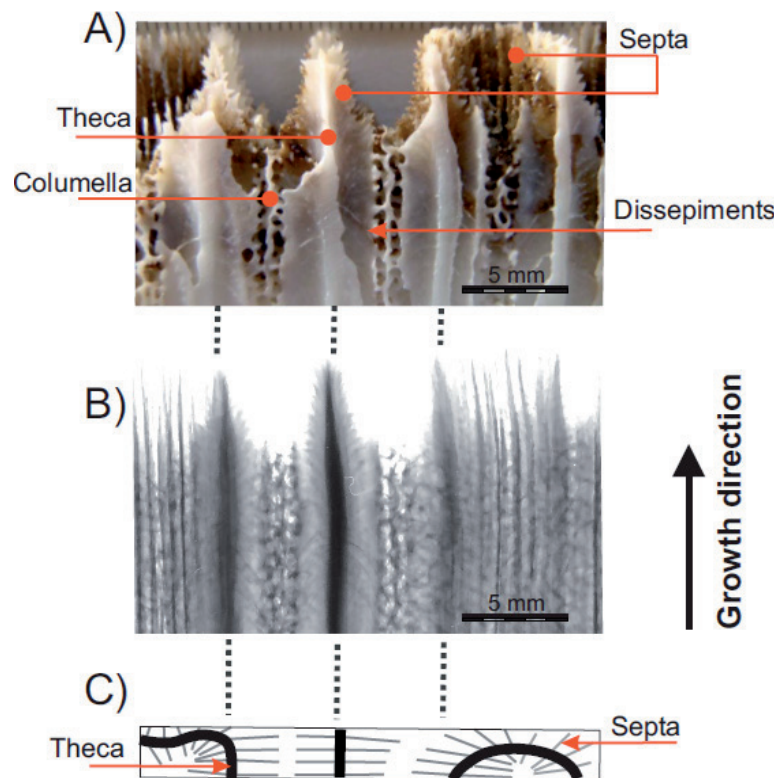


Figure 2.2: Mesoarchitecture of *Diploria strigosa* skeleton observed on the slab A) and the X-radiograph positive print B). Combined observations of the coral slab and corresponding X-radiograph are of relevance for identifying positions and orientations of skeletal elements constituting the slab C).

sampling accuracy of 0.05 mm. Coral XDS software (Helmle et al., 2002) was used to infer grey-scale variability within the slab in order to identify the exact position of annual density bands.

First, microsampling experiments along each skeletal element (septa, columella and the two opposite thecal walls) were conducted with constant increments of 0.5 mm over ten annual density bands (Figure 2.3). In order to ensure that ample skeletal material is extracted for both Sr/Ca and stable isotope analyses, the size of the drill bit was adjusted to the bulk density of the targeted skeletal element. Due to high-pore spaces, the columella and septa showing relatively low-bulk density on X-radiographs (Figure 2.2) were sampled with a 1.4 mm diameter drill bit. The two opposite thecal walls were sampled using two different microsampling techniques; microdrilling the centre of the theca using a 0.6 mm-diameter drill bit and microgrinding with a 1.4 mm-

diameter drill bit the opposite one after excavation of residual septal material, as illustrated in Figure 2.3. Using different drill bit size allows for investigating time averaging problems associated with microsampling the convoluted thecal wall (Dodge et al., 1984).

In order to investigate the spatial geochemical variability across the corallite, a second experiment was performed on a second slab facing the previous one. Cutting across long and meandering polyps of *Diploria strigosa* allows for investigating a single corallite on two different slabs. As the theca of *D. strigosa* is the commonly targeted skeletal element for climate reconstructions (Kuhnert et al., 2005; Hetzinger et al., 2006; Hetzinger et al., 2008; Hetzinger et al., 2010), microsamples with constant increments (0.5 mm) were extracted across and along a single thecal wall over a couplet of high/low density bands.

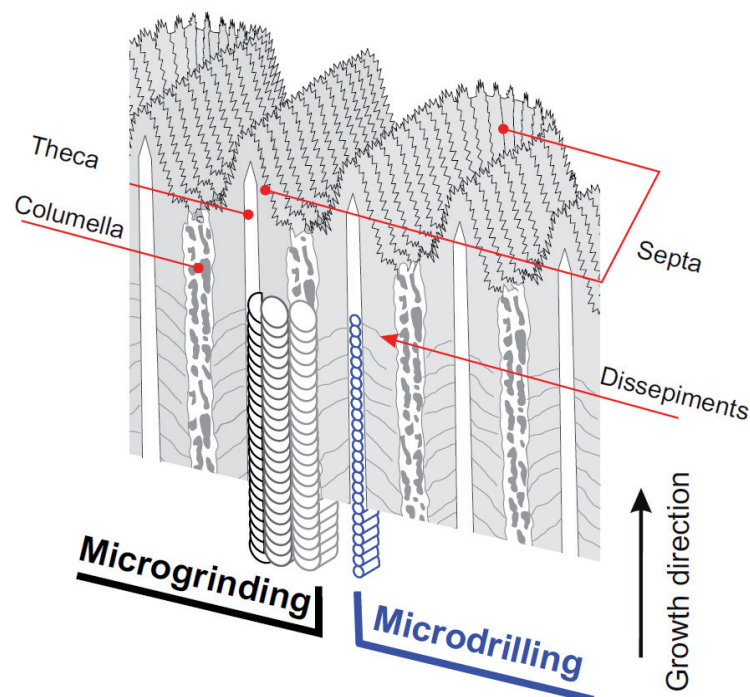


Figure 2.3: Scheme of the microsampling experiments conducted along a single corallite of *Diploria strigosa*: Microdrilling the centre of the thecal wall using a 0.6 mm diameter drill bit, and microgrinding the theca, septa and columella using a 1.4 mm diameter drill bit.

2.1.2.4 Sr/Ca and stable isotope analyses

Each powdered sample was split for both stable isotope and Sr/Ca analyses performed at MARUM and the Department of Geosciences of the University of Bremen, Germany. For stable isotope analyses, a Finnigan MAT 251 mass spectrometer was used to measure the $\delta^{18}\text{O}$ and $\delta^{13}\text{C}$ of ~0.05 mg of coral powder. Isotopic values are reported in ‰ relative Vienna peedee belemnite (VPDB) reference standard. Long term reproducibility for $\delta^{18}\text{O}$, deduced from replicate measurements of an internal carbonate standard, is better than $\pm 0.07\text{‰}$ (1σ).

For Sr/Ca analyses 0.25-0.30 mg sample powder was dissolved in 7 mL 2% suprapure HNO_3 containing 1 ppm Sc (Scandium) as internal standard. Measurements were performed on a Perkin-Elmer Optima 3300R simultaneous radial ICP-OES using a CETAC U5000-AT ultrasonic nebulizer. Element wavelengths were detected simultaneously in 3 replicates (Ca 317.933 nm, Ca 422.673 nm, Sr 421.552 nm, Sc 361.383 nm and Mg 280.271 nm). Ca concentrations measured on an atomic line (422.673 nm) were averaged with the concentrations from an ionic line (317.933 nm) to compensate for possible sensitivity drift in a radial ICP-OES. Measurements of a laboratory coral standard after each sample allowed offline correction for instrumental drift. Relative standard deviation of the Sr/Ca determinations was better than 0.2%.

2.1.3 Results

Many massive corals produce one couplet of high- and low-density band within a year that is detectable on X-radiographs (Knutson et al., 1972). Annual density-banding pattern in *Diploria strigosa* is the result of thickening of septa and columella (Helmle et al., 2000). Based on the annual-banding pattern observed on X-radiographs, we analysed Sr/Ca, $\delta^{18}\text{O}$ and $\delta^{13}\text{C}$ of individual skeletal elements over ten couplets of high/low density bands (Figure 2.3, 2.4). Figure 2.4 shows Sr/Ca, $\delta^{18}\text{O}$ and $\delta^{13}\text{C}$ records over ten annual growth increments from four individual profiles along distinct skeletal elements of the selected corallite. The results demonstrate that annual cycles in both Sr/Ca and $\delta^{18}\text{O}$ are partially resolved along skeletal elements. Moreover, discrepancies between individual profiles exist in the mean geochemical composition and in the amplitude and the position of resolved annual cycles.

2.1.3.1 Mean geochemical composition of skeletal elements

Averaged Sr/Ca, $\delta^{18}\text{O}$ and $\delta^{13}\text{C}$ values of each microsampling transect and their respective standard deviation and standard error of the mean are reported in Figure 2.5. The results indicate that significant differences in geochemical composition exist between individual transects. For instance, averaged values for microdrilling/microgrinding along the theca, microgrinding along the columella and along the septa are respectively 9.080/9.142, 9.331 and 9.346 mmol/mol for Sr/Ca; -4.27/-

4.02, -3.99 and -3.73‰ for $\delta^{18}\text{O}$ and -1.67/-0.29, -0.92 and +1.15‰ for $\delta^{13}\text{C}$.

Thecal material retrieved from the microdrilling experiment is significantly more depleted in Sr, ^{13}C and ^{18}O compared to skeletal material from adjacent profiles. The greatest difference in

mean Sr/Ca, $\delta^{18}\text{O}$ and $\delta^{13}\text{C}$ is found between microdrilling along the theca and microgrinding along the septa with 0.266 mmol/mol, 0.54‰ and 2.82‰, respectively. We also note significant discrepancies in the mean values of all measured proxies between the

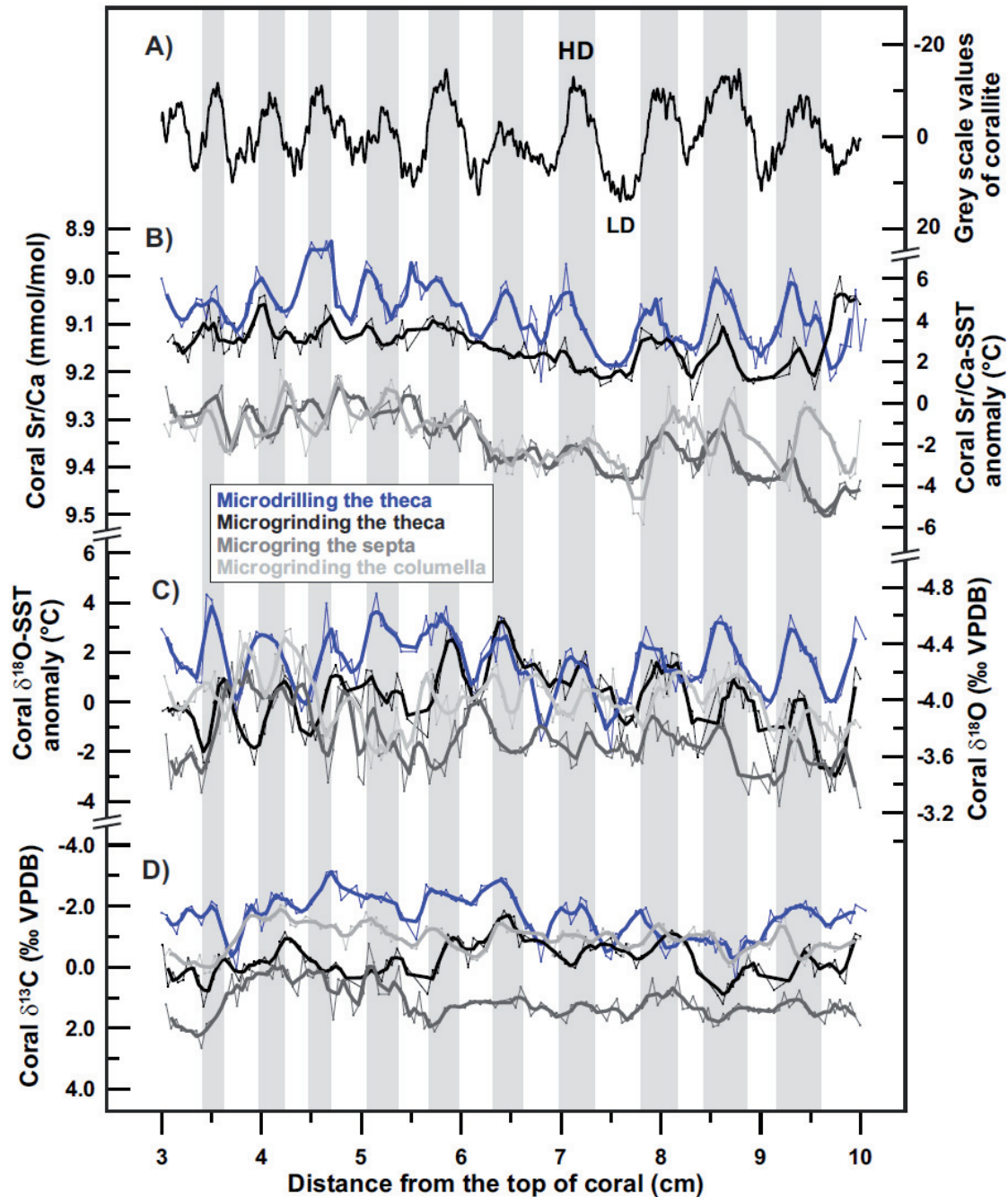


Figure 2.4: Annual density banding pattern A) and resolved Sr/Ca B), $\delta^{18}\text{O}$ C) and $\delta^{13}\text{C}$ D) annual cycles inferred from four microsampling transects (cf. Figure 2.3) and corresponding 3-point running means (*thick lines*) over a 10-year period. The relative density banding pattern of the selected corallite has been calculated with Coral XDS software (Helmle et al., 2002). Grey (white) bars indicate the high (low) density bands. The corresponding Sr/Ca-based sea surface temperature (SST) anomalies and $\delta^{18}\text{O}$ -based SST anomalies were calculated using the proxy-SST relationships of -0.041 mmol/mol per °C and -0.184 ‰ per °C, respectively, established for Caribbean *Diploria strigosa* corals (Hetzinger et al., 2006).

two microsampling experiments along the theca; microdrilling and microgrinding. The centre of the theca targeted with the microdrilling experiment is more depleted in Sr, ^{13}C and ^{18}O compared to the overall theca sampled with the microgrinding experiment (Figure 2.3). Both profiles show significant offsets in the mean values that are 0.062 mmol/mol, 0.25‰ and 1.42‰ for Sr/Ca, $\delta^{18}\text{O}$ and $\delta^{13}\text{C}$, respectively.

2.1.3.2 Subseasonally-resolved Sr/Ca, $\delta^{18}\text{O}$ and $\delta^{13}\text{C}$ records

The results of microsampling experiments performed along distinct skeletal elements indicate that the amplitude of the annual cycles in the Sr/Ca and $\delta^{18}\text{O}$ records is greater with microdrilling the centre of theca (Figure 2.4). As $\delta^{13}\text{C}$ is controlled by numerous environmental and physiological parameters (Carriquiry et al., 1994; Gagan et al., 1994;

Swart et al., 1996b; Felis et al., 1998; Grottoli and Wellington, 1999), the pattern of the $\delta^{13}\text{C}$ signal is not further discussed. While Sr/Ca records for individual profiles seem to exhibit some difficulties in reproducing seasonality, $\delta^{18}\text{O}$ records show a clearer seasonal pattern in both profiles along the theca. We note a breakdown of Sr/Ca annual cycle in the microgrinding theca experiment while the $\delta^{18}\text{O}$ signal still shows seasonality. In addition, we found that the position of the resolved annual cycles appears to be slightly offset between skeletal elements (Figure 2.4). Well-developed Sr/Ca annual cycles from the septa are in phase with the ones from the theca but offset with Sr/Ca annual cycles from the columella (Figure 2.4). In terms of distance from the top of the colony, the annual signal retrieved from the theca and the septa precedes the one from the columella by about 1-3 mm. The two

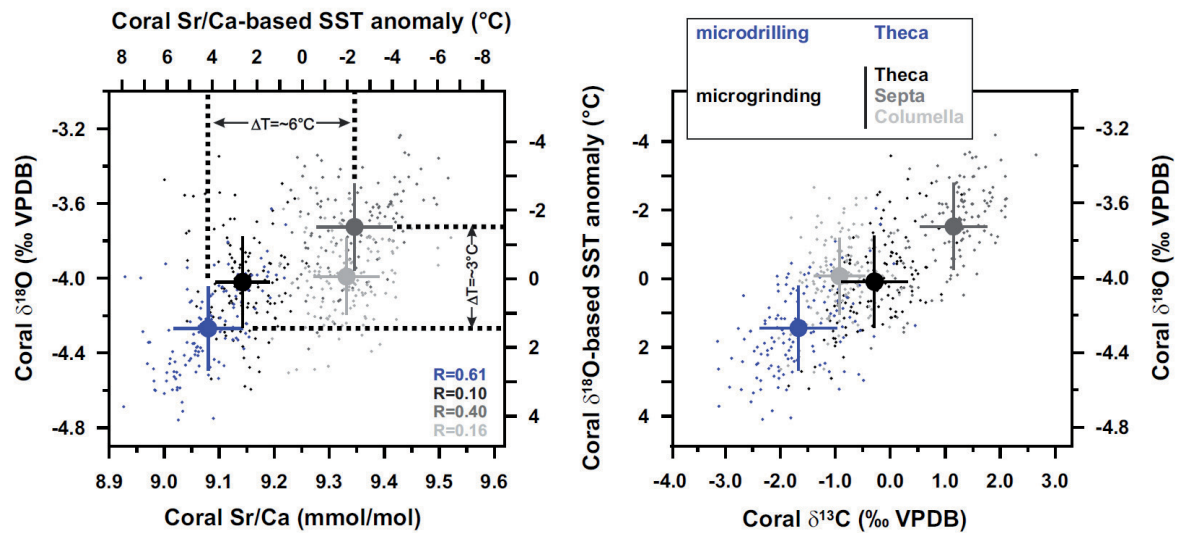


Figure 2.5: Geochemical signature of four different microsampling profiles along distinct skeletal elements of a single corallite of *Diploria strigosa*. Mean Sr/Ca, $\delta^{18}\text{O}$ and $\delta^{13}\text{C}$ values (large dots) of individual microsampling profiles and their respective standard deviations are also shown. The standard error of the mean is inferred by the size of the large dots. The corresponding Sr/Ca-based sea surface temperature (SST) anomalies and $\delta^{18}\text{O}$ -based SST anomalies were calculated using the proxy-SST relationships of -0.041 mmol/mol per °C and -0.184‰ per °C, respectively, established for Caribbean *D. strigosa* corals (Hetzinger et al., 2006). Correlation coefficients between Sr/Ca and $\delta^{18}\text{O}$ for individual microsampling transects are reported.

profiles from opposite theca walls (Figure 2.3) exhibit clear discrepancies in the amplitude of resolved annual cycles and in their mean Sr/Ca, $\delta^{18}\text{O}$ and $\delta^{13}\text{C}$ values. Our data suggest that the annual Sr/Ca cycles are not well-captured by microgrinding the thecal wall. However, it seems that microdrilling the centre of the theca can better capture clean annual cycles in both Sr/Ca and $\delta^{18}\text{O}$ (Figure 2.4).

2.1.3.3 Geochemical variability within the theca

Based on the banding pattern inferred from X-radiographs, geochemical variations across a single thecal wall are evaluated over one annual growth increment for Sr/Ca, $\delta^{18}\text{O}$ and $\delta^{13}\text{C}$ (Figure 2.6). Results of linear interpolation between measured proxies show that the centre of the theca is significantly depleted in Sr, ^{13}C and ^{18}O compared to its

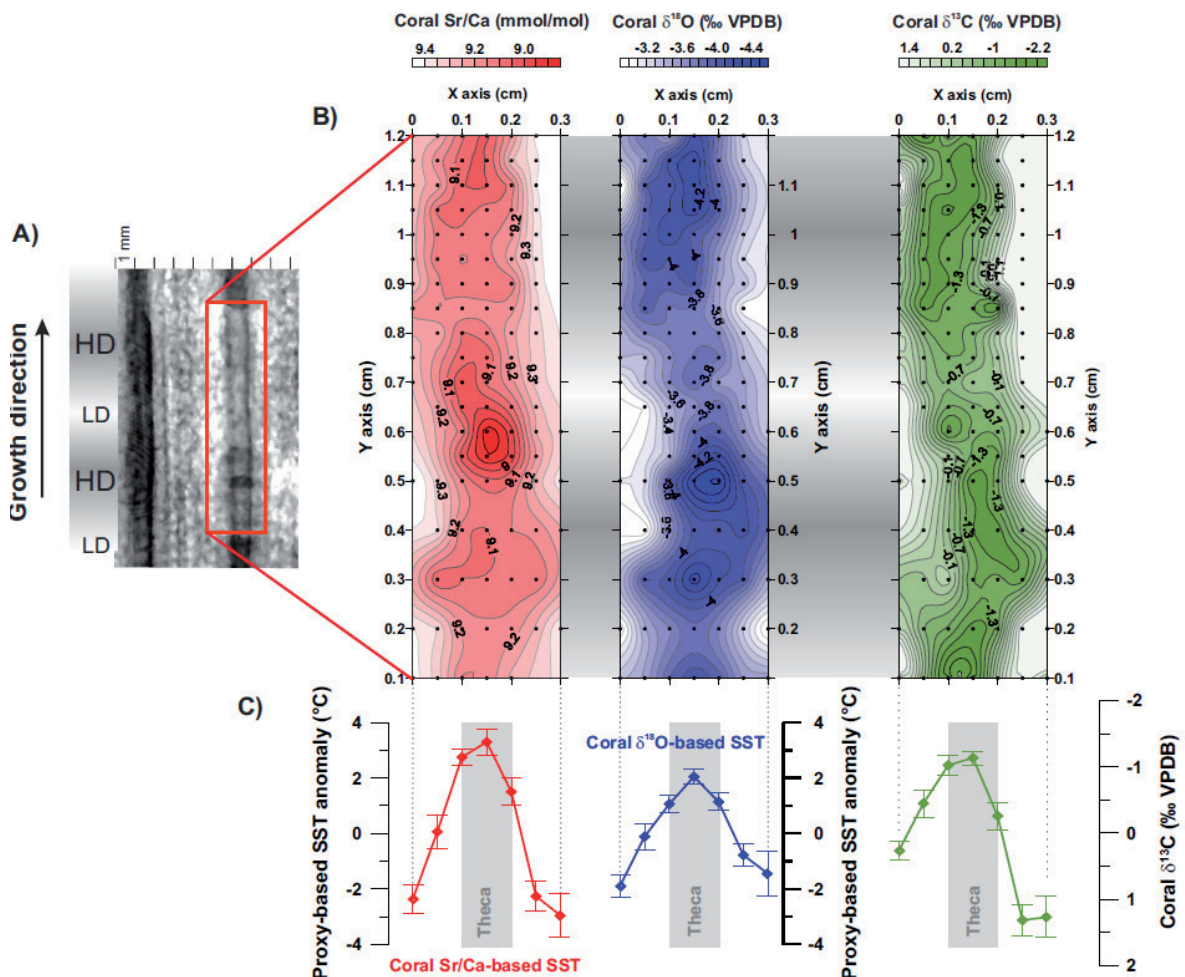


Figure 2.6: A) Geochemical variability is investigated for a single thecal wall over a couplet of high/low (HD/LD) density bands of *Diploria strigosa*. B) Linear interpolation between measured samples provide a picture of the Sr/Ca (red), $\delta^{18}\text{O}$ (blue) and $\delta^{13}\text{C}$ (green) variability within the theca. C) Apparent mean proxy-based SST anomalies based on Hetzinger et al., (2006) integrated vertically across the thecal wall and the corresponding standard errors of the mean are shown.

side. This spatial heterogeneity in climate proxies could lead to an apparent temperature drop of several degrees in a distance of 1-1.5 mm from the centre of the theca. Based on regression slopes from Hetzinger et al. (2006), such an apparent drop in reconstructed temperature can represent ~6 °C for Sr/Ca and ~4 °C for $\delta^{18}\text{O}$ (Figure 2.6). According to the annual density banding pattern, the depletion of the centre of the theca seems to be seasonally dependent. We note that the depleted skeletal material belonging to the centre of the theca shows to some degree higher amplitude of Sr/Ca and $\delta^{18}\text{O}$ annual cycles (Figure 2.6).

2.1.4 Discussion

It is well-established that the complex skeletal architecture of large-polyped corals is associated with geochemical heterogeneity between mesoskeletal elements which could lead to artificial climatic signals (Land et al., 1975; Pätzold, 1992; Leder et al., 1996; Swart et al., 2002) which makes it crucially important to identify coral specific sources of proxy-based uncertainties associated with conventional sampling of mesoskeletal elements. Recent contributions have highlighted the geochemical heterogeneity of large-polyped corals such as *Montastraea* sp. (Land et al., 1975; Leder et al., 1996; Watanabe et al., 2002; Smith et al., 2006), *Siderastrea* sp. (Moses et al., 2006; Maupin et al., 2008), *Diploastrea* sp. (Watanabe et al., 2003; Bagnato et al., 2004) and *Diploria* sp. (Pätzold, 1992).

2.1.4.1 Kinetic fractionation within a corallite

It is well-known that zooxanthellate corals do not precipitate their aragonitic skeleton in isotopic equilibrium with ambient seawater. The results of this disequilibrium are simultaneous depletion of ^{18}O and ^{13}C of the coral skeleton compared to inorganically precipitated aragonite (Weber and Woodhead, 1970; McConnaughey, 1989). These geochemical disequilibria or the so-called “vital effects” are not necessarily constant within a coral genus (Weber and Woodhead, 1970; Erez, 1978; Felis et al., 2003; Suzuki et al., 2005), within an individual polyp (Land et al., 1975; Pätzold, 1992) nor within the same skeletal element (Allison and Finch, 2004; Juillet-Leclerc et al., 2009). There are indications that these disequilibria are influenced by numerous biological mechanisms during calcification of the coral skeleton (Weber and Woodhead, 1970; Erez, 1978; Juillet-Leclerc and Reynaud, 2010). Those biological processes are also hypothesized to influence the incorporation of Sr from sea water into the coral skeleton (Weber, 1973; Cohen et al., 2001). In this study, all investigated skeletal elements from a single colony grew in a similar environment and thus biological processes are assumed to be the most likely cause of the observed mesoscale heterogeneity. Taking 1‰ (SMOW) as the mean $\delta^{18}\text{O}$ seawater value in the Southern Caribbean Sea (Schmidt, 1999; Chiang et al., 2002; McConnell et al., 2009), 0‰ (VPDB) as the mean $\delta^{13}\text{C}$ seawater value (Swart et al., 1996b) and 26.5 °C as the mean water temperature for the Bonaire gridbox at that time (Carton and Giese, 2008) results in isotopic equilibrium values for coral $\delta^{18}\text{O}$ and $\delta^{13}\text{C}$ of approximately -0.6‰ and 2.7‰ relative

to VPDB, respectively, following the procedure outlined by Heikoop et al., (2000) and using equations of Grossman and Ku (1986) and Romanek et al., (1992) for biogenic aragonite. In this sense, aragonite precipitated inorganically (Kinsman and Holland, 1969) at this temperature would be characterized by an aragonite Sr/Ca ratio of 9.64 mmol/mol. From these results, it follows that different geochemical compositions observed are the results of variable vital effects from one skeletal element to another.

Skeletal growth and calcification rate have long been thought to be important factors influencing the incorporation of stable isotopes and trace elements in coral skeletons (Weber and Woodhead, 1970; Goreau, 1977). For instance, more rapidly growing and/or calcifying parts of coral skeleton tend to show greater depletion in ^{18}O , ^{13}C (Land et al., 1975; Emiliani et al., 1978; McConnaughey, 1989; Felis et al., 2003; Maier et al., 2004) and Sr (de Villiers et al., 1995; Alibert and McCulloch, 1997; Allison and Finch, 2004; Goodkin et al., 2005; Saenger et al., 2008). Moreover, corals cultured in a controlled environment indicate that uptake of ^{18}O , ^{13}C and Sr relative to Ca might decrease at high calcification rate, consequently decreasing the isotopic and Sr/Ca values of the coral skeleton (Ferrier-Pagès et al., 2002; Inoue et al., 2007). Although our results show no negative correlation between the skeletal extension rate ranging from 4 to 9 mm/year and Sr/Ca, $\delta^{18}\text{O}$ and $\delta^{13}\text{C}$ (not shown), the significant depletion of Sr, ^{18}O and ^{13}C observed in the dense theca skeleton supports the calcification-related model controlling the incorporation of those elements in the skeleton of *Diploria strigosa*.

At microscale, it is known that every corallite is built by two mineralizing domains; the early mineralisation zone and the fibrous zone, commonly referred to as centre of calcification and rapidly extending fasciculi, respectively (Cohen and McConnaughey, 2003; Allison and Finch, 2004; Meibom et al., 2006; Juillet-Leclerc et al., 2009). Microscale analyses of these skeletal microstructures showed large scatter in both Sr/Ca (Adkins et al., 2003; Allison and Finch, 2004; Meibom et al., 2008) and $\delta^{18}\text{O}$ (Meibom et al., 2006; Juillet-Leclerc et al., 2009) indicating that biological processes occurring at mineralisation sites control the incorporation of stable isotopes and trace elements into growing aragonite crystals. The conventional sampling resolution used in the present study limits our understanding of the geochemistry of those microstructures in *Diploria strigosa* skeleton.

Isotopic disequilibria in biological carbonates have been previously classified according to the contributions of two different processes: “metabolic” and “kinetic” isotope effects (McConnaughey, 1989). “Kinetic” disequilibria involve simultaneous depletion of ^{18}O and ^{13}C whereas “metabolic” effects involve additional positive or negative modulation of skeletal $\delta^{13}\text{C}$, reflecting changes in the $\delta^{13}\text{C}$ of the dissolved inorganic carbon (DIC) pool, controlled primarily by photosynthetic activity of zooxanthellae (McConnaughey, 1989; Carriquiry et al., 1994). Numerous studies have demonstrated that photosynthesis tends to elevate the $\delta^{13}\text{C}$ of the DIC pool consequently increasing the skeletal $\delta^{13}\text{C}$ (Weber and Woodhead, 1970; Goreau, 1977; Swart, 1983; McConnaughey, 1989). The results of the present study indicate that septal materials are enriched in ^{13}C compared

to adjacent theca and columella. According to the skeletal architecture of *Diploria strigosa* (Dodge et al., 1984), the growth surface of septa constitutes the outer edge of the corallite that obviously receives more light than the theca built below the septal surface suggesting that the skeletal $\delta^{13}\text{C}$ differences within a corallite might reflect the rate of photosynthesis.

The geochemical composition of mesoskeletal structures of some corals have been attributed to the systematic influence of kinetic and metabolic effects on the modulation of stable isotopic fractionations in coral skeletal

elements (Pätzold, 1992). In the present study, we observe that thecal material is depleted in both ^{18}O and ^{13}C compared to the septa (Figure 2.4, 2.5 and 2.6), a geochemical heterogeneity which is consistent with those observed in *Diploria strigosa* colonies from Bermuda (Pätzold, 1992). In addition to that, we note that the theca is also depleted in Sr. To ensure that the observed geochemical variability in Sr/Ca, $\delta^{18}\text{O}$ and $\delta^{13}\text{C}$ is not an isolated signal, additional cross-theca experiments were performed on two other *D. strigosa* colonies from Bonaire (Figure 2.7). The result shows similar trends where the

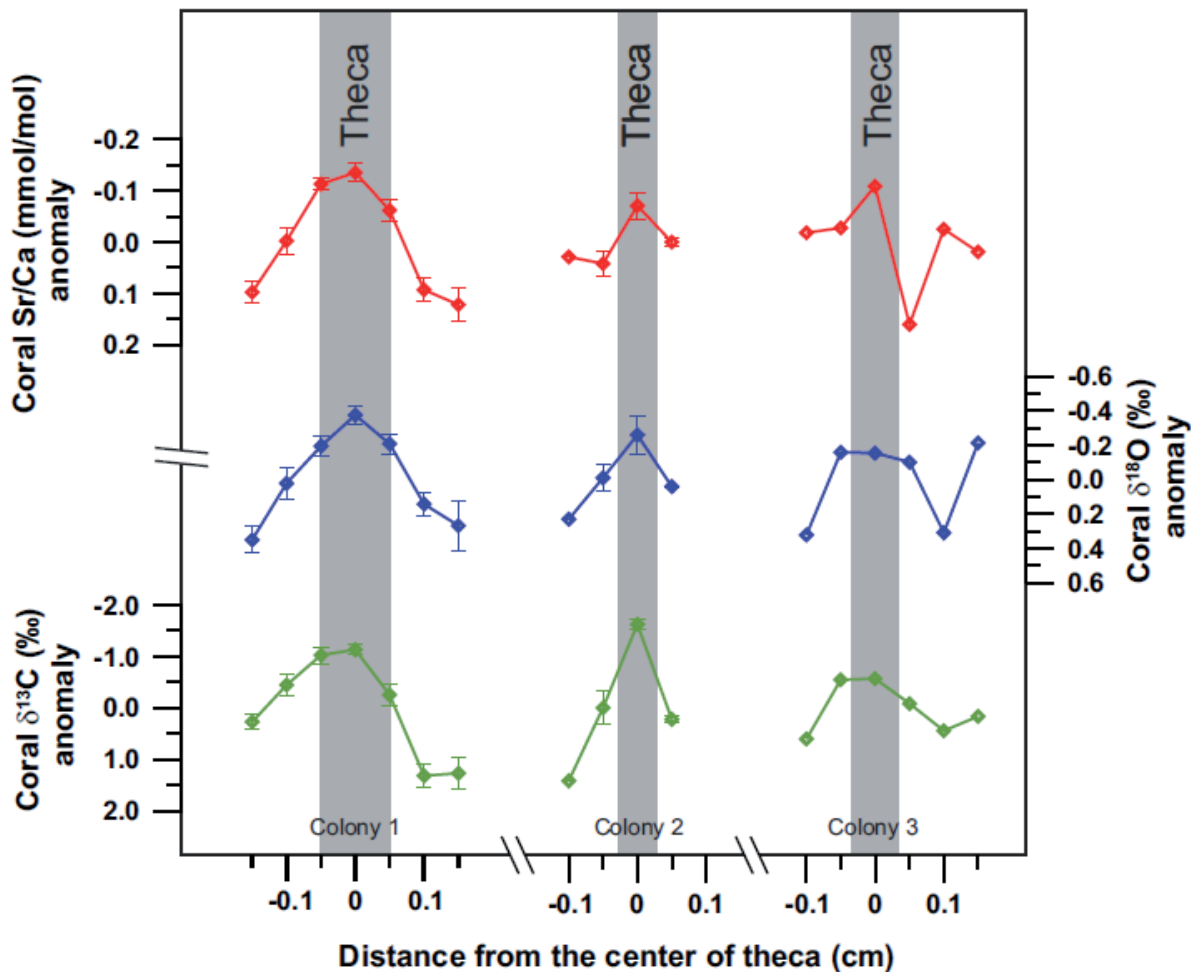


Figure 2.7: Mean Sr/Ca (red), $\delta^{18}\text{O}$ (blue) and $\delta^{13}\text{C}$ (green) anomalies and corresponding standard error of the mean integrated vertically across the thecal wall of three different *Diploria strigosa* colonies.

centre of the theca is significantly depleted in Sr, ^{13}C and ^{18}O compared to its side. However, the degree of this depletion is variable from a colony to another. This additional observation suggests that the depletion of the center of the thecal wall relative to its side is found in any *D. strigosa* colony. Therefore, we consider that the observed geochemical heterogeneity (Sr/Ca, $\delta^{18}\text{O}$ and $\delta^{13}\text{C}$) across the theca is a systematic feature of *D. strigosa* colonies. This systematic variation of stable isotopic compositions between the skeletal elements of the corallites has been attributed to variable skeletal fractionations that are controlled by biological processes. The dense theca is also characterized by low Sr/Ca values (Figure 2.4, 2.5, 2.6 and 2.7) and we assume that similar vital effects control the incorporation of Sr in the skeleton of *D. strigosa*.

2.1.4.2 Temperature dependence of climate proxies in *Diploria strigosa*

Since this *Diploria strigosa* was collected dead and has been dated with U/Th, there is no definitive time constraint on the portion of the coral sampled which allow for evaluating geochemical records in reference to environmental records. To circumvent this limitation, we alternatively investigate the correlation coefficient between the two SST proxies Sr/Ca and $\delta^{18}\text{O}$ as well as monthly-mean climatology proxy-SST relationships.

Coral Sr/Ca and $\delta^{18}\text{O}$ are known to be influenced by ambient SST. Therefore, the sensibility of both proxies retrieved from distinct skeletal material (Figure 2.3) to SST can be estimated by using the correlation coefficient between Sr/Ca and $\delta^{18}\text{O}$. A stronger correlation would support that both Sr/Ca and $\delta^{18}\text{O}$ from a microsampling profile are more

representative of SST rather than physiological processes. While salinity changes and their effects on $\delta^{18}\text{O}$ seawater are not considered here, our data show that the highest/lowest correlation coefficient between Sr/Ca and $\delta^{18}\text{O}$ ($r=0.61/r=0.10$) is found for the microdrilling/microgrinding the theca profile (Figure 2.4 and 2.5). This result suggests that skeletal material retrieved by microdrilling the centre of the theca is more representative of SST than skeleton from microgrinding the theca with a larger drill bit which might be complicated by skeletal growth and/or physiological processes.

Recent studies have emphasized problems associated with microsampling slow-growing *Diploria* sp. (Cohen et al., 2004; Goodkin et al., 2005; Cohen and Thorrold, 2007). Cohen et al. (2004) have shown that conventional microsampling of the convoluted skeleton of *D. labyrinthiformis* is associated with reduced amplitude of resolved Sr/Ca annual cycles. They found that the mixing of skeletal material precipitated at different times might smooth the reconstructed Sr/Ca annual cycle and thus, lower the slope of proxy-derived SST calibrations (Cardinal et al., 2001; Swart et al., 2002; Cohen and Thorrold, 2007). Cohen et al. (2007) proposed that only very fine scale sampling along the centre of the convoluted walls of *Diploria labyrinthiformis* will avoid this dampening and resolve the full seasonal range of SST variability. In the present study, we use a relatively slow-growing *D. strigosa* coral (0.65 cm/year) compared to the coral used for calibration purpose (Hetzinger et al., 2006). Monthly-mean Sr/Ca and $\delta^{18}\text{O}$ climatologies have been calculated for individual microsampling paths (Figure 2.3) and compared to monthly-mean SST

climatology for the period of interest spanning 1900-1929 (Figure 2.1). The results indicate a Sr/Ca-SST relationship derived from microdrilling the theca of -0.042 mmol/mol per °C while the three other transects show Sr/Ca-SST regression slopes of -0.015 mmol/mol per °C and less. A similar pattern is observed for the $\delta^{18}\text{O}$ -SST relationship which is -0.127‰ per °C for microdrilling the theca while the three other transects indicate -0.050‰ per °C and less. While microdrilling the center of the thecal wall provides a Sr/Ca-SST regression slope that is comparable to the one previously published for faster growing *D. strigosa* (Hetzinger et al., 2006), microgrinding the entire theca shows a relationship which indicates that the annual cycle retrieved from this microsampling experiment is dampened. Isotopic and trace element signals extracted with the large drill bit (1.4 mm diameter) are significantly smoothed compared to signals from the centre of the theca extracted with a smaller drill bit (0.6 mm diameter) (Figure 2.3). This result suggests that reconstructed annual cycles retrieved from microdrilling along the centre of the thecal walls (Figure 2.3) of *D. strigosa* are less dampened compared to those retrieved from microgrinding the thecal wall with a larger drill bit (Figure 2.3 and 2.4). Therefore, we assume that time-averaging problems in this *D. strigosa* colony are reduced by using a smaller drill bit. Moreover as the magnitude of mesoscale heterogeneity is larger than the annual cycle itself, we emphasize that mixing of mesoskeletal elements of different geochemical composition appears to be the main factor that can potentially affect the quality of the resolved climatic signal (Figure 2.5 and 2.6).

The incorporation of Sr and ^{18}O into the coral skeleton has been shown to be partially related to the annual extension rate (Goreau, 1977; Emiliani et al., 1978; McConnaughey, 1989; de Villiers et al., 1995; Felis et al., 2003; Goodkin et al., 2007). Annual mean Sr/Ca and $\delta^{18}\text{O}$ values in some colonies are negatively correlated with annual extension rate (Emiliani et al., 1978; Felis et al., 2003; Goodkin et al., 2005; Goodkin et al., 2007). The skeletal extension rate calculated from the microdrilling profile as the distance from the maximum Sr/Ca value in a given year to the maximum value of the following year does not show a negative correlation with annual mean Sr/Ca, but, our results indicate that, along the 10-year long record, low annual mean Sr/Ca and $\delta^{18}\text{O}$ values are associated with low skeletal extension rate. However, these positive non-significant correlations between annual extension rate and annual mean Sr/Ca ($r = 0.4$, $p = 0.22$) and $\delta^{18}\text{O}$ ($r = 0.5$, $p = 0.10$) suggest that there is no direct effect of skeletal extension rate on coral Sr/Ca and $\delta^{18}\text{O}$ in the skeleton of this *Diploria strigosa* colony. A likely explanation for these observed positive correlations is that this coral grew faster (slower) when SST was lower (higher), as observed at other locations in the western Atlantic (Dodge and Vaisnys, 1975; Carricart-Ganivet, 2004; Crueger et al., 2006; Saenger et al., 2009).

2.1.4.3 Implications for coral-based climate reconstruction

Our results suggest that systematic millimetre scale geochemical heterogeneity in *Diploria strigosa* skeleton is controlled by different vital effects between skeletal elements. This mesoscale heterogeneity can

potentially limit the quality of proxy-based environmental reconstructions retrieved from this large-polyped coral. Pätzold (1992) proposed that accurate microsampling should avoid mixing of mesoskeletal structures. Although our results support this suggestion, we observe that even at the scale of the commonly sampled thecal wall of *D. strigosa* (Kuhnert et al., 2005; Hetzinger et al., 2006; Hetzinger et al., 2008; Hetzinger et al., 2010) differences exist for $\delta^{18}\text{O}$, $\delta^{13}\text{C}$ and Sr/Ca. Therefore, appropriate sampling techniques are a prerequisite for high-resolution climate reconstructions.

Skeletal material retrieved by microdrilling the centre of the theca exhibits a higher correlation coefficient between Sr/Ca and $\delta^{18}\text{O}$, more depleted geochemical values and cleaner annual cycles than microgrinding the entire theca (Figure 2.3, 2.4 and 2.5). Moreover, Sr/Ca-SST relationships for both microdrilling and microgrinding the theca (-0.042 and -0.014 mmol/mol per °C, respectively) suggest that microdrilling the theca provides slope that is comparable to that of a recently published Sr/Ca-SST regression for a faster growing *Diploria strigosa* (Hetzinger et al., 2006). All these observations underline the importance of drill bit size in calibrating and reconstructing SST from the theca wall of *D. strigosa*. Therefore, any subseasonal proxy-based timeseries produced from the thecal walls of *D. strigosa* should consider this internal heterogeneity and cautious microsampling should integrate a constant proportion of skeletal material belonging to the centre of the theca. In addition, we note that the difference between septal and thecal material is greater for the Sr/Ca-based SST estimates suggesting that this temperature

proxy is more sensitive to mixing of skeletal material than $\delta^{18}\text{O}$ (Figure 2.5 and 2.6).

Based on these observations, we hypothesize that several factors such as sample size, sampling depth, quality of the microsampling path and the orientation of sampled skeletal elements relative to the sampling axis can affect the quality of the reconstructed climate signal in *D. strigosa*. As the thecal wall is systematically depleted in Sr, ^{18}O and ^{13}C compared to its side, samples that deviate from the centre of the theca will show enriched Sr/Ca, $\delta^{18}\text{O}$ and $\delta^{13}\text{C}$ values. The size of the drill bit influencing directly the proportion of depleted skeletal material extracted from the centre of the theca is positively correlated with a dampening of the resolved annual cycle. Therefore, proxy-derived SST calibrations established from “coarse” microsampling potentially underestimate the seasonal variability of the climate record compared to those generated with a finer drill bit along the theca of *D. strigosa*. Moreover, the quality of the sampling path can obviously affect the sinusoidal shape of the reconstructed annual cycle. For instance a “noisy” sampling transect along the centre of the thecal wall integrating a variable proportion of the targeted skeletal element is likely to produce a noisy annual cycle. Another additional source of uncertainty is associated with difficulties in sampling the targeted skeletal element due to its variable orientation within the slab, as illustrated in Figure 2.2. Finally, anomalous variations of coral proxies toward enriched values should be checked whether they are not associated with either sampling artefacts or orientation and position changes of the targeted skeletal element.

2.1.5 Conclusion

The skeletal Sr/Ca, $\delta^{18}\text{O}$ and $\delta^{13}\text{C}$ composition of the massive brain coral *Diploria strigosa* was investigated at millimetre scale. We found systematic mesoscale heterogeneity in Sr/Ca, $\delta^{18}\text{O}$ and $\delta^{13}\text{C}$ that is linked to different vital effects between skeletal elements. This finding has important implications for coral paleoclimatology as this geochemical heterogeneity in the skeleton of *D. strigosa* can lead to apparent temperature biases that are induced by incorporation of variable amounts of mesoskeletal elements. Microsampling experiments performed along different skeletal elements revealed that microdrilling along the centre of the thecal wall is the method that better captures the SST annual cycle in both Sr/Ca and $\delta^{18}\text{O}$ and provides more realistic proxies-SST relationships. Detailed investigations of the geochemical heterogeneity across the thecal walls reveal that its centre is depleted in Sr, ^{18}O and ^{13}C compared to its side. The corresponding apparent temperature signatures show differences of several degrees that are greater for Sr/Ca compared to $\delta^{18}\text{O}$.

Based on these observations, we stress the need for accurately microsampling a constant proportion of the centre of the theca because samples that deviate from the initial/optimal sampling path are characterized by higher Sr/Ca, $\delta^{18}\text{O}$ and $\delta^{13}\text{C}$ values that do not indicate a climatic signal but rather reflect vital effects. Consequently, anomalous excursions/trends toward higher Sr/Ca, $\delta^{18}\text{O}$ and $\delta^{13}\text{C}$ values, disturbance/loss of Sr/Ca and $\delta^{18}\text{O}$ seasonality are potential manifestations of such microsampling artefacts in the dense thecal wall of *Diploria strigosa*.

This study emphasizes the importance of the so-called vital effect in controlling the geochemical composition of different skeletal elements in *Diploria strigosa* corals. These different vital effects observed between mesoskeletal elements are to some extent linked to different calcification and photosynthesis rates (Erez, 1978; Juillet-Leclerc and Reynaud, 2010). In contrast to *D. strigosa*, small-polyped corals (e.g. *Porites* sp.) have less pronounced differences in density between individual skeletal elements and are therefore expected to be less or not affected by this mesoscale geochemical heterogeneity.

Acknowledgments

We thank the Government of the Island Territory of Bonaire (Netherlands Antilles) for research and fieldwork permission, E. Beukenboom (STINAPA Bonaire National Parks Foundation) for support, J. Pätzold for support with coral drilling and discussion, S. Pape for operating and maintaining the ICP-OES, M. Segl and her team for stable isotopes analyses, D. Scholz and C. Fensterer for U/Th dating, H. Kuhnert, K. Delong and M. McCulloch for discussion. We are also grateful to three anonymous reviewers for providing helpful suggestions that have significantly improved the manuscript. This work was funded by Deutsche Forschungsgemeinschaft (DFG) under the Special Priority Programme INTERDYNAMIC, through a grant to T.F. (FE 615/3-1, 3-2; CaribClim). C.G. acknowledges additional support by GLOMAR (Bremen International Graduate School for Marine Sciences) that is funded by DFG.

2.2 Assessing the potential of Southern Caribbean corals for reconstructions of Holocene temperature variability

Cyril Giry¹, Thomas Felis¹, Sander Scheffers² and Claudia Fensterer³

¹ MARUM - Center for Marine Environmental Sciences, University of Bremen, 28359 Bremen, Germany

² Marine Ecology Research Centre, Southern Cross University, Lismore, NSW 2480, Australia

³ Heidelberger Akademie der Wissenschaften, Forschungsstelle Radiometrie, Heidelberg, Germany.

Published in *IOP Conference Series: Earth and Environmental Science*

Abstract: We present a 40-year long monthly resolved Sr/Ca record from a fossil *Diploria strigosa* coral from Bonaire (Southern Caribbean Sea) dated with U/Th at 2.35 ka before present (BP). Secondary modifiers of this sea surface temperature (SST) proxy in annually-banded corals such as diagenetic alteration of the skeleton and skeletal growth-rate are investigated. Extensive diagenetic investigations reveal that this fossil coral skeleton is pristine which is further supported by clear annual cycles in the coral Sr/Ca record. No significant correlation between annual growth rate and Sr/Ca is observed, suggesting that the Sr/Ca record is not affected by coral growth. Therefore, we conclude that the observed interannual Sr/Ca variability was influenced by ambient SST variability. Spectral analysis of the annual mean Sr/Ca record reveals a dominant frequency centred at 6-7 years that is not associated with changes of the annual growth rate. The first monthly resolved coral Sr/Ca record from the Southern Caribbean Sea for preindustrial time suggests that fossil corals from Bonaire are suitable tools for reconstructing past SST variability. Coastal deposits on Bonaire provide abundant fossil *D. strigosa* colonies of Holocene age that can be accurately dated and used to reconstruct climate variability. Comparisons of long monthly resolved Sr/Ca records from multiple fossil corals will provide a mean to estimate seasonality and interannual to interdecadal SST variability of the Southern Caribbean Sea during the Holocene.

Citation: Giry, C., T. Felis, S. Scheffers, C. Fensterer (2010): *Assessing the potential of Southern Caribbean corals for reconstructions of Holocene temperature variability*. *IOP Conference Series: Earth and Environmental Science*, 9, 012021, doi:10.1088/1755-1315/9/1/012021.

2.2.1 Introduction

During their growth, massive scleractinian corals living in shallow water of tropical and subtropical oceans incorporate a large array of geochemical tracers in their annually-banded aragonite skeleton that can be measured to retrieve environmental parameters (Gagan et al., 2000; Felis and Pätzold, 2003). Robust chronological control allows coral skeleton microsampling at subseasonal resolution. Key oceanographic parameters such as sea surface temperature (SST) and sea surface salinity inferred from long-lived annually-banded coral colonies have recently improved our understanding of the tropical and subtropical climate system (Cole et al., 1993; Felis et al., 2000; Tudhope et al., 2001; Cobb et al., 2003; Felis et al., 2004; Linsley et al., 2006; Abram et al., 2008; Hetzinger et al., 2008). The strontium to calcium ratio (Sr/Ca) in coral skeletons (Smith et al., 1979; Beck et al., 1992) has been proven to be the most reliable salinity-independent SST proxy. In recent decades, the inverse relationship between SST and coral Sr/Ca has been largely used to evaluate past SST variability of tropical and subtropical oceans (Corrège et al., 2004; Asami et al., 2009; Felis et al., 2009). To date, establishment of long coral-based SST reconstructions of the Western North Atlantic and Caribbean that extend beyond sparse and short instrumental data are underrepresented. Exceptions include the studies by Winter et al., (2000), Kuhnert et al., (2002), Winter et al., (2003), Kuhnert et al., (2005), Kilbourne et al., (2008), Goodkin et al., (2008b) and Saenger et al., (2009).

Paleoclimate reconstructions of the tropical Atlantic inferred from sediment cores

and speleothems have provided evidence for variable hydrological conditions over the last thousands of years (Haug et al., 2001; Hodell et al., 2005; Cruz et al., 2009). On orbital timescales, Southern Caribbean rainfall changes are linked to the mean position of the Intertropical Convergence Zone (ITCZ) which is controlled by a meridional SST gradient in the equatorial sector. On shorter timescales such as interannual to interdecadal, instrumental observations suggest that the dynamics of the ITCZ and thus, regional SSTs, are influenced by natural modes of ocean/atmosphere variability of specific periodicity such as the El Niño/Southern Oscillation (ENSO), the North Atlantic Oscillation (NAO) and the Atlantic Multidecadal Oscillation (AMO) emanating from tropical and subtropical oceans (Marshall et al., 2001a; Hurrell et al., 2006). The competing influence of these modes of climate variability on tropical Atlantic climate is called the Tropical Atlantic Variability (TAV) (Hurrell et al., 2006).

In the Southern Caribbean Sea, a subdecadally-resolved bulk-Ti content record from anoxic sediment of the Cariaco Basin shows that rainfall changes over northern South America are influenced, on orbital timescales, by the mean latitudinal position of the ITCZ (Haug et al., 2001). Although this runoff proxy indicates long-term changes of local precipitation toward drier conditions driven by insolation decrease over the Northern Hemisphere during the Holocene, this record suggests that Southern Caribbean climate has encountered periods of highly-variable hydrological conditions with high-amplitude and high-frequency variability of regional rainfall (Haug et al., 2001; Cruz et al., 2009). Whether those abrupt hydrological shifts

are associated with changes in the magnitude of teleconnected modes of climate variability emanating from the Pacific or the Atlantic oceans still remains unclear.

In this study, we use a well-dated and well-preserved fossil coral from Bonaire to reconstruct seasonal and interannual SST variability during a time window of the late Holocene. Coral Sr/Ca in *Diploria strigosa* from Guadeloupe has been recently calibrated against SST and has proven capabilities for reconstructing interannual and interdecadal SST variability in the Caribbean (Hetzinger et al., 2006). Hetzinger *et al.*, (2006) found a monthly mean Sr/Ca-SST relationship of -0.041 mmol/mol per $^{\circ}\text{C}$ with instrumental SST data (Carton and Giese, 2008). Secondary modifiers of this SST proxy such as diagenetic alteration and skeletal growth-rate are investigated. Finally, the dominant frequency of

SST variability documented in the coral Sr/Ca record is discussed.

2.2.2 Material and Methods

2.2.2.1 Regional setting

Bonaire (Netherlands Antilles) is a small island in the Southern Caribbean Sea located ~ 100 km north of the Venezuelan coast ($12^{\circ}10'\text{N}$; $68^{\circ}18'\text{W}$) and ~ 400 km away from Cariaco Basin (Figure 2.8a). This open-ocean island lies at the southern edge of the hurricane belt (Meyer et al., 2003; Bries et al., 2004) and is partially fringed by coral reefs since the mid-Holocene (Focke, 1978; Scheffers, 2004). Tropical storms and hurricanes passing north of Bonaire create intense wave action that cause damage to the reef and significant shoreline modifications (Scheffers and Scheffers, 2006; Scheffers et al., 2009). Coastal deposits commonly found

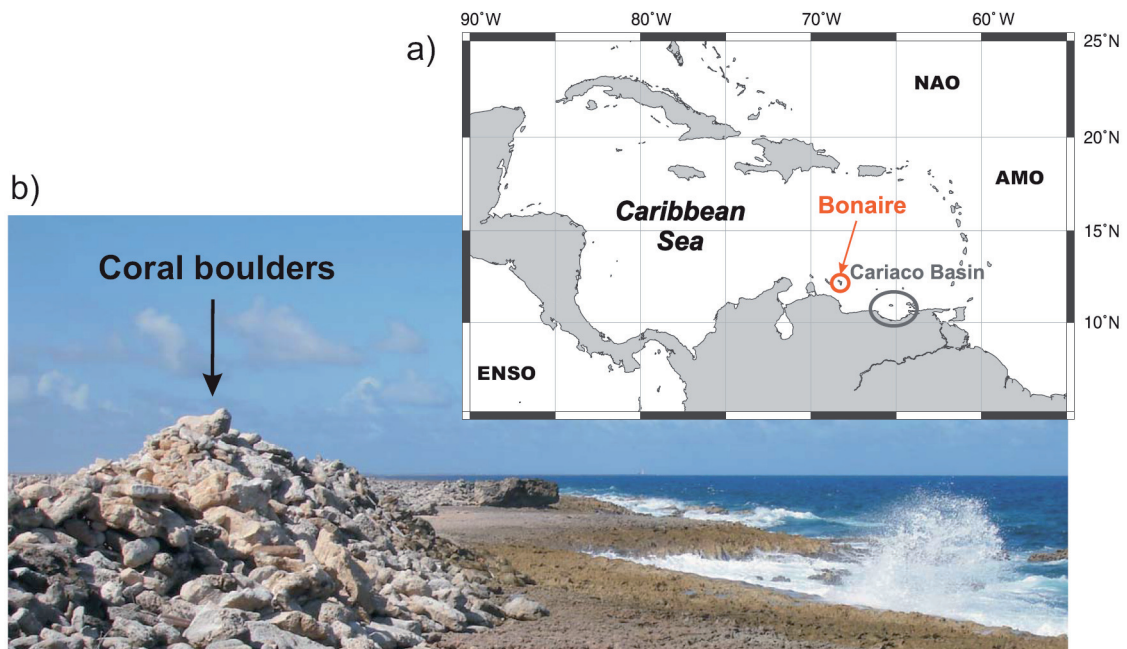


Figure 2.8 a) Bonaire is an open-ocean island located in the southern Caribbean Sea where local sea surface temperature variability is influenced by natural modes of ocean/atmosphere variability emanating from tropical and subtropical oceans, such as the El Niño-Southern Oscillation (ENSO), the North Atlantic Oscillation (NAO) and the Atlantic Multidecadal Oscillation (AMO). b) Accumulations of Holocene coral boulders transported by extreme waves (storm-induced and/or tsunamis-induced) form ramparts up to 10 m above sea level on Bonaire (Scheffers, 2004).

on Bonaire consist of decimetric to metric coral rubbles and boulders derived from adjacent coral reef (Figure 2.8b). The modern climate of Bonaire is tropical-arid characterised by low annual rainfall (~ 500 mm/year), high evaporation rate due to year-long easterly trade winds and high annual-mean SST (~26.8 °C) ranging from 25.7 °C (February) to 27.9 °C (October) (Carton and Giese, 2008).

2.2.2.2 Coral sampling and $^{230}\text{Th}/\text{U}$ -dating

Hurricane and/or tsunami deposits on Bonaire provide numerous fossil corals of Holocene age. A 40-cm-long core has been drilled from a fossil *Diploria strigosa* coral colony (BON-6-A) from one of these deposits at Washikemba (12°8'31.26"N, 68°11'53.10"W) on the windward coast of Bonaire (Figure 2.8b). $^{230}\text{Th}/\text{U}$ -dating at the Heidelberg Academy of Sciences indicates a coral age of 2.406 ± 0.049 ka (2 σ -uncertainty of 49 years), which is equivalent to 2.347 ± 0.049 ka before present (BP, where present is defined as AD 1950). Analyses were performed with a Finnigan Thermal Ionization Mass Spectrometer (TIMS) MAT 262 RPQ. Sample preparation and analytical details are similar as described in Scholz *et al.*, (2004). Calibration of the added U and Th spike solutions is described in Hoffmann *et al.*, (2007). Ages were calculated using the half-lives of Cheng *et al.*, (2000). All ages were corrected for the effect of detrital contamination using a bulk earth $^{232}\text{Th}/^{238}\text{U}$ weight ratio of 3.8 and assuming secular equilibrium between ^{238}U , ^{234}U and ^{230}Th . The effect of this correction, however, is 1 year and, thus, within the range of 2 σ -uncertainty of 49 years and negligible. The reliability of the determined $^{230}\text{Th}/\text{U}$ -age was checked using established criteria, such

as the initial ($^{234}\text{U}/^{238}\text{U}$) ratio in agreement with the ($^{234}\text{U}/^{238}\text{U}$) ratio of modern seawater (1.146, (Robinson *et al.*, 2004)) and U concentrations comparable to modern corals of the same species. For the studied fossil coral all these criteria are fulfilled. Thus, its age is considered as reliable.

2.2.2.3 Diagenetic investigations

The coral core was sectioned into 7 mm-thick slabs and investigated for possible diagenetic alteration of the skeleton using different methods. The slabs were X-rayed in order to identify both the annual density-banding pattern and areas of anomalous density patches potentially reflecting diagenetic alterations such as calcite or secondary aragonite infillings. In addition, for investigating diagenetic alteration that is representative of the entire coral slab, samples for powder X-ray diffraction (XRD), Scanning Electron Microscope (SEM) imaging and thin-section microscopy analyses were extracted from the middle of the slab. XRD was applied in order to quantify the calcite content of the sample. As crystals of inorganic aragonite cannot be detected with XRD, we used SEM and thin-section microscopy to identify the presence of secondary aragonite overgrowth that can potentially bias Sr/Ca-based SST reconstructions.

2.2.2.4 Microsampling

Based on the annual density-banding pattern of the coral skeleton observed on X-radiographs, we targeted a sampling resolution of about 12 samples per year, allowing an evaluation of proxy variability at monthly resolution. For each sample, an average of 1 mg skeletal powder was drilled along the

centre of the solid and dense theca wall, using a 0.6 mm diameter drill bit and applying a sampling depth of 1.5–2 mm and an average sampling increment of 0.55 mm.

2.2.2.5 Sr/Ca analyses

For Sr/Ca analyses 0.25–0.30 mg sample powder was dissolved in 7 mL 2 % suprapure HNO₃ containing 1 ppm Sc (Scandium) as internal standard. Measurements were performed on a Perkin-Elmer Optima 3300R simultaneous radial ICP-OES using a CETAC U5000-AT ultrasonic nebulizer (University of Bremen). Element wavelengths were detected simultaneously in 3 replicates (Ca 317.933 nm, Ca 422.673 nm, Sr 421.552 nm, Sc 361.383 nm and Mg 280.271 nm). Intensities of the two Ca lines were

averaged to compensate for possible plasma-induced variations in signal intensity. Measurements of a laboratory coral standard after each sample allowed offline correction for instrumental drift. Relative standard deviation of the Sr/Ca determinations was better than 0.2%.

2.2.2.6 Coral chronology

An average of 11.8 samples per year ranging from 8 to 14 has been extracted from the dense theca wall over 40 couplets of high- and low-density bands. The age model for the coral chronology is based on the seasonal banding pattern seen in the X-radiographs (Figure 2.9a) and the annual cycles in the skeletal Sr/Ca record. We assume that no significant changes the timing of the seasonal

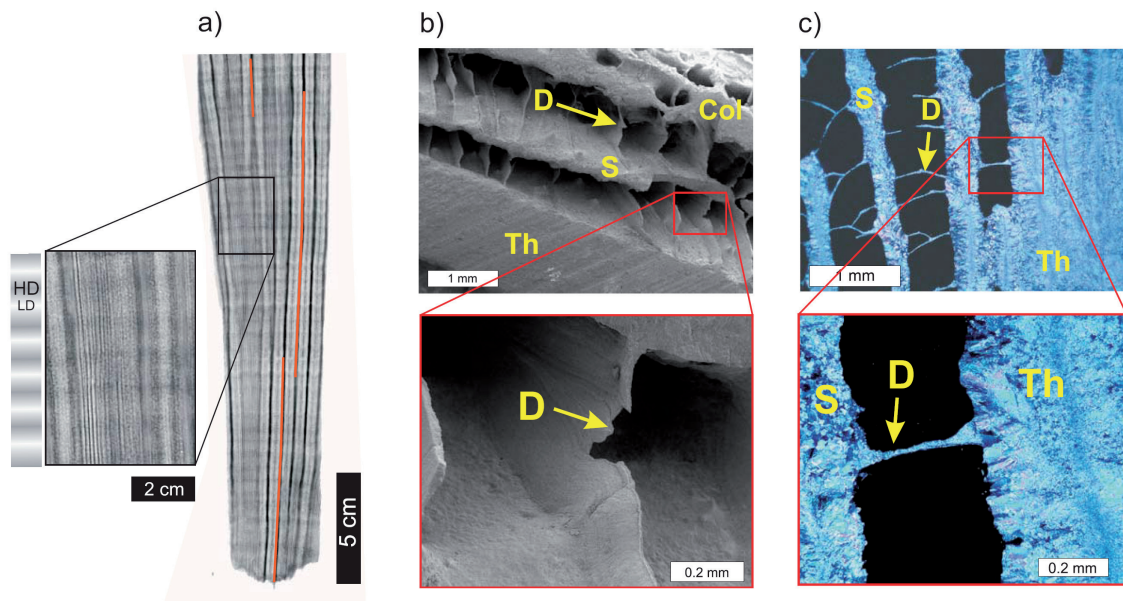


Figure 2.9: Investigation of the skeleton of the 2.35 ka BP Bonaire coral for possible diagenetic alteration. a) X-radiograph positive print of the coral slab (position of microsampling paths indicated by red lines) shows that powdered microsamples were extracted along the dense theca wall over annual couplets of high- and low-density bands (HD and LD, respectively). b) Scanning electron microscope images and c) thin section photomicrographs performed on samples from the centre of the slab reveal that individual skeletal elements such as theca (Th), septa (S), columella (Col) and dissepiments (D) have smooth surfaces with no indication for overgrowth by diagenetic cements, resulting in an excellent preservation of primary porosity of the coral skeleton.

maximum and minimum of SST occurred during the late Holocene. Therefore, maximum and minimum Sr/Ca values in any given year were assigned to the coldest (February) and warmest month (October) of present-day conditions, and subsequently interpolated to a monthly resolution following established procedures (Felis et al., 2000; Felis et al., 2004; Felis et al., 2009). The skeletal annual extension rate was calculated by using the distance from a maximum Sr/Ca value in a given year to the maximum value of the following year and annual mean Sr/Ca was calculated by averaging monthly data of each year.

2.2.3 Results and discussion

2.2.3.1 Preservation of coral skeleton

Diagenetic alterations such as dissolution, secondary precipitation of inorganic aragonite and calcite are known to influence the Sr/Ca ratio of coral skeletons (McGregor and Gagan, 2003; Cohen and Hart, 2004; Hendy et al., 2007; McGregor and Abram, 2008). XRD reveals a calcite content of <0.5 %. X-radiographs of the coral slab do not reveal anomalous density patches that are typical for diagenetic textures (Figure 2.9a). SEM analyses show a smooth surface of individual skeletal elements without any overgrowth or dissolution patterns (Figure 2.9b). Thin sections reveal that biogenic aragonite crystals are not overgrown by diagenetic cements and that centres of calcification are not dissolved (Figure 2.9c). In summary, diagenetic investigation of the 2.35 ka BP coral reveals that the skeleton is pristine. Therefore, we conclude that the Sr/Ca variability discussed in the next section is not affected by diagenetic alteration.

2.2.3.2 Coral Sr/Ca record

The 40-year long monthly resolved record shows clear annual cycles in Sr/Ca with average amplitude of 0.206 mmol/mol and displays interannual variability (Figure 2.10a). The Sr/Ca interannual variability calculated by the standard deviation of the annual mean Sr/Ca record is 0.028 mmol/mol. Using a relationship of -0.041 mmol/mol per °C, based on a monthly coral Sr/Ca-SST regression of a *Diploria strigosa* from Guadeloupe (Hetzinger et al., 2006), our coral record suggests that the average amplitude of the annual cycle of SST at 2.35 ka BP was 4.9 °C with an estimated interannual variability of 0.7 °C. However, using the commonly used relationship between coral Sr/Ca and SST of -0.06 mmol/mol per °C (Corrège, 2006) our proxy record indicates an average seasonality and interannual variability of 3.4 °C and 0.5 °C, respectively.

Observations of instrumental SST around Bonaire taken from the SODA reanalysis data set (gridbox centred at 68.25°W; 12.25°N) (Carton and Giese, 2008) for a 40-year period (1960-2000) reveals that the modern amplitude of the annual cycle and interannual variability is about 2-3 °C and 0.35 °C, respectively. These observations suggest that slightly higher SST seasonality and interannual variability compared to today are recorded in the Sr/Ca of the 2.35 ka BP coral.

Recent understanding in the calcification and architecture of the skeleton of brain corals revealed some problems related to microsampling such corals. Time-transgressive problems associated with microsampling the convoluted walls of slow-growing *Diploria* sp. and thus, integration of skeletal material precipitated at different months are known to

produce a dampened seasonal cycle (Cohen et al., 2004). Although our record is retrieved from a similar convoluted skeletal element of a *Diploria strigosa* coral growing at a rate of 0.62 cm per year, such problems can not explain the higher amplitude of the annual cycle of SST relative to today reconstructed from the 2.35 ka BP coral. Incorporation of strontium into the skeleton of *Diploria* sp. has been shown to be partially related to the annual extension rate, where annual mean Sr/Ca in some colonies is negatively correlated with annual growth-rate (Goodkin et al., 2005; Goodkin et al., 2007). In our study, the annual skeletal extension rate was calculated as the

distance from a maximum Sr/Ca value in a given year to the maximum value of the following year. The non-significant correlation ($r = 0.08$) between annual extension rate and the corresponding annual mean Sr/Ca suggests that extension rate is not affecting the skeletal Sr/Ca signal on interannual and longer timescales. Moreover, to ensure that there is in fact no influence of growth rate on the Sr/Ca signal, we further investigate the relationship between seasonal Sr/Ca and growth. Work by Goodkin et al., (2005) found differences in the winter and summer season calibrations to SST attributed to seasonal variations of extension rate. This study examined the relationship

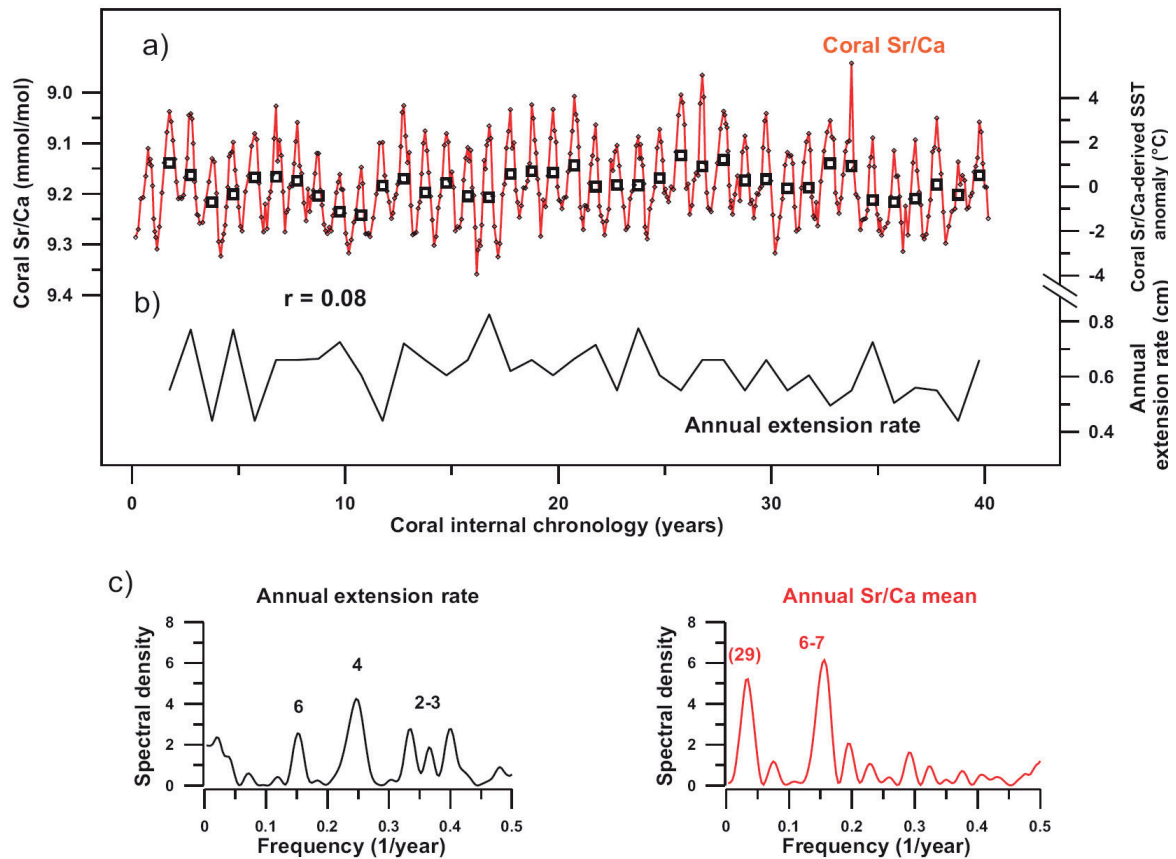


Figure 2.10: a) A 40-year long monthly resolved Sr/Ca record from a 2.35 ka BP coral from Bonaire (red line) reveals clear annual cycles and interannual variability. The corresponding annual mean record is also shown (open squares). Coral Sr/Ca-derived sea surface temperature anomaly is calculated by using the regression slope of -0.041 mmol/mol per $^{\circ}\text{C}$ from Hetzinger et al., (2006). The non-significant correlation between annual extension rate b) and the corresponding annual mean Sr/Ca record ($r = 0.08$) suggests that coral growth is not affecting skeletal Sr/Ca on interannual and longer timescales. c) Spectral analyses of the records of annual extension rate and annual mean Sr/Ca reveal that these two parameters seem to be influenced by distinct forcing. Prominent periodicities are indicated (years).

between Sr/Ca and annual growth rate and they found that the summer Sr/Ca correlates strongly to annual skeletal extension rate whereas winter Sr/Ca showed no correlation to growth rate. Their observation suggests that subannual changes in growth rate affect the Sr/Ca signal. Although a potential relationship between Sr/Ca and SST on seasonal timescales can not be investigated in our fossil coral, we found that seasonal Sr/Ca values for winter, spring, summer and fall do not show any significant correlations with annual extension rate (not shown). Therefore, we assume that a seasonal growth dependence of Sr/Ca observed in slow-growing *Diploria labyrinthiformis* corals from Bermuda (Cohen et al., 2004; Goodkin et al., 2005) is not affecting the Sr/Ca in our fossil *Diploria strigosa* coral from Bonaire.

2.2.3.3 Southern Caribbean interannual SST variability at 2.35 ka BP

Spectral analysis of the annual mean Sr/Ca record exhibits a dominant periodicity of 6-7 years (Figure 2.10c). Another spectral peak centred around 29 years is beyond the limit of low-frequency variability that can be inferred from the data, given the length of the time series (40 years). Spectral analysis of the annual growth-rate record indicates a dominant periodicity of 4 years which is not seen in the spectral analysis of the Sr/Ca record (Figure 2.10c). The discrepancies in the results of spectral analysis between annual growth rate and annual mean Sr/Ca further strengthen our conclusion that the Sr/Ca signal on interannual and longer timescales is not affected by growth rate, and therefore reflects past SST variability.

Instrumental observations of Southern Caribbean climate have demonstrated that

regional SST variations are linked to the strength and direction of trade winds which also control the regional evaporation/precipitation ratio (Giannini et al., 2000). The atmospheric circulation over the Southern Caribbean is controlled by the competing influence of modes of climate variability such as ENSO, NAO and AMO that control the magnitude of SST variability in tropical Atlantic sector (Hurrell et al., 2006). Modern coral records from western Atlantic Ocean have demonstrated the non-stationary features of low-latitude Atlantic multidecadal climate variability (Saenger et al., 2009). Moreover, instrumental observations reveal that the interannual component of SST variability is non-stationary making accurate climate forecasts more difficult to achieve (Sutton and Hodson, 2003). In this context, our preliminary finding that interannual variability in Southern Caribbean SST at 2.35 ka BP was dominated by a 6-7 year periodicity, which is not observed in our spectral analysis of regional SST (Carton and Giese, 2008) (not shown), support the non-steady behaviour of tropical Atlantic climate during the late Holocene. Future work on extending this Sr/Ca record over the entire growth period of the coral (>60 years) will provide a more robust estimate of interannual variations in Southern Caribbean SST during the late Holocene.

2.2.4 Conclusions

The present study investigates the potential of a fossil *Diploria strigosa* coral from Bonaire for reconstructing Southern Caribbean SST variability during the Holocene. The results suggest that fossil corals from this open-ocean island provide a unique opportunity for reconstructing interannual SST variability

because of their well-preserved skeleton and extension-rate independent skeletal Sr/Ca ratio on interannual and longer timescales. Our record provides the first monthly resolved Sr/Ca-based SST reconstruction of the Southern Caribbean Sea for preindustrial time and suggests that annually-banded fossil corals from Bonaire can provide seasonal and interannual oceanographic information of the Southern Caribbean sea surface during the Holocene. Furthermore, future work on paired analyses of Sr/Ca and $\delta^{18}\text{O}$ of Holocene corals will provide new insights into both SST and hydrology variability of the Southern Caribbean Sea on seasonal and interannual timescales, e.g., during intervals when the nearby Cariaco Basin sediments document highly variable hydrological conditions over northern South America. Finally, monthly-resolved Sr/Ca and $\delta^{18}\text{O}$ coral records from Bonaire are expected to shed more light on Pacific versus Atlantic and tropical versus extratropical controls on Southern Caribbean climate during the Holocene.

Acknowledgments

We thank the Government of the Island Territory of Bonaire (Netherlands Antilles) for research and fieldwork permission, Elsmarie Beukenboom (STINAPA Bonaire National Parks Foundation) for support, J. Pätzold for support with coral drilling and discussion, M. Kölling and S. Pape for Sr/Ca analyses, K.-H. Baumann for SEM analyses, D. Scholz, H. Kuhnert and M. McCulloch for discussion and two anonymous reviewers for valuable suggestions that greatly improved this manuscript. This work was funded by Deutsche Forschungsgemeinschaft (DFG) under the Special Priority Programme INTERDYNAMIC, through a grant to T.F. (FE 615/3-1; CaribClim). C.F. was supported by DFG (MA 821/37-1; CaribClim). C.G. acknowledges INTERDYNAMIK (DFG) for a travel grant to attend the PAGES YSM/OSM and additional support by GLOMAR (Bremen International Graduate School for Marine Sciences) that is funded by DFG.

2.3 Mid- to late Holocene changes in tropical Atlantic temperature seasonality and interannual to multidecadal variability documented in southern Caribbean coral records

Cyril Giry¹, Thomas Felis¹, Martin Kölling¹, Denis Scholz², Wei Wei³ and Sander Scheffers⁴

¹ MARUM - Center for Marine Environmental Sciences, University of Bremen, 28359 Bremen, Germany

² Heidelberger Akademie der Wissenschaften, Forschungsstelle Radiometrie, 69120 Heidelberg, Germany.

Now at Institute for Geosciences, University of Mainz, 55128 Mainz, Germany

³ Alfred Wegener Institute for Polar and Marine Research, 27570 Bremerhaven, Germany

⁴ School of Environmental Science and Management, Southern Cross University, PO 147 Lismore, Australia.

Submitted to *Earth and Planetary Science Letters*

Abstract: Proxy reconstructions of tropical Atlantic sea surface temperature (SST) that extend beyond the period of instrumental observations have primarily focused on centennial to millennial variability rather than on seasonal to multidecadal variability that is of relevance for reliable predictions of hazardous climate phenomena in this region. Here we present monthly-resolved records of Sr/Ca (a proxy of SST) from fossil annually-banded *Diploria strigosa* corals from Bonaire (southern Caribbean Sea). The individual corals provide time-windows of up to 68 years length, and the total number of 295 years of record allows for assessing the natural range of seasonal to multidecadal SST variability in the western tropical Atlantic during snapshots of the mid- to late Holocene. Comparable to modern climate, the coral Sr/Ca records reveal that mid- to late Holocene SST was characterised by clear seasonal cycles, persistent quasi-biennial and prominent interannual and inter- to multidecadal-scale variability. However, the magnitude of SST variations on these timescales has varied over the last 6.2 ka. The coral records, combined with climate model simulations reveal that southern Caribbean SST seasonality is influenced by insolation changes on orbital timescales, whereas internal dynamics of the climate system play an important role on shorter timescales. Interannual SST variability is linked to ocean-atmosphere interactions of Atlantic and Pacific origin. Pronounced interannual variability in the western tropical Atlantic is identified in the 2.35 ka coral, consistent with a strengthening of the variability of the El Niño/Southern Oscillation throughout the Holocene. Persistent inter- to multidecadal SST variability, possibly linked to Atlantic multidecadal variability, is evident in the coral records with enhanced amplitude in the mid-Holocene. Our coral data imply that short-term SST variability in the tropical Atlantic over the last 6.2 ka has arisen from dynamics internal to the climate system itself. This strengthens the need to fully understand the mechanisms underlying such natural variability.

Citation: Giry, C., T. Felis, M. Kölling, D. Scholz, W. Wei and S. Scheffers: *Mid- to late Holocene changes in tropical Atlantic temperature seasonality and interannual to multidecadal variability documented in southern Caribbean coral records*, (submitted).

2.3.1 Introduction

Improving skills in predicting climate phenomena that have large socio-economic impacts in the tropical Atlantic region (e.g., hurricane activity, Nordeste and Sahel rainfalls) relies on a better understanding of the forcing mechanisms that control regional sea surface temperature (SST) variability on seasonal and interannual to multidecadal timescales. Unlike the tropical Pacific, the tropical Atlantic is dominated by the competing influence of modes of climate variability emanating from tropical and extratropical oceans (Marshall et al., 2001; Czaja et al., 2002; Czaja, 2004; Hurrell et al., 2006) modulating the strength of the trade winds that affects SST and the distribution and intensity of rainfall over the surrounding landmasses (Enfield and Mayer, 1997; Giannini et al., 2000; Giannini et al., 2001b; Chiang et al., 2002). Mechanisms involved in SST variability in the Caribbean region are linked to sea level pressure (SLP) variations in the North Atlantic region (Hastenrath, 1984) mainly through changes in surface winds that in turn, affect the dynamics of the Atlantic Warm Pool (AWP) (Wang et al., 2007, 2008a). The AWP is a large body of water warmer than 28.5°C (Figure 2.11) which experiences modulations on several timescales including seasonal (Wang and Enfield, 2003), interannual (Wang et al., 2006; Wang et al., 2008a) and multidecadal (Wang et al., 2008b). During its maximum extent in boreal summer, the AWP affects summer climate of the western Hemisphere (Wang et al., 2006; Wang et al., 2007) and can induce thermal stress to coral reefs, as observed in the Caribbean in 2005 (Eakin et al., 2010). On interannual and multidecadal timescales, the AWP is modulated by the El Niño/Southern Oscillation (ENSO) and the Atlantic Multidecadal Oscillation (AMO)

(Wang et al., 2008a), respectively. The knowledge of tropical Atlantic SST variability on these timescales is based on short and sparse instrumental data. Proxy reconstructions from the tropical Atlantic that extend beyond the observational period have primarily focused on long-term changes in climate variability rather than focusing on short-term variability (i.e., seasonal to multidecadal), which is more relevant for predicting hazardous climate phenomena in this region.

We use a unique high-resolution climate archive, fossil annually-banded *Diploria strigosa* brain corals from the island of Bonaire (southern Caribbean Sea), to investigate patterns of short-term SST variability recorded in the strontium (Sr) to calcium (Ca) ratio of their skeletons (Smith et al., 1979; Beck et al., 1992) during the Holocene. Variations of Sr/Ca in massive corals are an established proxy for SST variability on seasonal (Gagan et al., 1998; Felis et al., 2004) and interannual to multidecadal timescales (Linsley et al., 2000; Felis et al., 2009), even during specific seasons of the year (Kuhnert et al., 2005; Hetzinger et al., 2006; Felis et al., 2010). Recent studies have shown that Sr/Ca records from modern *D. strigosa* corals are excellent proxies for seasonal and interannual to multidecadal variations in local to regional SST in the Caribbean (Hetzinger et al., 2006; Hetzinger et al., 2010). Our well-preserved fossil *D. strigosa* corals from Bonaire range in age up to 6220 years before present (BP) and provide unusually long time-windows of up to 68 years. U-series ages reveal that the individual corals represent snapshots throughout the mid- to late Holocene, which allows for evaluating reconstructed southern Caribbean SST

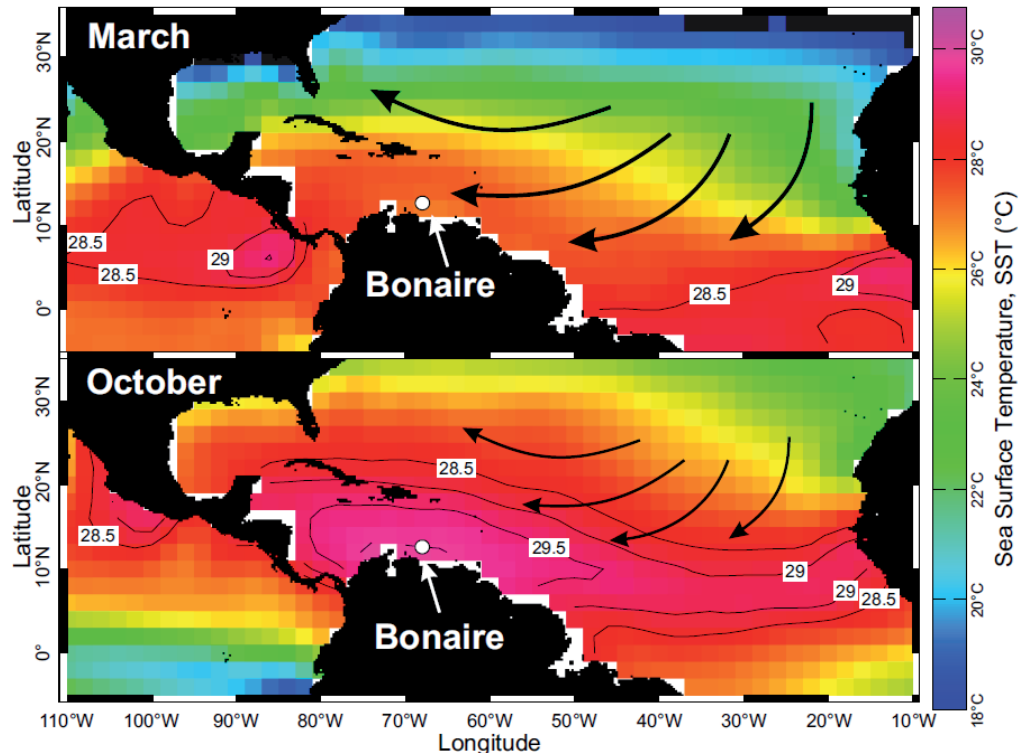


Figure 2.11: Sea surface temperature (SST) maps for March (*top*) and October (*bottom*) representing the months of minimum and maximum SST around Bonaire (*white circle*) (Smith et al., 2008). Maps are for the year 2010. Thin contour lines reveal SST warmer than 28.5°C that is characteristic of the Atlantic Warm Pool. Black arrows illustrate the direction and strength of dominant surface winds associated with the North Atlantic subtropical high.

variability under different climate background states.

Seasonal changes in insolation received in the northern and southern Hemisphere have significant effects on global climate variations (Wanner et al., 2008). The mid-Holocene was characterized by a stronger seasonality of insolation in the Northern Hemisphere which then steadily decreased toward the present (Berger, 1978). Holocene changes in insolation may have influenced the spatial distribution of surface heating and therefore, may have resulted in direct changes in temperature seasonality or in different oceanic and atmospheric circulation regimes. In addition, on shorter timescales, further mechanisms linked to both insolation changes on suborbital timescales (i.e., solar variability) and internal variability of

the climate system may have played a role in modulating Holocene climate change. Studies of past tropical Atlantic SST variability have essentially relied on foraminiferal $\delta^{18}\text{O}$ and Mg/Ca as well as alkenones in marine sediments providing insights into decadal to millennial scale variability (e.g., Rühlemann et al., 1999; Lea et al., 2003; Tedesco and Thunell, 2003). Our Bonaire coral Sr/Ca records allow us to investigate southern Caribbean SST variability at subseasonal resolution. We identify yet non-investigated fundamental features of tropical Atlantic climate variability and assess the natural range of seasonality and interannual to multidecadal SST variability in the southern Caribbean Sea during the mid- to late Holocene.

2.3.2 Material and Methods

2.3.2.1 Climatic setting of the study area

Bonaire (Netherlands Antilles) is an open-ocean island in the southern Caribbean Sea ($\sim 12^{\circ}10'N$, $68^{\circ}18'W$), located ~ 100 km north of Venezuela (Figure 2.11). The island has a tropical-arid climate characterised by low annual rainfall (~ 500 mm/year) and influenced by easterly trade winds. These also referred to as Caribbean low-level jet (CLLJ) (Wang and Lee, 2007; Muñoz et al., 2008) vary with Caribbean SLP anomalies that are connected to the North Atlantic subtropical high. Wang (2007) found that during both summer and winter Caribbean SST is negatively correlated with the strength of the CLLJ. Cold (warm) Caribbean SST anomalies are associated with high (low) SLP anomalies that are consistent with a strong (weak) CLLJ. A relatively high correlation

between the CLLJ and SST has been reported for the southern Caribbean Sea (Wang, 2007).

The monthly SST time series representative of a $2^{\circ} \times 2^{\circ}$ gridbox centred on Bonaire ($12^{\circ}N$; $68^{\circ}W$) (Smith et al., 2008) reveals pronounced annual cycles with a mean maximum of $28.6^{\circ}C$ in September/October and a mean minimum of $25.7^{\circ}C$ in February/March for the period 1930-2000 (Smith et al., 2008), indicating a SST seasonality of $2.9^{\circ}C$. Observational studies have shown that northern tropical Atlantic SST variability is remotely affected by the competing influence of ENSO and the North Atlantic Oscillation (NAO) on the strength of surface winds inducing changes in latent heating that in turn, generate SST anomalies (Czaja et al., 2002). Not all ENSO events manifest in exactly the same manner in the Caribbean Sea (Wang and Lee, 2007).

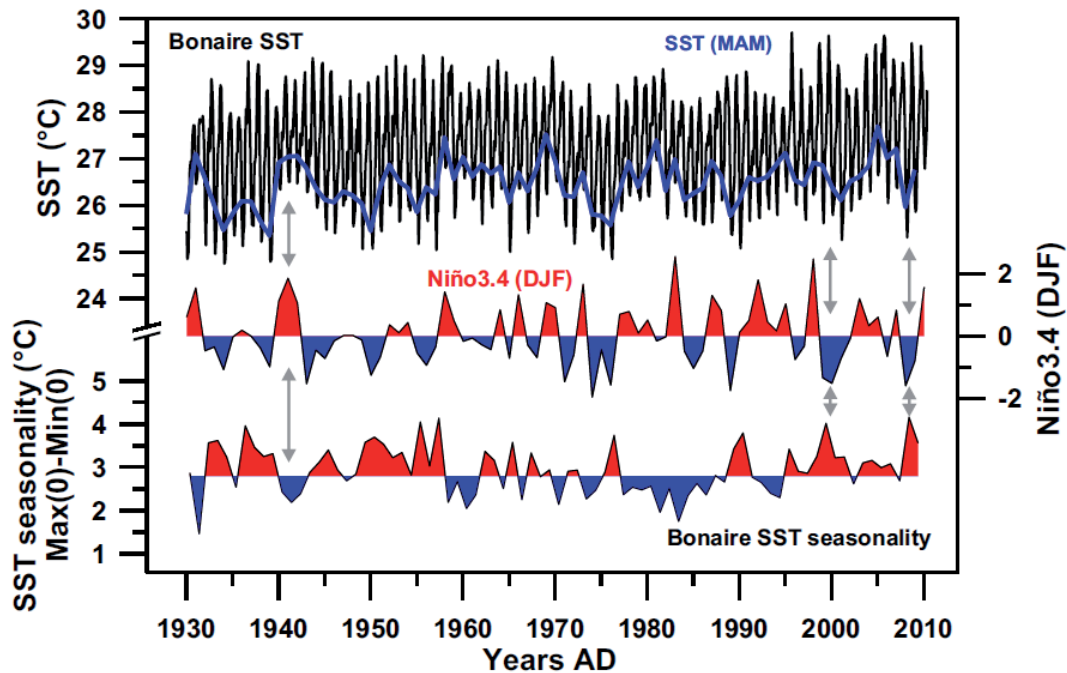


Figure 2.12: Monthly sea surface temperature (SST) for a $2^{\circ} \times 2^{\circ}$ gridbox centred on Bonaire ($12^{\circ}N$; $68^{\circ}W$) (ERSSTv3b (Smith et al., 2008)) (*top*). The March-April-May (MAM) Bonaire SST time series (*blue line*) is positively correlated ($r=0.61$) with the December-January-February (DJF) Niño3.4 index (Kaplan et al., 1998; Reynolds et al., 2002) (*middle*). SST seasonality (*bottom*) calculated as the difference between monthly maximum and minimum SST values in a single year, displays an inverse relationship with the Niño3.4 index (DJF) ($r=-0.48$). Gray arrows indicate major El Niño/La Niña events that were followed by anomalous SST seasonality around Bonaire.

There are some El Niño events that result in significant warm SST anomalies, while during other El Niño years no significant effects on SST are observed in the Caribbean. Instrumental observations have suggested that the NAO can play a key role in inhibiting the ENSO effect in the Caribbean resulting in a complex signal. For instance, a positive (negative) NAO phase implies stronger (weaker) than normal surface winds entering the Caribbean thus, generating negative (positive) SST anomalies (Giannini et al., 2001a). El Niño-related atmospheric anomalies are known to force a lagged warming of tropical North Atlantic (relative) SST through the weakening of the northeasterly trade winds and consequent reduction of surface fluxes (Giannini et al., 2004). Mature phases of ENSO occurring usually in December-January-February (DJF) affect remotely, via the so-called “atmospheric-bridge”, northern tropical Atlantic SST in spring (March-April-May: MAM) with a lag of 3-5 months (Enfield and Mayer, 1997). As shown in Figure 2.12, the high correlation ($r=0.61$) between the Niño3.4 index (DJF) and MAM Bonaire SST confirms that under present-day conditions ENSO-related atmospheric anomalies have a delayed influence on southern Caribbean SST. Moreover, given that ENSO affects primarily Bonaire SST anomalies in spring (MAM), the coldest season; it is indeed evident that the remote influence of ENSO affects Bonaire SST seasonality. El Niño events result in reduced amplitude and La Niña events result in increased amplitude of Bonaire SST seasonality (Figure 2.12). It is generally believed that interannual SST variability in the tropical North Atlantic is stronger (weakest) in boreal spring (early fall) (Czaja, 2004) which reflects primarily the remote forcing by NAO and ENSO,

but also the strength of local ocean–atmosphere coupling.

2.3.2.2 Coral collection and diagenetic investigations

Along the coast of Bonaire, prominent deposits of hurricane and/or tsunami origin occur. Those deposits consist of reef boulders and fossil coral colonies of Holocene age (Scheffers, 2004; Scheffers and Scheffers, 2006). Six fossil *Diploria strigosa* colonies recovered from these coastal deposits were drilled along the major growth axis. Similarly, two dead modern *D. strigosa* colonies from a storm deposit formed by hurricane Ivan in 2004 (Scheffers and Scheffers, 2006) were drilled. For calibration, a core from living *D. strigosa* was retrieved. Sampling sites are displayed in Supplementary Figure 1. Coral cores were cut along the growth direction using a circular diamond saw and 6-7 mm thick slabs were sliced from individual half-cores. Slabs were cleaned for 10 min in an ultrasonic bath, and then placed in a drying oven at 50°C overnight and subsequently X-rayed for 7 min at 45 kV. X-radiographs of the coral slabs are shown in Figure 2.13.

All corals used in this study were investigated for possible diagenetic alteration of their skeleton using different methods. First, the slabs were X-rayed in order to identify both the annual density-banding pattern and areas or patches of anomalously high density potentially reflecting diagenetic alterations such as secondary aragonite or calcite infillings. Slabs that did not show suspicious areas were further investigated for potential diagenetic textures by powder X-ray diffraction (XRD) analysis,

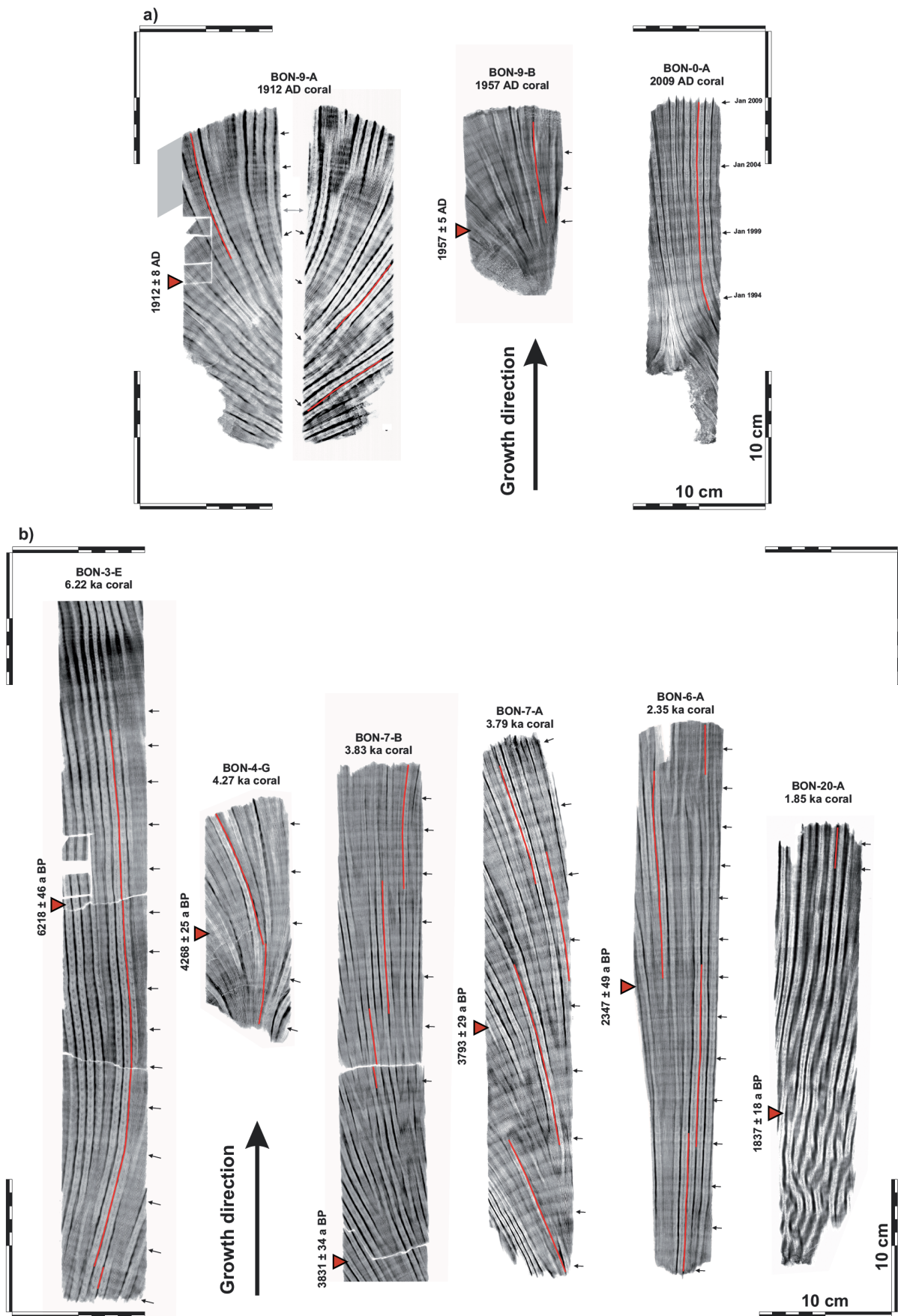


Figure 2.13: X-radiograph positive prints of slabs of a) modern and b) fossil Bonaire *Diploria strigosa* corals reveal the annual density banding pattern. Red lines indicate the position of the microsampling transects along the centre of the thecal walls. Red triangles indicate where samples for U/Th dating and diagenetic screening were taken. Black arrows indicate 5-year intervals based on annual high-density bands and grey shading marks changes in annual extension rate in coral BON-9-A.

Scanning Electron Microscope (SEM) imaging and thin-section microscopy, using a sample representative for the entire slab that was extracted from an area in the centre of the slab. XRD was applied in order to quantify the calcite content of the sample. As crystals of inorganic aragonite cannot be detected with XRD, SEM and thin-section microscopy were used to identify the presence of secondary aragonite.

2.3.2.3 $^{230}\text{Th}/\text{U}$ -dating of corals

$^{230}\text{Th}/\text{U}$ -dating was conducted on individual corals at the Heidelberg Academy of Sciences, Heidelberg, Germany. Analyses were performed with a Finnigan Thermal Ionization Mass Spectrometer MAT 262 RPK. Sample preparation and analytical details are similar as described in Scholz et al. (2004). Calibration of the added U and Th spike solutions is described in Hoffmann et al. (2007). Ages were calculated using the half-lives of Cheng et al. (2000). All ages were corrected for the effect of detrital contamination assuming a bulk earth $^{232}\text{Th}/^{238}\text{U}$ weight ratio of 3.8 and secular equilibrium between ^{238}U , ^{234}U and ^{230}Th . The reliability of the determined $^{230}\text{Th}/\text{U}$ -ages was checked using established criteria (Scholz and Mangini, 2007), such as initial ($^{234}\text{U}/^{238}\text{U}$) in agreement with ($^{234}\text{U}/^{238}\text{U}$) of modern seawater (i.e., 1.1466 ± 0.0025 , (Robinson et al., 2004)) and U concentrations comparable to modern corals of the same species. For the studied fossil corals all these criteria are fulfilled. Thus, their ages are considered as reliable. U/Th ages are presented in years before 1950 AD, with 2σ -error (Supplementary Table 1).

2.3.2.4 Microsampling, Sr/Ca analyses, chronology construction, time series analyses

Based on the annual-density banding pattern inferred from X-radiographs, we targeted a sampling resolution of about 12 samples per year. A combination of naked-eye observations of the slab-surface and density variations inferred from X-radiographs was used to identify the position and orientation of the dense thecal walls (Figure 2.13). Microsamples of skeletal powder were extracted by carefully drilling with constant sampling depth along the centre of the thecal wall using a 0.6 mm diameter bit. This careful sampling strategy has been successfully deployed and proved to yield the best signal of ambient SST variations (Giry et al., 2010a) and allowing to evaluate Sr/Ca variability at near-monthly resolution.

For Sr/Ca analyses, 0.25–0.30 mg coral powder was dissolved in 7 mL 2% suprapure HNO_3 containing 1 ppm Sc (Scandium) as internal standard. Measurements were performed on a Perkin-Elmer Optima 3300R simultaneous radial ICP-OES using a CETAC U5000-AT ultrasonic nebulizer at the Faculty of Geosciences, University of Bremen, Germany. Element wavelengths were detected simultaneously in 3 replicates (Ca 317.933 nm, Ca 422.673 nm, Sr 421.552 nm, Sc 361.383 nm and Mg 280.271 nm). Ca concentrations measured on an atomic line (422.673 nm) were averaged with the concentrations from an ionic line (317.933 nm) to compensate for possible sensitivity drift in a radial ICP-OES. Measurements of a laboratory coral standard after each sample allowed offline correction for instrumental drift. Relative standard deviation of the Sr/Ca determinations was better than 0.2%. Twenty five aliquots of the *Porites* coral powder reference material JCp-1 (Okai et al., 2002) were treated like samples and the average

Sr/Ca value obtained during the course of this study was 8.919 ± 0.008 mmol/mol.

Age models for coral Sr/Ca records are based on both annual density-banding patterns inferred from X-radiographs and annual cycles in Sr/Ca. We assumed that the timing of the annual SST cycle did not change during the investigated period, which is consistent with a climate model simulation (see section 3.3.2). Therefore, maximum and minimum coral Sr/Ca values in any given year were assigned to the on average coldest (February/March) and warmest months (September/October) according to present-day SST (Smith et al., 2008), respectively. Linear interpolation between these tie points resulted in time series that were subsequently interpolated to a monthly resolution following established procedures (Felix et al., 2009; Giry et al., 2010b). Skeletal annual growth rates were calculated as the distance from a maximum coral Sr/Ca value in a given year to the maximum value of the following year. Mean coral Sr/Ca values were calculated by averaging monthly data of each year and subsequently averaging the resulting annual means of all years. Coral Sr/Ca seasonality is defined as the difference between maximum and minimum monthly coral Sr/Ca values of a given year corresponding to the coldest and warmest months, respectively. Mean coral Sr/Ca seasonality was calculated by averaging the coral Sr/Ca seasonality of all years on record. We have applied Multitaper Method (MTM) spectral analysis with a red noise null hypothesis (Ghil et al., 2002) to the detrended and normalised coral Sr/Ca and instrumental SST records with the mean annual cycle removed.

2.3.2.5 Model description and experimental setup

The numerical experiments were performed with the coupled general circulation model ECHAM5/MPIOM/JSBACH developed by the Max-Planck-Institute for Meteorology that describes the dynamics of the atmosphere-ocean-sea ice-vegetation system (Marsland et al., 2003; Roeckner et al., 2003; Raddatz et al., 2007). The atmospheric model has a resolution of T31 ($3.75^\circ \times 3.75^\circ$) in horizontal and 19 vertical hybrid sigma pressure levels. The ocean part is run at $3^\circ \times 3^\circ$ averaged horizontal grid with 40 unevenly spaced vertical levels. We carried out two experiments: a pre-industrial (CTL) experiment and a mid-Holocene one (6 ka), by prescribing the appropriate orbital parameters and greenhouse gases, identical to those used in the Paleoclimate Modeling Intercomparison Project (PMIP) (Crucifix et al., 2005).

2.3.3 Results

2.3.3.1 Preservation of coral skeletons

The X-radiographs of the individual coral slabs (Figure 2.13) reveal clear annual-density banding patterns and do not indicate anomalous density patches that are typical for diagenetic alterations of the skeleton (Hendy et al., 2007). XRD analysis performed on fossil corals indicates calcite content $<0.5\%$ similar to that of the modern corals (Table 1.3). Thin sections indicate an excellent preservation of primary porosity of all coral skeletons, with no evidence for secondary aragonite or calcite cements (Figure 2.14). Furthermore, SEM analysis reveals that the skeletal elements of all corals have smooth surfaces free of both secondary

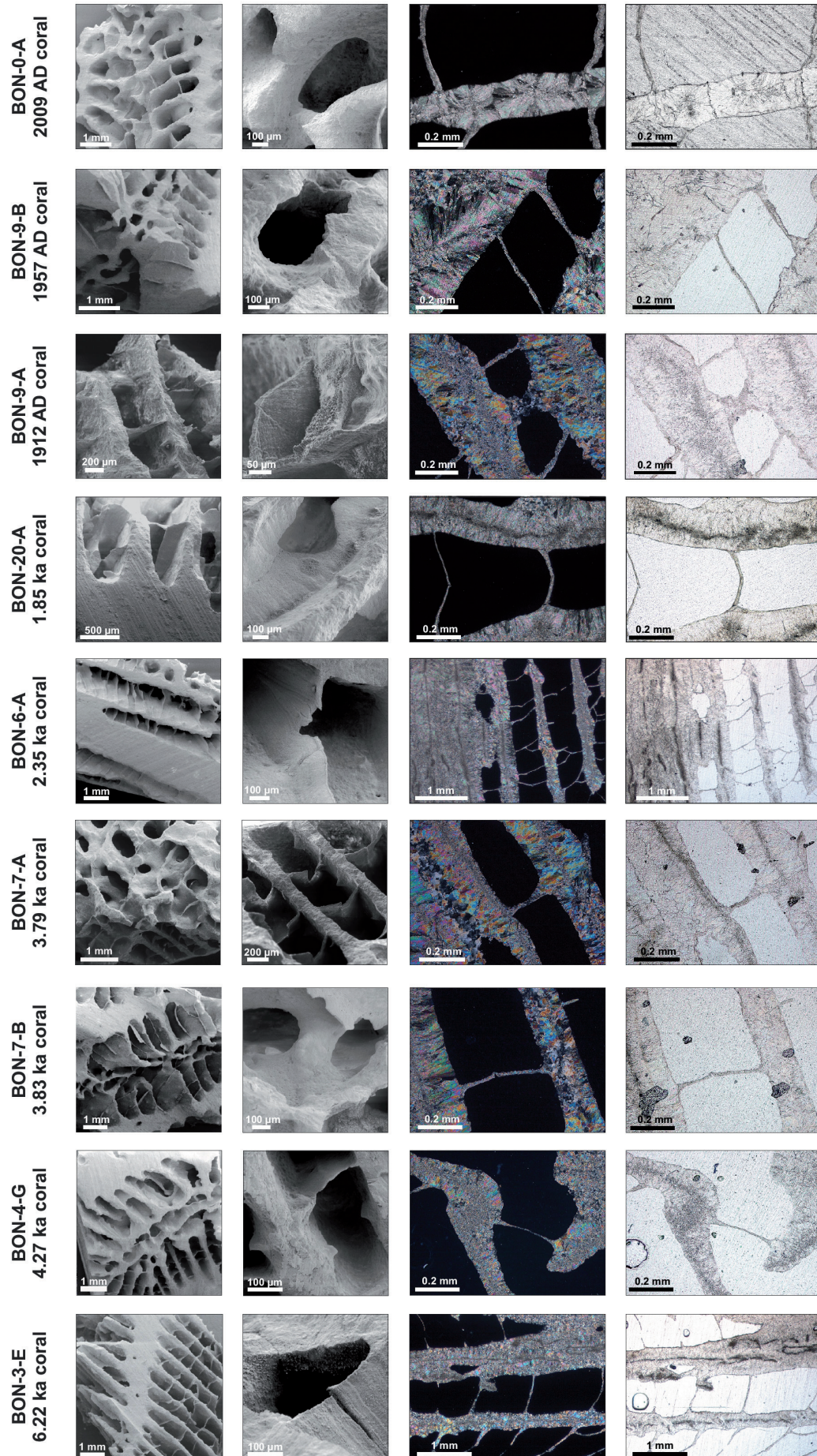


Figure 2.14: Scanning Electron Microscope images (*left and middle left*) and polarised- (*middle right*) and normal-light microscopy (*right*) of thin sections of Bonaire *Diploria strigosa* corals. Well-preserved skeletons are observed for both modern and fossil corals.

overgrowth and dissolution patterns. Dissepiments and especially the dense thecal walls, the target skeletal element for microsampling, are extraordinarily well preserved with no obvious differences between modern and fossil corals. Hence, our thorough diagenetic screening indicates that all corals used in this study have a pristine aragonitic skeleton, which is a prerequisite for reliable coral-based SST reconstructions.

2.3.3.2 Modern coral Sr/Ca-SST relationships

Reconstruction of SST variability from fossil corals requires a modern calibration of skeletal Sr/Ca. A rare calibration study of Sr/Ca variations in a modern *Diploria strigosa* is available from Guadeloupe in the Caribbean Sea (Hetzinger et al., 2006). This study reported significant Sr/Ca-SST relationships of -0.041 and -0.074 mmol/mol per °C for monthly and annual calibrations, respectively. We assess similar regression slopes for the *D. strigosa* collected live in Bonaire (BON-0-A) for the period 1993 to 2009. Monthly Sr/Ca correlates significantly with gridded SST data (Smith et al., 2008). The corresponding regression equation is:

$$\text{Sr/Ca (mmol/mol)} = -0.030(\pm 0.002) \times \text{SST} + 10.027(\pm 0.060) \quad (r^2=0.5, p<0.0001, N=188)$$

The regression equation for annual mean Sr/Ca values is:

$$\text{Sr/Ca (mmol/mol)} = -0.041(\pm 0.018) \times \text{SST} + 10.348(\pm 0.488) \quad (r^2=0.28, p=0.034, N=16).$$

Moreover, we investigate monthly Sr/Ca variability in reference to local SST data from Curaçao (an island ~80 km westwards), for a 18 months period spanning April 1999 to September 2000 (Bak et al., 2005). The resulting regression equation is:

$$\text{Sr/Ca (mmol/mol)} = -0.046(\pm 0.005) \times \text{SST} + 10.464(\pm 0.126) \quad (r^2=0.86, p<0.0001, N=18).$$

We note that when using local SST from a nearby island the slope of the regression equation is in the range of those typically reported for massive corals (Corrège, 2006) compared to using gridded SST data (Smith et al., 2008) for the same period.

U-series dating of the two dead modern corals (BON-9-A and BON-9-B) reveals ages of 1912 ± 8 years AD and 1957 ± 5 years AD, respectively. As the U/Th ages do not provide enough time constraint for direct comparison of coral Sr/Ca and instrumental SST records, we used the mean monthly climatologies of the corresponding time intervals for calibration (e.g., (Giry et al., 2010a)). The results show that Sr/Ca-SST relationships for BON-9-A and BON-9-B are -0.038 and -0.039 mmol/mol per °C,

Table 1.3: Details of the coral Sr/Ca records used in this study. Calcite contents were measured with X-ray diffraction.

| Sample ID | Age yr BP/AD ($\pm 1\sigma$) | Annual growth rate (cm/yr) ^b | Record length (yr) | Annual Mean Sr/Ca (mmol/mol) | STD (1 σ) | Standard error of the mean (1SE) | Sampling resolution (samples/yr) | Calcite content (%) |
|----------------------|-----------------------------------|--|-----------------------|---------------------------------|----------------------|-------------------------------------|-------------------------------------|------------------------|
| Modern corals | | | | | | | | |
| BON-0-A (living) | 2009 AD | 1.10 | 15 yr | 9.203 | 0.009 | 0.003 | 14.1 | ≤ 0.25 |
| BON-9-B (dead) | 1957 ± 5 AD | 0.75 | 13 yr | 9.062 | 0.025 | 0.007 | 14.6 | ≤ 0.5 |
| BON-9-A (dead) | 1912 ± 8 AD | 0.66 | 30 yr | 9.079 | 0.050 | 0.009 | 11.8 | ≤ 0.2 |
| Fossil corals | | | | | | | | |
| BON-20-A | 1837 ± 18 yr BP | 0.46 | 7 yr | 9.173 | 0.009 | 0.003 | 15.3 | ≤ 0.35 |
| BON-6-A | 2347 ± 49 yr BP | 0.61 | 68 yr | 9.178 | 0.028 | 0.004 | 11.2 | ≤ 0.5 |
| BON-7-A | 3793 ± 29 yr BP | 0.94 | 39 yr | 9.187 | 0.035 | 0.006 | 11.3 | ≤ 0.2 |
| BON-7-B | 3831 ± 34 yr BP | 0.71 | 33 yr | 9.272 | 0.028 | 0.005 | 13.0 | ≤ 0.5 |
| BON-4-G | 4268 ± 25 yr BP | 0.72 | 23 yr | 9.232 | 0.051 | 0.011 | 10.8 | ≤ 0.5 |
| BON-3-E | 6218 ± 46 yr BP | 0.63 | 67 yr | 9.289 | 0.052 | 0.007 | 11.4 | ≤ 0.5 |

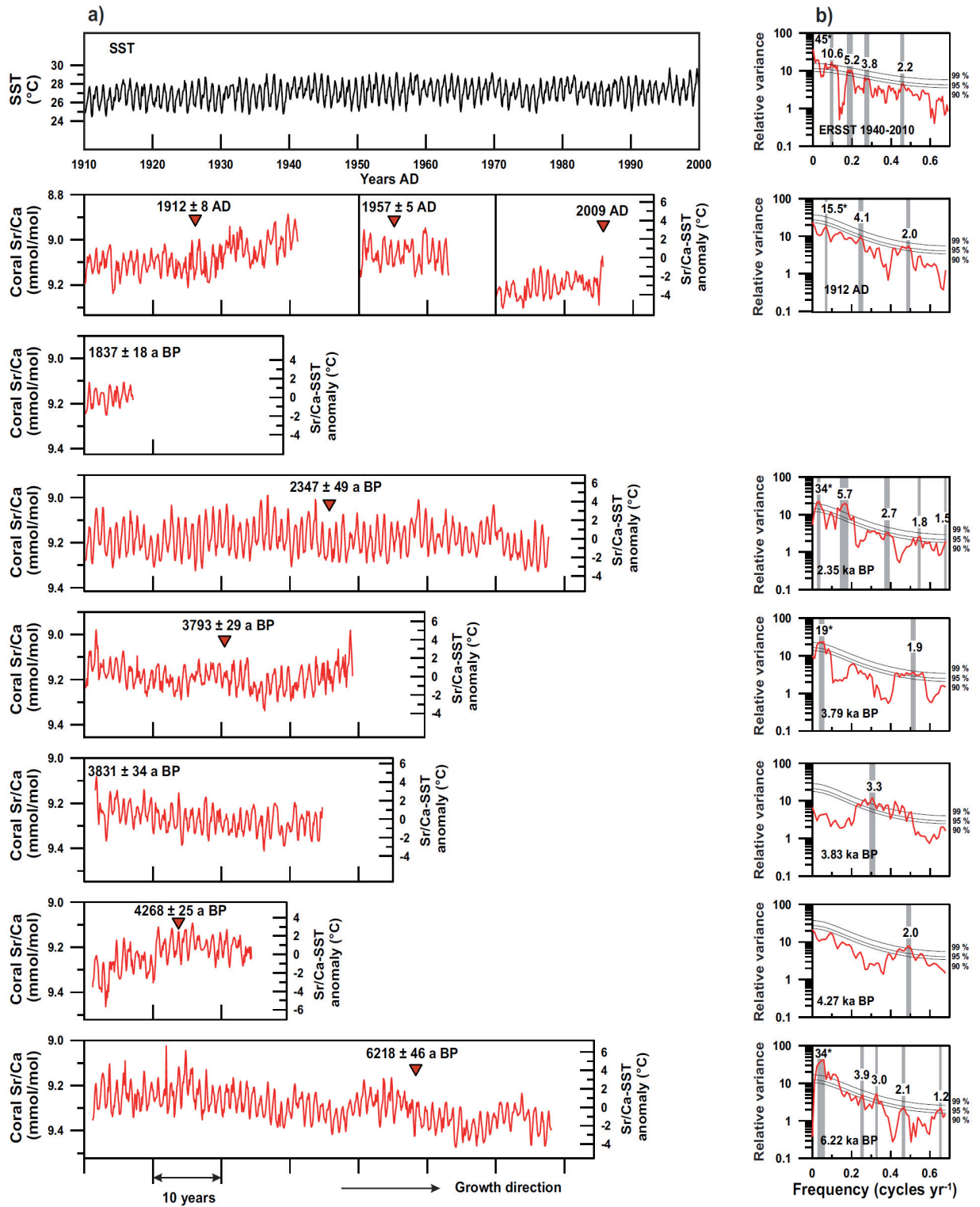


Figure 2.15: a) Monthly Bonaire coral Sr/Ca records and corresponding sea surface temperature (SST) anomalies. Monthly instrumental SST record for Bonaire ($2^{\circ} \times 2^{\circ}$ gridbox centred at 12°N ; 68°W) (Smith et al., 2008). U-series ages of individual corals are indicated (years before present; a BP). Coral Sr/Ca-based SST anomalies were calculated using the monthly relationship of -0.041 mmol/mol per $^{\circ}\text{C}$ (Hetzinger et al., 2006). b) Multitaper method (MTM) spectral analysis with a red noise null hypothesis (Ghil et al., 2002) (number of tapers 3; bandwidth parameter 2) of detrended and normalized coral Sr/Ca (of >20 years length) and SST records. 90%, 95%, and 99% significance levels and significant spectral peaks (in years) are indicated. Asterisk marks periodicities that are at the limit of detection with respect to the length of the time series.

respectively. These values are comparable to the ones previously published from Caribbean *D. strigosa* (Hetzinger et al., 2006). However, because the Hetzinger et al. (2006) coral Sr/Ca-SST relationships are based on more than 41 years we consider them as more robust, and use the corresponding monthly and annual relationships of -0.041 and -0.074 mmol/mol per $^{\circ}\text{C}$ for the interpretation of our coral Sr/Ca records.

2.3.3.3 Coral Sr/Ca-based SST variations throughout the mid- to late Holocene

The monthly-resolved coral Sr/Ca records of three modern and six fossil Bonaire corals provide a total of 295 years of record

since the mid-Holocene with individual time windows of up to 68 years length (Figure 2.15a). The records show clear annual cycles that correlate with the corresponding annual density-banding pattern in the coral skeleton. Therefore, robust internal chronologies could be established enabling accurate assessment of seasonal to multidecadal SST variability. Details of coral Sr/Ca records used in this study are displayed in Table 1.3.

2.3.3.3.1 Coral Sr/Ca-based variations in mean SST

The mean Sr/Ca values of the individual corals, based on monthly resolved records, are shown in Figure 2.16. The three corals which

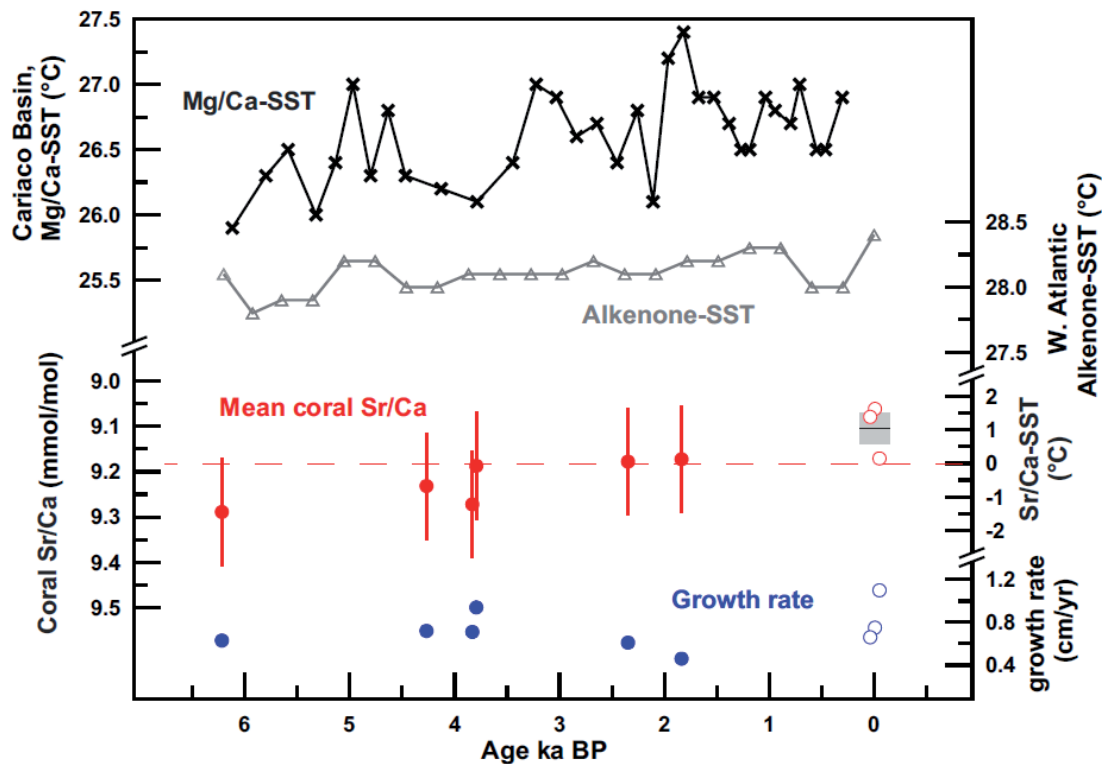


Figure 2.16: Comparison between Bonaire coral Sr/Ca-derived mean sea surface temperature (SST) estimates and other southern Caribbean Sea temperature reconstructions (Rühlmann et al., 1999; Lea et al., 2003). Error bars represent the combined error (root of the sum of the squares) of the standard deviation (2σ) of the mean Sr/Ca heterogeneity of three modern *Diploria strigosa* colonies and the standard error (2SE) of the mean Sr/Ca of each coral record, following established procedures (Abram et al., 2009). Dashed red line indicates the mean Sr/Ca value given by all mid- to late Holocene corals. The thin black line and gray area represent the mean Sr/Ca value given by the three modern corals and the corresponding standard error of the mean (2SE). Mean coral Sr/Ca-SST was calculated using the annual relationship of -0.074 mmol/mol per $^{\circ}\text{C}$ (Hetzinger et al., 2006). Note that mean Sr/Ca values are based on monthly records of up to 68 years length generated from individual corals.

grew during the last century exhibit between-colony offsets in mean Sr/Ca values ranging from 9.062 to 9.171 mmol/mol, which cannot be explained by corresponding SST changes (Smith et al., 2008). Such intercolony offsets have been reported for other massive corals and seem to be characteristic for some locations (Felis et al., 2004; Abram et al., 2009). The Bonaire intercolony variability in mean Sr/Ca has a standard deviation (1σ) of 0.059 mmol/mol. Using the annual relationship of -0.074 mmol/mol per °C (Hetzinger et al., 2006), this corresponds to a 1σ -uncertainty of ~0.8 °C. The mean coral Sr/Ca values of all 9 corals suggest a warming of the southern Caribbean since the mid-Holocene (Figure 2.16). Considering the combined error that takes into account modern intercolony offsets in mean Sr/Ca following established procedures (Abram et al., 2009) we find that cooler conditions at 6.22 ka BP are significant with respect to the average Sr/Ca value given by three modern corals. Taking into account the standard error of the mean, our result suggests that the southern Caribbean Sea was, at least, 0.4 °C cooler during the mid-Holocene than it is today. We note that the trend in mean coral Sr/Ca since the mid-Holocene cannot be attributed to any trend in mean coral growth rates (Goreau, 1977; de Villiers et al., 1995; Goodkin et al., 2007) (Table 1.3 and Figure 2.16) and thus, is interpreted to reflect SST changes.

2.3.3.3.2 Coral Sr/Ca-based SST seasonality

The Sr/Ca records of the three modern corals indicate a mean SST seasonality of 2.8 ± 0.3 °C (1SE) ranging from 2.3 to 3.1 °C (Figure 2.17), based on the monthly Sr/Ca-SST relationship of -0.041 mmol/mol per °C (Hetzinger et al., 2006), satisfactorily

documenting the present-day SST seasonality around Bonaire of 2.9 ± 0.1 °C (1SE) (1930-2000) (Smith et al., 2008). The between-colony differences in reconstructed SST seasonality cannot be attributed to actual differences in SST seasonality over the last century. Therefore, a combined error that takes into account modern intercolony differences (Abram et al., 2009) in coral Sr/Ca seasonality is considered for our estimates of Holocene SST seasonality (Figure 2.17).

The coral Sr/Ca records indicate a mean SST seasonality of 3.3 ± 0.3 °C (1SE) throughout the mid- to late Holocene. The 2.35 ka and the 6.22 ka corals indicate high SST seasonality. While the SST seasonality of 3.5 ± 1.0 °C at 6.22 ka BP is not significantly higher than modern values when taking into account our thorough error estimates, the 2.35 ka BP coral indicates a seasonality of 4.4 ± 1.0 °C that is significantly higher than both modern and mean mid- to late Holocene values. Spectral analysis of the coral Sr/Ca-SST seasonality records reveals significant interannual variability for almost all time intervals (Supplementary Figure 2).

2.3.3.3.3 Coral Sr/Ca-based interannual SST variability

Instrumental data reveal that SST variations around Bonaire were characterised by prominent quasi-biennial and interannual variability during the last century, with significant periodicities of 2.2, 3.8, and 5.2 years. The monthly coral Sr/Ca records indicate similar variability of SST at quasi-biennial and interannual periodicities during the mid- to late Holocene that is often superimposed on inter- to multidecadal variations (Figure 2.15). Significant

spectral peaks in the quasi-biennial (~ 2 -year) band are detected in almost all coral Sr/Ca records. Significant interannual variability ranging from 3 to 6 years is identified in most of the coral records. However, we note that the variance of interannual variability is relatively weak in the 6.22 ka coral record compared to that of 2.35 ka record and present-day SST variability, suggesting that the magnitude of interannual SST variability was reduced during the mid-Holocene (Figure 2.15). The 2.35 ka coral record displays significant variability at a prominent periodicity of 5.7 years that is

unprecedented in all other coral records. However, significant variability in the 5-6 year band is evident in instrumental records of SST around Bonaire.

2.3.3.3.4 Coral Sr/Ca-based inter- to multidecadal SST variability

Significant variance in the inter- to multidecadal band is detected in most of the coral Sr/Ca records as well as in instrumental Bonaire SST throughout the last century (Figure 2.15). Periodicities of 15.5, 19, and 34 years are identified in the coral records are, however, at

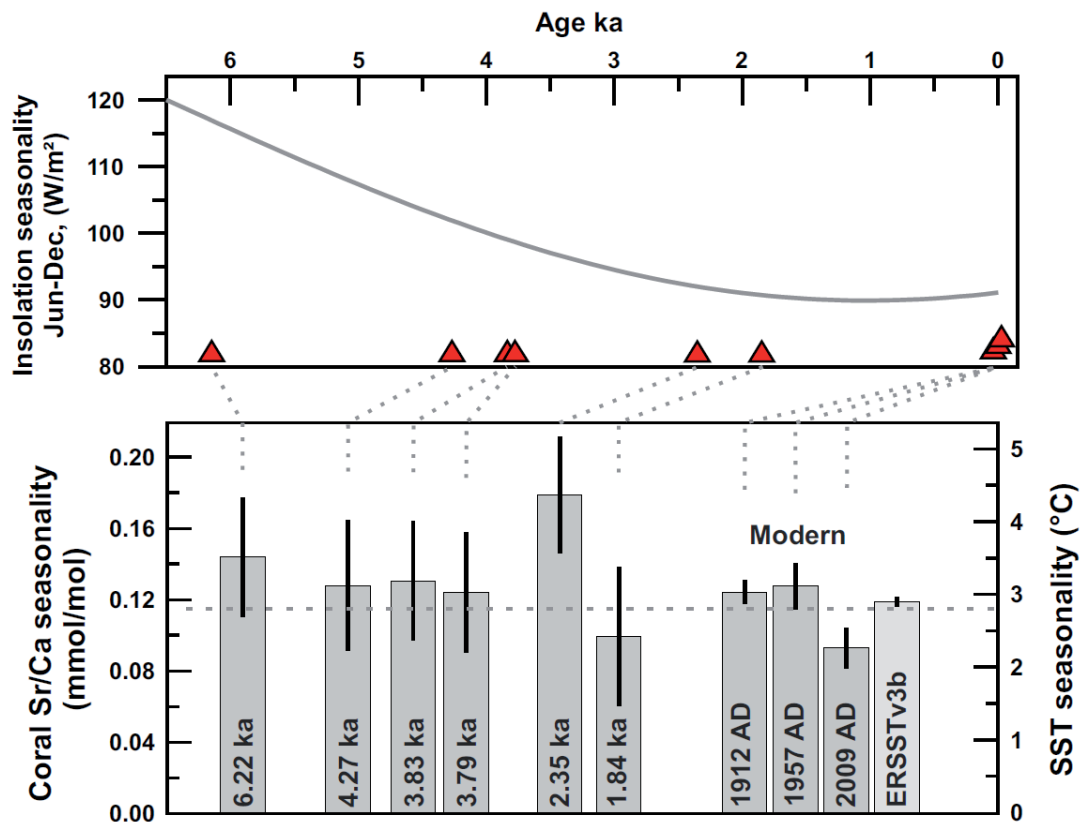


Figure 2.17: Top: Mid- to late Holocene change in seasonality of insolation (W/m^2) at the latitude of Bonaire (12.5°N) (Berger, 1978). Insolation seasonality is defined as the difference between June and December. **Bottom:** Bonaire coral Sr/Ca-derived SST seasonality calculated from individual coral records and instrumental SST data (1930-2000). Dashed line represents the mean modern Sr/Ca-SST seasonality (0.115 mmol/mol corresponding to 2.8°C) calculated from the mean seasonality of three modern corals. Error bars for fossil corals are the combined error (root of the sum of the squares) of the standard deviation (2σ) of the mean Sr/Ca seasonality of three modern *Diploria strigosa* and the standard error (2SE) of the averaged Sr/Ca seasonality of the fossil coral, following established procedures (Abram et al., 2009) but applied to reconstructed seasonality. 2SE for modern corals and instrumental data are presented. Coral Sr/Ca-SST seasonality was calculated using the monthly relationship of $-0.041 \text{ mmol/mol per } ^\circ\text{C}$ (Hetzinger et al., 2006). Note that mean Sr/Ca seasonality values are based on monthly records of up to 68 years length generated from individual corals.

the limit of detection with respect to the length of the considered time series, where oscillatory behaviour becomes indistinguishable from a secular trend. Nevertheless, the 6.22 ka coral record reveals enhanced inter- to multidecadal variability relative to the late Holocene records and present-day SST, suggesting that the magnitude of SST variability on these timescales was enhanced during the mid-Holocene. This is further supported by the standard deviation of the coral-based SST time series filtered in the inter- to- multidecadal band, which reveals a trend toward lower values since the mid-Holocene (supplementary Figure 3).

2.3.4 Discussion

2.3.4.1 Warming of the western tropical Atlantic over the last 6.2 ka

The Bonaire coral Sr/Ca records suggest that the southern Caribbean Sea was characterised by cooler conditions during the mid-Holocene compared to today. This result is consistent with alkenone- and foraminiferal Mg/Ca-based SST estimates from marine sediments that indicate a warming of the southern Caribbean Sea since the mid-Holocene (Rühlemann et al., 1999; Lea et al., 2003) (Figure 2.16). This warming of the western tropical Atlantic has been attributed to a trend in the NAO from a more positive phase in the early Holocene toward a more negative phase in the late Holocene, possibly linked to insolation changes associated with Earth's precessional cycle (Rimbu et al., 2003; Lorenz and Lohmann, 2004).

2.3.4.2 Forcing of SST seasonality in the western tropical Atlantic over the last 6.2 ka

The few studies that have addressed past SST seasonality in the Atlantic using coral

records have either focused on the last centuries or on the last interglacial period (Watanabe et al., 2001; Kuhnert et al., 2002; Winter et al., 2003; Kilbourne et al., 2010). The present study however, allows for estimating past SST seasonality in the western tropical Atlantic over the last 6.2 ka. Slightly increased SST seasonality is evident in the 6.22 ka Bonaire coral record. As expected from higher amplitude of the seasonal insolation cycle in the mid-Holocene relative to today (Figure 2.17), results suggest that direct insolation forcing plays, to some extent, a role in controlling the amplitude of the annual SST cycle in the southern Caribbean. In line with this, a coral record from the last interglacial revealed orbital control on Caribbean SST seasonality (Winter et al., 2003) and our climate model simulations forced with orbital parameters (Figure 2.18) reveal that increased Bonaire SST seasonality during the mid-Holocene is part of a large-scale feature in the North Atlantic region. This simulation indicates an opposite response in the eastern Equatorial Pacific, as already described by Clement et al. (1999). This suggests that northern tropical Atlantic climate is rather sensitive to orbitally driven changes in the seasonal insolation cycle, which are, nevertheless, more pronounced in the extratropics.

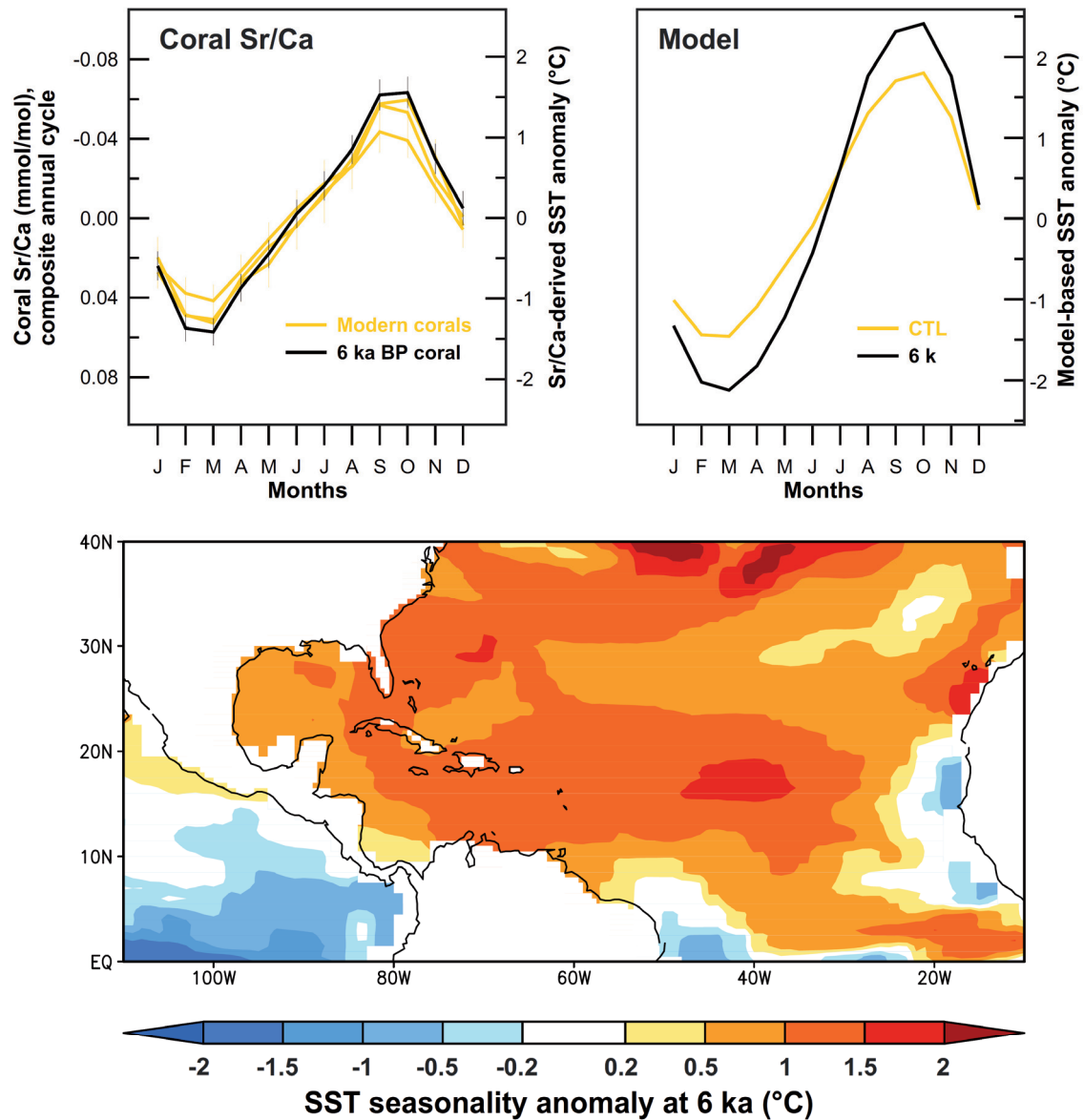


Figure 2.18: Top: Comparison of Bonaire sea surface temperature (SST) composite annual cycles inferred from coral Sr/Ca records (*left panel*) and COSMOS-aso simulations (*right panel*). **Top left:** Coral Sr/Ca composite annual cycles from 3 modern corals (*yellow lines*) are compared to the annual Sr/Ca cycle of a mid-Holocene coral (6.22 ka BP) (*black line*). Corresponding Sr/Ca-SST anomaly was calculated using the monthly Sr/Ca-SST relationship of -0.041 mmol/mol per $^{\circ}\text{C}$ (Hetzinger et al., 2006). **Top right:** COSMOS-aso simulation of monthly SST climatology of the Bonaire gridbox for pre-industrial (CTL) and mid-Holocene (6 ka) time slices. **Bottom:** SST seasonality anomaly at 6 ka inferred from COSMOS-aso simulation relative to pre-industrial (CTL) time. Note that increased SST seasonality in the mid-Holocene is a large-scale phenomenon in the tropical and subtropical North Atlantic sector.

Significantly increased SST seasonality at 2.35 ka together with prominent interannual variability of SST seasonality indicated by the Bonaire coral records suggests that additional forcing mechanisms are critical in controlling

occasional changes in the amplitude of the SST annual cycle in the southern Caribbean over the last 6.2 ka. Observational studies showed that the remote influence of ENSO on tropical north Atlantic SST is strongest in spring (Enfield and

Mayer, 1997; Czaja, 2004), as also observed in Bonaire SST (Figure 2.12). This seasonal emphasis in ENSO forcing produces significant interannual SST variability in the coldest season around Bonaire (Figure 2.19) that drives pronounced interannual variability of SST seasonality (Figure 2.12). Further mechanisms related to the influence of the NAO on spring Atlantic SST (Czaja, 2004), not discussed here, might also play a critical role in controlling SST seasonality on interannual timescales. In summary, while Southern Caribbean SST seasonality seems to reflect the overall influence of orbitally-induced changes in insolation over the last 6.2 ka, our results suggest that internal dynamics of the climate system play an important role in controlling short-term changes in SST seasonality.

2.3.4.3 Source of prominent quasi-biennial SST variability over the last 6.2 ka

The Bonaire coral records indicate significant quasi-biennial (~2-year) variations of southern Caribbean SST during the mid- to late Holocene. Since Atlantic hurricane activity fluctuates on very similar timescales (Gray, 1984), our coral records suggest that such prominent feature of southern Caribbean SST variability has been persistent over the last 6.2 ka.

Southern Caribbean SST variability is influenced by the strength of surface winds associated with the CLLJ, which has a high-frequency (1.25- and 2.3-year) component that varies in phase with the NAO (Wang, 2007). Quasi-biennial periodicities were also observed in a SST reconstruction from a modern Caribbean coral (Hetzinger et al., 2010), which were coherent with the quasi-biennial component of the NAO index as reported by

Hurrell and van Loon (1997). As the NAO is mainly a winter phenomenon (Hurrell, 1995), the significant quasi-biennial peaks found in any winter (DJF) coral time series (e.g., Figure 2.19) could support the persistence of the high-frequency component of the NAO over the last 6.2 ka.

2.3.4.4 Sources of interannual SST variability over the last 6.2 ka

The tropical Atlantic is subject to the competing influence of remote and local forcing. ENSO, the dominant source of global interannual climate variability, plays an important role in modulating modern tropical Atlantic climate (e.g., Enfield and Mayer, 1997; Giannini et al., 2001b). At interannual timescales, significant spectral power is observed in most Bonaire coral records indicating that southern Caribbean SST was characterised by prominent interannual variability over the last 6.2 ka. However, the magnitude of this interannual SST variability has changed through time, suggesting that the competing influence of remote and local forcing on southern Caribbean SST variability has changed since the mid-Holocene. To investigate this, two coral records of similar length that grew during contrasted periods of reduced/enhanced ENSO activity were used to assess the role of ENSO forcing on southern Caribbean interannual SST variability.

Periods of weak and enhanced ENSO activity were identified in tropical Pacific coral records (Tudhope et al., 2001; Woodroffe et al., 2003; McGregor and Gagan, 2004). Tudhope et al. (2001) reported a reduced ENSO activity during the mid-Holocene that was further supported by model simulations (Clement et al., 1999). Moreover, an analysis of Pacific corals

from diverse locations (Tudhope et al., 2001; Woodroffe et al., 2003; McGregor and Gagan, 2004) suggested that severe ENSO activity occurred during the time interval 2.5-1.7 ka (McGregor and Gagan, 2004).

The 6.22 ka Bonaire coral that grew during a period of weak ENSO activity indicates significant 3-4 year variability. The source of this variability is ambiguous because it can be attributed to air-sea interactions originating from both the Atlantic (Tourre et al., 1999; Xie and Carton, 2004; Chang et al., 2006) and the tropical Pacific (Tourre et al., 1999). In contrast, the 2.35 ka Bonaire coral which grew during a period of strong ENSO activity indicates enhanced spectral power at interannual periodicities centred at 5.7-years that is unprecedented in any other coral record. Comparable 5-6 year variability is evident in instrumental Bonaire SST, and cross-spectral analysis reveals coherence with Niño3.4 index but not with the NAO index at this timescale (supplementary Figure 4 and 5). Consequently, we interpret the strong interannual variability at typical ENSO periodicities in southern Caribbean SST at 2.35 ka together with the relatively weak interannual power at 6.22 ka as suggesting that while ocean-atmosphere interactions in the Atlantic have been minor but persistent sources of interannual variability, the intensification of ENSO activity throughout the mid- to late Holocene appears to be an important factor in controlling the magnitude of interannual SST variability in the southern Caribbean Sea.

2.3.4.5 Change in the seasonal pattern of interannual SST variability at 2.35 ka

The pattern of ENSO teleconnection to the Caribbean has been shown to have strong

seasonality as it affects predominantly tropical north Atlantic climate in a particular season, the boreal spring (e.g., Enfield and Mayer, 1997; Sutton et al., 2000; Giannini et al., 2001b; Czaja, 2004). Spectral analyses of instrumental Bonaire spring SST reveals a significant interannual peak centred at 5.2-years (Figure 2.19) that reflects the seasonal effect of ENSO on southern Caribbean SST. To test whether the seasonal pattern of the ENSO teleconnection has been stable over the past 6.2 ka, monthly coral records have been decomposed into seasonal time series and assessed for interannual signals during individual seasons (DJF, December-February; MAM, Mars-May; JJA, June-August; SON, September-November) (Figure 2.19).

The 6.22 ka coral, reflecting a period of reduced ENSO activity, indicates significant 3-4 year periodicities in the DJF, MAM and SON time series. Besides, a unique 8.3-year spectral peak was found in the JJA time series suggesting quasi-decadal variability in Bonaire summer SST at that time. The source of this quasi-decadal signal was also detected in instrumental data (Jury, 2009), and was attributed to modulation of the easterly trade-winds by the Atlantic subtropical high and summer convection (Jury, 2009) most likely stronger at 6.2 ka when the Intertropical Convergence Zone (ITCZ) was located farther north (Haug et al., 2001). The 6.22 ka coral record indicates that interannual SST variability was prominent in specific seasons, as observed in other coral records used in this study (not shown).

In contrast, the prominent periodicity centred at 5.7-years evident in the 2.35 ka coral record was not restricted to a particular season (as observed in instrumental data and other

coral records), but was significant in all seasons. As shown in Figure 2.19, warmer (colder) winters follow warmer (colder) summers, thus contributing to the pronounced interannual variability significant in all seasons. Giannini et al. (2001a) showed that interdecadal changes in the ENSO teleconnection to the Caribbean region can produce interference between ENSO and NAO producing statistically significant seasonal anomalies in Caribbean climate. Rogers (1984) focused on the temporal relationship between ENSO and NAO. He found strong coherence at a periodicity of 5.7-years. Later on, Huang et al., (1998) suggested that energy transfer from the tropical Pacific during

warm ENSO events might influence the NAO on these timescales. Consequently, the pronounced 5.7-year variability found in the 2.35 ka coral could suggest a reorganisation of atmospheric circulation possibly associated with changed ENSO-NAO interactions at that time.

Warm ENSO events and the negative phase of the NAO are known for generating warm tropical Atlantic SST anomalies in winter and spring (Giannini et al., 2001a; Czaja et al., 2002). However, it is not clear from the instrumental records that such constructive interferences between ENSO and NAO can produce SST anomalies that persist until the next summer and fall. Therefore, given that

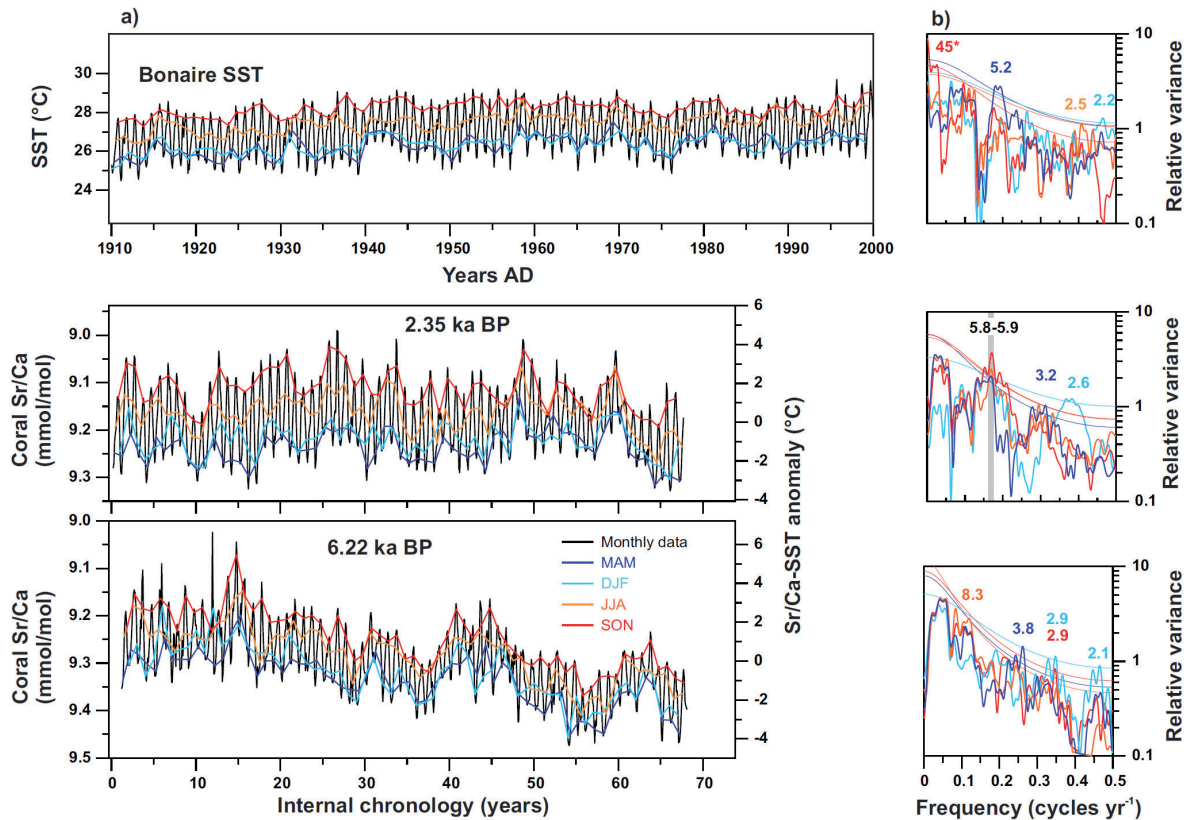


Figure 2.19: a) Monthly instrumental SST record for the Bonaire gridbox (12°N; 68°W) (Smith et al., 2008) (top), monthly coral Sr/Ca records from 2.35 ka (middle) and 6.22 ka BP (bottom) and corresponding seasonal coral Sr/Ca time series for winter (DJF), spring (MAM), summer (JJA) and fall (SON). Corresponding Sr/Ca-SST anomalies calculated using the monthly Sr/Ca-SST relationship of -0.041 mmol/mol per °C (Hetzinger et al., 2006) are shown. b) Multitaper method (MTM) spectral analysis with a red noise null hypothesis (Ghil et al., 2002) (number of tapers 3; bandwidth parameter 2) of seasonal time series detrended and normalized to unit variance. 95% significance level is indicated. Note that the 2.35 ka BP record displays a significant peak at 5.8-5.9 years that is significant in the SON and DJF time series at the 99% level and in the JJA and MAM time series at the 95% level.

modern ENSO forcing affects the north tropical Atlantic SST in a particular season (Enfield and Mayer, 1997; Sutton et al., 2000; Czaja, 2004), changes in the seasonality of ENSO teleconnection or positive ocean-atmosphere feedbacks (i.e., weakening of surface winds due to warm SST anomalies) might have driven the pronounced interannual SST variability at 2.35 ka BP. However, physical mechanisms involved in enhancing both SST seasonality and interannual variability in the southern Caribbean are not well understood. As this 2.35 ka coral record covers a period before the onset of the Roman Warm Period, modelling studies are needed to investigate the underlying mechanisms and assess their potential role in generating such large-scale climate anomalies.

2.3.4.6 Enhanced inter- to multidecadal SST variability in the mid-Holocene

On inter- to multidecadal timescales, observational studies revealed that Caribbean climate is influenced by the Atlantic Multidecadal Oscillation (AMO) (Enfield et al., 2001; Sutton and Hodson, 2005; Wang et al., 2008a). Given that regional SST proxy records could be linked to this Atlantic mode of multidecadal climate variability (e.g., Richey et al., 2007; Kilbourne et al., 2008; Poore et al., 2009; Saenger et al., 2009; Heslop and Paul, 2011), recent studies have demonstrated that Caribbean corals are ideal climate archives for recording variations of sea surface conditions associated with the AMO (Hetzinger et al., 2008; Kilbourne et al., 2008). Here, prominent inter- to multidecadal variability found in most of our Bonaire coral Sr/Ca records suggest a substantial AMO-like signature in southern Caribbean SST variability over the last 6.2 ka.

A coral $\delta^{18}\text{O}$ -based study from the Dominican Republic indicated interdecadal variability of precipitation in the mid-Holocene tropical Atlantic (Greer and Swart, 2006). These records suggest the possible role of tropical Atlantic in controlling interdecadal changes in northern Caribbean brought by the latitudinal shift of the ITCZ or increased storm activity. In line with this finding, the 6.22 ka Bonaire coral Sr/Ca record indicates strong multidecadal SST variations during the mid-Holocene. Knudsen et al. (2011) presented evidence that Caribbean precipitation over the last 8 ka has experienced multidecadal fluctuations linked to the AMO, yet the contribution of SST fields to the underlying climate variability on AMO-like timescales remains poorly constrained due to a lack of reliable high-resolution SST proxy records. Our coral Sr/Ca records from an AMO-sensitive region provide evidence for greater amplitude of inter- to multidecadal SST variability during the mid-Holocene. Further studies should investigate the role of large-scale ocean-atmosphere interactions in the Atlantic region in generating the greater amplitude of AMO-like SST variability, as observed in the mid-Holocene Bonaire coral.

2.3.5 Conclusion

The natural range of tropical Atlantic SST variability is investigated with a long-term perspective for the mid- to late Holocene using a total number of 295 years of monthly-resolved coral Sr/Ca records from Bonaire (southern Caribbean Sea). While this study provides additional evidence for cooler conditions in the western tropical Atlantic during the mid-Holocene, patterns of short-term SST variability have been investigated which can be summarised as follows:

(1) In combination with climate model simulations, the coral Sr/Ca records reveal that insolation changes on orbital timescales affect western tropical Atlantic SST seasonality.

(2) The significant increased SST seasonality at 2.35 ka together with prominent interannual variability of SST seasonality found in all coral records suggests that forcing mechanisms linked to the internal variability of the climate system are critical in modulating short-term changes in western tropical Atlantic SST seasonality.

(3) Prominent quasi-biennial and interannual SST variability in southern Caribbean SST during the mid- to late Holocene are linked to ocean-atmosphere interactions originating from both the Pacific and Atlantic oceans.

(4) Interannual SST variability at typical ENSO periods was low at 6.22 ka BP, whereas it was enhanced at 2.35 ka, reflecting the increasing influence of ENSO on western tropical Atlantic climate variability throughout the mid- to late Holocene.

(5) Significantly increased SST seasonality and enhanced interannual variability are documented by the 2.35 ka coral. Since similar interannual and seasonal temperature anomalies lasting for decades were not identified in observational data, we assume that a reorganisation of atmospheric circulation patterns possibly linked to interdecadal changes of teleconnection patterns (e.g., Giannini et al., 2001a) occurred at 2.35 ka BP.

(6) Enhanced inter- to multidecadal scale variability of western tropical Atlantic SST, i.e., on AMO timescales, is indicated by the 6.22 ka coral. Since the underlying mechanisms are poorly understood, further studies should investigate the role of different global climate states in modulating the amplitude of multidecadal tropical Atlantic climate variability.

As the period of instrumental observations might already contain anthropogenic imprints, the total number of 295 years of monthly-resolved coral Sr/Ca records used in this study provides unique insights into the natural range of tropical Atlantic SST variability since the mid-Holocene. These records indicate that short-term SST variability over the last 6.2 ka has arisen from internal dynamics of the climate system and suggest that a better understanding of changes in climate modes and their interactions are critical for successful predictions of tropical Atlantic climate variability under changing boundary conditions.

Acknowledgments

We thank the Government of the Island Territory of Bonaire (Netherlands Antilles) for research and fieldwork permission, E. Beukenboom (STINAPA Bonaire National Parks Foundation) for support, J. Pätzold for support with coral drilling and discussion, S. Pape for operating and maintaining the ICP-OES, M. Vermeij for help with local temperature data, H. Kuhnert for discussion, M. Zuther for X-ray diffraction analyses, K. Baumann for Scanning Electron Microscopy imaging, C. Fensterer and R. Eichstädter for assistance with U-series dating in the lab of A. Mangini, G. Lohmann for support with climate simulations and discussions, A.

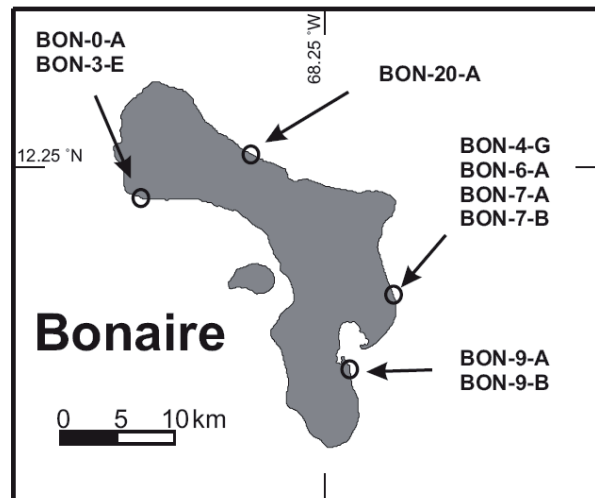
Scheffers and C. Maier for initiating this collaboration, and G. Wefer for overall support. This work was funded by Deutsche Forschungsgemeinschaft (DFG) under the Special Priority Programme INTERDYNAMIK,

through grants to T.F. (FE 615/3-1, 3-2; CaribClim). C.G. acknowledges additional support by GLOMAR (Bremen International Graduate School for Marine Sciences) that is funded by DFG.

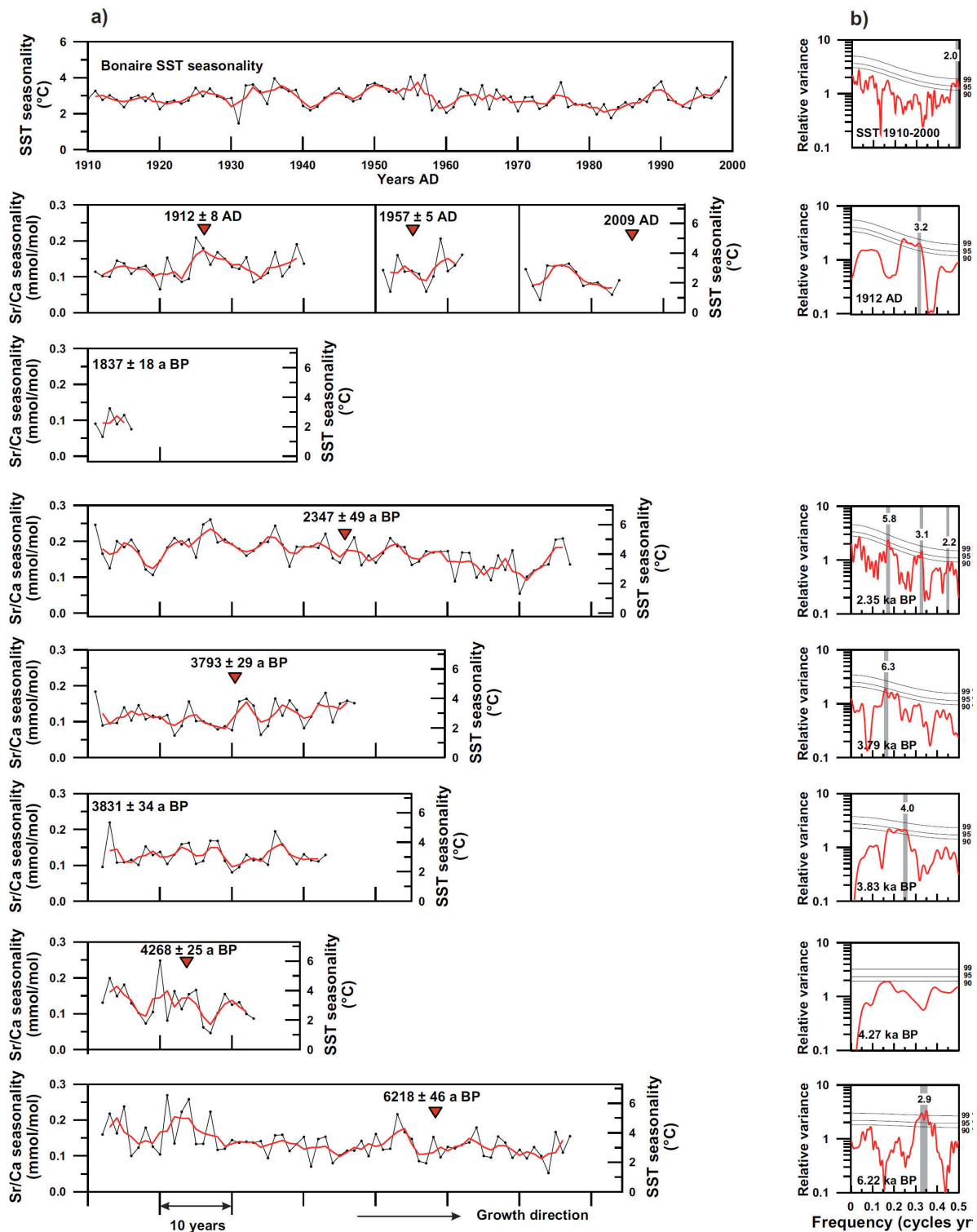
Supplementary information

Supplementary Table 1: Results of U-series dating of Bonaire corals. Corrected U-series ages (BP) are referenced to 1950 AD. n.d. signifies concentrations below the detection limit. Calcite contents were measured with X-ray diffraction.

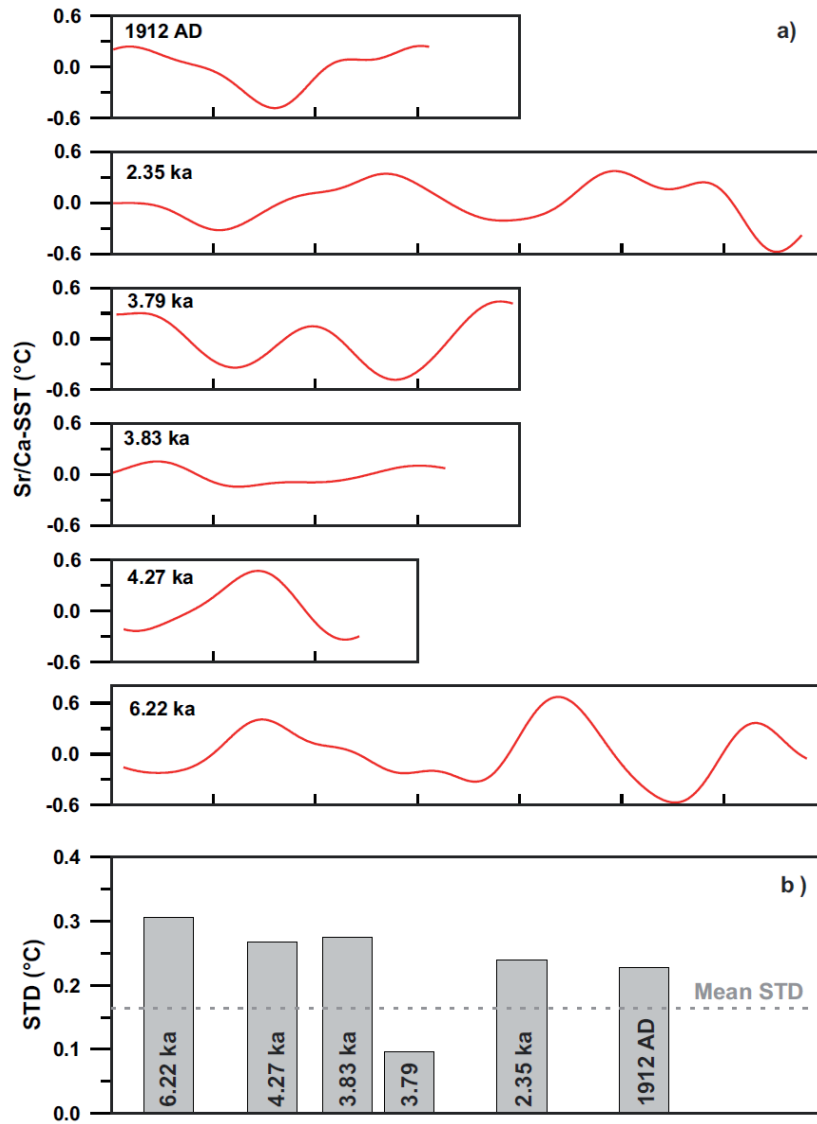
| Sample ID | δU (‰) | ^{238}U ($\mu g/g$) | ^{232}Th (ng/g) | ^{230}Th (pg/g) | $\delta^{234}U_{initial}$ (‰) | U-Th Age measured (ka) | U-Th Age (AD/BP) (a) | Calcite content (%) |
|----------------------|-------------------|----------------------------|--------------------------|--------------------------|----------------------------------|---------------------------|-------------------------|------------------------|
| Modern corals | | | | | | | | |
| BON-0-A (living) | - | - | - | - | - | - | - | ≤ 0.25 |
| BON-9-B (dead) | 144.1 ± 2.1 | 2.5360 ± 0.0025 | 0.0346 ± 0.0002 | 0.0227 ± 0.0020 | 144.1 ± 2.1 | 0.0518 ± 0.0049 | 1957 ± 5 AD | ≤ 0.5 |
| BON-9-A (dead) | 145.1 ± 1.9 | 2.2751 ± 0.0023 | 0.0276 ± 0.0004 | 0.0378 ± 0.0025 | 145.2 ± 1.9 | 0.0966 ± 0.0074 | 1912 ± 8 AD | ≤ 0.2 |
| Fossil corals | | | | | | | | |
| BON-20-A | 144.7 ± 1.6 | 2.6914 ± 0.0027 | n.d. | 0.8686 ± 0.0081 | 145.5 ± 1.6 | 1.897 ± 0.018 | 1837 ± 18 a BP | ≤ 0.35 |
| BON-6-A | 144.7 ± 1.7 | 2.7643 ± 0.0028 | 0.0560 ± 0.0003 | 1.129 ± 0.023 | 145.7 ± 1.7 | 2.406 ± 0.049 | 2347 ± 49 a BP | ≤ 0.5 |
| BON-7-A | 140.1 ± 1.6 | 2.5503 ± 0.0026 | 0.0736 ± 0.0003 | 1.651 ± 0.012 | 141.6 ± 1.6 | 3.852 ± 0.029 | 3793 ± 29 a BP | ≤ 0.2 |
| BON-7-B | 142.0 ± 1.6 | 2.8863 ± 0.0029 | n.d. | 1.890 ± 0.016 | 143.5 ± 1.6 | 3.891 ± 0.034 | 3831 ± 34 a BP | ≤ 0.5 |
| BON-4-G | 144 ± 1.8 | 2.4583 ± 0.0025 | 0.1029 ± 0.0003 | 1.791 ± 0.009 | 146.2 ± 1.8 | 4.327 ± 0.025 | 4268 ± 25 a BP | ≤ 0.5 |
| BON-3-E | 142.3 ± 1.7 | 3.2474 ± 0.0032 | n.d. | 3.395 ± 0.023 | 144.9 ± 1.8 | 6.278 ± 0.046 | 6218 ± 46 a BP | ≤ 0.5 |



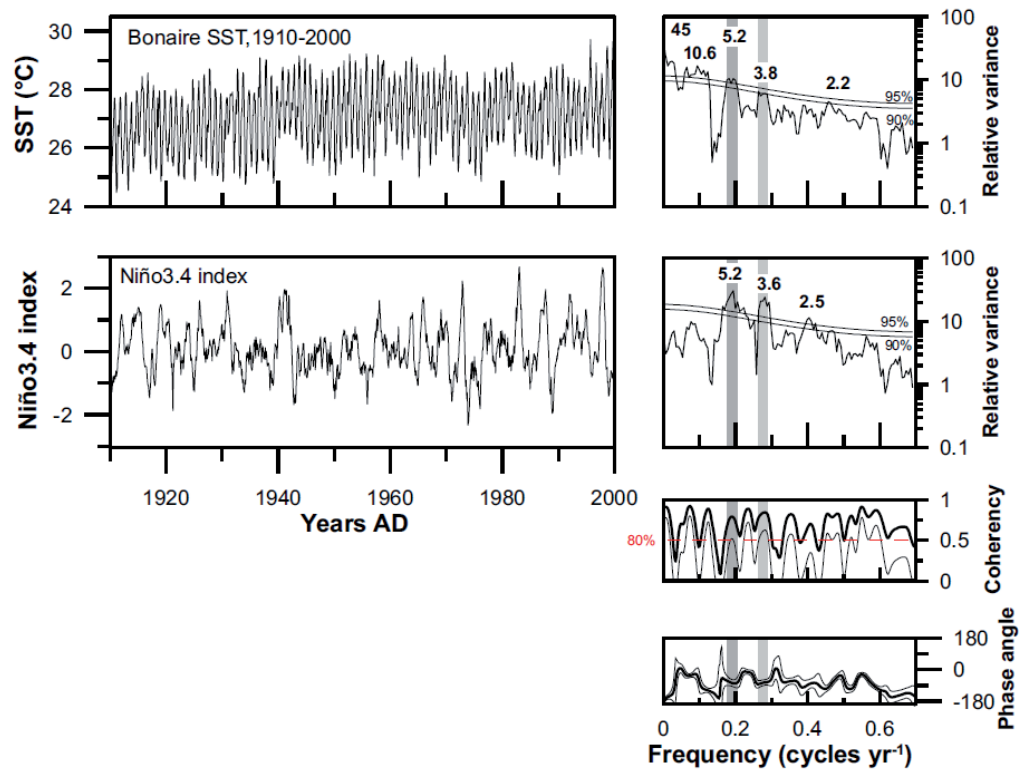
Supplementary Figure 1: Map of Bonaire showing locations of coral samples used in this study.



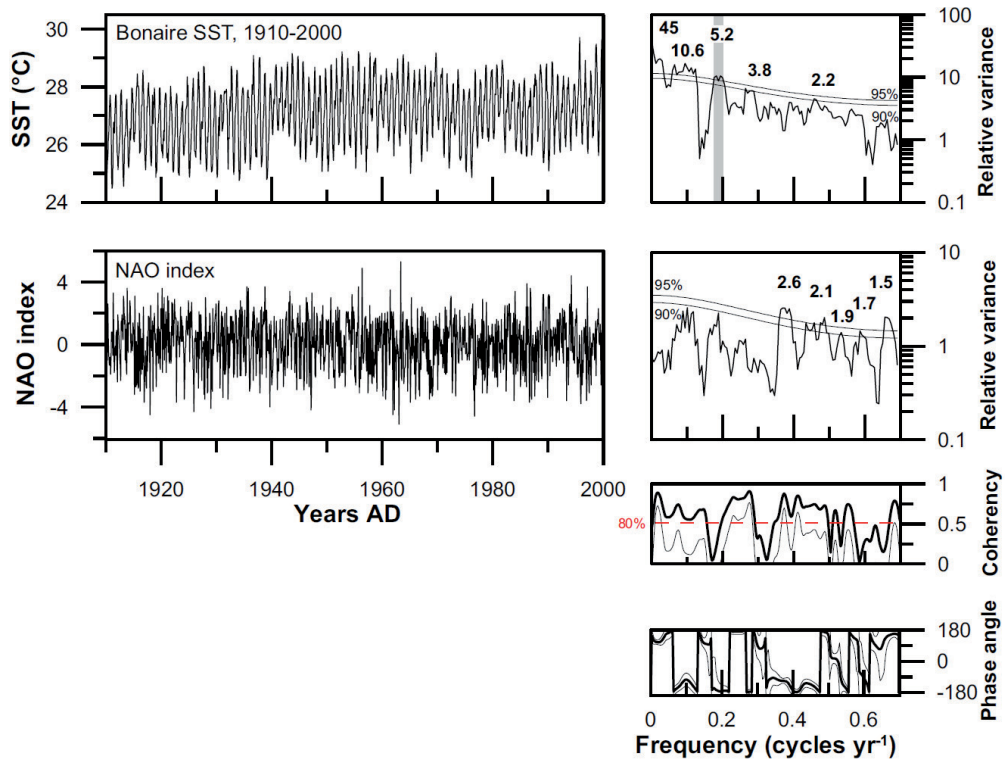
Supplementary Figure 2: a) Interannual variability of SST seasonality inferred from Bonaire monthly coral Sr/Ca records and instrumental SST (Smith et al., 2008) and corresponding 3-year running average (red line). b) Multitaper method (MTM) spectral analysis with a red noise null hypothesis (Ghil et al., 2002) (number of tapers 3, bandwidth parameter 2) of corresponding coral-based SST seasonality records of >20 year length and instrumental SST seasonality. Time series have been detrended and normalized to unit variance. 90%, 95%, and 99% significance levels are indicated.



Supplementary Figure 3: a) Interdecadal (10 – 40-year) bandpass filtered Sr/Ca-SST time series for all coral records used in this study (using the Sr/Ca-SST relationship of -0.074 mmol/mol per $^{\circ}\text{C}$, (Hetzinger et al., 2006) and b) corresponding standard deviations of the interdecadal bandpass filtered coral Sr/Ca-SST time series following established procedures (Tudhope et al., 2001). Horizontal dashed line indicates the mean value of standard deviation of the interdecadal bandpass filtered time series for all coral records used in this study. Note that the relatively high variance found in the 1912 AD coral Sr/Ca record is associated with a change in coral growth pattern as observed on X-radiographs (see Figure 2.13). Note that this experiment is sensible to changes in the Sr/Ca-SST regression slope which affects the absolute variance between corals rather than affecting the trend.



Supplementary Figure 4: Monthly time series of Bonaire SST (12°N; 68°W) (Smith et al., 2008) and the Niño3.4 index (*left panels*) and their spectral properties (*right panels*). Results of Multitaper method (MTM) spectral analysis with a red noise null hypothesis (Ghil et al., 2002) (number of tapers 3; bandwidth parameter 2) of detrended and normalized to unit variance time series with average annual cycles removed. 95% significance level is indicated. Cross-spectral analysis between the time series of the Bonaire SST and the Niño 3.4 index (*bottom right panels*). The 80% confidence level for coherency is indicated.



Supplementary Figure 5: Monthly time series of Bonaire SST (12°N; 68°W) (Smith et al., 2008) and the monthly NAO index (*left panels*) and their spectral properties (*right panels*). Results of Multitaper method (MTM) spectral analysis with a red noise null hypothesis (Ghil et al., 2002) (number of tapers 3; bandwidth parameter 2) of detrended and normalized to unit variance time series with average annual cycles removed. 95% significance level is indicated. Cross-spectral analysis between the time series of Bonaire SST and the NAO index (*bottom right panels*). The 80% confidence level for coherency is indicated.

Manuscript IV

2.4 Seasonal to multidecadal variability of sea surface hydrology in the southern Caribbean during the mid- to late Holocene

Cyril Giry¹, Thomas Felis¹, Martin Kölling¹ and Sander Scheffers²

¹ MARUM - Center for Marine Environmental Sciences, University of Bremen, 28359 Bremen, Germany

² School of Environmental Science and Management, Southern Cross University, PO 147 Lismore, Australia.

In preparation for *Paleoceanography*

Abstract: Long-term changes of sea surface hydrology in the Caribbean are related to the mean position of the Intertropical Convergence Zone (ITCZ) that fluctuates on glacial/interglacial cycles according to the strength of the Atlantic meridional overturning circulation (AMOC). However, due to a lack of suitable high-resolution marine archives little is known on short-term variability (i.e., seasonal to multidecadal) of past Caribbean hydrological cycle which could contribute to rapid changes in the strength of the AMOC. Here we reconstruct seasonality and interannual to multidecadal variability of sea surface hydrology of the southern Caribbean Sea by applying paired coral Sr/Ca and $\delta^{18}\text{O}$ measurements on pristine and well-dated annually-banded fossil corals from Bonaire (southern Caribbean Sea). Monthly resolved coral $\Delta\delta^{18}\text{O}$ records, a proxy for the oxygen isotopic composition of seawater ($\delta^{18}\text{O}_{\text{sw}}$), provide about 295 years of sea surface hydrology variability in one of the surface return flow of the AMOC. Modern annual $\delta^{18}\text{O}_{\text{sw}}$ cycles reconstructed from three modern corals can be justified by local precipitation, but rather reflect the strength of surface current through the Caribbean driven by surface winds. In contrast, the mid Holocene coral indicates sharp summer peak towards more negative $\delta^{18}\text{O}_{\text{sw}}$ values suggesting enhanced summer precipitation possibly associated with more northward position of the ITCZ at that time. Moreover, based on the systematic positive relationship between reconstructed sea surface temperature and salinity, we suggest that freshwater discharged from Orinoco and Amazon rivers and transported into the Caribbean by wind-driven surface currents are one critical factor influencing sea surface hydrology on interannual to multidecadal timescales at the study site. Finally, this study provides insight of freshwater budget of the southern Caribbean Sea during the mid- to late Holocene on timescales ranging from seasonal to multidecadal and suggests that rainfall over northern South America and surface winds play a critical role in controlling interannual to multidecadal variability of sea surface hydrology in the Caribbean.

Citation: Giry, C., T. Felis, M. Kölling and S. Scheffers: Seasonal to multidecadal variability of sea surface hydrology in the southern Caribbean during the mid- to late Holocene, (in preparation)

2.4.1 Introduction

Proxy records and model simulations indicate that tropical Atlantic hydrological cycle has experienced significant changes on glacial/interglacial timescales. Such millennial scale changes in the tropical hydrological cycle have been associated with both the mean latitudinal position of the Intertropical Convergence Zone (ITCZ) and the strength of the Atlantic Meridional Overturning Circulation (AMOC). The AMOC comprises a net northward surface flow of warm and salty water from low-latitude to the North Atlantic. The resulting heat transport to high-latitude affects north Atlantic climate which in turn, influences tropical hydrological cycle by shifting the ITCZ northward. High salinity anomalies were reported in the Caribbean during cold periods associated with a reduced AMOC and a southward shift of the ITCZ (Schmidt et al., 2004; Leduc et al., 2007; Carlson et al., 2008; Schmidt and Spero, 2011; Sepulcre et al., 2011). Moreover, Lynch-Stieglitz et al., (2007) found a decreased flow through the Caribbean at these times. The observed pattern of millennial scale variability indicates that cold periods are characterised by drier western tropical Atlantic and Caribbean combined with a reduced surface flow through the Caribbean. It is clear from both proxy records and model studies that changes in Caribbean freshwater budget due to tropical atmospheric circulations have profound effect on the salinity and density structure of the AMOC, all of which point to the critical role of the tropical Atlantic in mediating global climate changes. Furthermore, there are indications from recent development of oceanographic studies in the North Atlantic that the surface branch of the AMOC, bringing warm and salty waters from tropical to North

Atlantic, is characterised by energetic short-term variability (Cunningham et al., 2007; Cunningham and Marsh, 2010). Despite the relevance of such studies which revealed pronounced annual cycles, the observational period is too short to fully understand the nature of short-term variations of the surface flow of the AMOC. Nevertheless, recent model simulation found significant interannual variability of the AMOC that reflects the influence of ocean-atmosphere modes of interannual climate variability on the strength of the meridional overturning circulation (Vellinga and Wu, 2004). Furthermore, a recent study identified low-frequency variability of the North Brazilian Current transport as a potential indicator of the multidecadal variability of the surface return flow of the AMOC (Zhang et al., 2011).

Low latitude climate reconstructions have attributed evaporation/precipitation ratio (E/P) associated with latitudinal movement of the ITCZ as the main driver of Caribbean freshwater budget on millennial timescales (Schmidt et al., 2004; Leduc et al., 2007; Sepulcre et al., 2011). For example, during the early and mid-Holocene, there are indications for a more northward position of the ITCZ which has intensified precipitation over the north tropical Atlantic and the Caribbean (Hodell et al., 1991; Haug et al., 2001), whereas today, since the position of the ITCZ is in a more southerly position (Haug et al., 2001), net evaporation due to enhanced subsidence contributes to the negative freshwater budget of the Caribbean (Etter et al., 1987 and references therein). Subdecadally resolved titanium concentration data from Cariaco Basin sediment (Haug et al., 2001), a proxy for riverine input of terrigenous

materials from local rivers and the Orinoco River, revealed long-term changes in river runoff associated with the latitudinal migration of the ITCZ following orbitally-driven seasonal changes of insolation. Moreover, this high-temporally resolved record provides additional evidence for rapid changes (i.e., decadal to centennial scales) of hydrological conditions over northern South America. Mechanisms responsible for this short-term variability (i.e., interannual to multidecadal) are, however, poorly understood. Furthermore, due to a lack of suitable high-resolution proxy data that clearly resolve the annual cycle, the seasonal dynamic of the ITCZ under different climate background state have yet to be investigated in the western Atlantic in order to reconcile recent debate on the dynamic of the tropical rain belt over the course of the Holocene (e.g., Collins et al., 2011).

In order to investigate pattern of seasonal to multidecadal variability of sea surface hydrology in the Caribbean during the mid- to late Holocene, we use decades-long monthly resolved paired coral Sr/Ca and $\delta^{18}\text{O}$ records from fossil corals from Bonaire (southern Caribbean Sea) as proxy for the oxygen isotopic composition of seawater. Coral Sr/Ca is a proxy for sea surface temperature (SST) (Smith et al., 1979; Beck et al., 1992), whereas the $\delta^{18}\text{O}$ of coral skeleton varies in response to changes of both temperature and seawater $\delta^{18}\text{O}$ ($\delta^{18}\text{O}_{\text{sw}}$) which is linearly related to sea surface salinity (SSS) (Urey, 1947; Carriquiry et al., 1994; Wellington et al., 1996; Watanabe et al., 2001). Therefore, subseasonal paired measurements of coral $\delta^{18}\text{O}$ and Sr/Ca provide a unique opportunity to estimate simultaneously SST and SSS

changes recorded in the $\Delta\delta^{18}\text{O}$ of coral skeleton (Gagan et al., 1998). Ultimately, such subseasonally resolved coral records can shed more light on physical mechanisms responsible for changes in hydrological balance in the Caribbean on seasonal to multidecadal timescales throughout the mid- to late Holocene.

2.4.2 Regional setting of the study area

Coral colonies used in this study were collected on Bonaire (Netherland Antilles), an open-ocean island from the southern Caribbean Sea ($\sim 12^\circ 10' \text{N}$, $68^\circ 18' \text{W}$), located ~ 100 km off Venezuela. Caribbean climate is primarily forced by co-varying pattern of SST and trade winds associated with the seasonal migration of the ITCZ (Hastenrath, 1984). Bonaire has a tropical-arid climate characterised by low-annual mean rainfall ($\sim 500 \text{mm/yr}$). In contrast to other less-arid Caribbean Islands which received most of their yearly rain in summer (Giannini et al., 2000), Bonaire has the main rainy season from October through January followed by the dry season between February to May with a transition period called “small rains” season (Martis et al., 2002) from June to September. The seasonal pattern of the ITCZ affects the strength of northeast trade winds blowing over the western Atlantic and Caribbean. Trade winds weaken in boreal summer and strengthen in boreal winter and thus, affect the patterns of ocean circulation and precipitation in the Caribbean.

Freshwater budget in the Caribbean indicates the influence of two major processes: evaporation/precipitation (E/P) ratio (Etter et al., 1987) over the basin and freshwater input

from the Amazon and Orinoco rivers by advection of low salinity water masses by surface currents (Hellweger and Gordon, 2002). Net water loss due to year-long easterly trade-winds results in excessive evaporation (E) over precipitation (P) which is strong over the basin in wintertime (Hastenrath and Lamb, 1978; Etter et al., 1987; Giannini et al., 2000). Caribbean freshwater budget indicates that river discharges in the western Caribbean (west of 70°W) do not compensate for net water loss due to net evaporation (Etter et al., 1987), whereas it does in the western tropical Atlantic and eastern Caribbean (Hellweger and Gordon, 2002). This indicates that sea surface salinity (SSS) in the eastern Caribbean and the study site might reflect both E/P ratio and

freshwater supply from tropical rivers.

Caribbean hydrography is characterised by stratified upper 500m of the water column due to the presence of two dominant water masses with contrasted physical properties (Wüst, 1964). The North Atlantic Subtropical UnderWater (SUW), formed in the subtropical north Atlantic where E exceeds P, is characterised by salinity maximum (>36.5) that sinks below fresher surface water referred to as Caribbean Surface Water (CSW) (Wüst, 1964). The latter water mass is thought to be mixture of North Atlantic surface waters and freshwater from Amazon and Orinoco rivers and local freshwater runoff from South America that is transported northwestward by the Guyana and Caribbean

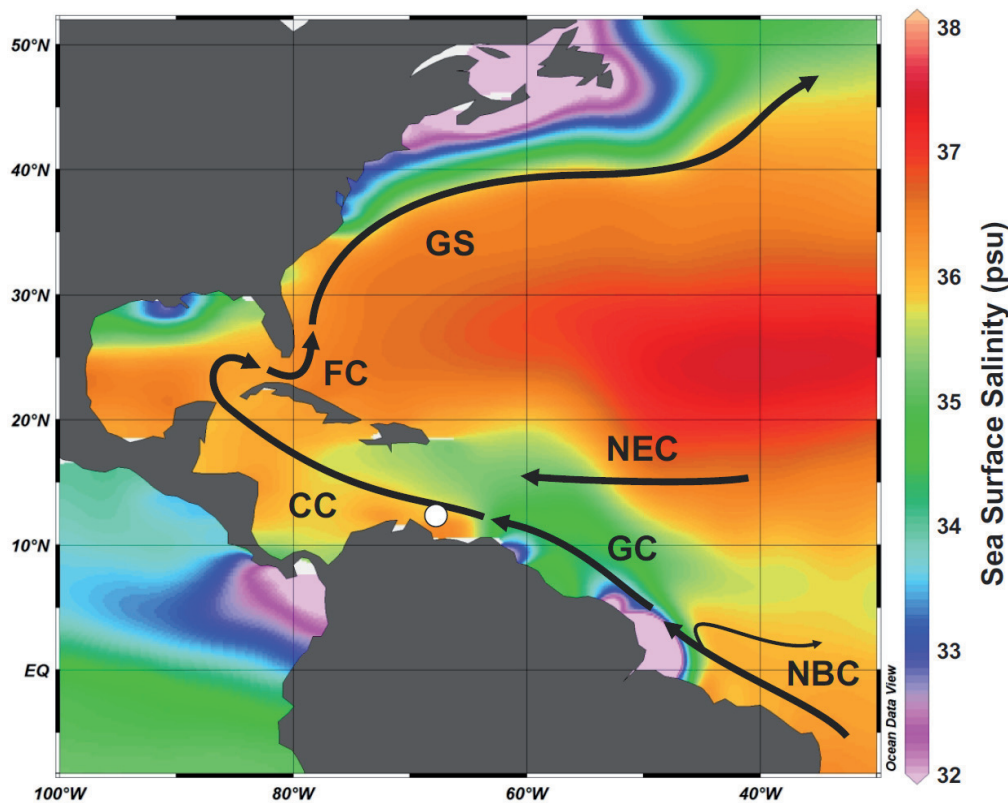


Figure 2.20: Modern oceanographic setting of the Caribbean and western North Atlantic. Schematic of major surface currents constituting the upper branch of the Atlantic meridional overturning circulation (AMOC) are superimposed on annual mean sea surface salinity map (Antonov et al., 2006). Major surface currents: North Brazilian Current (NBC), Guyana Current (GC), Caribbean Current (CC), Florida Current (FC), Gulf Stream (GS) and North Equatorial Current (NEC). White circle indicates the study site (Bonaire).

Currents (Figure 2.20). As the CSW is transported westward by the Caribbean Current, freshwater masses are evaporated and diluted in the eastern Caribbean Sea with the SUW (Gordon, 1967).

On interannual timescale, unlike the Pacific where the influence of El Niño/Southern Oscillation (ENSO) dominates, the tropical Atlantic is linked to the competing influence of local and remote forcing emanating from tropical and subtropical oceans. ENSO-related anomalous atmospheric circulation seems to be one of the dominant factors suppressing rainfall over the Caribbean (Chiang et al., 2002) on this timescale (Figure 2.21). They suggested that while teleconnection of warm ENSO to the tropical Atlantic results in an anomalous warm north/cool south SST gradient that shifts ITCZ anomalously north; warm ENSO induces strong anomalous Walker circulation that suppresses precipitation over the western tropical Atlantic and Caribbean.

Such pattern of ENSO teleconnection to the tropical Atlantic is consistent with other studies (Giannini et al., 2001b; Alexander and Scott, 2002).

On inter- to multidecadal timescales, the Atlantic Multidecadal Oscillation (AMO) plays a critical role in controlling both SST and rainfall in the Caribbean (Sutton and Hodson, 2005). Forcing mechanisms responsible for the leading large-scale pattern of multidecadal climate variability is partially related to variability in the oceanic thermohaline circulation on these timescales (Delworth and Mann, 2000; Knight et al., 2005), as recently identified along the northeastern coast of Brazil in the surface return flow of the AMOC (Zhang et al., 2011).

2.4.3 Material and Methods

U-series dating and screening for diagenesis were performed on all coral cores

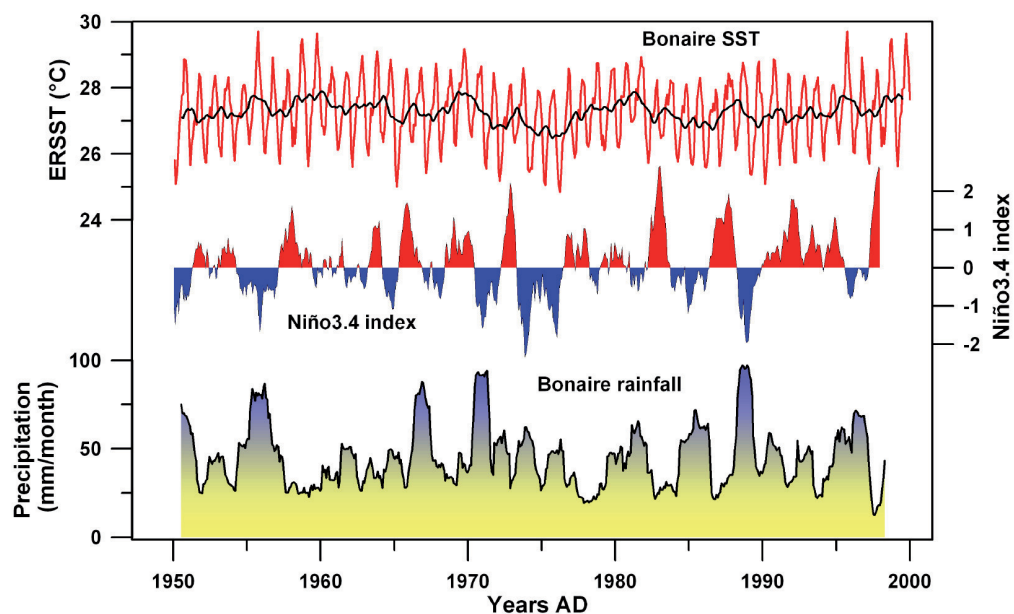


Figure 2.21: Monthly sea surface temperature (SST) for $2^{\circ} \times 2^{\circ}$ gridbox centred on Bonaire (12°N ; 68°W) (ERSSTv3b(Smith et al., 2008)) (*top*) and the corresponding 13 months running average (*black line*), Niño3.4 index (Kaplan et al., 1998; Reynolds et al., 2002) (*middle*) and corresponding 13 months running average of precipitation for gridbox centred on Bonaire (12.5°N ; 67.5°W) (*bottom*) (Hulme et al., 1998). Note that maximum rainfall events over Bonaire correspond to periods of negative tropical Pacific SST anomalies typical for La-Niña events.

used in this study as recently described (Giry et al., submitted) (Chapter 2.3). Briefly, based on the annual density bands inferred from X-radiographs, a sampling resolution of ~12 samples per year was targeted along the growth axis of pristine coral skeleton. For each sample, skeletal powder was carefully drilled using a 0.6 mm diameter drill bit along the centre of the dense thecal walls which is the skeletal element that provides the best environmental seasonal signal (Giry et al., 2010a). This careful sampling strategy allows for evaluating coral-based climate variability at near-monthly resolution. Each powdered sample was split for both stable isotope and Sr/Ca analyses performed at MARUM and the Department of Geosciences of the University of Bremen, Germany. Further details on stable isotope and Sr/Ca analyses have been described (Giry et al., 2010a; Giry et al., submitted).

The internal chronology of individual corals record is based on annual density-banding patterns inferred from both X-radiographs and annual Sr/Ca cycles. We assumed that the timing of annual SST cycle has not changed during the investigated period which was consistent with a numerical simulation (Giry et al., submitted). Therefore, maximum and minimum Sr/Ca values in any given year were assigned to the on average coldest (February/March) and warmest months (September/October) of present-day SST (Smith et al., 2008), respectively. This method introduces a non-cumulative error of ± 1 month in any given year. The same anchor points as for Sr/Ca were used for the age model construction of the corresponding $\delta^{18}\text{O}$ record derived from the same samples. To obtain monthly time series, coral Sr/Ca and $\delta^{18}\text{O}$

record were linearly interpolated to monthly resolution following established procedure (e.g., Felis et al., 2009; Giry et al., 2010b). However, as both Sr/Ca and $\delta^{18}\text{O}$ were measured on the same sample powder, the variation of Sr/Ca relative to that of $\delta^{18}\text{O}$ has no age uncertainty.

Subseasonal reconstruction of seawater $\delta^{18}\text{O}$ ($\delta^{18}\text{O}_{\text{sw}}$) is achieved by paired coral Sr/Ca and $\delta^{18}\text{O}$ measurements. The most commonly used method to calculate $\delta^{18}\text{O}_{\text{sw}}$ exploits proxy-SST regressions to convert $\delta^{18}\text{O}$ and Sr/Ca to temperature unit (McCulloch et al., 1994; Gagan et al., 1998). However, the regressions have generally different intercept due to different mean proxy values between different coral colonies (e.g., Felis et al., 2003; Abram et al., 2009). Therefore, omitting the intercept values in order to assess instantaneous changes of $\delta^{18}\text{O}_{\text{sw}}$ is critical (Ren et al., 2003). To do so, the centering method and the combined analytical error are used (Cahyarini et al., 2008). Multitaper Method (MTM) spectral analysis with a red noise null hypothesis (Ghil et al., 2002) is applied to the detrended and normalised $\delta^{18}\text{O}_{\text{sw}}$ and instrumental records with the mean annual cycle removed. Gaussian band-pass filtering is performed with AnalySeries software (Paillard et al., 1996).

2.4.4 Results

2.4.4.1 Modern coral $\delta^{18}\text{O}$ -SST relationship

Coral Sr/Ca variability in reference to SST has already been assessed from a modern *Diploria strigosa* coral from Bonaire (Giry et al., submitted). It has been shown that Sr/Ca-SST relationship are similar to previously published monthly values for

Diploria strigosa (Hetzinger et al., 2006). The $\delta^{18}\text{O}$ -SST relationship from the *D. strigosa* collected live in Bonaire (BON-0-A) which grew from 1993 to 2009 was assessed. The regression equation in reference to monthly SST data (Smith et al., 2008) is:

$$\delta^{18}\text{O} (\text{‰}) = -0.106(\pm 0.010) \times \text{SST} - 1.432(\pm 0.259) \\ (r^2 = 0.41, p < 0.01, N = 188)$$

Moreover, $\delta^{18}\text{O}$ variation is investigated in reference to local SST data from a nearby island, Curacao (distance ~80km), for a period of 18 months spanning April 1999 to September 2000 (Bak et al., 2005). The linear regression for this data is:

$$\delta^{18}\text{O} (\text{‰}) = -0.124(\pm 0.016) \times \text{SST} - 0.951(\pm 0.437) \\ (r^2 = 0.79, p < 0.0001, N = 18)$$

We note that the $\delta^{18}\text{O}$ -SST relationships are lower than the published values from *D. strigosa* from Guadeloupe (Hetzinger et al., 2006). The discrepancy might arise from distinct seasonal temperature and hydrological cycles between Bonaire and Guadeloupe that in turn affect the amplitude of the oxygen isotopic ratio of coral skeleton at both sites. Therefore, to investigate pattern of $\delta^{18}\text{O}_{\text{sw}}$ variability reconstructed from paired coral $\delta^{18}\text{O}$ and coral Sr/Ca records, a range of proxy-SST calibrations is considered rather than using single calibration values.

2.4.4.2 Mid- to late Holocene changes in southern Caribbean Sea surface hydrology

Monthly resolved coral Sr/Ca, coral $\delta^{18}\text{O}$ and $\delta^{18}\text{O}_{\text{sw}}$ of three modern and six fossil corals are shown in Figure 2.22. Each coral

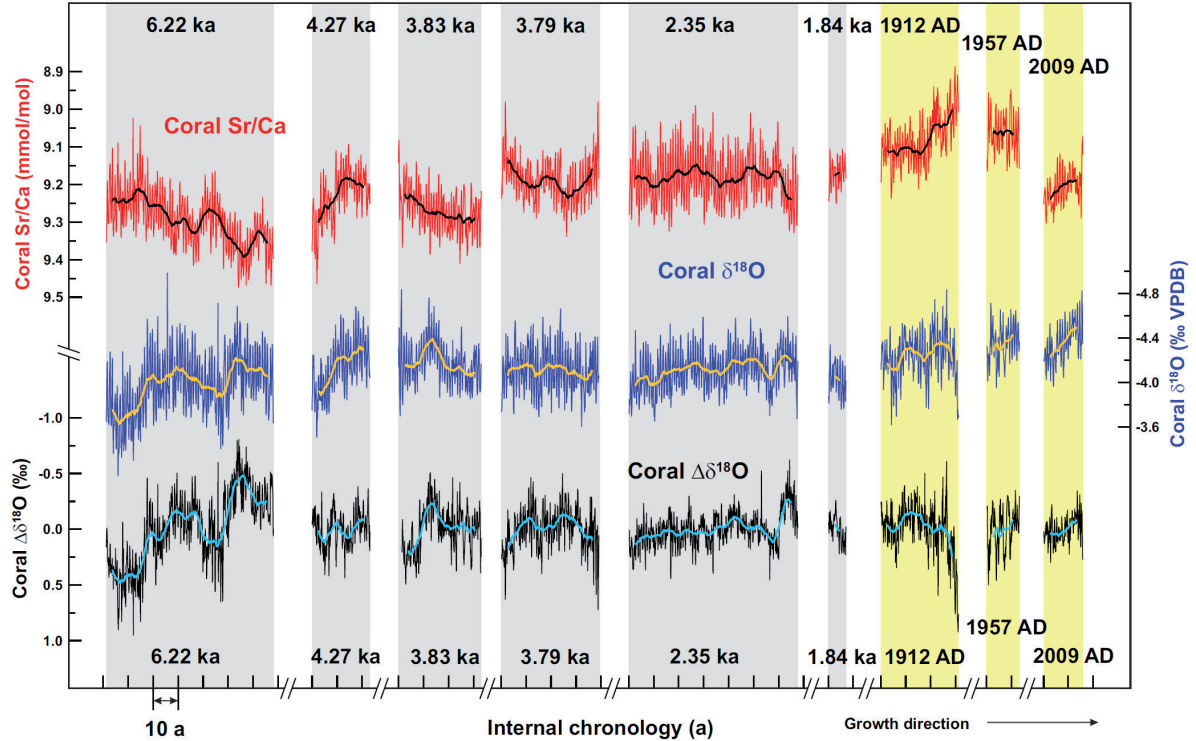


Figure 2.22: monthly resolved coral Sr/Ca (red), $\delta^{18}\text{O}$ (blue) and derived $\delta^{18}\text{O}_{\text{sw}}$ (black) records of modern (yellow shading) and fossil (grey shading) *Diploria strigosa* corals from Bonaire and corresponding 5-year running mean. The $\delta^{18}\text{O}_{\text{sw}}$ records were calculated using the centering method (Cahyarini et al., 2008) and Sr/Ca-SST and $\delta^{18}\text{O}$ -SST calibrations of -0.061 mmol/mol per $^{\circ}\text{C}$ and -0.180 ‰ per $^{\circ}\text{C}$ (Gagan et al., 1998; Corrège, 2006), respectively.

record shows clear annual cycles in both Sr/Ca and $\delta^{18}\text{O}$ records which correlate with the corresponding annual-density bands. Therefore, robust coral internal chronologies could be established enabling accurate assessment of seasonal to multidecadal variability of coral proxies.

2.4.4.2.1 Variation in mean $\delta^{18}\text{O}_{\text{sw}}$

Mean $\delta^{18}\text{O}_{\text{sw}}$ values were calculated by first averaging data of each year and subsequently averaging the resulting annual mean of all years constituting the coral record. The mean $\delta^{18}\text{O}_{\text{sw}}$ of individual coral records are shown in Figure 2.23. The three modern corals exhibit between colony offsets in mean $\delta^{18}\text{O}_{\text{sw}}$ values. The standard deviation of such intercolony variability is 0.161 ‰ (1σ). The mean $\delta^{18}\text{O}_{\text{sw}}$ values of all nine corals suggest a trend toward more positive values throughout the mid- to late Holocene. Considering the combined error that takes into account modern intercolony variability in mean $\delta^{18}\text{O}_{\text{sw}}$ (following

established procedure by Abram et al., (2009), but applied to mean $\delta^{18}\text{O}_{\text{sw}}$), more positive values found in the mid-Holocene are not significant with respect to modern $\delta^{18}\text{O}_{\text{sw}}$ values.

2.4.4.2.2 Seasonal changes of sea surface hydrology

Coral-based $\delta^{18}\text{O}$ seasonality

The coral $\delta^{18}\text{O}$ records of three modern corals indicate a mean $\delta^{18}\text{O}$ seasonality of 0.442 ± 0.057 ‰ ranging from 0.399 to 0.497 ‰ (Figure 2.24). It is assumed that the between-colony differences in coral $\delta^{18}\text{O}$ seasonality are not the result of changing environmental parameters over the last century, but rather reflect coral growth processes. Therefore, combined error (e.g., Abram et al., 2009) that takes into account modern intercolony offsets in coral $\delta^{18}\text{O}$ seasonality is considered for our estimates of Holocene coral $\delta^{18}\text{O}$ seasonality. Considering this uncertainty, Most of the fossil coral records show $\delta^{18}\text{O}$ seasonality that is not

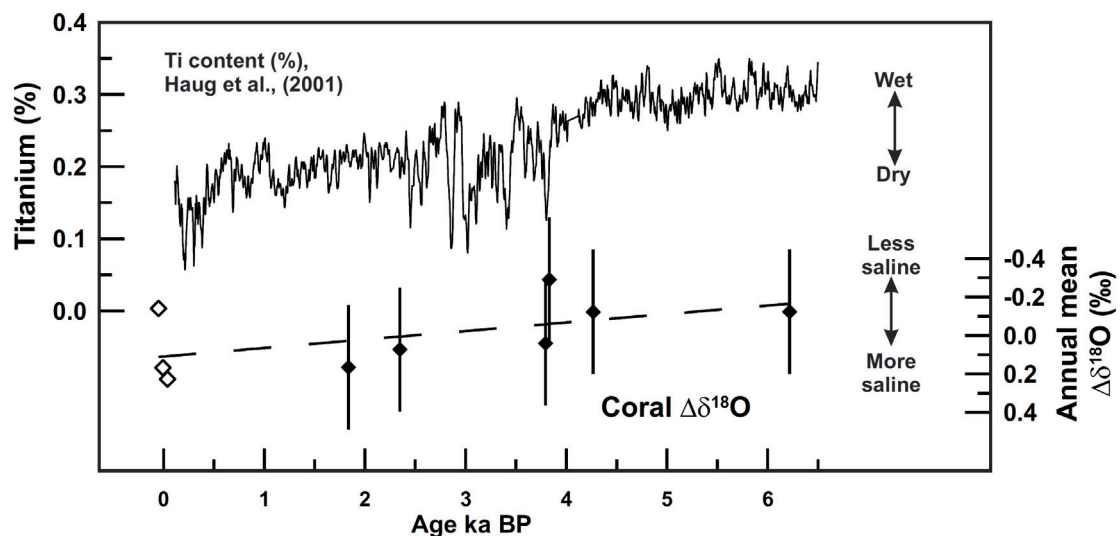


Figure 2.23: Comparison between mean coral $\Delta\delta^{18}\text{O}$ and Cariaco Basin Ti record (Haug et al., 2001). Coral $\Delta\delta^{18}\text{O}$ has been calculated for individual records using established procedures (Gagan et al., 1998; Corrège, 2006; Cahyarini et al., 2008). Error bars are the combined error (root of the sum of the squares) of the standard deviation (2σ) from mean coral $\Delta\delta^{18}\text{O}$ of three modern *Diploria strigosa* and the standard error (2SE) of the mean coral $\Delta\delta^{18}\text{O}$ value for individual corals, following established procedure (Abram et al., 2009) but applied to reconstructed coral $\Delta\delta^{18}\text{O}$. Note that coral $\Delta\delta^{18}\text{O}$ records indicate trend toward more saline conditions during the mid to late Holocene.

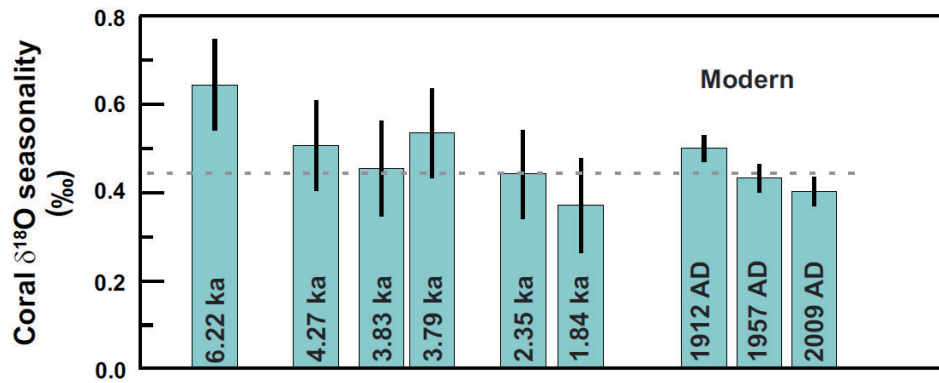


Figure 2.24: Coral $\delta^{18}\text{O}$ seasonality calculated for individual Bonaire coral records. Dashed line represents the mean modern $\delta^{18}\text{O}$ seasonality (0.442 ‰) calculated from the mean seasonality of three modern corals. Error bars for fossil corals are the combined error (root of the sum of the squares) of the standard deviation (2σ) from mean $\delta^{18}\text{O}$ seasonality of three modern *Diploria strigosa* and the standard error (2SE) of the averaged $\delta^{18}\text{O}$ seasonality measurements for individual coral records, following established procedure (Abram et al., 2009) but applied to reconstructed seasonality. 2SE for modern corals are presented. Note that the 6.2 ka coral shows significant increased $\delta^{18}\text{O}$ seasonality compared to that given by three modern corals.

significantly different from that given by three modern corals. However, significantly increased $\delta^{18}\text{O}$ seasonality (0.641 ± 0.103 ‰) is observed in the mid-Holocene coral (Figure 2.24).

Insight from measured coral Sr/Ca relative to coral $\delta^{18}\text{O}$

Composite annual Sr/Ca and $\delta^{18}\text{O}$ cycles derived from individual monthly resolved coral records indicate clear annual cycle for modern and fossil coral records (Figure 2.25a).

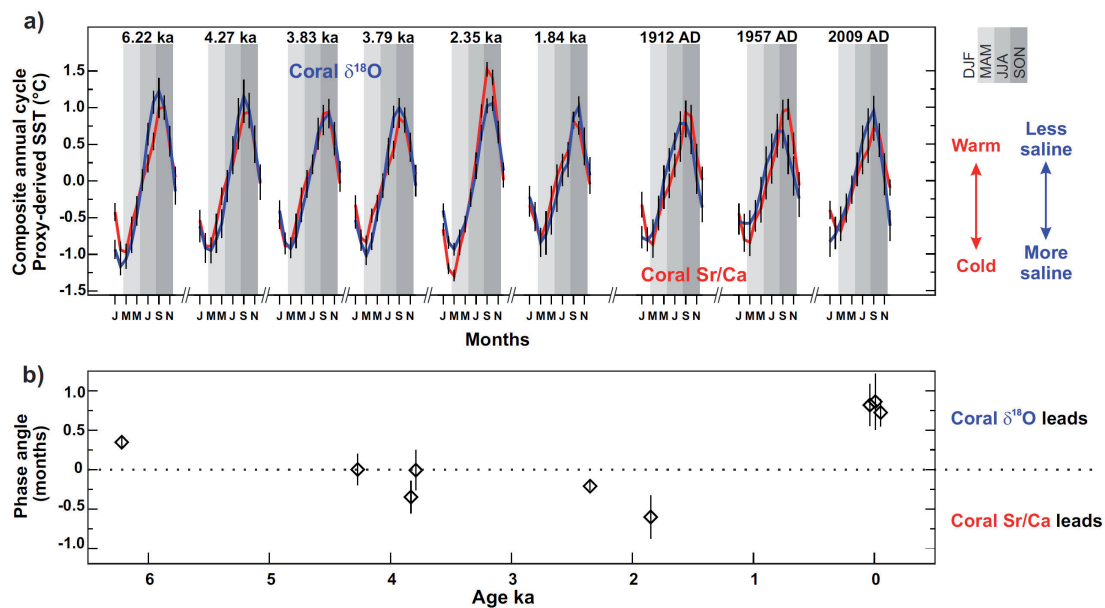


Figure 2.25: a) Composite annual cycles of coral Sr/Ca and $\delta^{18}\text{O}$ for each coral record used in this study converted in degree Celsius by using Sr/Ca-SST and $\delta^{18}\text{O}$ -SST relationships of -0.061 mmol/mol per $^{\circ}\text{C}$ and -0.180 ‰ per $^{\circ}\text{C}$ (Gagan et al., 1998; Corrège, 2006). Error bars indicate the standard error of the mean calculated for individual months. b) Phase angles of the annual cycle estimated by cross-spectral analyses between monthly coral Sr/Ca and coral $\delta^{18}\text{O}$ time series. Error bars indicate 80% confidence interval.

Changes in the timing between both proxies are assessed for the annual cycle. Cross-spectral analyses between measured coral proxies reveal that coral $\delta^{18}\text{O}$ annual cycle leads corresponding coral Sr/Ca records by about a month in modern corals. However, most of the fossil corals reveal that coral Sr/Ca either leads or is in phase with coral $\delta^{18}\text{O}$ (Figure 2.25b). The phase angles of modern coral records provide very similar values showing good reproducibility between modern coral colonies. Finally, the mid-Holocene coral

record which shows high amplitude annual $\delta^{18}\text{O}$ cycle (Figure 2.24) indicates that $\delta^{18}\text{O}$ leads Sr/Ca changes by only 0.3 month (Figure 2.25b).

Insight from calculated $\delta^{18}\text{O}_{\text{sw}}$

Composite annual $\delta^{18}\text{O}_{\text{sw}}$ cycles were calculated for individual coral records using a range of proxy-SST calibrations in order to test the impact of varying calibration on the reconstructed $\delta^{18}\text{O}_{\text{sw}}$ signal (Supplementary Figure 2.26). It is found that using calibrations

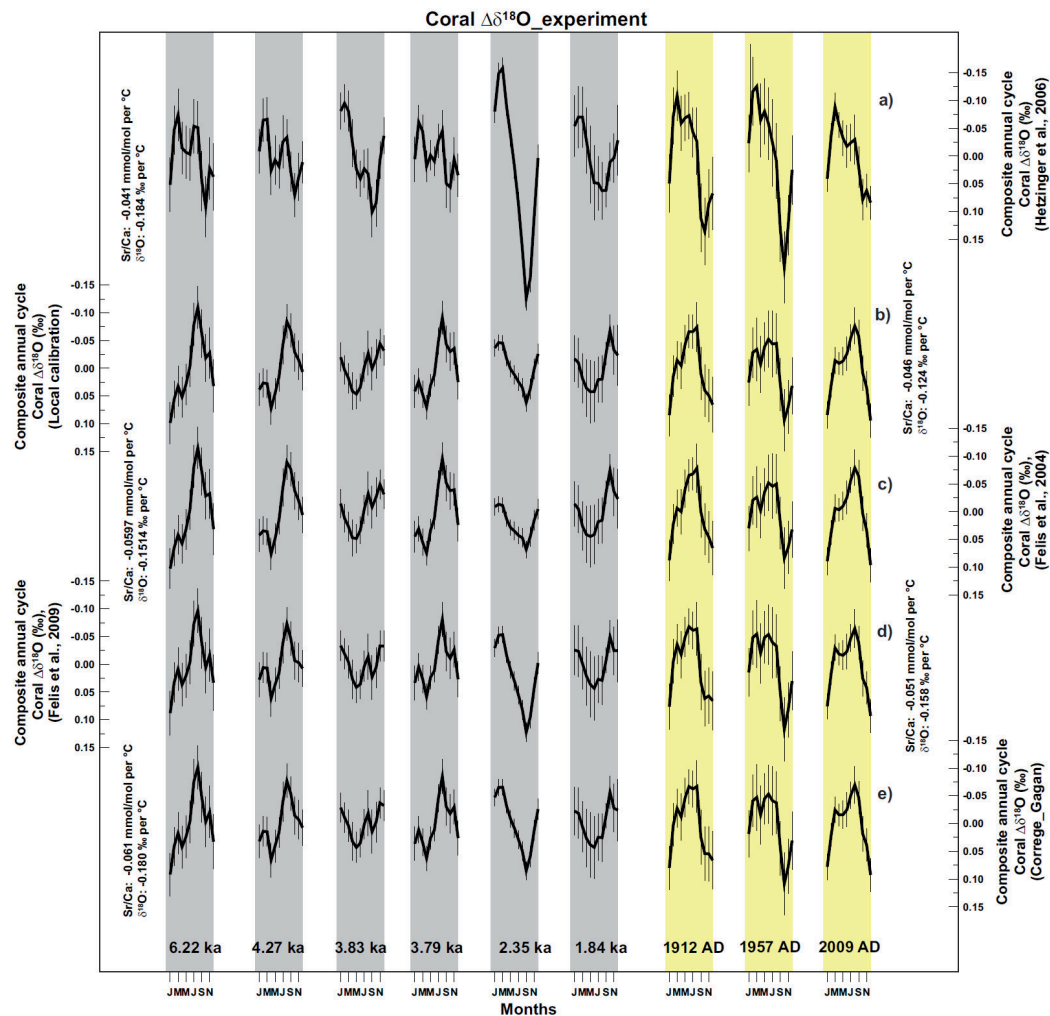


Figure 2.26: Response of reconstructed composite coral $\Delta\delta^{18}\text{O}$ annual cycle to different proxy-SST regression slopes. Composite annual cycles are calculated with the centring method (Cahyarini et al., 2008). Proxy-SST regression slopes used in this experiment are from a) Hetzinger et al., (2006), b) Coral Sr/Ca and $\delta^{18}\text{O}$ in reference to local SST data (this study), c) Felis et al., (2004), d) Felis et al., (2009) e) and well-accepted calibrations for coral $\delta^{18}\text{O}$ (Gagan et al., 1998) and coral Sr/Ca (Corrége, 2006). Note that experiment using calibration from Hetzinger et al., (2006) gives very different composite annual $\Delta\delta^{18}\text{O}$ cycle than all four other experiments which reveal very similar pattern for individual coral time window. Error bars represent the standard error of the mean of monthly values.

from Hetzinger et al., (2006) generate annual $\delta^{18}\text{O}_{\text{sw}}$ cycles that are very different than given by a set of four other calibrations, including local-SST calibrations (this study). Therefore, we rely on well-established proxy-SST calibrations (Gagan et al., 1998; Corrège, 2006) for the interpretation of fossil coral records.

Combined analytical uncertainties for reconstructing $\delta^{18}\text{O}_{\text{sw}}$ using Sr/Ca-SST relationship of -0.061 mmol/mol per $^{\circ}\text{C}$ (Corrège, 2006) and $\delta^{18}\text{O}$ -SST relationship of -0.18 ‰ per $^{\circ}\text{C}$ (Gagan et al., 1998) is ± 0.077 (Corrège, 2006) and $\delta^{18}\text{O}$ -SST relationship of -0.18 ‰ per $^{\circ}\text{C}$ (Gagan et al., 1998) is ± 0.077 ‰ (1σ). Consequently, coral $\Delta\delta^{18}\text{O}$ variability with amplitude greater than 0.154 ‰ are considered significant with respect to analytical uncertainty. Based on the above calibrations (Gagan et al., 1998; Corrège, 2006), reconstructed annual $\delta^{18}\text{O}_{\text{sw}}$ cycles from three modern coral records indicate lower values in spring and summer and higher values in fall and winter with average amplitude of 0.157 ‰

(Figure 2.27). Reconstructions of $\delta^{18}\text{O}_{\text{sw}}$ from Holocene coral records indicate similar seasonal hydrological regime (e.g., wet summer/dry winter) at 6.2 ka, 4.27 ka and 3.79ka, whereas different seasonal hydrological regime are observed at 3.83 ka, 2.35 ka and 1.84 ka. In addition, the mid-Holocene coral record reveals increased $\delta^{18}\text{O}_{\text{sw}}$ seasonality with amplitude of 0.193 ‰ that is 23% greater than the amplitude of the modern annual $\delta^{18}\text{O}_{\text{sw}}$ cycle given by three modern corals. Moreover, a period of reversed seasonality of hydrological cycle is detected at 2.35 ka BP. This record indicates more positive values in summer and more negative $\delta^{18}\text{O}_{\text{sw}}$ values with amplitude that is unprecedented in any other coral records.

2.4.4.2.3 Interannual to multidecadal $\delta^{18}\text{O}_{\text{sw}}$ variability

Multitaper method (MTM) spectral analysis of monthly coral $\Delta\delta^{18}\text{O}$ records indicates significant quasi-biennial, interannual variability that is often superimposed on multidecadal scale variability (Figure 2.28).

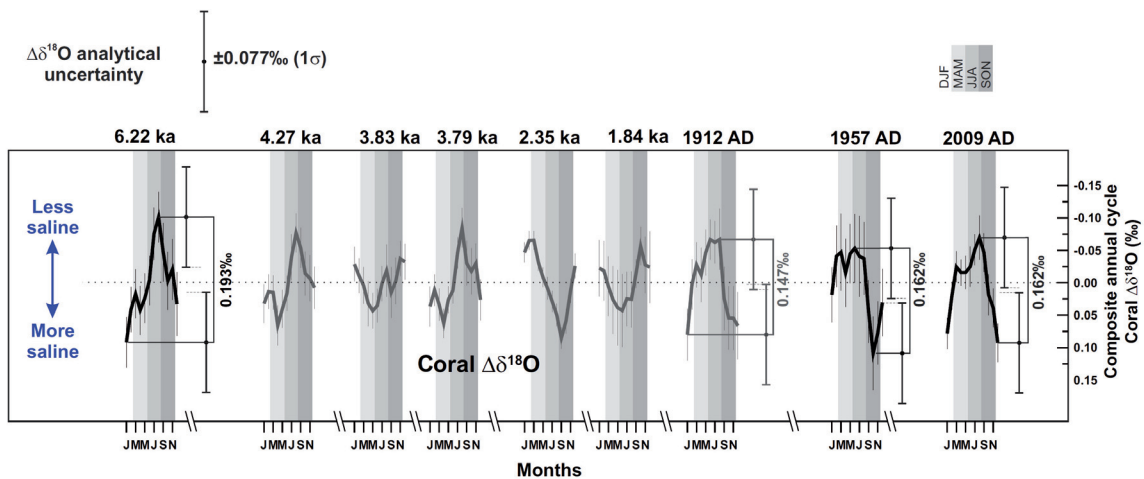


Figure 2.27: a) Composite annual coral $\Delta\delta^{18}\text{O}$ cycles for individual Bonaire coral records calculated using the centering method (Cahyarini et al., 2008) and Sr/Ca-SST and $\delta^{18}\text{O}$ -SST relationships of -0.061 mmol/mol per $^{\circ}\text{C}$ and -0.180 ‰ per $^{\circ}\text{C}$ (Gagan et al., 1998; Corrège, 2006). Combined analytical uncertainty is 0.154 ‰ (2σ). Composite annual cycles represented in black (gray) are characterised by amplitude of annual $\Delta\delta^{18}\text{O}$ cycle greater (lower) than 2σ . Vertical gray shading indicates seasons: winter (December-February, DJF), spring (March-May, MAM), summer (June-August, JJA) and fall (September-November, SON).

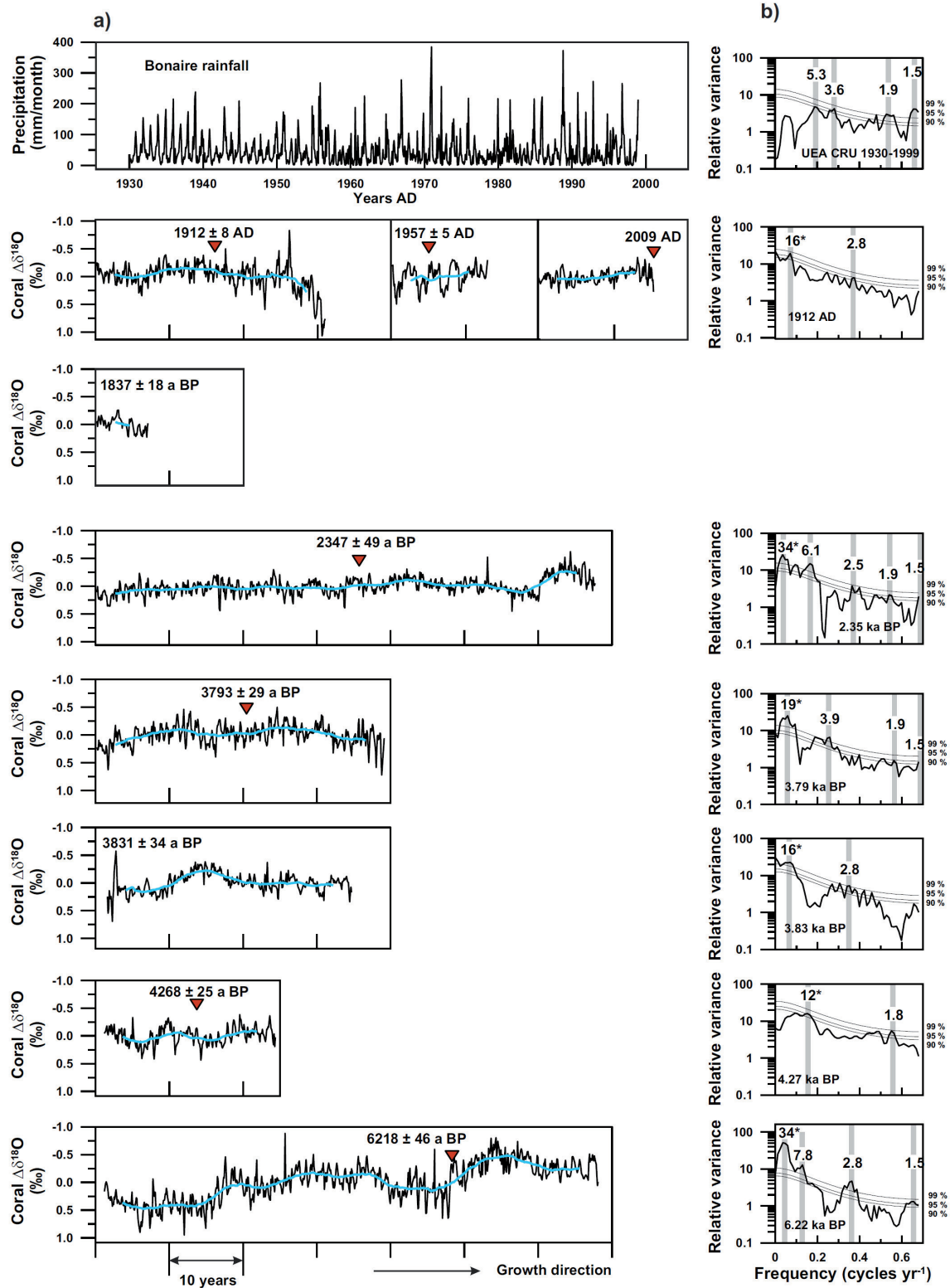


Figure 2.28: a) Monthly rainfall record from gridbox centred on Bonaire (12.5°N; 67.5°W) (*top*) (Hulme et al., 1998) and monthly reconstructed coral $\Delta\delta^{18}\text{O}$ records from Bonaire corals calculated using the centering method (Cahyarini et al., 2008). Sr/Ca-SST and $\delta^{18}\text{O}$ -SST regression coefficients used are -0.061 mmol/mol per °C and -0.180 mmol/mol per °C, respectively. b) Multitaper method (MTM) spectral analysis with a red noise null hypothesis (Ghil et al., 2002) (number of tapers 3; bandwidth parameter 2) of detrended and normalized to unit variance monthly precipitation and coral $\Delta\delta^{18}\text{O}$ records with length >20 years where mean annual cycle has been removed. 90%, 95%, and 99% significance levels are indicated.

Significant spectral peak in the quasi-biennial band (<2.3-year) is detected in all Bonaire corals. Interannual (2.3- to 7-year), near-decadal (7- to 15-year) as well as multidecadal (15- to 40-year) variability of coral $\Delta\delta^{18}\text{O}$ are identified in most of the coral records. Instrumental rainfall data (Hulme et al., 1998) reveal that precipitation over Bonaire are also characterised by significant quasi-biennial and interannual spectral peaks (Figure 2.28), whereas multidecadal variability of Bonaire precipitation is not significant over the period 1930-1999. Furthermore, while interannual variability seems to be a prominent feature of the coral-based $\delta^{18}\text{O}_{\text{sw}}$ records, the coral record at 2.3 ka indicates enhanced spectral power at interannual periodicity centred at 6.1-year and the 6.2 ka coral reveals pronounced variability at 7.8-year. Moreover, multidecadal periodicities seem to be a prominent feature in

Holocene coral $\Delta\delta^{18}\text{O}$ records where the strongest spectral power at multidecadal timescale is found in the 6.2 ka coral record.

To further investigate the strength of $\delta^{18}\text{O}_{\text{sw}}$ changes on different timescales throughout the mid- to late Holocene, individual coral $\Delta\delta^{18}\text{O}$ records have been filtered with a Gaussian bandpass filter (Paillard et al., 1996) to isolate quasi-biennial (<2.3-year), interannual (2.3- to 7-year), quasi-decadal (7- to 15-year) and multidecadal (15- to 40-year) components of variability (Figure 2.29). It is found that the amplitude of the quasi-biennial, interannual, and near-decadal coral $\Delta\delta^{18}\text{O}$ variability has not notably changed throughout the mid- to late Holocene compared to that of the multidecadal scale variability. This experiment reveals that the standard deviation of the 15- to 40-year bandpass-filtered time series of the 6.2 ka coral $\Delta\delta^{18}\text{O}$ record is twice

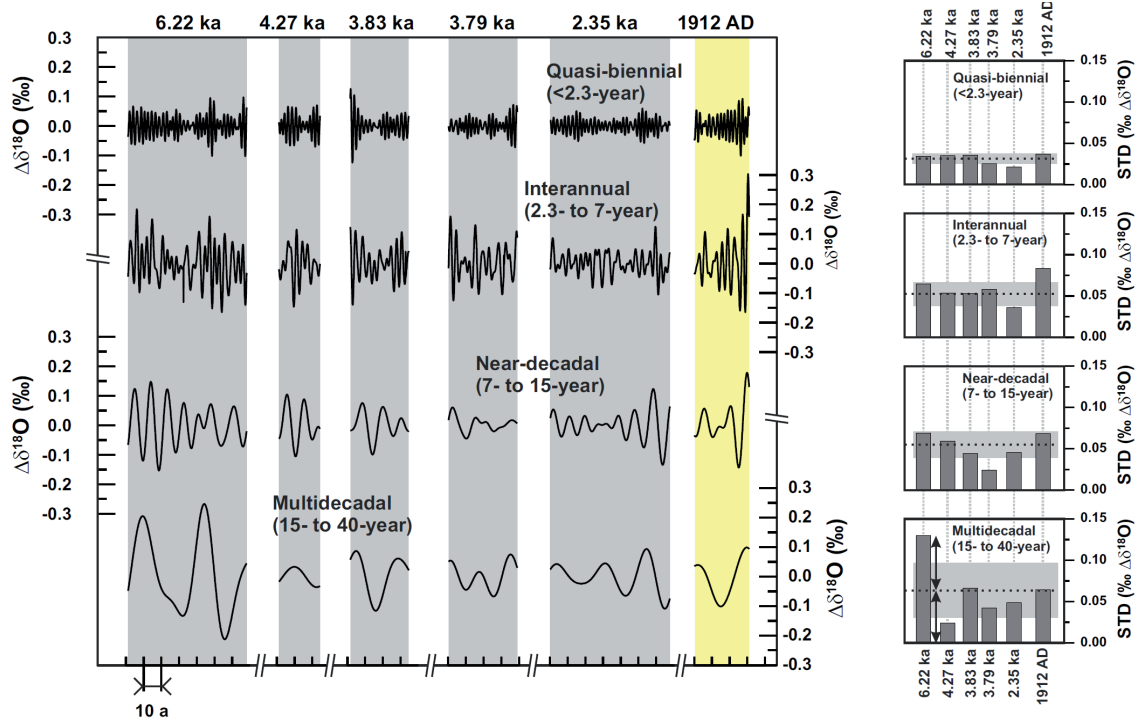


Figure 2.29: Quasi-biennial, interannual, near-decadal and multidecadal Gaussian bandpass filtered time series for individual coral $\Delta\delta^{18}\text{O}$ records (from Figure 2.22) with length > 20 years (*left panel*) and the corresponding standard deviations of filtered time series (*right panels*). Horizontal dashed lines indicate mean standard deviations of the filtered time series. Black arrows indicate that the variance of the multidecadal bandpass filtered time series of the 6.2 ka coral $\Delta\delta^{18}\text{O}$ record is twice as large as given by the corresponding mean standard deviation.

as large as the variance given by all coral records (Figure 2.29).

2.4.4.3 Relationship between $\delta^{18}\text{O}_{\text{sw}}$ and SST

The relationship between Sr/Ca-derived SST and $\Delta\delta^{18}\text{O}$ -related salinity is investigated for quasi-biennial, interannual, near-decadal, and multidecadal timescales (Figure 2.30) using the corresponding filtered time series. It is found that warmer than average SST are characterised by more saline conditions and *vice versa*. The sign of this relationship is true for all investigated timescales. The correlation coefficients between filtered time series are greater than 0.5 in most of the records suggesting that the observed relationship between SST and $\Delta\delta^{18}\text{O}$

related to salinity was prominent in the southern Caribbean Sea over the last 6.2 ka BP. In order to investigate the effect of different calibrations values on the sign of the relationship between $\Delta\delta^{18}\text{O}$ and Sr/Ca-SST records, similar experiment was performed by using $\Delta\delta^{18}\text{O}$ records derived with other proxy-SST calibrations (i.e., Hetzinger et al., 2006). It is found that calibrations used do not affect the sign of this relationship (not shown).

2.4.5 Discussion

2.4.5.1 $\delta^{18}\text{O}_{\text{sw}}$ changes of the western tropical Atlantic over the last 6.2 ka

Holocene climate conditions in low latitudes are mainly influenced by the convergence of subtropical northeasterly and

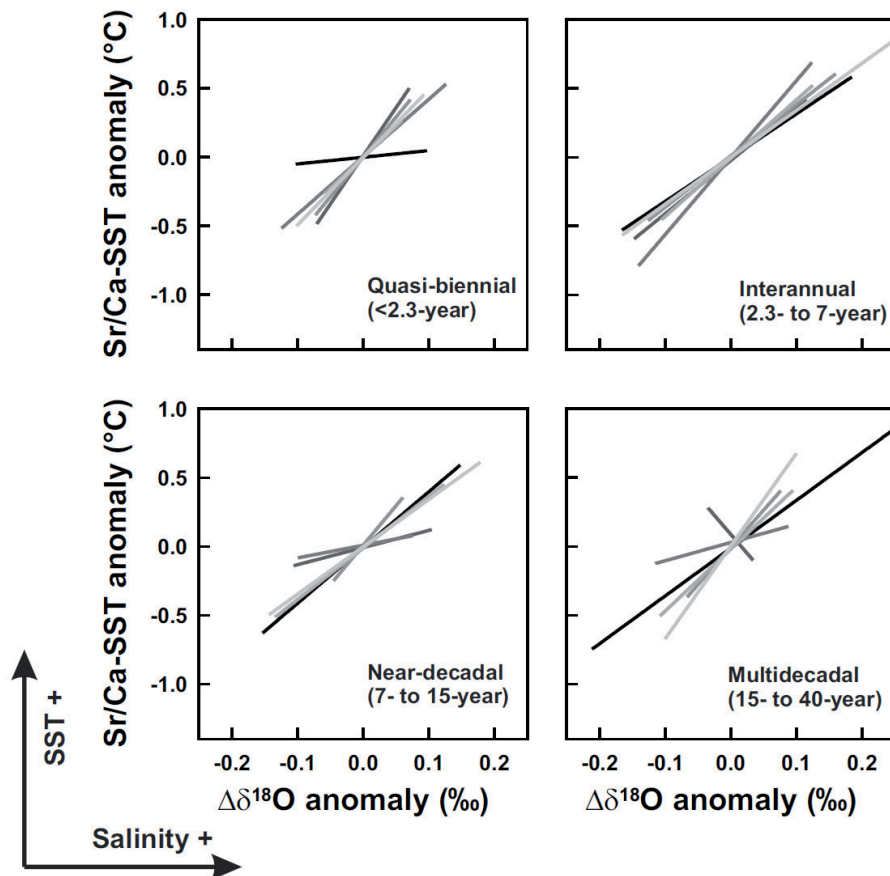


Figure 2.30: Linear regressions between Gaussian bandpass filtered coral $\Delta\delta^{18}\text{O}$ and Sr/Ca-SST records for Bonaire coral records with length > 20 years. Note that for all investigated timescales, coral records indicate positive correlation coefficient which suggest that periods of warmer than average sea surface temperatures (SST) are characterised by more saline conditions and *vice versa*.

southeasterly trade winds which form the Intertropical Convergence Zone (ITCZ). The ITCZ characterised by low pressure systems associated with a sharp zonal band of maximum precipitation migrates latitudinally according to seasonal changes of insolation. In the tropical Atlantic as well as other tropical locations, orbitally-driven changes in insolation received on top of the atmosphere have been shown to influence the latitudinal mean position of the ITCZ (e.g., Haug et al., 2001; Fleitmann et al., 2003). For instance, during the early and mid-Holocene, mid latitudes of the northern Hemisphere were characterised by greater summer insolation compared to winter and proxy reconstructions showed that zonal band of maximum rainfall associated with the ITCZ was located farther to the north relative to today thus, enhancing rainfall in more northern tropical latitudes. Haug et al., (2001) used titanium content of laminated sediment from Cariaco basin to infer relative changes of riverine terrigenous input throughout the Holocene that are linked to precipitation over northern South America. Although high-frequency variability of Titanium content was observed, they concluded that early to mid-Holocene rainfall over northern South America was enhanced due to a more northward position of the ITCZ linked to increased summer insolation in the northern Hemisphere at that time. In line with this finding, $\delta^{18}\text{O}_{\text{sw}}$ records indicate a trend towards more positive values throughout the mid- to late Holocene suggesting that the hydrological balance of the Southern Caribbean shifted from wetter conditions in the mid-Holocene towards drier conditions today. We caution the reader that this trend is barely significant possibly due to the combined effect of different vital effect

between coral colonies (Figure 2.23) and rapid shifts of the local hydrological conditions linked to tropical and extratropical forcing on the mean position of the ITCZ (Haug et al., 2001). Although accurate quantification of mean $\delta^{18}\text{O}_{\text{sw}}$ changes between 6.2 ka and today is difficult to infer from Bonaire corals, the decrease of $\delta^{18}\text{O}_{\text{sw}}$ over the last 6.2 ka did not exceed 0.322‰ (2 σ -uncertainty) which would correspond according to Watanabe et al., (2001) to salinity change less than 1.6 psu. Such slight change of tropical Atlantic salinity over the last 6.2 ka is further supported by model simulation by Oppo et al., (2007) which indicated less saline conditions and lower $\delta^{18}\text{O}_{\text{sw}}$ values in the tropics during the mid-Holocene.

2.4.5.2 Annual $\delta^{18}\text{O}_{\text{sw}}$ cycles over the last 6.2 ka: local precipitations Vs. oceanic advection

2.4.5.2.1 Reduced local precipitations at present

Annual $\delta^{18}\text{O}_{\text{sw}}$ cycle derived from modern corals revealed lower values in spring and summer and higher $\delta^{18}\text{O}_{\text{sw}}$ values in fall and winter. Climatological data from World Ocean Atlas 09 (Antonov et al., 2010) indicate salinity seasonality near Bonaire of ~1 psu with maximum and minimum SSS value occurring in May and September, respectively. However, according to SODA (Simple Ocean Data Assimilation Reanalysis) salinity dataset (Carton and Giese, 2008) for Bonaire gridbox, the seasonal cycle is ~0.6 psu in amplitude with maximum and minimum SSS values occurring in April and November, respectively (Figure 2.31). These two salinity datasets indicate that there is no consensus on the real

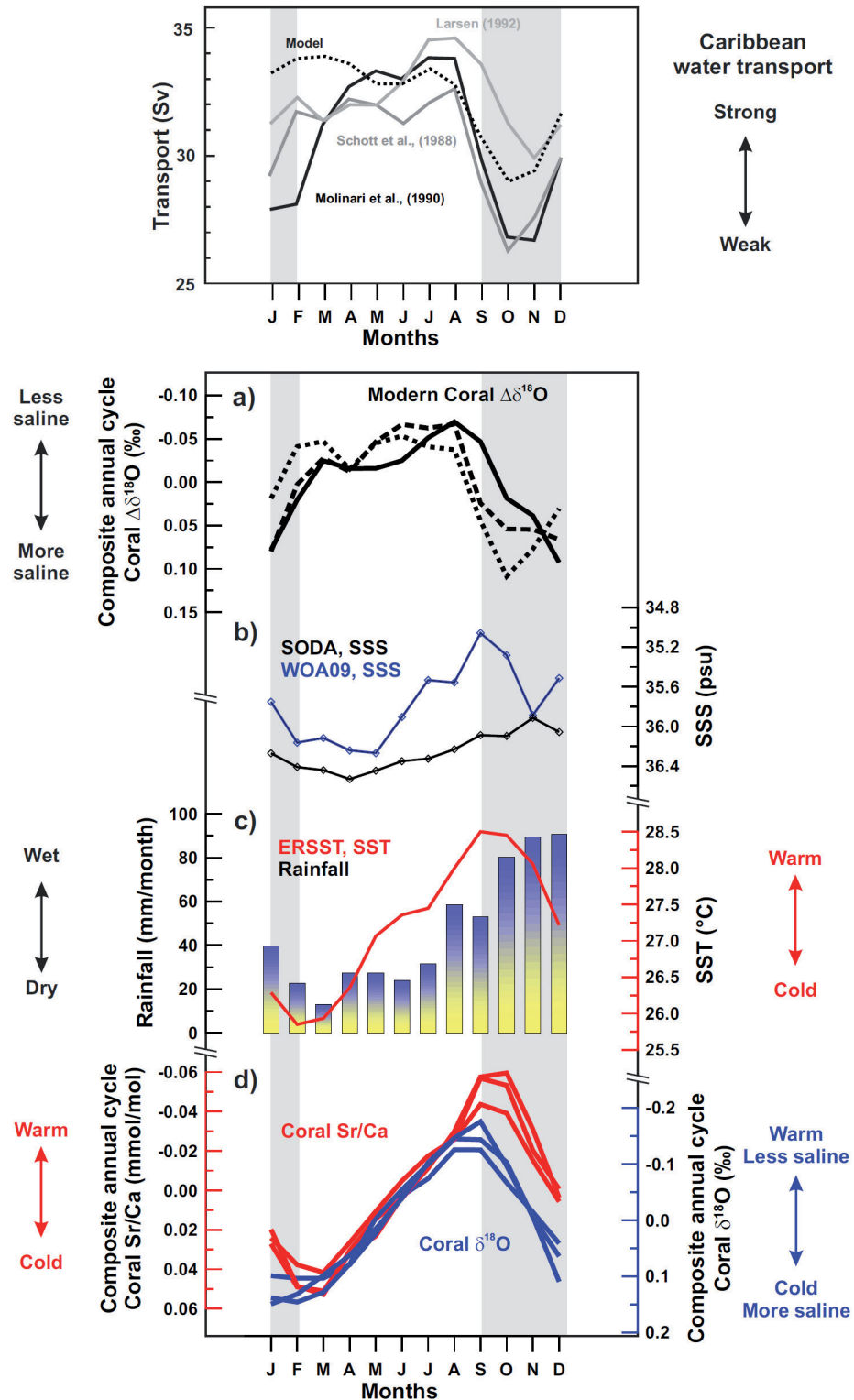


Figure 2.31: Top: Modelled (black dashed line) and observed annual cycle of the Florida Current (modified from Johns et al., 2002). **Bottom:** Monthly mean climatology of modern coral geochemical data and environmental parameters at the study, Bonaire. a) Composite annual coral $\Delta\delta^{18}\text{O}$ cycle of three modern corals, 1912 AD (dashed line), 1957 AD (dotted line) and 2009 AD (solid line) calculated as previously described (cf. Figure 2.22); b) Composite annual sea surface salinity cycles from World Ocean Atlas 09 (Antonov et al., 2010) in a $1^\circ \times 1^\circ$ gridbox (black) and from CARTON-GIESE SODA v2p0p2-4 (Carton and Giese, 2008) in a $0.5^\circ \times 0.5^\circ$ gridbox (blue); c) Sea Surface Temperature (SST) monthly climatology for 1970-2000 from ERSSTv3b (Smith et al., 2008) in a $2^\circ \times 2^\circ$ gridbox (red line) and climatology of monthly mean precipitation for the same period from UEA CRU Hulme Global prcp in a gridbox centred at 67.5° and 12.5° (Hulme et al., 1998) (vertical bars); d) Composite annual coral $\delta^{18}\text{O}$ (blue) and Sr/Ca (red) cycles of three modern corals. Grey areas indicate periods of more positive coral $\Delta\delta^{18}\text{O}$ values which correspond to periods of weaker surface water transport by the Florida Current.

amplitude and timing of the annual salinity cycle around Bonaire. The semi-arid climate of Bonaire is characterised by low annual mean rainfall with the rainy season occurring in fall. As the rainy season lag maximum SST values by a month, the rainfall amount can not explain the phase lag observed between coral $\delta^{18}\text{O}$ and Sr/Ca observed in three modern corals where $\delta^{18}\text{O}$ leads Sr/Ca (Figure 2.25). Consequently, since local rainfall and salinity data can not explained the annual $\delta^{18}\text{O}_{\text{sw}}$ cycles reconstructed from three modern corals, an alternate mechanism is proposed for explaining modern freshwater budget of Bonaire as documented by modern corals.

Bonaire lies in the pathway of the Caribbean Current which is the dominant surface current in the Caribbean Sea transporting surface warm water northwestward from the southeastern Caribbean to the Gulf of Mexico (Wüst, 1964). The outflow of this warm water mass from the Caribbean concentrates on Florida Strait between Florida Keys and Cuba to contribute to the Gulf Stream and the Western Boundary Current. The highest surface velocity in the Caribbean Sea (exceeding 100 cm/s) is found near the southern boundary along the coast of Venezuela and Netherland Antilles (Hernández et al., 2000; Fratantoni, 2001) suggesting that the southern Caribbean Sea is highly sensitive to change in surface water transport. Water masses transported through the Caribbean originate from the North Brazilian Current (NBC) and the Guyana Current (GC) which transport South Atlantic and freshwater discharged from Orinoco and Amazon Rivers, respectively, into the Caribbean (Hellweger and Gordon, 2002; Chérubin and Richardson, 2007) (Figure 2.20). The total flow through

the Caribbean displays a seasonal cycle that is stronger in the far southeastern Caribbean through the Windward Islands passages (Johns et al., 2002). Moreover, the inflow in the far southern Caribbean is intimately linked to the outflow from the Caribbean to the subtropical north Atlantic through the Florida Current (Johns et al., 2002). Extensive studies on surface water transport by the Florida Current indicate strong seasonality in water transport through the Florida Strait (Schott et al., 1988; Molinari et al., 1990; Larsen, 1992; Johns et al., 2002) (Figure 2.31). The outflow from the Caribbean shows maximum transport in spring and summer and minimum values in fall. From spring to summer, maximum transport appears to result from a strengthened NBC and GC primarily driven by changes in seasonal winds (Müller-Karger et al., 1989; Johns et al., 2002). The reduction of Atlantic inflow into the Caribbean in the second half of the year is thought to be linked to a weakened NBC and GC that redirect tropical fresher Atlantic water eastward at this time (Johns et al., 2002). Consequently, we suggest that the reconstructed $\delta^{18}\text{O}_{\text{sw}}$ annual cycle from three modern Bonaire corals primarily reflects the annual cycle of fresh water transported by the western boundary flow.

2.4.5.2.2 *Pronounced local precipitations in the mid-Holocene*

The seasonal migration of zonal band of maximum precipitation associated with the ITCZ is well documented in both observational and model studies. However, very little is known on the seasonal dynamic of the ITCZ under different climate background state mainly due to lack of suitable high-resolution proxy data that clearly resolve the annual

cycle. In order to assess pattern of southern Caribbean annual precipitation cycle in the mid-Holocene, we take advantage of the 6.2 ka coral which grew during a period of more northern position of the ITCZ (Haug et al., 2001).

The 6.2 ka coral indicates significant increased coral $\delta^{18}\text{O}$ seasonality, whereas Sr/Ca-SST annual cycle was slightly increased (this study, Figure 2.24; cf. Giry et al., (submitted), Figure 2.17). Moreover, coral $\delta^{18}\text{O}$ leads Sr/Ca record by about 0.3 month suggesting that more negative (positive) $\delta^{18}\text{O}$ values precede maximum (minimum) SST. These results indicate that annual $\delta^{18}\text{O}_{\text{sw}}$ was different at 6.2 ka than it is today and suggest that wetter conditions occurred before maximum SST peak and/or drier winter conditions occurred before minimum SST peak. Reconstructed $\delta^{18}\text{O}_{\text{sw}}$ in this mid-Holocene coral shows significant increased $\delta^{18}\text{O}_{\text{sw}}$ seasonality compared to that given by modern corals (Figure 2.27). This annual $\delta^{18}\text{O}_{\text{sw}}$ cycle indicates the lowest and highest values in August and January, respectively, with a sharp transition from more positive to more negative values occurring within less than two months. This sharp summer peak occurring in June-July is typical for transition from dry to wet conditions. Considering that local precipitation can explain the low $\delta^{18}\text{O}_{\text{sw}}$ value found in summer, this would mean that SST threshold for convection leading to strong local precipitation is reached prior to maximum SST value. However, one should not exclude the role of oceanic advection of freshwater through the Caribbean Current at that time. Haug et al., (2001) proposed that a more northerly mean annual position of the ITCZ in the mid-Holocene relative to today would

cause both more precipitation and less trade wind over northern South America. Considering that weaker trade winds would reduce the surface water inflow to the Caribbean (Müller-Karger et al., 1989; Johns et al., 2002), more negative summer $\delta^{18}\text{O}_{\text{sw}}$ values found in the 6.22 ka coral record provides strong support for more intense summer precipitation possibly brought by a more northern position of the ITCZ as the main driver of mid-Holocene annual sea surface hydrology in the southern Caribbean Sea. Therefore, our monthly resolved mid-Holocene $\delta^{18}\text{O}_{\text{sw}}$ record is consistent with the northward shift of the ITCZ (Haug et al., 2001). However, to further investigate the dynamic of the tropical rain belt over both South America and Africa, one should further develop monthly-resolved climate records from both hemispheres and along both continents.

2.4.5.2.3 Mid- to late Holocene transition

The mid-Holocene coral record suggests enhanced summer precipitations, whereas the three modern corals indicate advection of fresh surface water as the prevailing factor controlling sea surface hydrology at Bonaire. This suggests that a transition occurred since the mid-Holocene. The 4.27 and 3.79 ka corals show higher $\delta^{18}\text{O}$ seasonality having no phase lag with corresponding annual Sr/Ca record suggesting that more negative (positive) $\delta^{18}\text{O}$ values occurred in phase with warmer (colder) SST. This suggests wet summers and/or dry winters. As for the 6.22 ka coral record, “sharp” $\delta^{18}\text{O}_{\text{sw}}$ summer peaks towards more negative values are observed in the composite annual cycle of these two coral records suggesting that wet summers were potentially characteristic in the

southern Caribbean climate at those times. However, this “wet summer/dry winter” pattern is less pronounced in more recent coral records and especially in modern corals suggesting that either loss of summer precipitation or reduced advection of fresher water through the Caribbean Current in summer occurred throughout the mid- to late Holocene thus, damping the “sharp” summer peak towards more negative values in more recent coral records.

The 3.83 and 1.84 ka coral records indicate that annual coral Sr/Ca record leads corresponding $\delta^{18}\text{O}$ record by about half a month suggesting that wetter (drier) conditions occurred after maximum (minimum) SST values. It is indeed evident from the measured coral Sr/Ca and $\delta^{18}\text{O}$ data that changes in the timing between annual SST and hydrological cycles occurred in the southern Caribbean Sea throughout the mid- to late Holocene possibly driven by the competing influence of local precipitation and oceanic advection of freshwater originating from Orinoco and Amazon rivers.

An exceptionally large increased SST seasonality compared to both today and the mid-Holocene is indicated by a Bonaire coral for 2.3 ka BP (Giry et al., 2010b; Giry et al., submitted). This is accompanied by a reversal of $\delta^{18}\text{O}_{\text{sw}}$ annual cycle as inferred from coral $\Delta\delta^{18}\text{O}$, resulting in a dampening of coral $\delta^{18}\text{O}$ seasonality despite of an enhanced coral Sr/Ca seasonality. This reversal in the seasonality of the hydrological balance around 2.3 ka BP indicates low (high) $\delta^{18}\text{O}_{\text{sw}}$ values in winter (summer). Assuming that local rainfall was the main driver of seasonal $\delta^{18}\text{O}_{\text{sw}}$ variations, enhanced precipitation/reduced evaporation during winter and/or reduced

precipitation/enhanced evaporation during summer/fall relative to today could possibly explain the observed annual $\Delta\delta^{18}\text{O}$ cycle at 2.35ka. However, reduced advection of freshwater during the warm season and/or enhanced advection during the cold season could be an alternate explanation. To validate the latter, surface winds would modulate both SST (i.e., wind-induced heat loss) and hydrological condition (i.e., wind-induced oceanic advection of freshwater from tropical Atlantic) at sea surface. In this sense, weakened (strengthened) surface winds in summer (winter) could generate positive (negative) SST anomaly and reduce (intensify) transport of fresh tropical water to the study site.

To summarise, it is found that local precipitation was dominating annual hydrological cycle in the mid-Holocene. In contrast, oceanic advection of freshwater discharged from the Orinoco and the Amazon rivers by wind-driven surface currents dominates the annual $\delta^{18}\text{O}_{\text{sw}}$ cycle at Bonaire today due to strengthened trade winds associated with the modern southward shift of the ITCZ.

2.4.5.3 Control of surface winds on SST and sea surface hydrology

Holocene coral Sr/Ca-SST and coral $\Delta\delta^{18}\text{O}$ records reveal that period of warmer than average SST around Bonaire were characterised by more saline conditions (Figure 2.30). This relationship is true for all investigated timescales including quasi-biennial, interannual and multidecadal timescales. On quasi-biennial timescale, the Quasi-Biennial Oscillation of zonal winds of the tropical troposphere with a typical periodicity of

2.3-year has been shown to be associated with sea level pressure anomalies and hurricane activity in the Atlantic (Gray, 1984). On interannual timescale, ENSO is known to play a major role in controlling both the tropical Atlantic SST and precipitation (Giannini et al., 2000; Alexander and Scott, 2002; Chiang et al., 2002). Observational study by Chiang et al., (2002) demonstrated that warm ENSO teleconnection to the tropical Atlantic results in anomalous warm north tropical Atlantic mainly through a warming of the tropical troposphere due to anomalous heating in the eastern equatorial Pacific. In addition, warming of the troposphere in the Atlantic reduces convection and thus, precipitation over the tropical Atlantic. Moreover, intense convection in the tropical Pacific associated with warm ENSO leads to suppression of rainfall over northern South America and Amazon Basin (Garreaud et al., 2009). Although ENSO activity was reduced in the mid-Holocene (Clement et al., 1999; Tudhope et al., 2001), we find that the 6.22 ka coral record also shows similar relationship between salinity and SST on interannual timescale suggesting that a unique physical mechanisms responsible for such relationship were present over the last 6.2 ka BP around Bonaire. On multidecadal timescales, the Atlantic Multidecadal Oscillation mode of multidecadal fluctuations of SST in the north Atlantic sector is known to play critical a role in controlling tropical Atlantic precipitation anomalies (Sutton and Hodson, 2005). For instance, during the warm phase of the AMO the tropical Atlantic and Caribbean experience positive summer precipitation anomalies, whereas summer precipitation over northern South America and Amazon Basin

seems to show a inverse relationship with the AMO (Sutton and Hodson, 2005).

Given that the relationship between SST and salinity at Bonaire (i.e., warmer/colder conditions go along with more/less saline conditions) is true for a wide range of timescales ranging from quasi-biennial to multidecadal, we assume that a single physical mechanism was responsible for the sign of this relationship over the last 6.2 ka. We propose that changes in surface winds modulate both SST and the strength of oceanic advection of tropical Atlantic freshwater into the southern Caribbean Sea as illustrated in Figure 2.32. In a previous study (Giry et al., submitted), pronounced quasi-biennial to multidecadal variability of southern Caribbean SST recorded in coral Sr/Ca record was reported. Since SST and surface winds are very strongly correlated in the far southern Caribbean around Bonaire (Figure 9 from Wang, 2007), we assume that changes of surface winds on a broad range of timescale drive SST there. Moreover, as modern Caribbean throughflow shows strong wind-driven seasonality (e.g., Johns et al., 2002), we suggest that surface winds force the inflow of fresh tropical water into the Caribbean via Ekman transport through the North Brazilian-Guyana-Caribbean current system. For instance, strengthened surface winds contribute to stronger heat loss that cool down SST at Bonaire, while it forces Ekman transport and oceanic surface circulation that transport fresher tropical Atlantic water into the Caribbean thus, contributing to colder and fresher conditions at Bonaire (Figure 2.32).

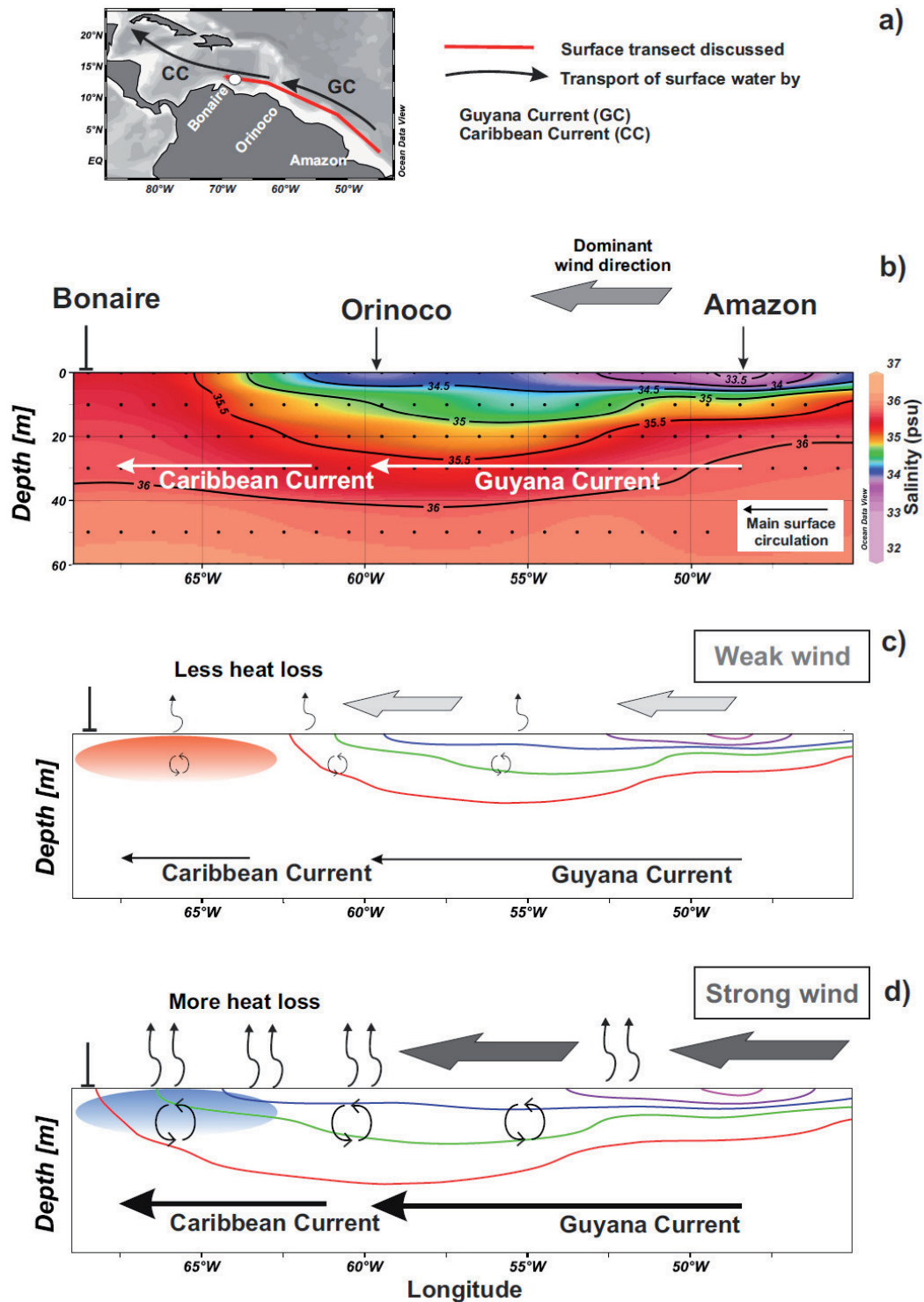


Figure 2.32: a) Map showing positions of section of interest (*red line*) and dominant surface currents (Guyana Current, GC; Caribbean Current, CC). b) Observed sea surface Salinity (SSS) in the upper 60 m along the section from the western tropical Atlantic to the southeastern Caribbean Sea. Freshwater discharged by the Amazon and Orinoco rivers contribute to freshening of the western tropical Atlantic that extend northwestward due to transport by Guyana and Caribbean Currents. c) and d) Response of sea surface conditions under two different surface wind strength scenarios. c) Weak wind scenario: reduced extent of fresh water (*contour color lines*) transport northwestward due to reduced Guyana/Caribbean current system, and reduced heat loss and vertical mixing at sea surface that in turn contribute to warmer sea surface temperature (SST). d) Strong wind scenario: intensification of surface water transport from the western tropical Atlantic to the Caribbean by surface current system and enhanced heat loss and vertical mixing at sea surface which in turn reduce SST thus, contributing to colder and less saline conditions around Bonaire.

2.4.5.4 Enhanced multidecadal variability at 6.2 ka

Coral $\Delta\delta^{18}\text{O}$ records from Bonaire indicate prominent interdecadal to multidecadal periodicities (Figure 2.29) suggesting a well-marked feature of southern Caribbean sea surface hydrological conditions. The 6.22 ka coral $\Delta\delta^{18}\text{O}$ record shows enhanced multidecadal variability (Figure 2.28) that is further supported by Gaussian band-pass filtering method (Figure 2.29). Moreover, the amplitude of this multidecadal $\Delta\delta^{18}\text{O}$ signal ($\sim 0.3\text{‰}$) is larger than the corresponding annual cycle, indeed providing evidence for enhanced multidecadal variability of southern Caribbean sea surface hydrology in the mid-Holocene.

Previous coral $\delta^{18}\text{O}$ -based study from Dominican Republic indicated significant interdecadal variability of tropical Atlantic precipitation in the mid-Holocene (Greer and Swart, 2006). They suggested that the latitudinal migration of ITCZ or increased storm activity have modulated interdecadal changes of northern Caribbean precipitations captured in the Enriquillo Valley. Moreover, it has been recently reported that multidecadal climate variability associated with the Atlantic Multidecadal Oscillation (AMO) were persistent throughout the mid- to late Holocene (Knudsen et al., 2011). Knudsen et al., (2011) showed that Caribbean precipitations inferred from Titanium record from Cariaco Basin have experienced multidecadal fluctuations linked to the AMO over the last 8 ka.

Given that sea surface hydrology of the southern Caribbean has experienced pronounced multidecadal variations in the mid-Holocene, one has to investigate the sources of this variability and unravel the role of tropical

surface water advection amongst local precipitation amount effect. On seasonal timescale, the coral $\Delta\delta^{18}\text{O}$ record at 6.2 ka provides evidence for enhanced summer precipitation (cf. section 4.2.2). Consequently, as the hypothesis of SST threshold for convection can potentially explain annual $\delta^{18}\text{O}_{\text{sw}}$ cycle, we propose to assess the role of summer precipitation in producing the pronounced multidecadal variability inferred from the mid-Holocene coral $\Delta\delta^{18}\text{O}$ record.

To test the role of SST threshold for convection in controlling multidecadal summer precipitation potentially associated with the AMO (i.e., warmer Caribbean SST leads to more summer precipitation) (Sutton and Hodson, 2005), the difference between negative (wet month) and positive (dry month) $\delta^{18}\text{O}_{\text{sw}}$ values is assessed for any single year of the 6.22 ka coral. Assuming that $\delta^{18}\text{O}_{\text{sw}}$ of dry months represent mainly mean oxygen isotopic composition of sea water, it is found that warmer than average SST are characterised by more summer precipitation (Figure 2.33c). This result supports the effect of local SST on summer precipitation known from the AMO (Sutton and Hodson, 2005). However, more saline conditions found during warm periods can not be explained by the influence of local summer precipitation. Consequently, the enhanced amplitude of multidecadal mean sea surface hydrology variability observed in the 6.2 ka coral record was presumably influenced by other mechanisms possibly linked to the impact of surface winds on SSS and SST (cf. section 2.4.5.3).

Nevertheless, other mechanisms reported in the literature could explain the sign of the relationship observed between SSS and SST and possibly explain the enhanced

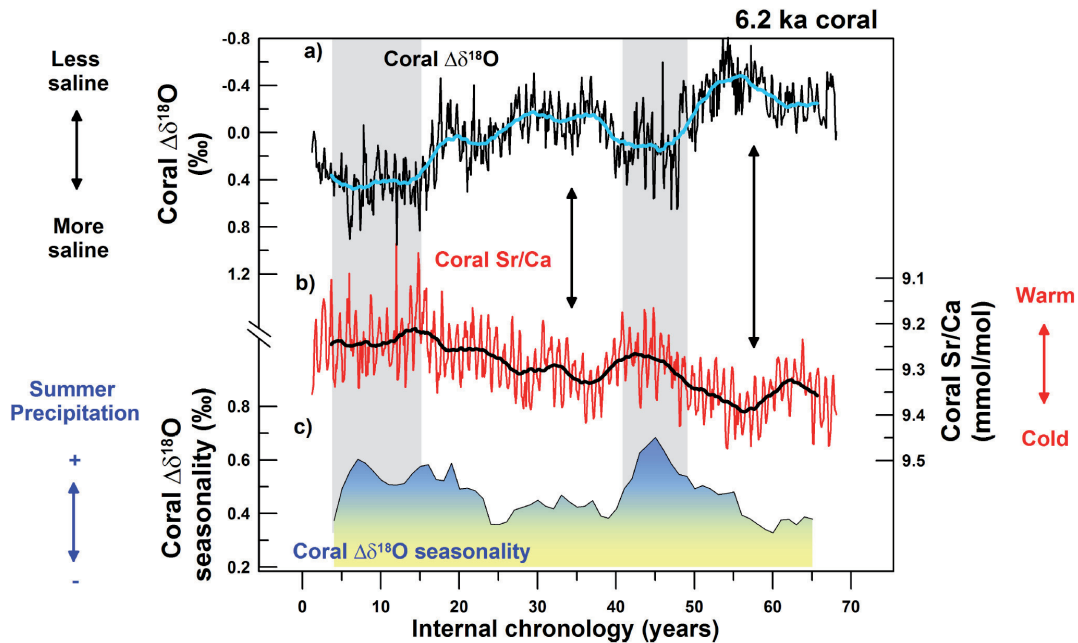


Figure 2.33: a) monthly coral $\Delta\delta^{18}\text{O}$ record of the 6.2 ka coral (black line) and corresponding 5-year running mean (blue line). b) Monthly coral Sr/Ca record (red line) and corresponding 5-year running mean (thick black line). c) 5-year running mean coral $\Delta\delta^{18}\text{O}$ seasonality calculated as the difference between minimum and maximum $\Delta\delta^{18}\text{O}$ values of any single year. Coral $\Delta\delta^{18}\text{O}$ seasonality reflects the intensity of summer precipitation. Grey shadings indicate periods of enhanced summer precipitation which correspond to periods of warmer than average SST and more saline conditions. Black arrows show periods colder than average characterised by less saline conditions.

multidecadal variability as documented in the mid-Holocene coral records. On multidecadal timescales, the AMO is linked to the strength of the Atlantic meridional overturning circulation (AMOC) (Delworth and Mann, 2000; Knight et al., 2005). During stronger AMOC, meridional heat transport through ocean circulation from low to high latitude influences SST in the north Atlantic realm which is then characterised by warmer than average SST characteristic of the positive phase of the AMO (Sutton and Hodson, 2003). There is a general agreement from water hosing experiments that the resulting slow down of the AMOC cools down the entire North Atlantic (Stouffer et al., 2006). However, similar water hosing experiment using a high-resolution coupled ocean-atmosphere model (Wan et al., 2009) revealed that atmospheric processes in response to a

weakened AMOC indeed produce surface cooling in most of the north Atlantic realm, whereas a narrow strip of warmer surface water appears along the northern coast of South America. Wan and colleagues suggested that a weakening of the AMOC produce a weakening of the western boundary current off Venezuela and Guyana coasts. They argue that such reduced western boundary current produces a strong subsurface temperature warming that extends to surface mixed layer. In addition to that, there is a general consensus in water hosing experiments that the mean position of the ITCZ is shifted southward during a weakened AMOC thus, bringing negative precipitation anomalies over the tropical north Atlantic and northern South America (e.g., Vellinga and Wood, 2002; Lohmann, 2003; Zhang and Delworth, 2005;

Stouffer et al., 2006). Since abrupt shifts from warm and saline to cold and fresh conditions in the southern Caribbean sea were associated with a collapse of the thermohaline circulation (e.g., Younger Dryas), we assume that on multidecadal timescale, a scale relevant for ocean circulation, the positive relationship between SST and SSS derived from Bonaire coral records could be partially explained by multidecadal changes in the strength of the AMOC. Moreover, if this is proven true, enhanced multidecadal climate variability observed in the mid-Holocene Caribbean climate (e.g., Greer and Swart, 2006; Giry et al., submitted) would reflect multidecadal changes in the strength of the AMOC.

2.4.6. Conclusion

Seasonality and interannual to multidecadal variability of $\delta^{18}\text{O}_{\text{sw}}$ in the southern Caribbean was reconstructed from paired coral Sr/Ca and $\delta^{18}\text{O}$ measurements in ~295 years inferred from Holocene corals from Bonaire. Well-distributed coral time-windows indicate trend towards more positive over the last 6.2 ka suggesting that the Caribbean was wetter during the mid-Holocene than it is today. Significant short-term variability of sea surface hydrological conditions recorded in coral $\Delta\delta^{18}\text{O}$ are observed on timescales ranging from seasonal to multidecadal. On seasonal timescale, strong correspondence is found between reconstructed annual $\delta^{18}\text{O}_{\text{sw}}$ cycles from modern corals and fresh surface water transported into the Caribbean by Guyana/Caribbean current system today. However, the mid-Holocene annual $\delta^{18}\text{O}_{\text{sw}}$ cycle indicates rapid shift towards more negative values in summer suggesting that enhanced summer precipitation was the

dominant factor influencing annual sea surface conditions at 6.2 ka. Mid- to late Holocene coral records also indicate sharp summer peak which becomes less apparent in more recent coral records suggesting either a less pronounced summer precipitation or reduced Caribbean through flow in summer towards the late Holocene. On interannual and multidecadal timescales, it is found that warmer conditions than average are characterised by more saline conditions and *vice versa*. Since this systematic relationship is found for very short timescales relevant for atmospheric circulation, we proposed that surface wind-driven oceanic advection of fresh surface water from the Amazon and Orinoco Rivers could explain the sign of the relationship between SSS and SST. Moreover, the mid-Holocene was characterised by enhanced multidecadal variability of sea surface hydrology which point to enhanced AMO-like variability in the mid-Holocene possibly associated with multidecadal variability of the strength of the AMOC. In addition, although this study do not rule out E/P ratio as the dominant factor controlling millennial scales changes of sea surface hydrology in the Southern Caribbean, preliminary interpretations suggest that shorter-term variability (i.e., interannual to multidecadal, and possibly centennial) of southern Caribbean sea surface hydrology results from the combination of both the amount of precipitation over northern South America and the strength of wind-driven surface currents. Finally, given that salinity changes in the Caribbean can have drastic impact on pattern of thermohaline circulation and heat transport from low to high latitude, we strongly recommend the modelling community to further investigate short-term

variability of western tropical Atlantic climate as a potential feedback mechanism on the strength of the AMOC.

Acknowledgments

We thank the Government of the Island Territory of Bonaire (Netherlands Antilles) for research and fieldwork permission, E. Beukenboom (STINAPA Bonaire National Parks Foundation) for support, J. Pätzold for support with coral drilling and discussion, S. Pape for operating and maintaining the ICP-

OES, M. Segl and her team for stable isotope analysis, H. Kuhnert for discussion, and A. Scheffers and C. Maier for initiating this collaboration. This work was funded by Deutsche Forschungsgemeinschaft (DFG) under the Special Priority Programme INTERDYNAMIK, through grants to T.F. (FE 615/3-1, 3-2; CaribClim). C.G. acknowledges additional support by GLOMAR (Bremen International Graduate School for Marine Sciences) that is funded by DFG.

3. Summary and conclusions

Since coral-based climate records from *Diploria strigosa* corals have been shown to correlate with instrumental data, this brain coral is a potential archive of the tropical and subtropical Atlantic climate (Kuhnert et al., 2005; Hetzinger, 2007). However, complications associated with its complex mesoskeletal architecture must be firmly established prior to generating accurate reconstructions of past climate when no instrumental data are available. Therefore, the first goals of this dissertation were to provide a better understanding of the geochemistry of the coral skeleton of *D. strigosa* in order to accurately document past changes in the Southern Caribbean climate. While modern coral cores were used for calibration purpose, fossils coral cores of Holocene age were utilised to reconstruct the natural variability of southern Caribbean climate for pre-industrial times. The following paragraphs summarise the major conclusions of each study.

In the first study (**Manuscript I**), the geochemical composition of a *Diploria strigosa* coral skeleton was investigated at millimetre scale in order to, first, assess potential complications associated with microsampling its meandroid coral skeleton, and second, to identify the best microsampling technique that will yield to accurate climate record derived from fossil coral skeletons. Systematic mesoscale geochemical heterogeneity linked to different vital effects between skeletal elements were identified. This first result indicates that mixing different skeletal elements during microsampling is inappropriate for robust climate reconstructions from the skeleton of *D. strigosa*. Moreover, microsampling experiments along different skeletal elements were performed using different drill bit sizes. Based on the monthly mean climatology relationship between climate proxies and SST, it was found that fine microsampling the center of the thecal wall of *D. strigosa* yield to the best estimate of seasonal changes of environmental parameters. This finding was further supported by the high correlation coefficient between the two SST proxies in coral skeleton (i.e., Sr/Ca and $\delta^{18}\text{O}$). Finally, this first study showed the capability of reconstructing seasonality from *D. strigosa* coral skeleton growing at a rate of 0.65 cm/year with the precondition that accurate microsampling strategy (i.e., fine microsampling a constant proportion of skeleton along the center of the theca walls) is adopted for generating robust monthly resolved climate records from fossil *D. strigosa* corals.

In the second study (**Manuscript II**), the aforementioned microsampling technique was applied to generate a 40-year long monthly resolved Sr/Ca record from a fossil *Diploria strigosa* coral from Bonaire (southern Caribbean Sea) dated with U/Th at 2.35 ka BP. Secondary modifiers of this SST proxy, such as diagenetic alteration and skeletal growth-rate were investigated. Extensive diagenetic investigations revealed pristine coral skeleton which was further supported by clear annual cycles in the coral Sr/Ca record. No significant correlation between annual extension-rate and coral Sr/Ca were observed, suggesting that the Sr/Ca record was not affected by coral growth. Therefore, we concluded that the reconstructed interannual Sr/Ca variability was influenced by ambient SST variability. Finally, this first monthly resolved coral Sr/Ca record from the southern

Caribbean Sea for pre-industrial time suggested that fossil corals from Bonaire are suitable archives for reconstructing past SST variability.

Short-term variability (i.e., seasonal to multidecadal) of SST in the tropical Atlantic is critical component of climate for predicting hazardous climate phenomena in this region. However, knowledge about this short-term SST variability is essentially based on the short instrumental data period covering only few decades. In the third study (**Manuscript III**), short-term SST variability in the tropical Atlantic was extended beyond pre-industrial times in order to investigate its natural variability recorded in the coral Sr/Ca ratio of six well-dated fossil corals from Bonaire. Alike modern instrumental data, where trade winds influence SST through heat loss from the ocean to the atmosphere, coral Sr/Ca-SST records indicated that SST around Bonaire was characterised by clear annual cycles, persistent quasi-biennial and prominent interannual and inter- to multidecadal scales variability. However, the magnitude of SST variation on these timescales has changed over the last 6.2 ka and the causes of these changes are summarised below:

SST seasonality: slight increased SST seasonality inferred from the 6.22 ka coral indicated orbital-control on the tropical Atlantic SST seasonality. This result was further supported by numerical simulation which revealed that this increased SST seasonality was a large-scale phenomenon of the north Atlantic sector associated with seasonal insolation changes at mid-latitudes. Moreover, significantly large increased SST seasonality at 2.35 ka together with persistent year-to-year variability of SST seasonality suggested a strong influence of the climate dynamics in controlling short-term SST seasonality around Bonaire.

Interannual SST variability: prominent quasi-biennial and interannual SST variability in the southern Caribbean Sea are linked to air-sea interactions emanating from both the Pacific and the Atlantic Oceans. Interannual SST variability at typical El Niño/Southern Oscillation (ENSO) period was reduced at 6.2 ka BP, whereas it was enhanced at 2.3 ka BP suggesting increasing effect of ENSO on tropical Atlantic climate throughout the mid- to late Holocene. Finally, pronounced 5.7-year variability persistent in all seasons found in the 2.35 ka coral pointed to a reorganisation of tropical Atlantic atmospheric circulation at that time.

Inter- to multidecadal SST variability: prominent variability in this timescale was evident in the longest coral records. However, these records were too short to assess the underlying periodicities with sufficient accuracy. Nevertheless, bandpass filtering method helped identifying a period of enhanced multidecadal variability at 6.2 ka BP which was possibly linked to enhanced Atlantic Multidecadal Oscillation-like variations.

To summarise, the data presented in this third study represents ~ 295 years of monthly SST record. Such data imply that short-term SST variability in the tropical Atlantic for pre-industrial is unprecedented over the short instrumental period.

The island of Bonaire, located in the southern Caribbean Sea, lies in the pathway of the Caribbean Current, the dominant surface current within the Caribbean basin. This current transports surface water northwestward and is part of the surface return flow of the Atlantic

meridional overturning circulation (AMOC) which brings heat from low to high latitudes. The fourth study (**Manuscript IV**) assessed short-term variability of sea surface hydrological conditions around Bonaire documented in coral $\Delta\delta^{18}\text{O}$ records. Using the well-established approach of paired coral Sr/Ca and $\delta^{18}\text{O}$ measurements, the isotopic composition of seawater ($\delta^{18}\text{O}_{\text{sw}}$) was reconstructed at monthly resolution.

It was found that southern Caribbean Sea surface hydrology has changed on both seasonal and interannual to multidecadal timescales throughout the mid- to late Holocene. Reconstructed annual $\delta^{18}\text{O}_{\text{sw}}$ cycles from three modern corals revealed that fresh water transported into the Caribbean Sea by wind-driven surface currents influences annual sea surface hydrology today. However, the annual $\delta^{18}\text{O}_{\text{sw}}$ cycle reconstructed from the mid-Holocene coral revealed a rapid shift towards more negative $\delta^{18}\text{O}_{\text{sw}}$ values in summer, thus suggesting that enhanced summer precipitation, associated with a more northward position of the ITCZ, was the prevailing mechanism controlling annual sea surface hydrology in the mid-Holocene.

In addition, significant periodicities at interannual to multidecadal timescales were found in most of the coral $\Delta\delta^{18}\text{O}$ records. The persistent positive relationship between sea surface temperature and salinity found for all timescales indicated that a unique physical mechanism was responsible for the sign of this relationship. Oceanic advection of fresh surface waters from the Amazon and Orinoco Rivers forced by surface winds was suggested as the prevailing factor influencing the sea surface hydrology in the Southern Caribbean on interannual to multidecadal time scales. Moreover, since significant salinity changes in the Caribbean can have a drastic impact on the strength of the thermohaline circulation and resulting heat transport from low to high latitude, this study implied that the amount of precipitation over northern South America and wind-driven surface currents are possible mechanisms influencing its short-term variability.

To conclude, while the period of instrumental observations might already contain anthropogenic imprints, the total number of 295 years of monthly resolved coral-based climate record accurately generated within the framework of this thesis provides, for the first time, relevant insights onto the natural short-term variability of the tropical Atlantic climate for pre-industrial times. As the reconstructed climate variability from Holocene time-windows indicates that the magnitude of interannual and multidecadal variability exceeded corresponding variability known from the observation period, this PhD thesis implies that short-term changes in climate can arise from dynamics internal to the climate system itself. Finally, this study provides valuable high resolution data for comparison with climate models, which is important for successful predictions of the tropical Atlantic climate under changing boundary conditions.

4. Outlook - Future research directions

4.1 Biological effects on geochemical proxies in corals

Geochemical variations preserved in the aragonitic skeleton of massive corals have the exceptional potential to produce highly-resolved paleoenvironmental reconstructions spanning many centuries. However, this potential has not been fully exploited because biological processes referred to as “vital effects” have hindered generation of paleoenvironmental records. The understanding of the potential non-climatic influences and sources of error on coral-based climate reconstructions is a prerequisite for developing more reliable tropical climate and environmental records (e.g., Lough, 2010). In manuscript I, a strategy was designed in order to circumvent such complications of temperature proxies (i.e., Sr/Ca and $\delta^{18}\text{O}$) preserved in the coral skeleton of *Diploria strigosa*. Although effects of biological processes on both coral Sr/Ca and $\delta^{18}\text{O}$ is well-documented in the literature (Weber, 1973; Erez, 1978; de Villiers et al., 1995), its effect on other geochemical environmental proxies (i.e., $\delta^{11}\text{B}$, $\Delta^{14}\text{C}$, Mg/Ca, U/Ca, Ba/Ca, and Cd/Ca, among others) incorporated in coral skeletons is, however, poorly understood (e.g., Vengosh et al., 1991; Carriquiry and Villaescusa, 2010). In order to test the effect of biological processes on the aforementioned proxies, measurements of these environmental proxies could be performed on individual skeletal elements of a single *D. strigosa*. If vital effects on such proxies are proven true for *D. strigosa* skeletal elements which grew in a single environment, then, accurate sampling strategy should be designed in order to accurately reconstruct paleoenvironmental parameters preserved in fossil coral skeletons. In addition, such an experiment performed on the coral skeleton of *D. strigosa* and other large-polyped corals (i.e., *Colpophyllia* sp., *Diploastrea* sp., etc...) will ultimately shed more light on biological processes controlling on the incorporation of geochemical elements into the aragonitic coral skeleton.

4.2 Climate reconstructions from Pleistocene corals

The present PhD thesis identified the dense and solid thecal walls of *Diploria strigosa* as the skeletal element that provides the best environmental signal of surrounding seawater. Such dense, large and solid thecal walls are free of pores and therefore, ensure ample material for sampling and diminish concerns of diagenetic alteration or secondary precipitation, known for distortion of the climate signals preserved in the coral skeleton (Hendy et al., 2007). Consequently, one has to benefit from fossil *Diploria strigosa* coral colonies of more distant past (e.g., interglacial reef terraces) to shed more light on southern Caribbean climate variability under different boundary conditions and especially during warm periods without anthropogenic interferences (Sime et al., 2009). Recent works performed on Pleistocene corals from others tropical and subtropical locations were successful in reconstructing climate variability from last interglacial corals (e.g., Winter et al., 2003; Felis et al., 2004; Ayling et al., 2006). In a recent study, it has been reported that uplifted reef terraces on Bonaire provide fossil corals in growth position (Meyer et al., 2003). Such reef terraces are expected to have formed during last interglacial periods (i.e., Marine Isotopic Stage MIS 5, MIS

9 and probably MIS 11) characterised by high sea-level stand (de Buissonjé, 1974; Kim and Lee, 1999). Therefore, proxy records from the thecal walls of Pleistocene *D. strigosa* corals from Bonaire will significantly expand our understanding of the natural range of seasonality and interannual to multidecadal variability in this region during the last interglacial periods, which is up to now based on a single 4-year coral record from the northeastern Caribbean indicating an SST seasonality at 127 ka BP, 1-2 °C larger than at present.

4.3 Monthly resolved coral records of past Atlantic climate variability

Coral-based climate reconstructions provide a unique insight into past climate variability at a temporal resolution that cannot be achieved with any other climate archives. In the present study, a sampling resolution of 12 samples per year was undertaken in order to achieve the scientific objectives and accurately reconstruct seasonally phase-locked climate variations in the tropical Atlantic. Such monthly reconstruction allowed for investigation of variability within seasons. Such variability retrieved from the convoluted thecal walls of *Diploria strigosa* corals could not be identified with sufficient accuracy using lower sampling resolution (e.g., Leder et al., 1996; Quinn et al., 1996). If bimonthly sampling resolution was adopted, the slight increased SST seasonality in the mid-Holocene would probably not have been detected and supported with climate model simulation. Moreover, as patterns of ENSO and NAO teleconnection to the tropical Atlantic have strong seasonality (e.g., Sutton et al., 2000), lower sampling resolution may have yielded different conclusions or it would have even resulted in overlooking such important features of the tropical climate system. In addition, reconstructed enhanced local summer precipitation in the mid-Holocene coral, associated with the northward shifted ITCZ, would not have been possible with lower sampling resolution. Therefore, the high-sampling resolution performed within the framework of this study is justified, although very costly.

For future studies focussing on interannual to multidecadal climate variability only, lower sampling resolution could be considered. However, it should be kept in mind that the tropical Atlantic climate is seasonally phase-locked and influenced by the ENSO and the NAO teleconnection pattern which indicate strong seasonality today (Sutton et al., 2000). There are some indications that global climate anomalies, such as the Medieval Climate Anomaly (MCA) and Little Ice Age (LIA) were associated with strong ENSO-NAO interactions (Seager and Burgman, 2011). Therefore, monthly resolved tropical Atlantic climate reconstructions from fossil corals provide information on potential changes of seasonality associated with yet unknown interbasin couplings.

4.4 Extended coral-based reconstructions of mid-Holocene climate

Monthly resolved climate reconstructions from fossil corals can provide unique insights of past climate variability in the tropical Atlantic sector under different boundary conditions (i.e., LIA, MCA and last interglacials). The mid-Holocene is a period of particular interest to the understanding of the Earth's climate system because of the high abundance of detailed regional paleoclimatic records (see reviews by Mayewski et al., 2004; Wanner et al., 2008). The mid-

Holocene was characterized by a stronger seasonality of insolation in the Northern Hemisphere relative to today (Berger, 1978). This enhanced the thermal contrast between land and sea in northern tropics producing strong summer monsoons over Africa (Gasse, 2000).

Coral-based climate records have been successful in reconstructing mid-Holocene climate variability using *Porites* sp. corals (Gagan et al., 1998; Corrège et al., 2000; Moustafa et al., 2000; McGregor and Gagan, 2004; Montaggioni et al., 2006; Deng et al., 2009; Yokoyama et al., 2011). This dissertation showed that it is now possible to apply similar reconstruction of mid-Holocene climate using Atlantic corals from Bonaire, in the north tropical Atlantic. These corals indicate that summer precipitation was enhanced in the mid-Holocene, most likely caused by a northward shift of the ITCZ at that time (Haug et al., 2001).

Recently, Collins et al., (2011) proposed that the range of seasonal oscillation of the African rain belt has expanded during the mid-Holocene rather than migrating to the north as proposed by other studies (Haug et al., 2001; Fleitmann et al., 2003). Since we have only sampled the northern hemisphere, our coral records from Bonaire cannot distinguish between a northward shift and a change in the range of the seasonal oscillation. However, it should be possible to develop monthly resolved coral-based climate records from both hemispheres in order to test whether summer precipitation has increased similarly at southern latitudes during the mid-Holocene. More specifically, the monthly resolution achievable in coral studies would allow for the determination of the timing and intensity of rainfall throughout the year. Along the Atlantic coast of South America, promising open-ocean reef complexes (e.g., Abrolhos reef system) provide modern corals from southern latitudes. Such coral reefs in the western south Atlantic might provide fossil corals of Holocene age according to Leao and Kikuchi (1999) that could be used to reconstruct past climate variability in southern latitudes at subseasonal resolution (Domingues et al., 2010; Kikuchi et al., 2010). Such an approach may also be possible over the African and Asian monsoon regions (e.g., Deng et al., 2009).

References

- Abram, N.J., Gagan, M.K., Cole, J.E., Hantoro, W.S. and Mudelsee, M., 2008. Recent intensification of tropical climate variability in the Indian Ocean. *Nature Geoscience* 1, 849-853.
- Abram, N.J., McGregor, H.V., Gagan, M.K., Hantoro, W.S. and Suwargadi, B.W., 2009. Oscillations in the southern extent of the Indo-Pacific Warm Pool during the mid-Holocene. *Quaternary Science Reviews* 28, 2794-2803.
- Adkins, J.F., Boyle, E.A., Curry, W.B. and Lutringer, A., 2003. Stable isotopes in deep-sea corals and a new mechanism for "vital effects". *Geochimica et Cosmochimica Acta* 67, 1129-1143.
- Alexander, M. and Scott, J., 2002. The influence of ENSO on air-sea interaction in the Atlantic. *Geophys. Res. Lett.* 29, 1701.
- Alibert, C. and McCulloch, M.T., 1997. Strontium/Calcium Ratios in Modern *Porites* Corals From the Great Barrier Reef as a Proxy for Sea Surface Temperature: Calibration of the Thermometer and Monitoring of ENSO. *Paleoceanography*, 12(3), 345-363.
- Allison, N. and Finch, A.A., 2004. High-resolution Sr/Ca records in modern *Porites lobata* corals: Effects of skeletal extension rate and architecture. *Geochemistry Geophysics Geosystems* 5, Q05001, doi:10.1029/2004GC000696.
- Antonov, J.I., R. A. Locarnini, T. P. Boyer, A. V. Mishonov and H. E. Garcia, 2006. World Ocean Atlas 2005, Volume 2: Salinity. S. Levitus (Ed.), NOAA Atlas NESDIS 62, U.S. Government Printing Office, Washington, D.C., 182 pp.
- Antonov, J.I., D. Seidov, T. P. Boyer, R. A. Locarnini, A. V. Mishonov, H. E. Garcia, O. K. Baranova, M. M. Zweng and D. R. Johnson, 2010. World Ocean Atlas 2009, Volume 2: Salinity, S. Levitus, Ed. NOAA Atlas NESDIS 69, U.S. Government Printing Office, Washington, D.C., 184 pp.
- Asami, R., Felis, T., Deschamps, P., Hanawa, K., Iryu, Y., Bard, E., Durand, N. and Murayama, M., 2009. Evidence for tropical South Pacific climate change during the Younger Dryas and the Bølling-Allerød from geochemical records of fossil Tahiti corals. *Earth and Planetary Science Letters* 288, 96-107.
- Ayling, B.F., McCulloch, M.T., Gagan, M.K., Stirling, C.H., Andersen, M.B. and Blake, S.G., 2006. Sr/Ca and $\delta^{18}\text{O}$ seasonality in a *Porites* coral from the MIS 9 (339-303 ka) interglacial. *Earth and Planetary Science Letters* 248, 462-475.
- Bagnato, S., Linsley, B.K., Howe, S.S., Wellington, G.M. and Salinger, J., 2004. Evaluating the use of the massive coral *Diploastrea heliopora* for paleoclimate reconstruction. *Paleoceanography* 19.
- Bak, R., Nieuwland, G. and Meesters, E., 2005. Coral reef crisis in deep and shallow reefs: 30 years of constancy and change in reefs of Curacao and Bonaire. *Coral Reefs* 24, 475-479.
- Bak, R.P.M., 1975. Ecological aspects of the distribution of reef corals in the Netherlands Antilles. *Transactions VIIth Caribbean Geol. Conf.*, Guadeloupe
- Bak, R.P.M., 1977. Coral reefs and their zonation in the Netherlands Antilles. *Studies in Geology* 4:3-16.
- Beck, J.W., Edwards, R.L., Ito, E., Taylor, F.W., Recy, J., Rougerie, F., Joannot, P. and Henin, C., 1992. Sea-Surface Temperature from Coral Skeletal Strontium/Calcium Ratios. *Science* 257, 644-647.

- Berger, A., 1978. Long-Term Variations of Daily Insolation and Quaternary Climatic Changes. *Journal of the Atmospheric Sciences* 35, 2362-2367.
- Bries, J.M., Debrot, A.O. and Meyer, D.L., 2004. Damage to the leeward reefs of Curaçao and Bonaire, Netherlands Antilles from a rare storm event: Hurricane Lenny, November 1999. *Coral Reefs* 23, 297-307.
- Broecker, W.S. and Peng, T.H., 1982. Tracers in the sea. Eldigio Press Lamont Doherty Geological Observatory, 690 pp.
- Budd, A.F. and Johnson, K.G., 1999. Origination Preceding Extinction during Late Cenozoic Turnover of Caribbean Reefs. *Paleobiology* 25, 188-200.
- Cahyarini, S.Y., Pfeiffer, M., Timm, O., Dullo, W.-C. and Schönberg, D.G., 2008. Reconstructing seawater $\delta^{18}\text{O}$ from paired coral $\delta^{18}\text{O}$ and Sr/Ca ratios: Methods, error analysis and problems, with examples from Tahiti (French Polynesia) and Timor (Indonesia). *Geochimica et Cosmochimica Acta* 72, 2841-2853.
- Cardinal, D., Hamelin, B., Bard, E. and Pätzold, J., 2001. Sr/Ca, U/Ca and $\delta^{18}\text{O}$ records in recent massive corals from Bermuda: relationships with sea surface temperature. *Chemical Geology* 176, 213-233.
- Carlson, A.E., Oppo, D.W., Came, R.E., LeGrande, A.N., Keigwin, L.D. and Curry, W.B., 2008. Subtropical Atlantic salinity variability and Atlantic meridional circulation during the last deglaciation. *Geology* 36, 991-994.
- Carricart-Ganivet, J.P., 2004. Sea surface temperature and the growth of the West Atlantic reef-building coral *Montastraea annularis*. *Journal of Experimental Marine Biology and Ecology* 302, 249-260.
- Carriquiry, J., Risk, M.J. and Schwarcz, H.P., 1994. Stable isotope geochemistry of corals from Costa Rica as proxy indicator of the EL Niño/southern Oscillation (ENSO). *Geochimica et Cosmochimica Acta* 58, 335-351.
- Carriquiry, J.D. and Villaescusa, J.A., 2010. Coral Cd/Ca and Mn/Ca records of ENSO variability in the Gulf of California. *Climate of the Past* 6, 401-410.
- Carton, J.A., Cao, X., Giese, B.S. and Da Silva, A.M., 1996. Decadal and Interannual SST Variability in the Tropical Atlantic Ocean. *Journal of Physical Oceanography* 26, 1165-1175.
- Carton, J.A. and Giese, B.S., 2008. A Reanalysis of Ocean Climate Using Simple Ocean Data Assimilation (SODA). *Monthly Weather Review* 136, 2999-3017.
- Chang, P., Ji, L. and Li, H., 1997. A decadal climate variation in the tropical Atlantic Ocean from thermodynamic air-sea interactions. *Nature* 385, 516-518.
- Chang, P., Fang, Y., Saravanan, R., Ji, L. and Seidel, H., 2006. The cause of the fragile relationship between the Pacific El Niño and the Atlantic Niño. *Nature* 443, 324-328.
- Cheng, H., Edwards, R.L., Hoff, J., Gallup, C.D., Richards, D.A. and Asmerom, Y., 2000. The half-lives of uranium-234 and thorium-230. *Chemical Geology* 169, 17-33.
- Chérubin, L.M. and Richardson, P.L., 2007. Caribbean current variability and the influence of the Amazon and Orinoco freshwater plumes. *Deep Sea Research Part I: Oceanographic Research Papers* 54, 1451-1473.
- Chiang, J.C.H., Kushnir, Y. and Giannini, A., 2002. Deconstructing Atlantic Intertropical Convergence Zone variability: Influence of the local cross-equatorial sea surface

- temperature gradient and remote forcing from the eastern equatorial Pacific. *J. Geophys. Res.* 107, 4004.
- Clement, A.C., Seager, R. and Cane, M.A., 1999. Orbital Controls on the El Niño/Southern Oscillation and the Tropical Climate. *Paleoceanography* 14, 441-456.
- Cobb, K.M., Charles, C.D., Cheng, H. and Edwards, R.L., 2003. El Niño/Southern Oscillation and tropical Pacific climate during the last millennium. *Nature* 424, 271-276.
- Cohen, A.L., Layne, G.D., Hart, S.R. and Lobel, P.S., 2001. Kinetic control of skeletal Sr/Ca in a symbiotic coral: Implications for the paleotemperature proxy. *Paleoceanography*, 16(1), 20-26.
- Cohen, A.L., Owens, K.E., Layne, G.D. and Shimizu, N., 2002. The Effect of Algal Symbionts on the Accuracy of Sr/Ca Paleotemperatures from Coral. *Science* 296, 331-333.
- Cohen, A.L. and McConnaughey, T.A., 2003. Geochemical Perspectives on Coral Mineralization. *Reviews in Mineralogy and Geochemistry* 54, 151-187.
- Cohen, A.L. and Hart, S.R., 2004. Deglacial sea surface temperatures of the western tropical Pacific: A new look at old coral. *Paleoceanography* 19.
- Cohen, A.L., Smith, S.R., McCartney, M.S. and Etten, J.v., 2004. How brain corals record climate: an integration of skeletal structure, growth and chemistry of *Diploria labyrinthiformis* from Bermuda. *Marine Ecology Progress Series* 271, 147-158.
- Cohen, A.L. and Thorrold, S.R., 2007. Recovery of temperature records from slow-growing corals by fine scale sampling of skeletons. *Geophysical Research Letters* 34, L17706, doi:10.1029/2007GL030967.
- Cole, J.E., Fairbanks, R.G. and Shen, G.T., 1993. Recent Variability in the Southern Oscillation: Isotopic Results from a Tarawa Atoll Coral. *Science* 260, 1790-1793.
- Collins, J.A., Schefuss, E., Heslop, D., Mulitza, S., Prange, M., Zabel, M., Tjallingii, R., Dokken, T.M., Huang, E., Mackensen, A., Schulz, M., Tian, J., Zarriess, M. and Wefer, G., 2011. Interhemispheric symmetry of the tropical African rainbelt over the past 23,000 years. *Nature Geosci* 4, 42-45.
- Corrège, T., Delcroix, T., Rège, J., Beck, W., Cabioch, G. and Le Cornec, F., 2000. Evidence for Stronger El Niño-Southern Oscillation (ENSO) Events in a Mid-Holocene Massive Coral. *Paleoceanography* 15, 465-470.
- Corrège, T., Gagan, M.K., Beck, J.W., Burr, G.S., Cabioch, G. and Le Cornec, F., 2004. Interdecadal variation in the extent of South Pacific tropical waters during the Younger Dryas event. *Nature* 428, 927-929.
- Corrège, T., 2006. Sea surface temperature and salinity reconstruction from coral geochemical tracers. *Palaeogeography, Palaeoclimatology, Palaeoecology* 232, 408-428.
- Craig, H. and Gordon, L.I. (Editors), 1965. Deuterium and oxygen 18 variations in the ocean and the marine atmosphere. *Stable Isotopes in Oceanographic Studies and Paleotemperatures*, Cons. Naz. di Rech., Spoleto, Italy, 121 pp.
- Crucifix, M., Braconnot, P., Harrison S.P. and Otto-Bliesner B., 2005. Second Phase of Paleoclimate Modelling Intercomparison Project. *Eos Trans. AGU*, 86(28), doi:10.1029/2005EO280003
- Crueger, T., Kuhnert, H., Pätzold, J. and Zorita, E., 2006. Calibrations of Bermuda corals against large-scale sea surface temperature and sea level pressure pattern time series and

- implications for climate reconstructions. *Journal Geophysical Research* 111, D23103, doi:10.1029/2005jd006903.
- Cruz, F.W., Vuille, M., Burns, S.J., Wang, X., Cheng, H., Werner, M., Lawrence Edwards, R., Karmann, I., Auler, A.S. and Nguyen, H., 2009. Orbitally driven east-west antiphasing of South American precipitation. *Nature Geosci* 2, 210-214.
- Cunningham, S.A., Kanzow, T., Rayner, D., Baringer, M.O., Johns, W.E., Marotzke, J., Longworth, H.R., Grant, E.M., Hirschi, J.J.-M., Beal, L.M., Meinen, C.S. and Bryden, H.L., 2007. Temporal Variability of the Atlantic Meridional Overturning Circulation at 26.5°N. *Science* 317, 935-938.
- Cunningham, S.A. and Marsh, R., 2010. Observing and modeling changes in the Atlantic MOC. *Wiley Interdisciplinary Reviews: Climate Change* 1, 180-191.
- Curtis, J.H., Hodell, D.A. and Brenner, M., 1996. Climate Variability on the Yucatan Peninsula (Mexico) during the Past 3500 Years, and Implications for Maya Cultural Evolution. *Quaternary Research* 46, 37-47.
- Curtis, S. and Hastenrath, S., 1995. Forcing of anomalous sea surface temperature evolution in the tropical Atlantic during Pacific warm events. *J. Geophys. Res.* 100, 15835-15847.
- Czaja, A., van der Vaart, P. and Marshall, J., 2002. A Diagnostic Study of the Role of Remote Forcing in Tropical Atlantic Variability. *Journal of Climate* 15, 3280-3290.
- Czaja, A., 2004. Why Is North Tropical Atlantic SST Variability Stronger in Boreal Spring? *Journal of Climate* 17, 3017-3025.
- Dana, J.D., 1846. Zoophytes, United States Exploring Expedition during the Years 1838-1842 under the Command of Charles Wilkes., pp. 121-708.
- de Buissonjé, P.H., 1974. Neogene and Quaternary Geology of Aruba, Curaçao and Bonaire, PhD thesis, Universiteit Utrecht, The Netherlands.
- de Villiers, S., Shen, G.T. and Nelson, B.K., 1994. The Sr/Ca-temperature relationship in coralline aragonite: Influence of variability in $(\text{Sr}/\text{Ca})_{\text{seawater}}$ and skeletal growth parameters. *Geochimica et Cosmochimica Acta* 58, 197-208.
- de Villiers, S., Nelson, B.K. and Chivas, A.R., 1995. Biological Controls on Coral Sr/Ca and $\delta^{18}\text{O}$ Reconstructions of Sea Surface Temperatures. *Science* 269, 1247-1249.
- de Villiers, S., 1999. Seawater strontium and Sr/Ca variability in the Atlantic and Pacific oceans. *Earth and Planetary Science Letters* 171, 623-634.
- Delaygue, G., Jouzel, J. and Dutay, J.-C., 2000. Oxygen 18-salinity relationship simulated by an oceanic general circulation model. *Earth and Planetary Science Letters* 178, 113-123.
- Delworth, T.L. and Mann, M.E., 2000. Observed and simulated multidecadal variability in the Northern Hemisphere. *Climate Dynamics* 16, 661-676.
- deMenocal, P., Ortiz, J., Guilderson, T., Adkins, J., Sarnthein, M., Baker, L. and Yarusinsky, M., 2000a. Abrupt onset and termination of the African Humid Period: rapid climate responses to gradual insolation forcing. *Quaternary Science Reviews* 19, 347-361.
- deMenocal, P., Ortiz, J., Guilderson, T. and Sarnthein, M., 2000b. Coherent High- and Low-Latitude Climate Variability During the Holocene Warm Period. *Science* 288, 2198-2202.

- Deng, W.-f., Wei, G.-j., Li, X.-h., Yu, K.-f., Zhao, J.-x., Sun, W.-d. and Liu, Y., 2009. Paleoprecipitation record from coral Sr/Ca and $\delta^{18}\text{O}$ during the mid Holocene in the northern South China Sea. *The Holocene* 19, 811-821.
- Dodge, R.E. and Vaisnys, J.R., 1975. Hermatypic coral growth banding as environmental recorder. *Nature* 258, 706-708.
- Dodge, R.E., Wyers, S.C., Frith, H.R., Knap, A.H., Smith, S.R. and Sleeter, T.D., 1984. The effects of oil and oil dispersants on the skeletal growth of the hermatypic coral *Diploria strigosa*. *Coral Reefs* 3, 191-198.
- Domingues, R., Kikuchi, R.K., Lentini, C., Zucchi, M. and Costa, A., 2010. THE POTENTIAL OF BRAZILIAN CORALS AS PALEOCEANOGRAPHIC PROXIES. *Eos Trans. AGU*, 91(26), Meet. Am. Suppl., Abstract PP44A-08.
- Eakin, C.M., Morgan, J.A., Heron, S.F., Smith, T.B., Liu, G., Alvarez-Filip, L., Baca, B., Bartels, E., Bastidas, C., Bouchon, C., Brandt, M., Bruckner, A.W., Bunkley-Williams, L., Cameron, A., Causey, B.D., Chiappone, M., Christensen, T.R.L., Crabbe, M.J.C., Day, O., de la Guardia, E., Díaz-Pulido, G., DiResta, D., Gil-Agudelo, D.L., Gilliam, D.S., Ginsburg, R.N., Gore, S., Guzmán, H.M., Hendee, J.C., Hernández-Delgado, E.A., Husain, E., Jeffrey, C.F.G., Jones, R.J., Jordán-Dahlgren, E., Kaufman, L.S., Kline, D.I., Kramer, P.A., Lang, J.C., Lirman, D., Mallela, J., Manfrino, C., Maréchal, J.-P., Marks, K., Mihaly, J., Miller, W.J., Mueller, E.M., Muller, E.M., Orozco Toro, C.A., Oxenford, H.A., Ponce-Taylor, D., Quinn, N., Ritchie, K.B., Rodríguez, S., Ramírez, A.R., Romano, S., Samhuri, J.F., Sánchez, J.A., Schmahl, G.P., Shank, B.V., Skirving, W.J., Steiner, S.C.C., Villamizar, E., Walsh, S.M., Walter, C., Weil, E., Williams, E.H., Roberson, K.W. and Yusuf, Y., 2010. Caribbean Corals in Crisis: Record Thermal Stress, Bleaching, and Mortality in 2005. *PLoS ONE* 5, e13969.
- Ellis, J. and Solander, D., 1786. The Natural History of many curious and uncommon Zoophytes, collected from various parts of the Globe. Systematically arranged and described by the late Daniel Solander, Benjamin White & Son, London, pp. 1-206.
- Elsner, J.B., Liu, K.-b. and Kocher, B., 2000. Spatial Variations in Major U.S. Hurricane Activity: Statistics and a Physical Mechanism. *Journal of Climate* 13, 2293-2305.
- Emiliani, C., Hudson, J.H., Shinn, E.A. and George, R.Y., 1978. Oxygen and Carbon Isotopic Growth Record in a Reef Coral from the Florida Keys and a Deep-Sea Coral from Blake Plateau. *Science* 202, 627-629.
- Enfield, D.B. and Mayer, D.A., 1997. Tropical Atlantic sea surface temperature variability and its relation to El Niño-Southern Oscillation. *J. Geophys. Res.* 102, 929-945.
- Enfield, D.B., Mestas, Nuñez, A.M. and Trimble, P.J., 2001. The Atlantic Multidecadal Oscillation and its relation to rainfall and river flows in the continental U.S. *Geophys. Res. Lett.* 28, 2077-2080.
- Engel, M., Brückner, H., Wennrich, V., Scheffers, A., Kelletat, D., Vött, A., Schäbitz, F., Daut, G., Willershäuser, T. and May, S.M., 2010. Coastal stratigraphies of eastern Bonaire (Netherlands Antilles): New insights into the palaeo-tsunami history of the southern Caribbean. *Sedimentary Geology* 231, 14-30.
- Erez, J., 1978. Vital effect on stable-isotope composition seen in foraminifera and coral skeletons. *Nature* 273, 199-202.
- Etter, P.C., Lamb, P.J. and Portis, D.H., 1987. Heat and Freshwater Budgets of the Caribbean Sea with Revised Estimates for the Central American Seas. *Journal of Physical Oceanography* 17, 1232-1248.

- Felis, T., Pätzold, J., Loya, Y. and Wefer, G., 1998. Vertical water mass mixing and plankton blooms recorded in skeletal stable carbon isotopes of a Red Sea coral. *Journal Geophysical Research*, 103(C13), 30731-30739.
- Felis, T., Pätzold, J., Loya, Y., Fine, M., Nawar, A.H. and Wefer, G., 2000. A coral oxygen isotope record from the northern Red Sea documenting NAO, ENSO, and North Pacific teleconnections on Middle East climate variability since the year 1750. *Paleoceanography*, 15(6), 679-694.
- Felis, T. and Pätzold, J. (Editors), 2003. Climate records from corals. *Marine Science Frontiers for Europe*. Springer-Verlag, Berlin, 11-27 pp.
- Felis, T., Pätzold, J. and Loya, Y., 2003. Mean oxygen-isotope signatures in *Porites* spp. corals: inter-colony variability and correction for extension-rate effects. *Coral Reefs* 22, 328-336.
- Felis, T., Lohmann, G., Kuhnert, H., Lorenz, S.J., Scholz, D., Patzold, J., Al-Rousan, S.A. and Al-Moghrabi, S.M., 2004. Increased seasonality in Middle East temperatures during the last interglacial period. *Nature* 429, 164-168.
- Felis, T., Suzuki, A., Kuhnert, H., Dima, M., Lohmann, G. and Kawahata, H., 2009. Subtropical coral reveals abrupt early-twentieth-century freshening in the western North Pacific Ocean. *Geology* 37, 527-530.
- Felis, T., Suzuki, A., Kuhnert, H., Rimbu, N. and Kawahata, H., 2010. Pacific Decadal Oscillation documented in a coral record of North Pacific winter temperature since 1873. *Geophys. Res. Lett.* 37, L14605.
- Ferrier-Pagès, C., Boisson, F., Allemand, D. and Eric, T., 2002. Kinetics of strontium uptake in the scleractinian coral *Stylophora pistillata*. *Marine Ecology Progress Series* 245, 93-100.
- Fleitmann, D., Burns, S.J., Mudelsee, M., Neff, U., Kramers, J., Mangini, A. and Matter, A., 2003. Holocene Forcing of the Indian Monsoon Recorded in a Stalagmite from Southern Oman. *Science* 300, 1737-1739.
- Focke, J.W., 1978. Holocene development of coral fringing reefs, leeward off Curaçao and Bonaire (Netherlands Antilles). *Marine Geology* 28, M31-M41.
- Fratantoni, D.M., 2001. North Atlantic surface circulation during the 1990's observed with satellite-tracked drifters. *J. Geophys. Res.* 106, 22067-22093.
- Gagan, M.K., Chivas, A.R. and Isdale, P.J., 1994. High-resolution isotopic records from corals using ocean temperature and mass-spawning chronometers. *Earth and Planetary Science Letters* 121, 549-558.
- Gagan, M.K., Ayliffe, L.K., Hopley, D., Cali, J.A., Mortimer, G.E., Chappell, J., McCulloch, M.T. and Head, M.J., 1998. Temperature and Surface-Ocean Water Balance of the Mid-Holocene Tropical Western Pacific. *Science* 279, 1014-1018.
- Gagan, M.K., Ayliffe, L.K., Beck, J.W., Cole, J.E., Druffel, E.R.M., Dunbar, R.B. and Schrag, D.P., 2000. New views of tropical paleoclimates from corals. *Quaternary Science Reviews* 19, 45-64.
- Garreaud, R.D., Vuille, M., Compagnucci, R. and Marengo, J., 2009. Present-day South American climate. *Palaeogeography, Palaeoclimatology, Palaeoecology* 281, 180-195.
- Gasse, F., 2000. Hydrological changes in the African tropics since the Last Glacial Maximum. *Quaternary Science Reviews* 19, 189-211.

- George, S.E. and Saunders, M.A., 2001. North Atlantic Oscillation impact on tropical North Atlantic winter atmospheric variability. *Geophys. Res. Lett.* 28, 1015-1018.
- Ghil, M., Allen, M.R., Dettinger, M.D., Ide, K., Kondrashov, D., Mann, M.E., Robertson, A.W., Saunders, A., Tian, Y., Varadi, F. and Yiou, P., 2002. Advanced spectral methods for climatic time series. *Rev. Geophys.* 40, 1003.
- Giannini, A., Kushnir, Y. and Cane, M.A., 2000. Interannual Variability of Caribbean Rainfall, ENSO, and the Atlantic Ocean*. *Journal of Climate* 13, 297-311.
- Giannini, A., Cane, M.A. and Kushnir, Y., 2001a. Interdecadal Changes in the ENSO Teleconnection to the Caribbean Region and the North Atlantic Oscillation*. *Journal of Climate* 14, 2867-2879.
- Giannini, A., Chiang, J.C.H., Cane, M.A., Kushnir, Y. and Seager, R., 2001b. The ENSO Teleconnection to the Tropical Atlantic Ocean: Contributions of the Remote and Local SSTs to Rainfall Variability in the Tropical Americas*. *Journal of Climate* 14, 4530-4544.
- Giannini, A., Saravanan, R. and Chang, P., 2004. The preconditioning role of Tropical Atlantic Variability in the development of the ENSO teleconnection: implications for the prediction of Nordeste rainfall. *Climate Dynamics* 22, 839-855.
- Giry, C., Felis, T., Kölling, M. and Scheffers, S., 2010a. Geochemistry and skeletal structure of *Diploria strigosa*, implications for coral-based climate reconstruction. *Palaeogeography, Palaeoclimatology, Palaeoecology* 298, 378-387.
- Giry, C., Felis, T., Scheffers, S. and Fensterer, C., 2010b. Assessing the potential of Southern Caribbean corals for reconstructions of Holocene temperature variability. *IOP Conference Series: Earth and Environmental Science* 9, doi: 10.1088/1755-1315/9/1/012021.
- Giry, C., Felis, T., Kölling, M., Scholz, D., Wei, W. and Scheffers, S., submitted. Mid- to late Holocene changes in tropical Atlantic temperature seasonality and interannual to multidecadal variability documented in southern Caribbean coral records *Earth and Planetary Science Letters*.
- Goldenberg, S.B., Landsea, C.W., Mestas-Nunez, A.M. and Gray, W.M., 2001. The Recent Increase in Atlantic Hurricane Activity: Causes and Implications. *Science* 293, 474-479.
- Goodkin, N.F., Huguen, K.A., Cohen, A.L. and Smith, S.R., 2005. Record of Little Ice Age sea surface temperatures at Bermuda using a growth-dependent calibration of coral Sr/Ca. *Paleoceanography*, 20, PA4016, doi:10.1029/2005PA001140.
- Goodkin, N.F., Huguen, K.A. and Cohen, A.L., 2007. A multicoral calibration method to approximate a universal equation relating Sr/Ca and growth rate to sea surface temperature. *Paleoceanography*, 22, PA1214, doi:10.1029/2006PA001312.
- Goodkin, N.F., Huguen, K.A., Curry, W.B., Doney, S.C. and Ostermann, D.R., 2008a. Sea surface temperature and salinity variability at Bermuda during the end of the Little Ice Age. *Paleoceanography*, 23, PA3203, doi:10.1029/2007pa001532.
- Goodkin, N.F., Huguen, K.A., Doney, S.C. and Curry, W.B., 2008b. Increased multidecadal variability of the North Atlantic Oscillation since 1781. *Nature Geoscience* 1, 844-848.
- Gordon, A.L., 1967. Circulation of the Caribbean Sea. *J. Geophys. Res.* 72, 6207-6223.
- Goreau, T.J., 1977. Coral Skeletal Chemistry: Physiological and Environmental Regulation of Stable Isotopes and Trace Metals in *Montastrea annularis*. *Proceedings of the Royal Society of London. Series B, Biological Sciences* 196, 291-315.

- Gray, W.M., 1984. Atlantic Seasonal Hurricane Frequency. Part I: El Niño and 30 mb Quasi-Biennial Oscillation Influences. *Monthly Weather Review* 112, 1649-1668.
- Greer, L. and Swart, P.K., 2006. Decadal cyclicity of regional mid-Holocene precipitation: Evidence from Dominican coral proxies. *Paleoceanography*, 21, PA2020, doi:10.1029/2005PA001166.
- Grossman, E.L. and Ku, T.-L., 1986. Oxygen and carbon isotope fractionation in biogenic aragonite: Temperature effects. *Chemical Geology: Isotope Geoscience section* 59, 59-74.
- Grottoli, A.G. and Wellington, G.M., 1999. Effect of light and zooplankton on skeletal $\delta^{13}\text{C}$ values in the eastern Pacific corals *Pavona clavus* and *Pavona gigantea*. *Coral Reefs* 18, 29-41.
- Guilderson, T.P., Fairbanks, R.G. and Rubenstone, J.L., 1994. Tropical Temperature Variations Since 20,000 Years Ago: Modulating Interhemispheric Climate Change. *Science* 263, 663-665.
- Hastenrath, S. and Lamb, P.J., 1978. Heat Budget Atlas of the Tropical Atlantic and Eastern Pacific Oceans University of Wisconsin Press 104 pp.
- Hastenrath, S., 1984. Interannual Variability and Annual Cycle: Mechanisms of Circulation and Climate in the Tropical Atlantic Sector. *Monthly Weather Review* 112, 1097-1107.
- Haug, G.H., Hughen, K.A., Sigman, D.M., Peterson, L.C. and Rohl, U., 2001. Southward Migration of the Intertropical Convergence Zone Through the Holocene. *Science* 293, 1304-1308.
- Haug, G.H., Günther, D., Peterson, L.C., Sigman, D.M., Hughen, K.A. and Aeschlimann, B., 2003. Climate and the Collapse of Maya Civilization. *Science* 299, 1731-1735.
- Heikoop, J.M., Dunn, J.J., Risk, M.J., Schwarcz, H.P., McConnaughey, T.A. and Sandeman, I.M., 2000. Separation of kinetic and metabolic isotope effects in carbon-13 records preserved in reef coral skeletons. *Geochimica et Cosmochimica Acta* 64, 975-987.
- Hellweger, F.L. and Gordon, A.L., 2002. Tracing Amazon River water into the Caribbean Sea. *Journal of Marine Research* 60, 537-549.
- Helmle, K.P., Dodge, R.E. and Ketcham, R.A., 2000. Skeletal architecture and density banding in *Diploria strigosa* by X-ray computed tomography. *Proceedings 9th International Coral Reef Symposium, Bali, Indonesia* 1, 365-371.
- Helmle, K.P., Kohler, K.E. and Dodge, R.E., 2002 Relative Optical Densitometry and The Coral X-radiograph Densitometry System: CoralXDS, *Int. Soc. Reef Studies 2002 European Meeting*. Cambridge, England.
- Hendy, E.J., Gagan, M.K., Lough, J.M., McCulloch, M. and deMenocal, P.B., 2007. Impact of skeletal dissolution and secondary aragonite on trace element and isotopic climate proxies in *Porites* corals. *Paleoceanography* 22, PA4101.
- Hernández, Guerra, A. and Joyce, T.M., 2000. Water masses and circulation in the surface layers of the Caribbean at 66°W. *Geophys. Res. Lett.* 27, 3497-3500.
- Heslop, D. and Paul, A., 2011. Can oceanic paleothermometers reconstruct the Atlantic Multidecadal Oscillation? *Climate of the Past* 7, 151-159.
- Hetzinger, S., Pfeiffer, M., Dullo, W.-C., Ruprecht, E. and Garbe-Schönberg, D., 2006. Sr/Ca and $\delta^{18}\text{O}$ in a fast-growing *Diploria strigosa* coral: Evaluation of a new climate archive for the tropical Atlantic. *Geochemistry Geophysics Geosystems* 7, Q10002, doi:10.1029/2006GC001347.

- Hetzinger, S., 2007. Stable oxygen isotopes and Sr/Ca-ratios in modern *Diploria strigosa* corals from different sites in the Caribbean Sea : evaluation of a new climate archive for the tropical Atlantic, Mathematisch-Naturwissenschaftliche Fakultät der Christian-Albrechts-Universität zu Kiel, 107 pp.
- Hetzinger, S., Pfeiffer, M., Dullo, W.-C., Keenlyside, N., Latif, M. and Zinke, J., 2008. Caribbean coral tracks Atlantic Multidecadal Oscillation and past hurricane activity. *Geology* 36, 11-14.
- Hetzinger, S., Pfeiffer, M., Dullo, W.-C., Garbe-Schönberg, D. and Halfar, J., 2010. Rapid 20th century warming in the Caribbean and impact of remote forcing on climate in the northern tropical Atlantic as recorded in a Guadeloupe coral. *Palaeogeography, Palaeoclimatology, Palaeoecology* 296, 111-124.
- Hodell, D.A., Curtis, J.H., Jones, G.A., Higuera-Gundy, A., Brenner, M., Binford, M.W. and Dorsey, K.T., 1991. Reconstruction of Caribbean climate change over the past 10,500 years. *Nature* 352, 790-793.
- Hodell, D.A., Brenner, M., Curtis, J.H. and Guilderson, T., 2001. Solar Forcing of Drought Frequency in the Maya Lowlands. *Science* 292, 1367-1370.
- Hodell, D.A., Brenner, M. and Curtis, J.H., 2005. Terminal Classic drought in the northern Maya lowlands inferred from multiple sediment cores in Lake Chichancanab (Mexico). *Quaternary Science Reviews* 24, 1413-1427.
- Hoffmann, D.L., Prytulak, J., Richards, D.A., Elliott, T., Coath, C.D., Smart, P.L. and Scholz, D., 2007. Procedures for accurate U and Th isotope measurements by high precision MC-ICPMS. *International Journal of Mass Spectrometry* 264, 97-109.
- Huang, J., Higuchi, K. and Shabbar, A., 1998. The relationship between the North Atlantic Oscillation and El Niño/Southern Oscillation. *Geophys. Res. Lett.* 25, 2707-2710.
- Hughen, K.A., Schrag, D.P., Jacobsen, S.B. and Hantoro, W., 1999. El Niño during the Last Interglacial Period recorded by a fossil coral from Indonesia. *Geophys. Res. Lett.* 26, 3129-3132.
- Hulme, M., Osborn, T.J. and Johns, T.C., 1998. Precipitation sensitivity to global warming: Comparison of observations with HadCM2 simulations. *Geophys. Res. Lett.* 25, 3379-3382.
- Human, P. and Deloach, N., 2008. Reef coral identification: Florida, Caribbean, Bahamas. New World Publication, Inc.
- Hurrell, J.W., 1995. Decadal Trends in the North Atlantic Oscillation: Regional Temperatures and Precipitation. *Science* 269, 676-679.
- Hurrell, J.W. and Van Loon, H., 1997. Decadal variations in climate associated with the North Atlantic Oscillation. *Climatic Change* 36, 301-326.
- Hurrell, J.W., Visbeck, M., Busalacchi, A., Clarke, R.A., Delworth, T.L., Dickson, R.R., Johns, W.E., Koltermann, K.P., Kushnir, Y., Marshall, D., Mauritzen, C., McCartney, M.S., Piola, A., Reason, C., Reverdin, G., Schott, F., Sutton, R., Wainer, I. and Wright, D., 2006. Atlantic Climate Variability and Predictability: A CLIVAR Perspective. *Journal of Climate* 19, 5100-5121.
- Inoue, M., Suzuki, A., Nohara, M., Hibino, K. and Kawahata, H., 2007. Empirical assessment of coral Sr/Ca and Mg/Ca ratios as climate proxies using colonies grown at different temperatures. *Geophysical Research Letters* 34, L12611, doi:10.1029/2007GL029628.
- Johns, W.E., Townsend, T.L., Frantantoni, D.M. and Wilson, W.D., 2002. On the Atlantic inflow to the Caribbean Sea. *Deep Sea Research Part I: Oceanographic Research Papers* 49, 211-243.

- Juillet-Leclerc, A., Reynaud, S., Rollion-Bard, C., Cuif, J.P., Dauphin, Y., Blamart, D., Ferrier-Pagès, C. and Allemand, D., 2009. Oxygen isotopic signature of the skeletal microstructures in cultured corals: Identification of vital effects. *Geochimica et Cosmochimica Acta* 73, 5320-5332.
- Juillet-Leclerc, A. and Reynaud, S., 2010. Light effects on the isotopic fractionation of skeletal oxygen and carbon in the cultured zooxanthellate coral, *Acropora*: implications for coral-growth rates. *Biogeosciences* 7, 893-906.
- Jury, M.R., 2009. A quasi-decadal cycle in Caribbean climate. *J. Geophys. Res.* 114, D13102.
- Kaplan, A., Cane, M.A., Kushnir, Y., Clement, A.C., Blumenthal, M.B. and Rajagopalan, B., 1998. Analyses of global sea surface temperature 1856-1991. *J. Geophys. Res.* 103, 18567-18589.
- Kaplan, A., Kushnir, Y. and Cane, M.A., 2000. Reduced Space Optimal Interpolation of Historical Marine Sea Level Pressure: 1854–1992*. *Journal of Climate* 13, 2987-3002.
- Kerr, R.A., 2000. A North Atlantic Climate Pacemaker for the Centuries. *Science* 288, 1984-1985.
- Kikuchi, R.K., Oliveira, M.D. and Leão, Z.M., 2010. Coral Density Banding Pattern in Western South Atlantic. *Eos Trans. AGU*, 91(26), Meet. Am. Suppl., Abstract PP31A-07.
- Kilbourne, K.H., Quinn, T.M. and Taylor, F.W., 2004. A fossil coral perspective on western tropical Pacific climate <350 ka. *Paleoceanography* 19, PA1019.
- Kilbourne, K.H., Quinn, T.M., Webb, R., Guilderson, T., Nyberg, J. and Winter, A., 2008. Paleoclimate proxy perspective on Caribbean climate since the year 1751: Evidence of cooler temperatures and multidecadal variability. *Paleoceanography*, 23, PA3220, doi:10.1029/2008PA001598.
- Kilbourne, K.H., Quinn, T.M., Webb, R., Guilderson, T., Nyberg, J. and Winter, A., 2010. Coral windows onto seasonal climate variability in the northern Caribbean since 1479. *Geochem. Geophys. Geosyst.* 11, Q10006.
- Kim, K.H. and Lee, D.-J., 1999. Distribution and depositional environments of coralline lithofacies in uplifted Pleistocene coral reefs of Bonaire, Netherland Antilles. *J. Paleont. Soc. Korea* 15, 18.
- Kinsman, D.J.J. and Holland, H.D., 1969. The co-precipitation of cations with CaCO₃--IV. The co-precipitation of Sr²⁺ with aragonite between 16° and 96°C. *Geochimica et Cosmochimica Acta* 33, 1-17.
- Knight, J.R., Allan, R.J., Folland, C.K., Vellinga, M. and Mann, M.E., 2005. A signature of persistent natural thermohaline circulation cycles in observed climate. *Geophys. Res. Lett.* 32, L20708.
- Knudsen, M.F., Seidenkrantz, M.-S., Jacobsen, B.H. and Kuijpers, A., 2011. Tracking the Atlantic Multidecadal Oscillation through the last 8,000 years. *Nat Commun* 2, 178.
- Knutson, D.W., Buddemeier, R.W. and Smith, S.V., 1972. Coral Chronometers: Seasonal Growth Bands in Reef Corals. *Science* 177, 270-272.
- Kuhnert, H., Pätzold, J., Schnetger, B. and Wefer, G., 2002. Sea-surface temperature variability in the 16th century at Bermuda inferred from coral records. *Palaeogeography, Palaeoclimatology, Palaeoecology* 179, 159-171.
- Kuhnert, H., Crueger, T. and Pätzold, J., 2005. NAO signature in a Bermuda coral Sr/Ca record. *Geochemistry Geophysics Geosystems* 6, Q04004, doi:10.1029/2004GC000786.

- Kushnir, Y., Robinson, W.A., Chang, P. and Robertson, A.W., 2006. The Physical Basis for Predicting Atlantic Sector Seasonal-to-Interannual Climate Variability*. *Journal of Climate* 19, 5949-5970.
- Lachniet, M.S., Burns, S.J., Piperno, D.R., Asmerom, Y., Polyak, V.J., Moy, C.M. and Christenson, K., 2004. A 1500-year El Niño/Southern Oscillation and rainfall history for the Isthmus of Panama from speleothem calcite. *J. Geophys. Res.* 109, D20117.
- Land, L.S., Lang, J.C. and Barnes, D.J., 1975. Extension rate: A primary control on the isotopic composition of West Indian (Jamaican) scleractinian reef coral skeletons. *Marine Biology* 33, 221-233.
- Landsea, C.W., 1999. Atlantic Basin Hurricanes: Indices of Climatic Changes. *Climatic Change* 42, 89-129.
- Larsen, J.C., 1992. Transport and Heat Flux of the Florida Current at 27 degrees N Derived from Cross-Stream Voltages and Profiling Data: Theory and Observations. *Philosophical Transactions: Physical Sciences and Engineering* 338, 169-236.
- Latif, M., Collins, M., Pohlmann, H. and Keenlyside, N., 2006. A Review of Predictability Studies of Atlantic Sector Climate on Decadal Time Scales. *Journal of Climate* 19, 5971-5987.
- Le Tissier, M.D.A.A., Clayton, B., Brown, B.E. and Davis, P.S., 1994. Skeletal correlates of coral density banding and an evaluation of radiography as used in sclerochronology. *Marine Ecology Progress Series* 110, 29-44.
- Lea, D.W., Pak, D.K., Peterson, L.C. and Hughen, K.A., 2003. Synchronicity of Tropical and High-Latitude Atlantic Temperatures over the Last Glacial Termination. *Science* 301, 1361-1364.
- Leão, Z.M.A.N. and Kikuchi, R.K.P., 1999. The Bahian Coral Reefs - from 7000 years BP to 2000 years AD. *Ci. Cult. J. Braz. Ass. Adv. Sci.* 51(3/4):262-273. .
- Leder, J.J., Swart, P.K., Szmant, A.M. and Dodge, R.E., 1996. The origin of variations in the isotopic record of scleractinian corals: I. Oxygen. *Geochimica et Cosmochimica Acta* 60, 2857-2870.
- Leduc, G., Vidal, L., Tachikawa, K., Rostek, F., Sonzogni, C., Beaufort, L. and Bard, E., 2007. Moisture transport across Central America as a positive feedback on abrupt climatic changes. *Nature* 445, 908-911.
- LeGrande, A.N. and Schmidt, G.A., 2006. Global gridded data set of the oxygen isotopic composition in seawater. *Geophys. Res. Lett.* 33, L12604, DOI 10.1029/2006gl026011.
- Linnaeus, 1758.
- Linsley, B.K., Messier, R.G. and Dunbar, R.B., 1999. Assessing between-colony oxygen isotope variability in the coral *Porites lobata* at Clipperton Atoll. *Coral Reefs* 18, 13-27.
- Linsley, B.K., Wellington, G.M. and Schrag, D.P., 2000. Decadal Sea Surface Temperature Variability in the Subtropical South Pacific from 1726 to 1997 A.D. *Science* 290, 1145-1148.
- Linsley, B.K., Kaplan, A., Gouriou, Y., Salinger, J., deMenocal, P.B., Wellington, G.M. and Howe, S.S., 2006. Tracking the extent of the South Pacific Convergence Zone since the early 1600s. *Geochemistry Geophysics Geosystems* 7, Q05003, doi:10.1029/2005GC001115.
- Locarnini, R.A., A. V. Mishonov, J. I. Antonov, T. P. Boyer and H. E. Garcia, 2006. World Ocean Atlas 2005, Volume 1: Temperature. S. Levitus, Ed. NOAA Atlas NESDIS 61, 182 pp.

- Lohmann, G., 2003. Atmospheric and oceanic freshwater transport during weak Atlantic overturning circulation. *Tellus A* 55, 438-449.
- Lorenz, S.J. and Lohmann, G., 2004. Acceleration technique for Milankovitch type forcing in a coupled atmosphere-ocean circulation model: method and application for the Holocene. *Climate Dynamics* 23, 727-743.
- Lough, J.M., 2004. A strategy to improve the contribution of coral data to high-resolution paleoclimatology. *Palaeogeography, Palaeoclimatology, Palaeoecology* 204, 115-143.
- Lough, J.M., 2010. Climate records from corals. *Wiley Interdisciplinary Reviews: Climate Change* 1, 318-331.
- Lund, D.C., Lynch-Stieglitz, J. and Curry, W.B., 2006. Gulf Stream density structure and transport during the past millennium. *Nature* 444, 601-604.
- Lynch-Stieglitz, J., Adkins, J.F., Curry, W.B., Dokken, T., Hall, I.R., Herguera, J.C., Hirschi, J.J.-M., Ivanova, E.V., Kissel, C., Marchal, O., Marchitto, T.M., McCave, I.N., McManus, J.F., Mulitza, S., Ninnemann, U., Peeters, F., Yu, E.-F. and Zahn, R., 2007. Atlantic Meridional Overturning Circulation During the Last Glacial Maximum. *Science* 316, 66-69.
- Maier, C., Felis, T., Pätzold, J. and Bak, R.P.M., 2004. Effect of skeletal growth and lack of species effects in the skeletal oxygen isotope climate signal within the coral genus *Porites*. *Marine Geology* 207, 193-208.
- Marshall, J., Kushnir, Y., Battisti, D., Chang, P., Czaja, A., Dickson, R., Hurrell, J., McCartney, M., Saravanan, R. and Visbeck, M., 2001a. North Atlantic climate variability: phenomena, impacts and mechanisms. *International Journal of Climatology* 21, 1863-1898.
- Marshall, J., Yochanan, K., David, B., Ping, C., Arnaud, C., Robert, D., James, H., Michael, M., Saravanan, R. and Martin, V., 2001b. North Atlantic climate variability: phenomena, impacts and mechanisms, pp. 1863-1898.
- Marshall, J.F. and McCulloch, M.T., 2002. An assessment of the Sr/Ca ratio in shallow water hermatypic corals as a proxy for sea surface temperature. *Geochimica et Cosmochimica Acta* 66, 3263-3280.
- Marsland, S., Haak, H., Jungclaus, J., Latif, M. and Röske, F., 2003. The Max-Planck-Institute global ocean/sea ice model with orthogonal curvilinear coordinates. *Ocean Modelling*, 5, 91-127.
- Martis, A., van Oldenborgh, G.J. and Burgers, G., 2002. Predicting rainfall in the Dutch Caribbean—more than El Niño? *International Journal of Climatology* 22, 1219-1234.
- Maupin, C.R., Quinn, T.M. and Halley, R.B., 2008. Extracting a climate signal from the skeletal geochemistry of the Caribbean coral *Siderastrea siderea*. *Geochemistry Geophysics Geosystems* 9, Q12012, doi:10.1029/2008GC002106.
- Mayewski, P.A., Rohling, E.E., Curt Stager, J., Karlén, W., Maasch, K.A., David Meeker, L., Meyerson, E.A., Gasse, F., van Kreveld, S., Holmgren, K., Lee-Thorp, J., Rosqvist, G., Rack, F., Staubwasser, M., Schneider, R.R. and Steig, E.J., 2004. Holocene climate variability. *Quaternary Research* 62, 243-255.
- McConnaughey, T., 1989. ^{13}C and ^{18}O isotopic disequilibrium in biological carbonates: I. Patterns. *Geochimica et Cosmochimica Acta* 53, 151-162.
- McConnell, M.C., Thunell, R.C., Lorenzoni, L., Astor, Y., Wright, J.D. and Fairbanks, R., 2009. Seasonal variability in the salinity and oxygen isotopic composition of seawater from the

- Cariaco Basin, Venezuela: Implications for paleosalinity reconstructions. *Geochemistry Geophysics Geosystems* 10, Q06019, doi:10.1029/2008GC002035
- McCulloch, M.T., Gagan, M.K., Mortimer, G.E., Chivas, A.R. and Isdale, P.J., 1994. A high-resolution Sr/Ca and $\delta^{18}\text{O}$ coral record from the Great Barrier Reef, Australia, and the 1982-1983 El Niño. *Geochimica et Cosmochimica Acta* 58, 2747-2754.
- McGregor, H.V. and Gagan, M.K., 2003. Diagenesis and geochemistry of porites corals from Papua New Guinea: Implications for paleoclimate reconstruction. *Geochimica et Cosmochimica Acta* 67, 2147-2156.
- McGregor, H.V. and Gagan, M.K., 2004. Western Pacific coral $\delta^{18}\text{O}$ records of anomalous Holocene variability in the El Niño/Southern Oscillation. *Geophys. Res. Lett.* 31, L11204.
- McGregor, H.V. and Abram, N.J., 2008. Images of diagenetic textures in Porites corals from Papua New Guinea and Indonesia. *Geochem. Geophys. Geosyst.* 9.
- Meibom, A., Yurimoto, H., Cuif, J.-P., Domart-Coulon, I., Houlbreque, F., Constantz, B., Dauphin, Y., Tambutté, E., Tambutté, S., Allemand, D., Wooden, J. and Dunbar, R., 2006. Vital effects in coral skeletal composition display strict three-dimensional control. *Geophysical Research Letters* 33, L11608, doi:10.1029/2006GL025968.
- Meibom, A., Cuif, J.-P., Houlbreque, F., Mostefaoui, S., Dauphin, Y., Meibom, K.L. and Dunbar, R., 2008. Compositional variations at ultra-structure length scales in coral skeleton. *Geochimica et Cosmochimica Acta* 72, 1555-1569.
- Meyer, D.L., Bries, J.M., Greenstein, B.J. and Debrot, A.O., 2003. Preservation of *in situ* reef framework in region of low hurricane frequency: Pleistocene of Curacao and Bonaire, southern Caribbean. *Lethaia* 36, 273-286.
- Molinari, R.L., Johns, E. and Festa, J.F., 1990. The Annual Cycle of Meridional Heat Flux in the Atlantic Ocean at 26.5°N. *Journal of Physical Oceanography* 20, 476-482.
- Molinari, R.L. and Mestas-Núñez, A.M., 2003. North Atlantic decadal variability and the formation of tropical storms and hurricanes. *Geophys. Res. Lett.* 30, 1541.
- Montaggioni, L.F., Le Cornec, F., Corrège, T. and Cabioch, G., 2006. Coral barium/calcium record of mid-Holocene upwelling activity in New Caledonia, South-West Pacific. *Palaeogeography, Palaeoclimatology, Palaeoecology* 237, 436-455.
- Morrison, J. and Nowlin, W.J., 1982. General Distribution of Water Masses Within the Eastern Caribbean Sea During the Winter of 1972 and Fall of 1973. *J. Geophys. Res.* 87, 4207-4229.
- Morton, R.A., Richmond, B.M., Jaffe, B.E. and Gelfenbaum, G., 2008. Coarse-Clast Ridge Complexes of the Caribbean: A Preliminary Basis for Distinguishing Tsunami and Storm-Wave Origins. *Journal of Sedimentary Research* 78, 624-637.
- Moses, C.S., Swart, P.K. and Dodge, R.E., 2006. Calibration of stable oxygen isotopes in *Siderastrea radians* (Cnidaria:Scleractinia): Implications for slow-growing corals. *Geochemistry Geophysics Geosystems* 7, PA3010, doi:10.1029/2005PA001257.
- Moustafa, Y.A., Pätzold, J., Loya, Y. and Wefer, G., 2000. Mid-Holocene stable isotope record of corals from the northern Red Sea. *International Journal of Earth Sciences* 88, 742-751.
- Müller-Karger, F.E., McClain, C.R., Fisher, T.R., Esaias, W.E. and Varela, R., 1989. Pigment distribution in the Caribbean sea: Observations from space. *Progress In Oceanography* 23, 23-64.

- Muñoz, E., Busalacchi, A.J., Nigam, S. and Ruiz-Barradas, A., 2008. Winter and Summer Structure of the Caribbean Low-Level Jet. *Journal of Climate* 21, 1260-1276.
- Nobre, P. and Strukla, J., 1996. Variations of Sea Surface Temperature, Wind Stress, and Rainfall over the Tropical Atlantic and South America. *Journal of Climate* 9, 2464-2479.
- Okai, T., Suzuki, A., Kawahata, H., Terashima, S. and Imai, N., 2002. Preparation of a New Geological Survey of Japan Geochemical Reference Material: Coral JCp-1. *Geostandards Newsletter* 26, 95-99.
- Oppo, D.W., Schmidt, G.A. and LeGrande, A.N., 2007. Seawater isotope constraints on tropical hydrology during the Holocene. *Geophys. Res. Lett.* 34, L13701.
- Paillard, D., Labeyrie, L. and Yiou, P., 1996. Macintosh program performs time-series analysis. *Eos Trans. AGU* 77, 379.
- Pätzold, J., 1992. Variation of Stable Oxygen and Carbon Isotopic Fractionation within the Skeletal Elements of Reef Building Corals from Bermuda. *Proceedings of the Seventh International Coral Reef Symposium, Guam* 1, 196-200.
- Pfeiffer, M., Timm, O., Dullo, W.-C. and Garbe-Schönberg, D., 2006. Paired coral Sr/Ca and $\delta^{18}\text{O}$ records from the Chagos Archipelago: Late twentieth century warming affects rainfall variability in the tropical Indian Ocean. *Geology* 34, 1069-1072.
- Poore, R., DeLong, K., Richey, J. and Quinn, T., 2009. Evidence of multidecadal climate variability and the Atlantic Multidecadal Oscillation from a Gulf of Mexico sea-surface temperature-proxy record. *Geo-Marine Letters* 29, 477-484.
- Quinn, T.M., Taylor, F.W., Crowley, T.J. and Link, S.M., 1996. Evaluation of Sampling Resolution in Coral Stable Isotope Records: A Case Study Using Records from New Caledonia and Tarawa. *Paleoceanography* 11, 529-542.
- Raddatz, T., Reick, C., Knorr, W., Kattge, J., Roeckner, E., Schnur, R., Schnitzler, K.G., Wetzel, P. and Jungclaus, J., 2007. Will the tropical land biosphere dominate the climate-carbon cycle feedback during the twenty-first century? *Climate Dynamics* 29, 565-574.
- Ren, L., Linsley, B.K., Wellington, G.M., Schrag, D.P. and Hoegh-guldberg, O., 2003. Deconvolving the $\delta^{18}\text{O}$ seawater component from subseasonal coral $\delta^{18}\text{O}$ and Sr/Ca at Rarotonga in the southwestern subtropical Pacific for the period 1726 to 1997. *Geochimica et Cosmochimica Acta* 67, 1609-1621.
- Reynolds, R.W., Rayner, N.A., Smith, T.M., Stokes, D.C. and Wang, W., 2002. An Improved In Situ and Satellite SST Analysis for Climate. *Journal of Climate* 15, 1609-1625.
- Richey, J.N., Poore, R.Z., Flower, B.P. and Quinn, T.M., 2007. 1400 yr multiproxy record of climate variability from the northern Gulf of Mexico. *Geology* 35, 423-426.
- Rimbu, N., Lohmann, G., Kim, J.H., Arz, H.W. and Schneider, R., 2003. Arctic/North Atlantic Oscillation signature in Holocene sea surface temperature trends as obtained from alkenone data. *Geophys. Res. Lett.* 30, 1280.
- Robinson, L.F., Belshaw, N.S. and Henderson, G.M., 2004. U and Th concentrations and isotope ratios in modern carbonates and waters from the Bahamas. *Geochimica et Cosmochimica Acta* 68, 1777-1789.
- Roeckner, E., Bäuml, G., Bonaventura, L., Brokopf, R., Esch, M., Giorgetta, M., Hagemann, S., Kirchner, I., Kornblueh, L., Manzini, E., Rhodin, A., Schlese, U., Schulzweida, U. and Tompkins, A., 2003. The Atmospheric General Circulation Model ECHAM5. Part One: Model Description Report No.349. Max Planck Institute for Meteorology.

- Rogers, J.C., 1984. The Association between the North Atlantic Oscillation and the Southern Oscillation in the Northern Hemisphere. *Monthly Weather Review* 112, 1999-2015.
- Romanek, C.S., Grossman, E.L. and Morse, J.W., 1992. Carbon isotopic fractionation in synthetic aragonite and calcite: Effects of temperature and precipitation rate. *Geochimica et Cosmochimica Acta* 56, 419-430.
- Rühlemann, C., Mulitza, S., Muller, P.J., Wefer, G. and Zahn, R., 1999. Warming of the tropical Atlantic Ocean and slowdown of thermohaline circulation during the last deglaciation. *Nature* 402, 511-514.
- Saenger, C., Cohen, A.L., Oppo, D.W. and Hubbard, D., 2008. Interpreting sea surface temperature from strontium/calcium ratios in *Montastraea* corals: Link with growth rate and implications for proxy reconstructions. *Paleoceanography*, 23, PA3102, doi:10.1029/2007PA001572.
- Saenger, C., Cohen, A.L., Oppo, D.W., Halley, R.B. and Carilli, J.E., 2009. Surface-temperature trends and variability in the low-latitude North Atlantic since 1552. *Nature Geoscience* 2, 492-495.
- Saravanan, R. and Chang, P., 2000. Interaction between Tropical Atlantic Variability and El Niño–Southern Oscillation. *Journal of Climate* 13, 2177-2194.
- Saunders, M.A., Chandler, R.E., Merchant, C.J. and Roberts, F.P., 2000. Atlantic hurricanes and NW Pacific typhoons: ENSO spatial impacts on occurrence and landfall. *Geophys. Res. Lett.* 27, 1147-1150.
- Scheffers, A., 2004. Tsunami imprints on the Leeward Netherlands Antilles (Aruba, Curaçao, Bonaire) and their relation to other coastal problems. *Quaternary International* 120, 163-172.
- Scheffers, A. and Scheffers, S., 2006. Documentation of the Impact of Hurricane Ivan on the Coastline of Bonaire (Netherlands Antilles). *Journal of Coastal Research* 22, 1437-1450.
- Scheffers, S.R., Haviser, J., Browne, T. and Scheffers, A., 2009. Tsunamis, hurricanes, the demise of coral reefs and shifts in prehistoric human populations in the Caribbean. *Quaternary International* 195, 69-87.
- Schmidt, G.A., 1999. Forward Modeling of Carbonate Proxy Data from Planktonic Foraminifera Using Oxygen Isotope Tracers in a Global Ocean Model. *Paleoceanography* 14, 482-497.
- Schmidt, G.A., Bigg, G.R. and Rohling, E.J., 1999. Global Seawater Oxygen-18 Database.
- Schmidt, M.W., Spero, H.J. and Lea, D.W., 2004. Links between salinity variation in the Caribbean and North Atlantic thermohaline circulation. *Nature* 428, 160-163.
- Schmidt, M.W. and Spero, H.J., 2011. Meridional shifts in the marine ITCZ and the tropical hydrologic cycle over the last three glacial cycles. *Paleoceanography* 26, PA1206.
- Scholz, D., Mangini, A. and Felis, T., 2004. U-series dating of diagenetically altered fossil reef corals. *Earth and Planetary Science Letters* 218, 163-178.
- Scholz, D. and Mangini, A., 2007. How precise are U-series coral ages? *Geochimica et Cosmochimica Acta* 71, 1935-1948.
- Schott, F.A., Lee, T.N. and Zantopp, R., 1988. Variability of Structure and Transport of the Florida Current in the Period Range of Days to Seasonal. *Journal of Physical Oceanography* 18, 1209-1230.

- Schrag, D.P., 1999. Rapid Analysis of High-Precision Sr/Ca Ratios in Corals and Other Marine Carbonates. *Paleoceanography* 14, 97-102.
- Seager, R. and Burgman, R.J., 2011. Medieval hydroclimate revisited. *PAGES News*, E. Xoplaki, D. Fleitmann, H. Diaz, I. von Gunten and T. Kiefer (Eds), Vol. 19, No 1, March 2011.
- Sepulcre, S., Vidal, L., Tachikawa, K., Rostek, F. and Bard, E., 2011. Sea-surface salinity variations in the northern Caribbean Sea across the Mid-Pleistocene Transition. *Climate of the Past* 7, 75-90.
- Shen, C.-C., Lee, T., Chen, C.-Y., Wang, C.-H., Dai, C.-F. and Li, L.-A., 1996. The calibration of D[Sr/Ca] versus sea surface temperature relationship for *Porites* corals. *Geochimica et Cosmochimica Acta* 60, 3849-3858.
- Sime, L.C., Wolff, E.W., Oliver, K.I.C. and Tindall, J.C., 2009. Evidence for warmer interglacials in East Antarctic ice cores. *Nature* 462, 342-345.
- Smith, D.M., Eade, R., Dunstone, N.J., Fereday, D., Murphy, J.M., Pohlmann, H. and Scaife, A.A., 2010. Skilful multi-year predictions of Atlantic hurricane frequency. *Nature Geosci* 3, 846-849.
- Smith, J.M., Quinn, T.M., Helmle, K.P. and Halley, R.B., 2006. Reproducibility of geochemical and climatic signals in the Atlantic coral *Montastraea faveolata*. *Paleoceanography*, 21, PA1010, doi:10.1029/2005PA001187.
- Smith, S.V., Buddemeier, R.W., Redalje, R.C. and Houck, J.E., 1979. Strontium-Calcium Thermometry in Coral Skeletons. *Science* 204, 404-407.
- Smith, T.M., Reynolds, R.W., Peterson, T.C. and Lawrimore, J., 2008. Improvements to NOAA's Historical Merged Land-Ocean Surface Temperature Analysis (1880-2006). *Journal of Climate* 21, 2283-2296.
- Solomon, S., D. Qin, M. Manning, Z. Chen, M. Marquis, K.B. Averyt, M. Tignor and H.L. Miller (eds.), 2007. *The Physical Science Basis: Contribution of Working Group I to the Fourth Assessment Report of the Intergovernmental Panel on Climate Change*, 2007, Cambridge, United Kingdom and New York, NY, USA.
- Stoll, H.M. and Schrag, D.P., 1998. Effects of Quaternary Sea Level Cycles on Strontium in Seawater. *Geochimica et Cosmochimica Acta* 62, 1107-1118.
- Stouffer, R.J., Yin, J., Gregory, J.M., Dixon, K.W., Spelman, M.J., Hurlin, W., Weaver, A.J., Eby, M., Flato, G.M., Hasumi, H., Hu, A., Jungclaus, J.H., Kamenkovich, I.V., Levermann, A., Montoya, M., Murakami, S., Nawrath, S., Oka, A., Peltier, W.R., Robitaille, D.Y., Sokolov, A., Vettoretti, G. and Weber, S.L., 2006. Investigating the Causes of the Response of the Thermohaline Circulation to Past and Future Climate Changes. *Journal of Climate* 19, 1365-1387.
- Sun, D., Gagan, M.K., Cheng, H., Scott-Gagan, H., Dykoski, C.A., Edwards, R.L. and Su, R., 2005. Seasonal and interannual variability of the Mid-Holocene East Asian monsoon in coral [$\delta^{18}\text{O}$] records from the South China Sea. *Earth and Planetary Science Letters* 237, 69-84.
- Sutton, R.T., Jewson, S.P. and Rowell, D.P., 2000. The Elements of Climate Variability in the Tropical Atlantic Region. *Journal of Climate* 13, 3261-3284.
- Sutton, R.T. and Hodson, D.L.R., 2003. Influence of the Ocean on North Atlantic Climate Variability. *Journal of Climate* 16, 3296-3313.

- Sutton, R.T. and Hodson, D.L.R., 2005. Atlantic Ocean Forcing of North American and European Summer Climate. *Science* 309, 115-118.
- Suzuki, A., Hibino, K., Iwase, A. and Kawahata, H., 2005. Intercolony variability of skeletal oxygen and carbon isotope signatures of cultured *Porites* corals: Temperature-controlled experiments. *Geochimica et Cosmochimica Acta* 69, 4453-4462.
- Swart, P.K., 1983. Carbon and oxygen isotope fractionation in scleractinian corals: a review. *Earth-Science Reviews* 19, 51-80.
- Swart, P.K., Dodge, R.E. and Hudson, H.J., 1996a. A 240-Year Stable Oxygen and Carbon Isotopic Record in a Coral from South Florida: Implications for the Prediction of Precipitation in Southern Florida. *PALAIOS* 11, 362-375.
- Swart, P.K., Leder, J.J., Szmant, A.M. and Dodge, R.E., 1996b. The origin of variations in the isotopic record of scleractinian corals: II. Carbon. *Geochimica et Cosmochimica Acta* 60, 2871-2885.
- Swart, P.K., Elderfield, H. and Greaves, M.J., 2002. A high-resolution calibration of Sr/Ca thermometry using the Caribbean coral *Montastraea annularis*. *Geochemistry Geophysics Geosystems* 3, 8402, doi:10.1029/2002GC000306.
- Tedesco, K. and Thunell, R., 2003. High resolution tropical climate record for the last 6,000 years. *Geophys. Res. Lett.* 30, 1891.
- Tourre, Y.M., Rajagopalan, B. and Kushnir, Y., 1999. Dominant Patterns of Climate Variability in the Atlantic Ocean during the Last 136 Years. *Journal of Climate* 12, 2285-2299.
- Tudhope, A.W., Chilcott, C.P., McCulloch, M.T., Cook, E.R., Chappell, J., Ellam, R.M., Lea, D.W., Lough, J.M. and Shimmield, G.B., 2001. Variability in the El Niño-Southern Oscillation Through a Glacial-Interglacial Cycle. *Science* 291, 1511-1517.
- Urey, H.C., 1947. The thermodynamic properties of isotopic substances. *Journal of the Chemical Society* 562-581.
- Van Duyl, F.C., 1985. Atlas to the living reefs of Curaçao and Bonaire (Netherlands Antilles), Utrecht.
- Vellinga, M. and Wood, R.A., 2002. Global Climatic Impacts of a Collapse of the Atlantic Thermohaline Circulation. *Climatic Change* 54, 251-267.
- Vellinga, M. and Wu, P., 2004. Low-Latitude Freshwater Influence on Centennial Variability of the Atlantic Thermohaline Circulation. *Journal of Climate* 17, 4498-4511.
- Vengosh, A., Kolodny, Y., Starinsky, A., Chivas, A.R. and McCulloch, M.T., 1991. Coprecipitation and isotopic fractionation of boron in modern biogenic carbonates. *Geochimica et Cosmochimica Acta* 55, 2901-2910.
- Veron, J.E.N., 2000. Corals of the World. Vol 3. Australia: Australian Institute of Marine Sciences and CRR Qld Pty Ltd. Australian Institute of Marine Sciences and CRR Qld Pty Ltd., 3, 206-209 pp.
- Wan, X., Chang, P., Saravanan, R., Zhang, R. and Schmidt, M.W., 2009. On the interpretation of Caribbean paleo-temperature reconstructions during the Younger Dryas. *Geophys. Res. Lett.* 36, L02701.
- Wang, C. and Enfield, D.B., 2003. A Further Study of the Tropical Western Hemisphere Warm Pool. *Journal of Climate* 16, 1476-1493.

- Wang, C., Enfield, D.B., Lee, S.-k. and Landsea, C.W., 2006. Influences of the Atlantic Warm Pool on Western Hemisphere Summer Rainfall and Atlantic Hurricanes. *Journal of Climate* 19, 3011-3028.
- Wang, C., 2007. Variability of the Caribbean Low-Level Jet and its relations to climate. *Climate Dynamics* 29, 411-422.
- Wang, C. and Lee, S.-k., 2007. Atlantic warm pool, Caribbean low-level jet, and their potential impact on Atlantic hurricanes. *Geophys. Res. Lett.* 34, L02703.
- Wang, C., Lee, S.-k. and Enfield, D.B., 2007. Impact of the Atlantic Warm Pool on the Summer Climate of the Western Hemisphere. *Journal of Climate* 20, 5021-5040.
- Wang, C., Lee, S.-K. and Enfield, D.B., 2008a. Atlantic Warm Pool acting as a link between Atlantic Multidecadal Oscillation and Atlantic tropical cyclone activity. *Geochem. Geophys. Geosyst.* 9, Q05V03.
- Wang, C., Lee, S.-K. and Enfield, D.B., 2008b. Climate Response to Anomalous Large and Small Atlantic Warm Pools during the Summer. *Journal of Climate* 21, 2437-2450.
- Wanner, H., Beer, J., Bütikofer, J., Crowley, T.J., Cubasch, U., Flückiger, J., Goosse, H., Grosjean, M., Joos, F., Kaplan, J.O., Küttel, M., Müller, S.A., Prentice, I.C., Solomina, O., Stocker, T.F., Tarasov, P., Wagner, M. and Widmann, M., 2008. Mid- to Late Holocene climate change: an overview. *Quaternary Science Reviews* 27, 1791-1828.
- Watanabe, T., Winter, A. and Oba, T., 2001. Seasonal changes in sea surface temperature and salinity during the Little Ice Age in the Caribbean Sea deduced from Mg/Ca and $18\text{O}/16\text{O}$ ratios in corals. *Marine Geology* 173, 21-35.
- Watanabe, T., Winter, A., Oba, T., Anzai, R. and Ishioroshi, H., 2002. Evaluation of the fidelity of isotope records as an environmental proxy in the coral *Montastraea*. *Coral Reefs* 21, 169-178.
- Watanabe, T., Gagan, M.K., Corrège, T., Scott-Gagan, H., Cowley, J. and Hantoro, W.S., 2003. Oxygen isotope systematics in *Diploastrea heliophora*: new coral archive of tropical paleoclimate. *Geochimica et Cosmochimica Acta* 67, 1349-1358.
- Weber, J.N. and Woodhead, P.M.J., 1970. Carbon and oxygen isotope fractionation in the skeletal carbonate of reef-building corals. *Chemical Geology* 6, 93-117.
- Weber, J.N. and Woodhead, P.M.J., 1972. Temperature dependence of oxygen-18 concentration in reef coral carbonates. *Journal of Geophysical Research* vol. 77, 463.
- Weber, J.N., 1973. Incorporation of strontium into reef coral skeletal carbonate. *Geochimica et Cosmochimica Acta* 37, 2173-2190.
- Wellington, G.M., Dunbar, R.B. and Merlen, G., 1996. Calibration of Stable Oxygen Isotope Signatures in Galápagos Corals. *Paleoceanography*, 11(4), 467-480.
- Winter, A., Goenaga, C. and Maul, G.A., 1991. Carbon and Oxygen Isotope Time Series From an 18-Year Caribbean Reef Coral. *Journal Geophysical Research* 96(C9), 16673-16678.
- Winter, A., Ishioroshi, H., Watanabe, T., Oba, T. and Christy, J., 2000. Caribbean Sea Surface Temperatures: Two-to-Three Degrees Cooler than Present During The Little Ice Age. *Geophysical Research Letters* 27(20), 3365-3368.
- Winter, A., Paul, A., Nyberg, J., Oba, T., Lundberg, J., Schrag, D. and Taggart, B., 2003. Orbital control of low-latitude seasonality during the Eemian. *Geophysical Research Letters* 30, 1163, doi:10.1029/2002GL016275.

- Woodley, J.D., Chornesky, E.A., Clifford, P.A., Jackson, J.B.C., Kaufman, L.S., Knowlton, N., Lang, J.C., Pearson, M.P., Porter, J.W., Rooney, M.C., Rylaarsdam, K.W., Tunnicliffe, V.J., Wahle, C.M., Wulff, J.L., Curtis, A.S.G., Dallmeyer, M.D., Jupp, B.P., Koehl, M.A.R., Neigel, J. and Sides, E.M., 1981. Hurricane Allen's Impact on Jamaican Coral Reefs. *Science* 214, 749-755.
- Woodroffe, C.D., Beech, M.R. and Gagan, M.K., 2003. Mid-late Holocene El Niño variability in the equatorial Pacific from coral microatolls. *Geophys. Res. Lett.* 30, 1358.
- Wüst, G., 1964. Stratification and Circulation in the Antillean-Caribbean Basins, Part 1, Spreading and mixing of the water types with an oceanographic atlas, Columbia University Press, New York, 201 pp.
- Xie, S.-P. and Carton, J.A. (Editors), 2004. Tropical Atlantic variability: Patterns, mechanisms, and impacts, 147, 121-142 pp.
- Yokoyama, Y., Suzuki, A., Siringan, F., Maeda, Y., Abe-Ouchi, A., Ohgaito, R., Kawahata, H. and Matsuzaki, H., 2011. Mid-Holocene palaeoceanography of the northern South China Sea using coupled fossil-modern coral and atmosphere-ocean GCM model. *Geophys. Res. Lett.* 38, L00F03.
- Zhang, D., Msadek, R., McPhaden, M.J. and Delworth, T., 2011. Multidecadal variability of the North Brazil Current and its connection to the Atlantic meridional overturning circulation. *J. Geophys. Res.* 116, C04012.
- Zhang, R. and Delworth, T.L., 2005. Simulated Tropical Response to a Substantial Weakening of the Atlantic Thermohaline Circulation. *Journal of Climate* 18, 1853-1860.
- Zinke, J., Dullo, W.C., Heiss, G.A. and Eisenhauer, A., 2004. ENSO and Indian Ocean subtropical dipole variability is recorded in a coral record off southwest Madagascar for the period 1659 to 1995. *Earth and Planetary Science Letters* 228, 177-194.